PB 189 759

BULK TRANSPORT OF WASTE SLURRIES TO INLAND AND OCEAN DISPOSAL SITES. VOLUME III. TECHNICAL ASPECTS OF PIPELINING OF WASTE MATERIALS

J. P. Kenny

Bechtel Corporation
San Francisco, California

September 1969

CLEARINGHOUSE
FOR FEDERAL SCIENTIFIC AND TECHNICAL INFORMATION

Distributed . . . 'to foster, serve and promote the nation's economic development and technological advancement.'

U.S. DEPARTMENT OF COMMERCE/National Bureau of Standards

This document has been approved for public release and sale.

Abstracted by USGS
Del. 3-6-70

14010EHS09/69
DAST - 18

PB189759

W70-04007

BULK TRANSPORT OF WASTE SLURRIES TO INLAND AND OCEAN DISPOSAL SITES

VOLUME III

TECHNICAL ASPECTS OF PIPELINING OF WASTE MATERIALS

BECHTEL

September 1969

Reproduced by the
CLEARINGHOUSE
for Federal Scientific & Technical
Information Springfield Va. 22151

222

CONTENTS

Page

1 INTRODUCTION 1-1

2 SUMMARY AND CONCLUSIONS 2-1

3 STATE OF THE ART 3-1

3.1 Hydrodynamics 3-1
3.2 Operability 3-18
3.3 Corrosion/Erosion 3-21
3.4 Mechanical Equipment 3-25

4 DISCUSSION OF DESIGN PROCEDURE 4-1

5 HYDRAULIC TEST EQUIPMENT 5-1

6 LABORATORY PROCEDURES AND DATA 6-1

6.1 Testing Methods 6-1
6.2 Digested Sludge 6-4
6.3 Fly Ash 6-9
6.4 Sludge/Fly Ash Mixtures 6-16
6.5 Maintenance Dredging 6-17
6.6 Sludge/Dredgings Mixtures 6-23
6.7 Water Treatment Plant Sludge 6-23

7 PIPE TESTS ON DIGESTED SLUDGE 7-1

7.1 Pipelining of Digested Sludge 7-1
7.2 Rheology 7-4
7.3 Hydraulic Data 7-16

8 PIPE TESTS ON FLY ASH SLURRIES 8-1

8.1 Pipelining of Fly Ash Slurries 8-1
8.2 Rheology 8-5
8.3 Hydraulic Data 8-9
8.4 Pipeline Operability 8-28

9 PIPE TESTS ON SLUDGE/FLY ASH MIXTURES 9-1

9.1 Pipelining of Sludge/Fly Ash Mixtures 9-1
9.2 Rheology 9-3
9.3 Hydraulic Data 9-7
9.4 Pipeline Operability 9-15

APPENDIX A A-1

A.1 Water Runs A-1
A.2 Digested Sludge Runs A-6
A.3 Fly Ash Runs A-10
A.4 Sludge/Fly Ash Runs A-21

CONTENTS (cont.)

Page

APPENDIX B

NOMENCLATURE B-1

APPENDIX C

REFERENCES C-1

PREFACE

Contract No. 14-12-156 was issued to Bechtel Corporation by the Federal Water Pollution Control Administration of the Department of the Interior on April 10, 1968. The purpose of the contract was to determine the technical feasibility and economics of transporting sewage treatment plant sludge and dredging spoils by currently available transportation methods for the purpose of both land and ocean disposal. To ensure the general application of this concept, regional considerations were emphasized. Two other bulk waste materials, fly ash and water treatment plant sludge, were also investigated for possible inclusion in the disposal system

The report summarizing the work performed under this contract has been presented in three volumes. This volume is concerned with the technical aspects of the use of pipelines for transportation of the waste materials. The use of pipelines, as opposed to trucks or railroads, requires an understanding of the technology of solid-liquid flow and this volume is intended to provide this necessary information. Volume I presents a detailed evaluation of two typical regional systems, the Northeast Ohio land disposal system and the Baltimore-Washington ocean disposal system. Included is a recommended demonstration plan of the bulk transport and disposal concept. Volume II is devoted to environmental criteria for regional waste management systems.

ACKNOWLEDGEMENTS

The following people contributed to this report:

NAME	CONTRIBUTION
J. P. Kenny*	Experimental, Data Correlation, Report Writing, State of Art Section
P. E. Snoek*	Experimental
J. C. Carney*	Experimental, Data Correlation
W. J. Stump*	Experimental
Dr. Iraj Zandi**	Reviewer and Author of Section 3, State of the Art

* Bechtel Corporation
** University of Pennsylvania, Towne School of Engineering

We also wish to thank the Consolidation Coal Company Division of Continental Oil Company for making available the very extensive Cadiz test facilities at no cost to the public.

E. J. Wasp
Project Manager

Section 1

INTRODUCTION

This report is part of the Waste Management Study undertaken at the request of the FWPCA (Contract No. 14-12-156). Volume II of the study presents the technical and environmental criteria for a regional waste disposal system, and in Volume I, these general criteria are applied to develop waste management systems for two specific regions.

The transportation of wastes from their sources to disposal areas is a major economic factor in any disposal system. The purpose of this section of the study is to establish the feasibility of using pipelines to transport waste materials, and to develop a reliable procedure for the design of such pipelines. As opposed to alternative modes of transportation such as trucks and rail, the design of a successful pipeline system to transport solid wastes requires an understanding of the technology of solids-liquid flow. To this end a series of laboratory and pipeline tests was performed and is described in this study. The object of the test program was to arrive at a suitable design procedure by correlation of measured friction losses.

The bases and procedures of data correlation are discussed in detail in Section 3, but the rationale used in applying these techniques can be summarized as follows:

1. The recommended design procedure should enable the hydraulic design of a commercial pipeline to be made from the laboratory measurement of basic flow parameters.
2. The recommended design procedure must be applicable to widely differing material.

3. The recommended design procedure must be applicable to commercial pipe diameters.

4. Since commercial slurry pipelines normally operate in the turbulent regime, the design model must include a reliable criterion for the prediction of laminar/turbulent transition.

Digested sewage sludge and fly ash were chosen as representative materials for the tests. The physical characteristics of these materials differ widely. Fly ash is a fast settling, high density material; sludge solids are fibrous, have low density and have extremely low settling rates. However, it was expected, and was also demonstrated, that both materials - sludge because of its fibrous nature and fly ash because the particles are very fine - would be transported in homogenous flow in the turbulent regime. Samples taken from the top and the middle of the pipe test sections confirmed that this was indeed the case.

These materials, individually and in various combinations of the two, were tested at various velocities in 1/2-inch, 12-inch, and 16-inch pipe test sections, for a number of solids concentrations, thus providing a very wide range of data.

In order to ensure the successful operation of any solid/liquid pipeline, the operability of a given system with regard to shutdown and startup must be established, and tests were performed for this purpose on fly ash and a fly ash/sludge mixture.

The tests were performed at the experimental facilities of the Hanna Coal Company Division of Consolidation Coal, located at Cadiz, Ohio. As a public service, the Consolidation Coal Company provided the facilities for the tests without charge. The sludge was obtained from the Southerly Sewage Treatment Plant in Cleveland and fly ash was obtained from Ohio Edison's Sammis Plant.

To provide information relevant to transportation of other waste materials, laboratory analyses were performed on samples of sludge from Washington Water Pollution Control plants, maintenance dredgings from Cleveland Harbor, and water treatment plant sludge from Cleveland.

Section 2

SUMMARY AND CONCLUSIONS

The hydraulic and laboratory data gathered on the materials under study show that digested sludge, fly ash, and fly ash/sludge mixtures can be successfully transported by pipelines.

The rheological characteristics of the materials were established using a rotational viscometer. From these data, head losses were predicted for a wide range of pipe diameters, and the predictions were successfully correlated with measured pipe data.

The pipeline operability, with regard to shut-down and startup, was evaluated for each material, and the internal corrosion rates to be expected in the pipeline transportation of these materials were determined.

Specific conclusions regarding such pipelines are outlined below.

2.1 HYDRODYNAMIC DESIGN

Various correlation procedures were applied to the hydraulic data for flow of these waste materials in pipes. It was shown that a model assuming homogeneous suspension of the solids gives good prediction of friction losses for a wide range of pipe diameters. An example of the accuracy of prediction of hydraulic test data is shown in Figure 2.1.

The basis of this model is that flow of a homogeneous suspension is very similar to that of a true, or Newtonian, fluid. Provided that a suitable viscosity of the slurry can be obtained, head losses can be calculated from the standard friction factor-Reynolds Number relationships for Newtonian fluids. Section 4 presents a detailed discussion of the basis for and the use of the homogeneous model, and shows that

FIGURE 2-1

COMPARISON OF PREDICTED
AND MEASURED FRICTION LOSSES
SOUTHERLY DIGESTED SLUDGE

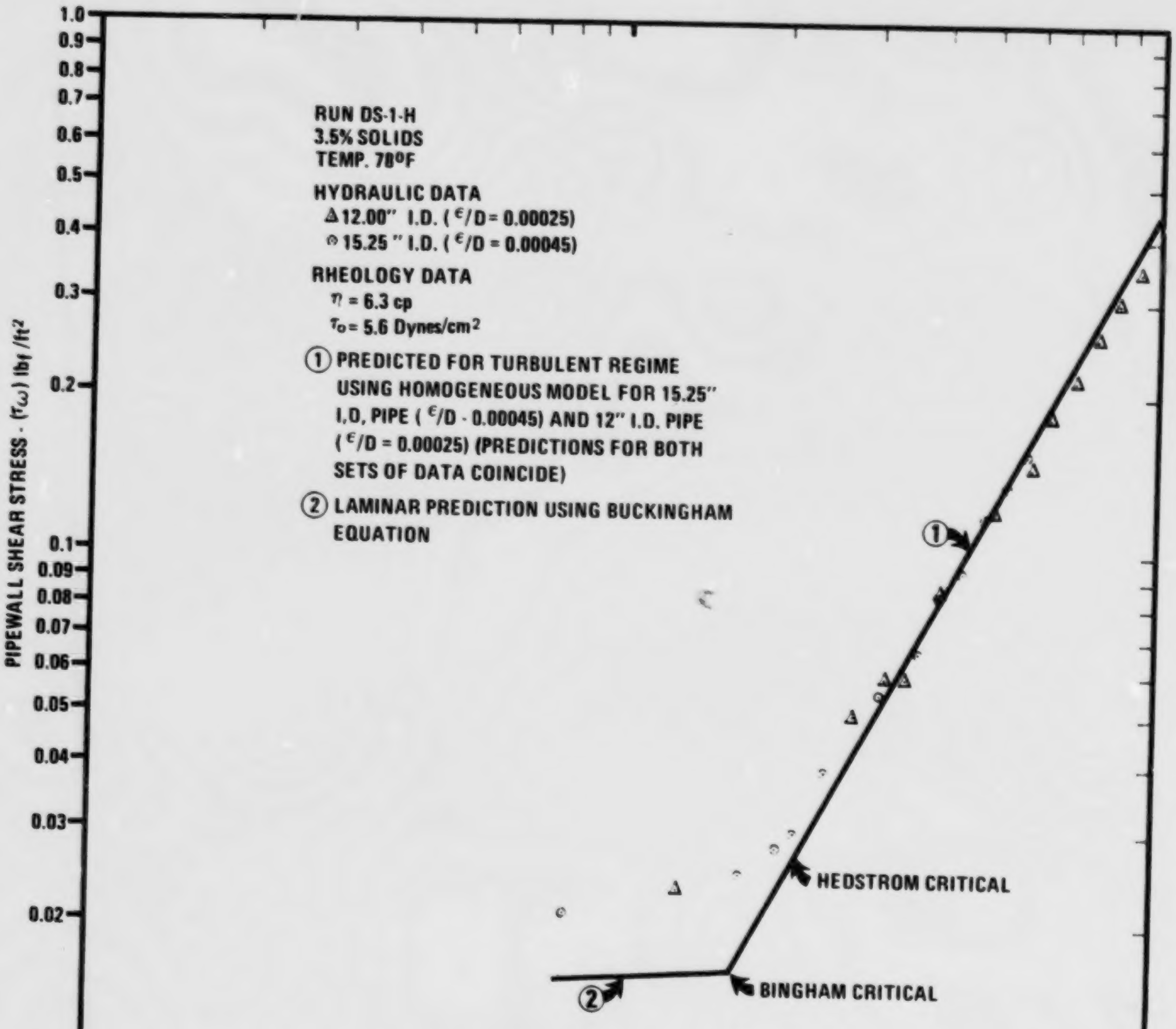

RUN DS-1-H
3.5% SOLIDS
TEMP. 78°F

HYDRAULIC DATA
△ 12.00" I.D. ($\epsilon/D = 0.00025$)
○ 15.25" I.D. ($\epsilon/D = 0.00045$)

RHEOLOGY DATA
$\eta = 6.3$ cp
$\tau_o = 5.6$ Dynes/cm^2

① PREDICTED FOR TURBULENT REGIME USING HOMOGENEOUS MODEL FOR 15.25" I.D. PIPE (ϵ/D - 0.00045) AND 12" I.D. PIPE ($\epsilon/D = 0.00025$) (PREDICTIONS FOR BOTH SETS OF DATA COINCIDE)

② LAMINAR PREDICTION USING BUCKINGHAM EQUATION for a slurry exhibiting plastic properties, the coefficient of rigidity is a suitable viscosity with which to define the Reynolds Number.

The study shows that this model is a reliable procedure for the design of pipeline waste disposal systems, provided that accurate information as to system rheology is available. A rotational viscometer was used in this study to generate such rheological data. In the turbulent regime, which is the area of interest to commercial pipelines, the study materials are transported as homogeneous fluids (with certain concentration limitations in the case of fly ash). The data show that the Hedstrom critical velocity (Refs. 18 and 19) gives good predictions of laminar/turbulent transition, and is, therefore, a useful method of ensuring that a given system is in the turbulent flow regime.

Digested sludge and sludge/fly ash mixtures are closely represented by the homogeneous model. Indeed, it appears that adding fly ash to digested sludge is an ideal method of transporting fly ash (or similar waste materials), since addition of significant quantities of fly ash (10:1 on sludge solids) does not result in a drastic increase in friction losses. Data for fly ash/water slurries indicate a dampening of turbulence due to the presence of solids. The suppressant action in some instances is almost within the limits of experimental error.

2.2 OPERABILITY

Laboratory and test loop datashow that pipelines transporting these waste materials can be successfully restarted following a shutdown. The findings of the tests are supported by the fact that successful installations for the transportation of both sludge and fly ash have been in operation for a number of years.

2.3 CORROSION

The corrosion rates to be expected in the pipelining of sludge, fly ash, and fly ash/sludge mixtures were evaluated by laboratory tests. The test procedure used has been related to actual rates experienced in a commercial pipeline (Ref. 57), and is a reliable method of establishing pipeline corrosion rates.

The tests show that corrosion rates for these materials are very moderate (1 to 2 mils per year) and will present no particular problems in a cross-country pipeline.

Section 3

STATE OF THE ART

3.1 HYDRODYNAMICS

The behavior of solid/liquid systems can be very complex, and in many cases the design of a non-Newtonian pipeline system is as much an art as a science. However, in the simple case of homogeneous flow, the design can be essentially a science.

Homogeneous flow occurs when the solid particles are fine and of low specific gravity or when the mean velocity of flow is sufficiently high to keep the particles uniformly suspended throughout the cross-section of the pipe. Normally, but not necessarily, the slurry exhibits a shear stress/shear rate relationship that is different from that of the conveying fluid. When the conveying fluid is water, the slurry behavior may be non-Newtonian. (Refs. 1 through 6.)

This nondeposit, nonstratified flow is encountered in the transportation of fine sand, fine coal, clays, thorium oxide, drilling muds, sewage sludge, and many other finely ground materials. Numerous criteria have been presented as tests for homogeneity. Durand (Ref. 49) suggest that the particles normally carried in the homogeneous regime are below 30 microns in diameter (about 400 mesh), and Govier and Charles (Ref. 48) propose that if the terminal settling velocity of particles in a stationary liquid is less than 0.002 fps it is likely that the solids will be transported in the homogeneous regime.

However, the homogeneous regime, as defined here, comes into being as a result of a combination of particle size, solid and liquid density, and mean velocity of flow. The only criterion used for homogeneity is uniformity of solids distribution in the pipeline. As will be discussed later, fly ash slurries with a size consist of essentially 100 mesh x 0 containing 57 percent solids (of specific gravity 2.5) or greater are transported in the homogeneous regime for the usual range of commercial pipeline velocities. In the absence of actual measurement, comparison with these conditions of particle size, concentration, and solids specific gravity can be used to obtain the approximate requirements for homogeneous flow for another slurry system.

The homogeneous flow regime may be divided into those regimes in which the solid/liquid interaction does not significantly alter the rheological properties of the conveying fluid, and into those in which it does.

3.1.1 Dilute Suspensions of Relatively Large Particles

It has been observed that the flow of water carrying a small amount of particulate matter results in lower head losses than for the flow of water alone, all other conditions being equal. Under certain conditions, this head loss suppression may be considerable and may result in increased pumping efficiency. Much has been written pointing to this unexpected phenomenon. Motivated by McMath (Ref. 8), who, on the basis of data for the Mississippi River, observed that a stream at a given stage would flow faster when turbid than when clear, Vanoni (Ref. 9) made measurements of friction factors in a laboratory flume for various values of flow rate, slope of channel, size and amount of suspended load. He found that the resistance to flow decreased as a result of suspended sediment and therefore sediment-laden water flowed faster than comparable clear water.

A recent paper by Zandi (Ref. 10) indicates that the same phenomenon is observed when low concentrations of either fine coal, fine charcoal, or fine ash are added to flowing water. Zandi suggests a number of possible mechanisms for this suppressant action. A number of investigations have attributed the decrease in friction factor to a damping of system turbulence due to the presence of solid particles (Refs. 8 and 11).

Where the system is such that flow is in the homogeneous regime, because of the combination of concentration, particle size, and velocity, but is not of the type exhibiting the friction factor suppression effect, the friction factor, and therefore, the head losses, can be predicted from the normal friction factor/Reynolds Number charts, provided that the density and viscosity of the slurry are used to define Reynolds Number. As a first approximation, the viscosity of the suspension may be assumed to be equal to that of the suspending medium. However, a more accurate viscosity may be estimated by means of approximate rheological constants (Refs. 12 and 13), e.g., coefficient of rigidity if a slurry has a plastic behavior.

3.1.2 Non-Newtonian Suspensions

Figure 3-1 shows the isothermal shear stress/shear rate relationships for typical time-independent fluids. These relationships can be approximated by the following equations:

Pseudoplastic and Dilatant $\tau = K\left(\frac{dU}{dr}\right)^n$ (1)

Plastic $\tau = \tau_o + \left(\frac{dU}{dr}\right)\eta$ (2)

where the symbols are as defined in Appendix B.

The rheological significance of equations 1 and 2 can be seen by reference to Figure 3-1, which shows the major classifications of non-Newtonian fluids and the typical rheological differences between them and a true fluid. It can be seen that a Newtonia (true) fluid exhibits a linear shear stress/rate of shearing strain characteristic which passes through the origin. Hence, establishing a viscosity for a Newtonian fluid is relatively simple, it being, by definition, the slope of the shear stress/shear rate curve.

FIGURE 3-1

FLUID CLASSIFICATION

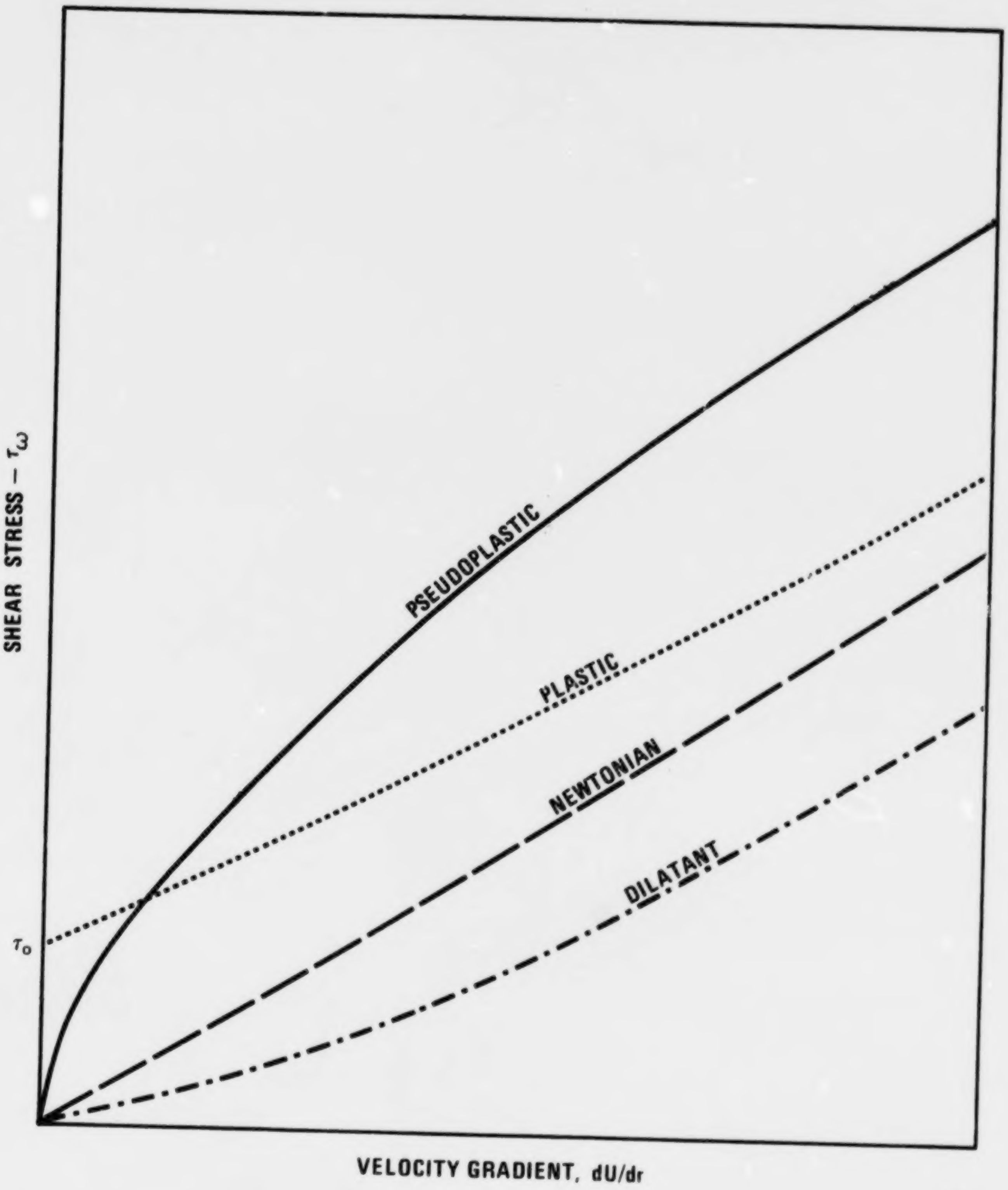

A Bingham (true) plastic also exhibits a linear characteristic, but differs from a Newtonian system in that at zero shear rate the characteristic shows an intercept on the shear stress axis. This intercept is known as the yield stress of the material and is a measure of the force which must be applied before the fluid can begin to move. The slope of the line is equivalent to the coefficient of rigidity of the material.

Pseudoplastics and dilatant materials do not exhibit a yield stress, and at lower shear rates the materials exhibit a varying viscosity. However, at high shear rates, the shear stress/shear rate characteristics become linear, and a limiting viscosity can be identified.

Equation (1) is the power law or Ostwald-de Waele Model, and equation (2) is known as the Bingham plastic model. Both laminar and turbulent flow of these suspensions are possible and are commercially significant. The aspect of these types of flow which is of interest and which will be discussed here is prediction of head loss. Concentration distribution across the pipe cross-section is, of course, uniform.

3.1.2.1 Laminar Flow of Non-Newtonian Suspensions: Head Loss. For a Bingham plastic suspension, Buckingham (Ref. 16) integrated equation (2) for a pipe and obtained:

$$\frac{8V}{D} = \frac{\tau_w g_o}{\eta}\left[1 - \frac{4}{3}\left(\frac{\tau_o}{\tau_w}\right) + \frac{1}{3}\left(\frac{\tau_o}{\tau_w}\right)^4\right] \qquad (3)$$

which enables one to calculate τ_w and hence pressure loss, Δp, from the knowledge of mean velocity, pipe diameter, and rheological parameters of the suspension. Another method of calculating head loss is through the estimation of friction factor.

On the basis of work by Govier and Winning (Ref. 17) and Hedstrom (Ref. 18) and through dimensional analysis, Metzner (Ref. 15) showed that the Fanning friction factor, as defined by $f = (\Delta pD/4L)/(\rho V^2/2g_c)$ is not only a function of Reynolds Number, but also of a dimensionless number, known as the Hedstrom Number, which is given by:

$$N_{He} = N_{Re} \times P_L \qquad (4)$$

P_L is the plasticity number and is defined as $(\tau_o/\eta)/(V/D)$. The physical significance of the plasticity number is readily seen to be the ratio of shearing strain in the in the fluid $\left(\frac{dU}{dr} = \frac{\tau_o}{\eta}\right)$ to the shearing strain in the pipe (V/D).

The relationship between N_{Re}, N_{He} and friction factor is given as follows:

$$\frac{1}{N_{Re}} = \frac{f}{16} - \frac{1}{6}\left(\frac{N_{He}}{N_{Re}{}^2}\right) + \frac{1}{3}\left(\frac{N_{He}{}^4}{f^3 N_{Re}{}^8}\right) \qquad (5)$$

This relationship is shown in Figure 3-2 and is an equally satisfactory representation of laminar flow for Bingham plastic fluids.

It is interesting to note that equation (5) and Figure 3-2 are also applicable to the turbulent flow of Bingham plastics. Hanks (Ref. 19) has developed this to include the variation of Reynolds Number at

FIGURE 3-2

FRICTION FACTOR – REYNOLDS NUMBER DIAGRAM FOR BINGHAM PLASTICS

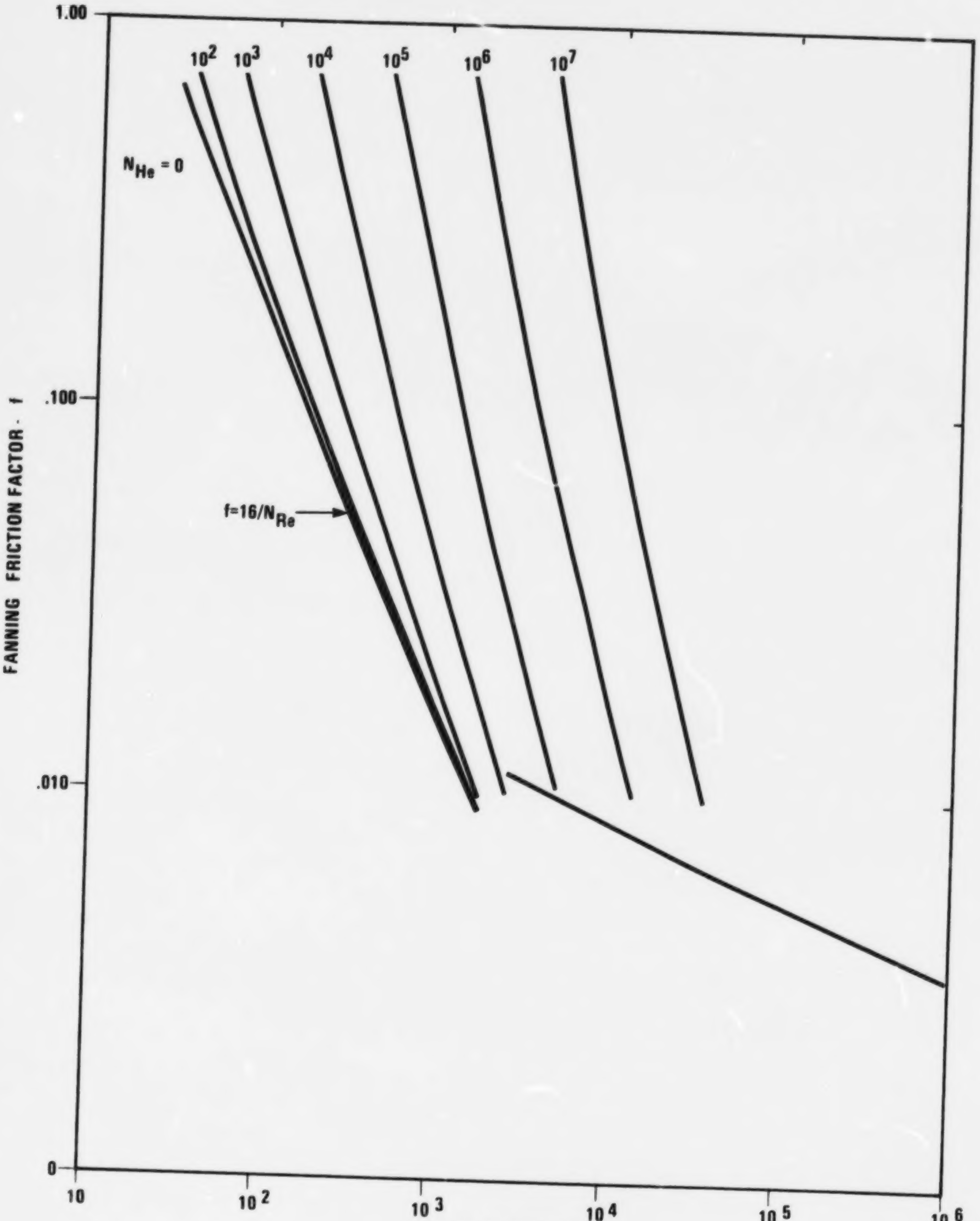

turbulent/laminar transition, with the Hedstrom Number, as shown in Figure 3-3.

It can be seen that at values of the Hedstrom Number less than 10^5, the data given by Hanks are in good agreement with the Hedstrom prediction of critical Reynolds Number. However, at Hedstrom Numbers greater than 10^5 there is a significant divergence. Hanks, by use of the Powell-Eyring model, develops an analogue of the Hedstrom Number which gives a better fit to the data. The approach used in the present study is more direct, the critical Reynolds Number being obtained from an empirical line through the data points and the Hedstrom Number being defined on the Bingham plastic basis.

For a Bingham plastic suspension, Tomita (Ref. 14) equated the shearing force on the surface of any arbitrary cylindrical shape of fluid to the difference of pressure forces between two arbitrary cross-sections and derived a modified friction factor and a modified Reynolds Number for the correlation of turbulent flow of Bingham plastics.

The modified values are given as follows:

$$f^* = f\left(\frac{1}{1-c}\right) \qquad (6)$$

$$N_{Re}^* = N_{Re}\left[\frac{(1-c)(c^4 - 4c + 3)}{3}\right] \qquad (7)$$

where

$$c = \tau_o / \tau_w \qquad (8)$$

As c approaches zero, i.e., as the system approaches Newtonian behavior, the modified values, f* and N* tend toward f and N_{Re}.

Figure 3-3

VARIATION OF N_{Re_c} WITH N_{He} FOR BINGHAM FLOW IN PIPES

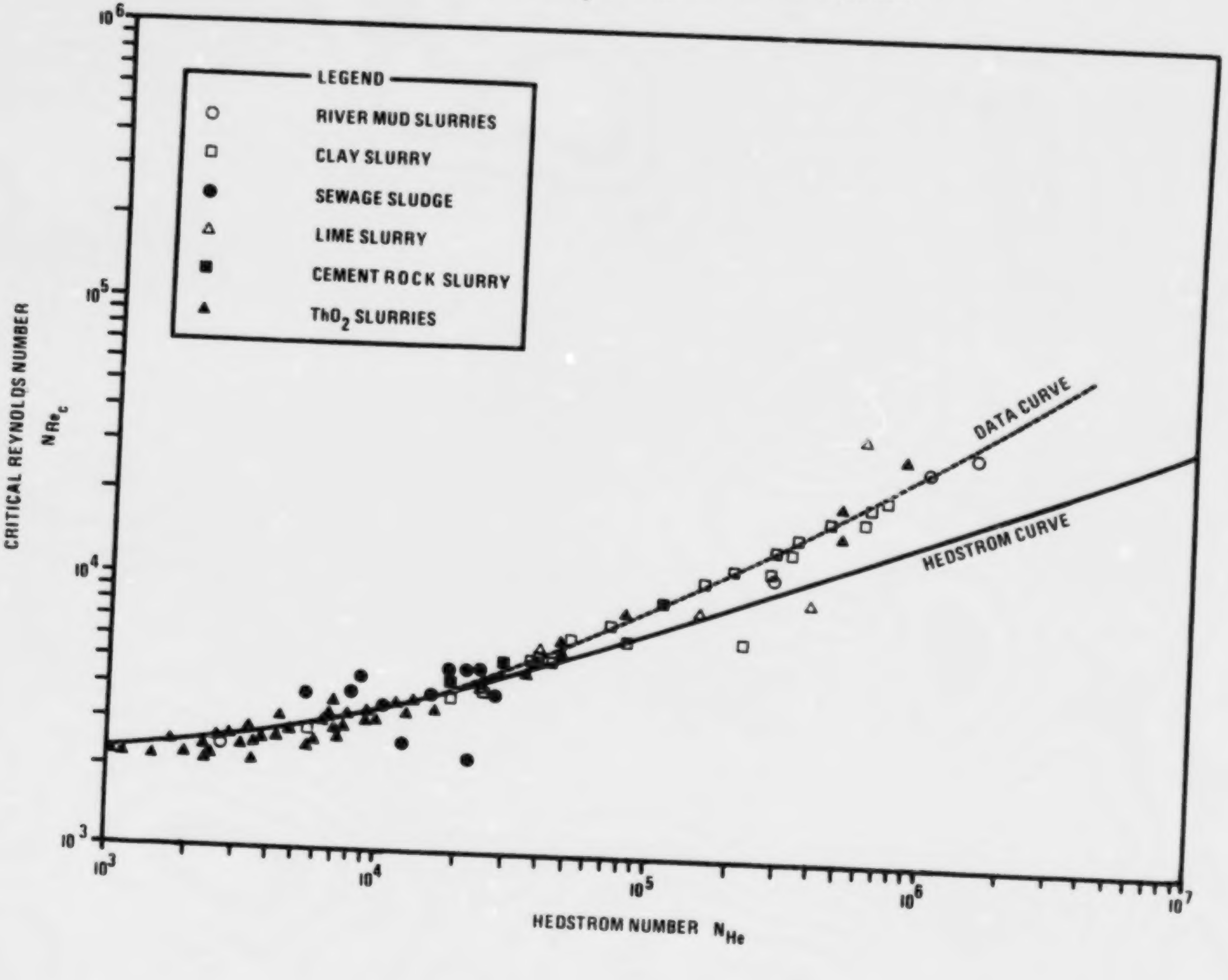

For a power law fluid the approach for ascertaining the head loss depends on the type of rheological data available. If the data from a capillary tube viscometer are available, the procedure is rather simple. Mooney (Ref. 20) has shown that in the laminar regime the relationship between the shear stress at the wall of a pipe or tube, $\Delta p D/4L$, and the term $(8V/D)$ is independent of diameter of the tube. Behn (Ref. 21) has shown that this is also true for sludges. Therefore, data from a capillary tube viscometer can directly be extrapolated to larger pipes. It is important to be careful that extrapolation is made in the range of $(8V/D)$ of the viscometer's data.

However, if only data from a rotational viscometer are available, that is to say, if one has only the rheological relationship expressed in equation (2) or its equivalent, then the answer may be found by integration of equation (2) as suggested by Rankin (Ref. 22).

$$\Delta P = 4K \left(\frac{6n + 2}{n}\right)^n \frac{V^n L}{D^n + 1} \qquad (9)$$

A somewhat more general approach has been suggested by Metzner and Reed (Ref. 23) who showed that the Fanning friction factor can be rigorously related to a generalized Reynolds Number, N^*_{Re} in the following manner:

$$f = 16/N^*_{Re} \qquad (10)$$

where N^*_{Re} is defined as:

$$N^*_{Re} = \frac{DV\rho}{\mu\,\mathrm{eff}} \qquad (11)$$

where μ_{eff} is the effective viscosity at a given wall shear. Now μ_{eff} is, by definition, $\tau_w/(8V/D)$, which can be rewritten as:

$$\mu_{eff} = K^* \left(\frac{8V}{D}\right)^{n^* - 1} \qquad (12)$$

hence:

$$N^*_{Re} = \frac{D^{n^*} V^{(2-n)} \rho}{g_c K^* 8^{(n^* - 1)}} \qquad (13)$$

For most fluids of practical importance n* and K* are related to K and n of equation (1) as follows: (Ref. 23).

$$n^* = n \qquad (14)$$

$$K^* = K\left(\frac{3n^* + 1}{4n^*}\right)^{n^*} \qquad (15)$$

It is obvious that once K and n are known through equations (10), (13), (14), and (15) head loss can be calculated.

3.1.2.2 Turbulent Flow of Non-Newtonian Suspensions: Friction Factor. A literature survey clearly indicates that a universally acceptable technique for accurately predicting the head losses of turbulent flows of non-Newtonian suspensions and fluids in pipes does not exist. All available correlations are completely empirical or do not refer to the basic nature of turbulent flow and are based on limited data. At the present time, the standard Newtonian relationship between the Reynolds number, N_{Re}, and the friction factor, f, is used to design pipelines conveying non-Newtonian fluids. The difficulty arises in the calculation of N_{Re}, because for non-Newtonian fluids viscosity is a function of shear rate. The primary task has been to define a constant viscosity known as the "apparent viscosity."

As early as 1941, Caldwell and Babbitt (Ref. 24) studied the flow of muds, sludges, and suspensions in circular pipes and concluded that in the turbulent regime the head loss can be predicted from the conventional Newtonian friction factor and the Reynolds Number relationship if the density of the slurry and a proper viscosity defined under laminar conditions as:

$$\mu = (g \ \tau_w D)/8V \tag{16}$$

is used, where g is acceleration of gravity in ft/sec^2.

Alves, Boucher, and Pigford (Ref. 25) who experimented with titanium-dioxide slurries; Whilhelm, Wroughton, and Loeffel (Ref. 26) who studied ground cement rock suspension flow; and Winding, Baumann and Krainch (Ref. 27) who worked with synthetic latices of the GR-S type; and others (Refs. 28 and 29) suggested use of a somewhat different viscosity, i.e., limiting viscosity at infinite shear, μ_∞. They reported that the plot of f versus N_{Re} correlates well for turbulent pseudoplastic data if μ_∞ is used. Bogue (Ref. 30) pointed out that Ward had indicated the limitation of μ_∞ by noting that it may become a somewhat nebulous quantity to measure. The concept of μ_∞ was extended by Weltman (Ref. 31), Hedstrom (Ref. 18), Wang (Ref. 32), and Thomas (Refs. 33 and 34) to Bingham plastic fluids (Thomas experimented with thorium oxide suspensions).

Alves, et al. (Ref. 25), and Binder and Busher (Ref. 35) suggested the use of turbulent viscosity, μ_t. Evaluation of μ_t requires the turbulent pressure drop and flow rate data and the result is usually higher for slurries than the viscosity of the conveying fluid. Alves, et al. (Ref. 25) reported an accuracy of 25 percent in pressure drop calculations if μ_t is used. Because μ_t is a function of pipe size and shear rate, pilot plant data are necessary for scale up and design.

According to Dodge (Ref. 36), Ito redefined both friction factor and Reynolds Number and on the basis of data collected on clay suspensions claimed a unique relationship for these values in the turbulent regime. Dodge also indicated the inconsistency of Ito's conclusion.

Metzner and Reed (Ref. 23) used the ordinary Fanning friction factor but defined a generalized Reynolds Number in the form of equation (14). They plotted most of the data available in the literature at low or intermediate shear rates in the form of f versus N_{Re}^* and found that the end of the laminar flow occurs at about 2100 to 2300 and is followed by a very broad transition region extending to $N_{Re}^* = 70,000$. Few data were avilable for N_{Re}^* exceeding 70,000. Metzner and Reed recommended as a conservative measure that the usual Newtonian turbulent curve should be used for design. Most of the conclusions were based essentially upon the small amount of data available in the turbulent regime. On the basis of dimensional analysis, Bird (Ref. 37), confirmed the results obtained by Metzner and Reed for laminar flow but cast some doubt on the validity of assuming a power law model in the turbulent regime. Dodge (Ref. 36) presented a critical examination of the work of Metzner and Reed (Ref. 23) and showed that the flow behavior index n* used in their correlation was incorrect for a very significant fraction of their transition and turbulent points. Dodge suggested the possibility that most of the fluids involved were changing from non-Newtonian to Newtonian at the shear stresses prevalent in the apparent transition region, and this rheological change was responsible for the constancy of the friction factor for Reynolds Numbers exceeding 2100.

An analytical study of the true non-Newtonian systems in the turbulent regime was undertaken by Dodge and Metzner (Ref. 38) who began with dimensional analysis and employed the general method that was first used by Millikan (Ref. 39). From these studies they developed the following friction factor/Reynolds Number relationships:

$$\sqrt{\frac{1}{f}} = A_m \log \left[N^*_{Re} \, f^{(2-n^*)/2} \right] + C_m \qquad (17)$$

where A_m and C_m are unknown constants. Since in the derivation of equation (3) reference was not made to the basic nature of turbulence and the physical mechanism of the flow, constants A_m and C_m cannot be obtained solely on the basis of theoretical considerations. These investigators measured friction factors for clay suspensions and aqueous solutions of carboxymethylcellulose (CMC) and carbopol. Based on their data, they evaluated A_m and C_m and found that equation (3) described the data fairly well.

Simultaneously with the work of Dodge and Metzner, an experimental paper was published by Shaver and Merrill (Ref. 40). From data of dilute aqueous solution of CMC, alginate, carbopol, and polyisobutylene in cyclohexane, they found that the friction factor and a pseudoplastic Reynolds Number defined as:

$$N_{Re}'' = \left[\frac{D^n \gamma^{2-n} \rho}{K}\right] \frac{8}{\left[2\,(3 + 1/n)\right]^n} \qquad (18)$$

may be correlated by equation

$$f = \frac{0.079}{n^5 N_{Re}'' \gamma} \qquad (19)$$

where $\gamma = \frac{2.63}{(10.5)^n}$. They found that in turbulent flow the relationship between f and N_{Re}'' consists of a family of curves with each curve depending on n (flow behavior index) in such a way that the friction factor decreases with decreasing n at a given N_{Re}''. The use of equation (4) and (5) is restricted for $n>0.40$.

Thomas (Refs. 33, 34, 41, 42, 43, 44) undertook a comprehensive review of the knowledge available in the area of non-Newtonian suspensions and fluids. In one of his papers (Ref. 44), he reported the turbulent flow friction factors for flocculated suspensions of thoria, kaolin, and titania (their shear rate/shear stress data may be correlated with the Bingham plastic model). In all cases the friction factors were less than for Newtonian fluids. The departure from Newtonian friction factors was attributed to the thickening of the laminar sublayer due to non-Newtonian characteristics. For yield stress less than 0.5 lb_f/ft^2, the friction factor tended to approach Newtonian values as the Reynolds Number was increased.

In contrast to this, for values of yield stress more than 0.5, the friction factor tended to diverge from Newtonian values. Both sets of data were correlated with the Blasius-type relation which states that

$$f = BN_{Re}^{-b} \tag{20}$$

where N_{Re} is defined as $\frac{DV\rho}{\eta}$ and according to Thomas:

$$B = 0.079 \left[\left(\frac{\mu}{\eta} \right)^{0.48} + \left(\frac{g_c \rho \tau_o (6 \times 10^{-6})}{\mu^2} \right)^2 \right] \tag{21}$$

$$b = 0.025 \left[\left(\frac{\mu}{\eta} \right)^{0.15} + \left(\frac{g_c \rho \tau_o (6 \times 10^{-6})}{\mu^2} \right)^2 \right] \tag{22}$$

and μ is the viscosity of conveying liquid.

Another recent paper is by Eissenberg (Ref. 45) who measured and correlated turbulent friction factors of thoria suspensions at elevated temperatures. The correlation is based on wall shear stress viscosity defined by Bogue and Metzner (Ref. 46).

A different approach from those mentioned above is taken by Murthy and Zandi (Ref. 47). The key to their analysis, for the evaluation of head loss, is the ability to predict, accurately, the velocity profile. The velocity profile equation in combination with the equation of material balance provides the necessary instruments for the predictions of the head loss for turbulent flow of an Ostwald-deWaele suspension in a pipe. Starting with the Navier-Stokes equation, Murthy and Zandi developed two relationships which permit one, a priori, to evaluate velocity profiles and head losses in a smooth pipe from the knowledge of pipe diameters, mean velocities, and properties of the suspensions.

3.2 OPERABILITY

In recent years, the feasibility of pipeline transportation of solids has been demonstrated on commercial installations throughout the world. Although the concept is not new, short lines having been in use since early this century, it is only in the last 20 years that long distance transportation of solids in pipelines has become an industrial reality.

Table 3-1 is a summary of long distance slurry pipelines which have been built in recent years.

In any slurry pipeline, the main concern from an operations standpoint is that the line can be easily restarted following a shutdown. Although for certain materials, such as digested sludge, no such problem exists, it can be readily seen that in a particulate system, such as coal slurry, the possibility of depositing a tightly packed bed in the pipeline could have serious consequences.

Laboratory tests on equilibrium settled slurries and actual pipeline testing can provide the information by which the operability characteristics of a given slurry can be accurately evaluated. In

Table 3-1

SUMMARY OF COMMERCIA

	Location	Material	Length (miles)	Diam (inc
Consolidation Coal	Ohio	Coal	108	10
American Gilsonite	Utah	Gilsonite	72	6
Rugby Cement	England	Limestone	57	10
Columbia Cement	Columbia	Limestone	9.2	5
South African Companies	South Africa	Gold Tailings	21.5	6 &
Savage River Mines	Tasmania	Iron Concentrate	54	9
Black Mesa Pipeline, Inc.	Arizona	Coal	273	18
Hyperion Wastewater Treatment Plant	Los Angeles	Digested Sewage Sludge	7.5	22
Mogden Wastewater Treatment Plant	England	Digested Sewage Sludge	7	12
Easterly Pollution Control Center	Cleveland	Raw Sewage	13	12

*Commercial operation ceased in 1963 for non-technical reasons
Now maintained in standby condition

A

Table 3-1

F COMMERCIAL SLURRY PIPELINES

gth es)	Diameter (inches)	Throughput (million tons per year)	Solids Specific Gravity	Weight (percent solids)	Years in Operation or Status
	10	1.30	1.40	52	6 *
	6	0.38	1.05	46	11
	10	0.70	2.70	61	5
	5	0.35	2.70	55	25
	6 & 9	1.05	2.70	50	14
	9	2.25	4.90	60	2
	18	5.70	1.40	50	Under Construction
	22	--	1.80	1.0	11
	12	--	1.80	4.0	33
	12	--	1.80	3.0	32

1

B

general, slurries with relatively fine solids tend to be rather fluid in the settled condition, and present little problem on start-up, whereas coarse solids tend to pack in the settled condition. It is not uncommon that the design size consist of solids in a pipeline is dictated, not from process or product requirements, but from the hydraulic standpoint in order to achieve an operable balance between fine and coarse constituents.

The successful pipeline operation of slurries as widely differing as coal and iron ore (Ref. 58) is testimony as to the state of the art concerning these problems.

The pipelining of digested sludge could present problems that are not normally encountered in solids pipelines.

The generation of methane gas due to continued digestion in transit through the line should be considered in any design. Operating experience available at this time is limited to relatively short lines, using only one pump station. One such line, a 7-mile outfall line from Hyperion Treatment Plant in Los Angeles, has encountered no problems regarding gas generation in the line (Ref. 50). However, it is conceivable that a long distance line with many pumping stations could experience difficulties in this regard, especially on shutdown. Simple precautions, such as installing degassification chambers at the pump suction, will alleviate problems due to gas.

The build-up of deposits on the inner pipewall has been experienced at the Los Angeles plant. The nature of these deposits is not fully known but they could consist of grease and chemical deposits such as urate crystals. The occasional pigging of the line has successfully removed this build-up. It is reported that pipelines transporting raw sludge (Refs. 51 and 52) have considerable deposits of grease in the line but, again, pigging is an adequate solution to the problem. Since most of the grease is removed prior to the digestion process, this is not a major consideration for a digested sludge pipeline, but the facility for pigging the line should be included in any installation, so that deposits of a biological or chemical nature (such as urate crystals) can be removed from the pipe wall.

3.3 CORROSION AND EROSION

In order to ensure that a pipeline will be operable for the whole span of its projected lifetime, it is necessary that the degree of corrosion be established, so that allowances can be included to account for any such metal loss.

Obviously, the degree of corrosion is a function of pipe material, soil conditions, and the slurry characteristics. Corrosion of the exterior surface can be controlled reasonably well by application of a suitable coating and a cathodic protection rectifier system. Internal corrosion, however, may be serious if proper precautions are not taken. Experience with commercial pipelines indicates that internal corrosion is rather severe in the initial part of the pipeline without protective measures. This initial corrosion appears to be due to oxygen. Once oxygen is depleted the corrosion still continues but at much lower rates. In most cases a combination of pH control and addition of a suitable inhibitor will prevent excessive initial corrosion. Swan, et al. (Ref. 53) reported the experimental work conducted on the Cadiz pipeline where a proper inhibitor system was selected and its effectiveness in the pipeline was determined. The laboratory experiment showed that both sodium dichromate and sodium sulfite should provide protection. However, although the field test proved the effectiveness of sodium dichromate (approximately 20 ppm Cr^{+6} at a cost of 1.5¢/ton), it also showed the ineffectiveness of a sulfite-phosphate mixture. Normally, chromates increase the tendency to pitting which can be countered by addition of sodium hexametaphosphate. This addition proved unnecessary in the Cadiz line. Table 3-2 shows the effect of an inhibitor on corrosion rate and indicates that with no inhibitor the initial corrosion would be serious. The quantity of inhibitor used is a matter of economics. It should be established whether it is less expensive to prevent corrosion or to increase the thickness of the pipeline. Table 3-2 also shows that the actual corrosion rates observed in the Cadiz line were successfully duplicated by the use of a laboratory test procedure. This procedure (as discussed in Section 6.1) was used to establish the corrosion/erosion characteristics of the fly ash and digested sludge used in this study.

Table 3-2

LABORATORY CORROSION/ EROSION RATES VERSUS FULL SCALE PIPELINE TEST RESULTS (Ref. 57)

Inhibitor	Position (miles down pipeline)	Corrosion/Erosion Rate (mils/year) Pipeline	Corrosion/Erosion Rate (mils/year) Laboratory
None	0	114	105
133 ppm Na_2SO_3 & 45 ppm hexametaphosphate	0	54	50
17 ppm Cr^{+6} and 48 ppm hexametaphosphate	0	2.2	2.4
34 ppm Cr^{+6} and 90 ppm hexametaphosphate	0	1.0	1.0
	30	1.2	1.1
	60	2.9	1.4
20 ppm Cr^{+6}	0	0.8	1.9
	30	1.4	2.4
	60	3.8	2.8
	108	3.5	2.8

A very encouraging observation during the operation of the Cadiz line was that at no time was significant corrosion observed in the test installation on the basis of weight loss and micrometer data or in the line itself by visual observation. According to Swan, et al. (Ref. 53), after more than 5 years of continuous operation, machine grooves in flanges still were clearly visible.

Erosion was at no time a significant factor in the Cadiz pipeline. Apparently this was due to a proper combination of particle size and particle shape. Erosion, however, could be very serious whenever the particles are abrasive and have sharp edges. The problem is more acute in bends and fittings where the shock wear may be pronounced. Abnormal wear is sometimes found at the pipe flanges and at the bottom of the pipe. According to Condolios and Chapus, (Ref. 61) both friction wear and shock wear vary approximately with the cube of the velocity of the system; therefore, the mean velocity of the flow should be kept within reasonable limits (normally 4 to 6 ft/sec) to minimize wear.

Bain (Ref. 54) discussed a program of research for the purpose of assessing the relative erosion characteristics of different combinations of pipe material, flow regimes, water chemistry, and coal type. The results of this work are not yet published but they should provide extremely useful information. Smith and Wasp (Ref. 55) suggest that mean velocities must be kept below 9 to 10 ft/sec in order to permit the protective film formed by an inhibitor to remain on the pipe wall.

Montgomery, Craytown and Girdwood (Ref. 56) have observed that the wear of pipe associated with hydraulic back fill is very small. Beatz (Ref. 56) claims that in such a system the greatest wear has been observed to occur on the side of the pipe, but this is probably due to the existence of a static or slow moving bed which would tend to protect the bottom of the pipe from turbulent erosion.

In general, it appears that most designers of slurry pipelines after construction and operation of their system have been pleasantly surprised at the actual level of erosion and corrosion of pipe.

3.4 MECHANICAL EQUIPMENT

Pumps

The oil industry had long been involved in pumping slurries in the oil fields, in the form of drilling mud. Because of the high pressure requirements (up to 5,000 psi) extreme conditions (such as heavy abrasion due to sand trapped in the mud), and the need for reliability, satisfactory pump designs evolved.

The Ohio Coal Pipeline investigated piston and plunger types (see Figure 3.4 and 3.5) which are both used in the oil fields. Consolidation Coal elected to use piston-type pumps with an approximate discharge pressure of 1100 psi on their 108 mile coal pipeline. Free pyrites made the abrasion fairly severe. Initially, the valve insert life was about 30 hrs. The insert was originally made of composition rubber, but the eventual use of polyurethane inserts provided an insert life of 1200 hrs.

The Black Mesa coal pipeline in Arizona (Ref. 64) will utilize a newer version of this piston pump which has a capability of 1600 psi

EXHIBIT 3.4

SCHEMATIC OF PISTON PUMP – FLUID END

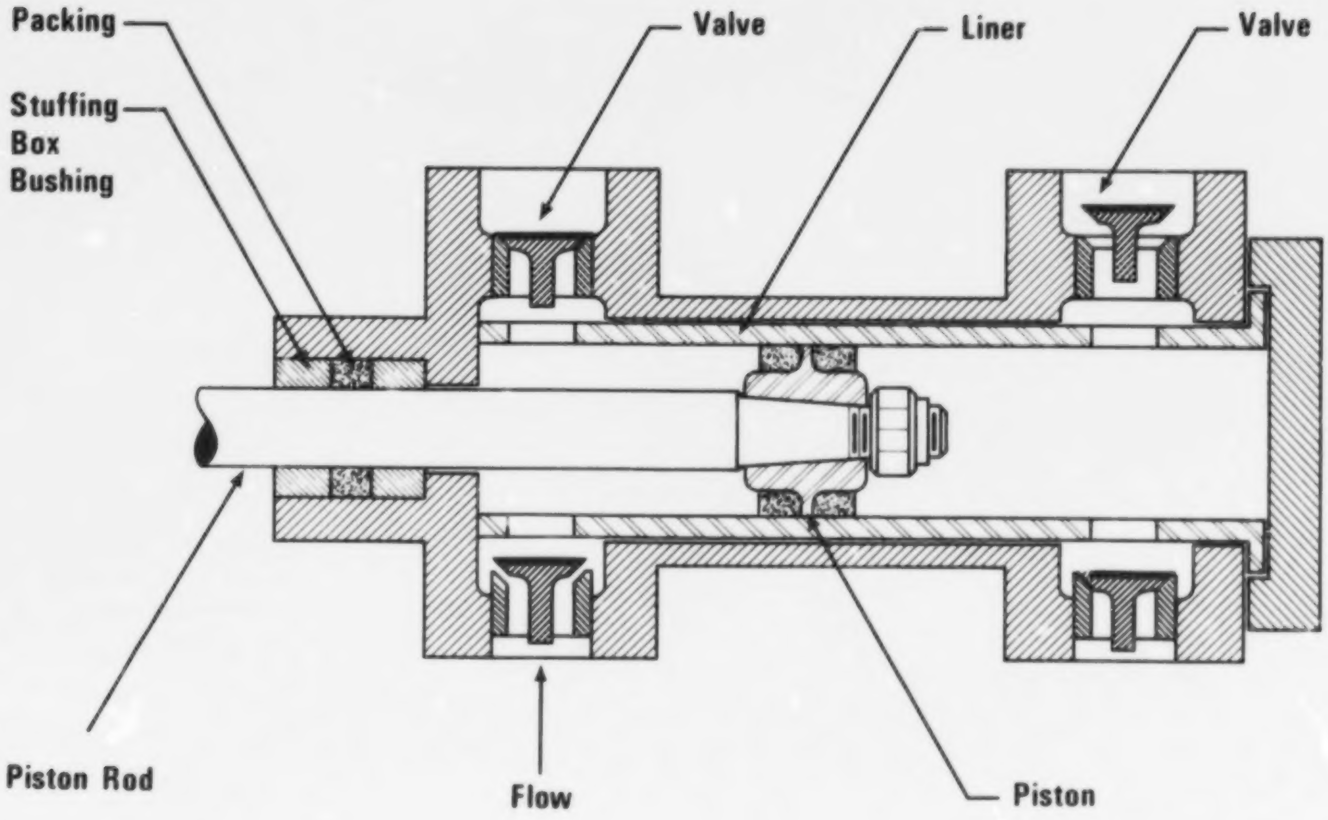
Packing
Stuffing Box Bushing
Valve
Liner
Valve
Piston Rod
Flow
Piston

EXHIBIT 3.5

SCHEMATIC OF PLUNGER PUMP - FLUID END

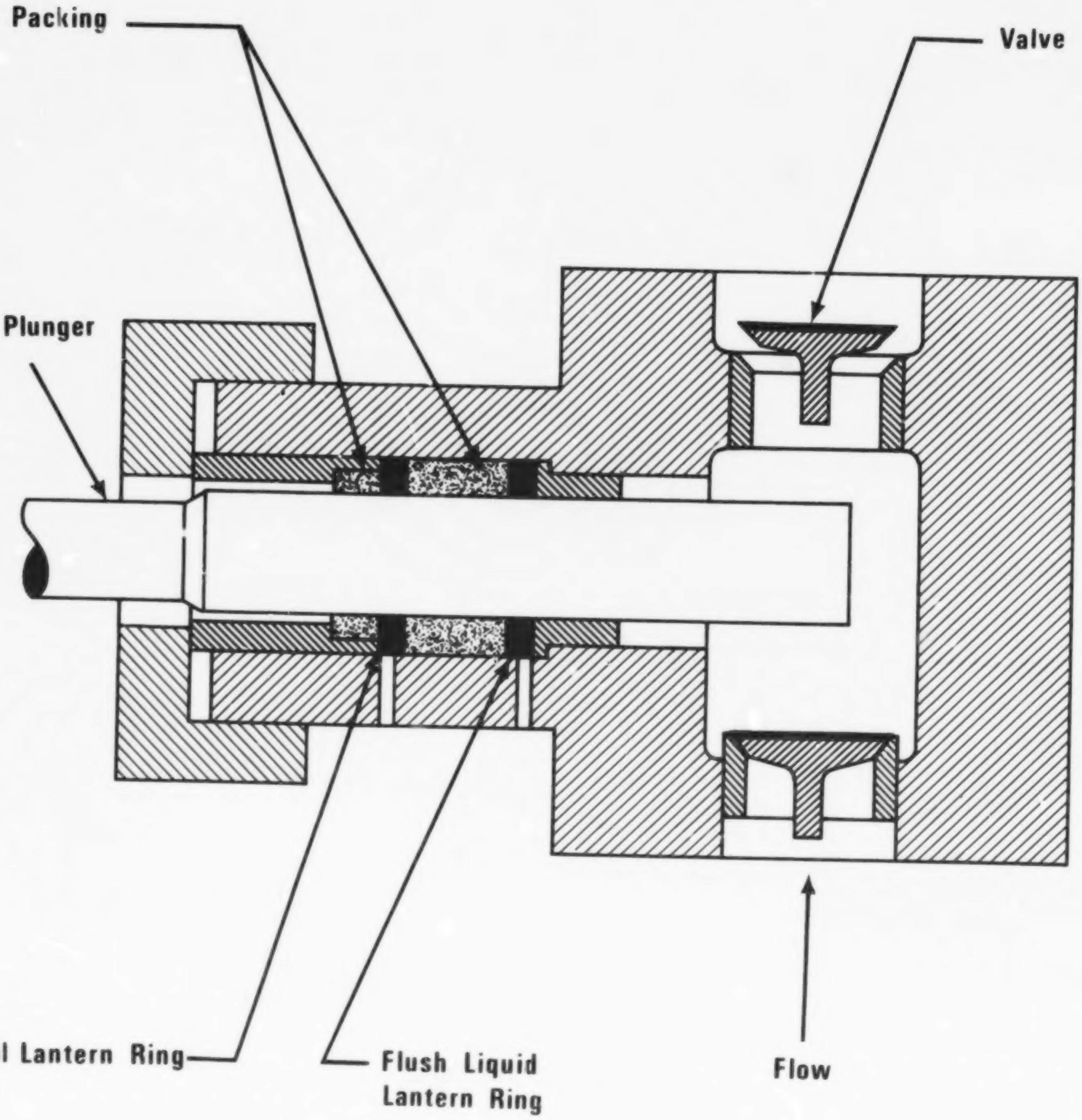
Packing
Valve
Plunger
Oil Lantern Ring
Flush Liquid Lantern Ring
Flow

discharge pressure and 1400 gpm (1750 hp).

The choice of piston versus plunger type pump largely depends on the abrasiveness of the slurry to be pumped. Highly abrasive slurries such a magnetite require installation of plunger-type pumping units so as to obtain a longer service life of displacing member. Piston pumps are the more common of the two and are used in the majority of long distance slurry pipelines; they are available is sizes up to 1750 HP. By comparison, the plunger-type pumps are only available up to 560 HP. The main wearing parts in the piston pump are pistons, liners, valves and valve seats. In the plunger pump the wearing parts are plunger sleeves, packing lantern rings, bushings, valves and valve seats. The actual part life depends upon abrasiveness of the slurry, piston or plunger speed and discharge pressure. High pressure pump tests, using an actual slurry sample, can be performed to estimate part life. As the number of commercial slurry pipelines increases, more data, based on operating experience, will become available.

Centrifugal pumps have been successfully applied to pumping slurries in the mining field. In general, the pumps are limited to a low head capability of up to 110 feet of slurry. They are lined with rubber, hard steel or other wear resisting material and their efficiency is low, but within these limitations they are an excellent means of moving material in process. For longer distance pumping, such as in mine tailings lines where distances are limited to about 3 to 4 miles, it is necessary to connect the units in series either in one pump station or as booster pumps spaced along the line. Each pump in the series develops between 80 to 110 feet of slurry head. Some commercial installations have up to 7 pumps in a series in one pump station, the pumps in these installations have heavy type casing to withstand higher total discharge pressure (up to 500 psi).

Valves

Depending upon the system pressure, there is a range of valve types which are suitable for slurry service. For low pressure service (up to 150 lb. ASA), the choice of valve depends on the abrasiveness of the slurry. Gate-type valves are not satisfactory in an abrasive environment but rubber sleeve pinch valves, plug valves, jacket-type sleeve valves, and ball valves are acceptable. These types of valves are generally used in the suction piping of any high pressure pumping installation. High pressure valves are limited to ball and plug-type valves of similar type used in commercial long distance oil and gas pipelines. These types have proven themselves to be reliable in the Ohio Coal pipeline. The choice of these valves rests primarily on the fact that there are no places in the flow passage where solids may become trapped which would hinder the operation and/or sealing ability of the valve. Their smooth continuous interior also prevents localized erosion from occuring.

Tanks & Agitators

Slurry storage tanks differ only slightly from normal oil storage tanks. This difference stems from the need to keep the soild phase of the slurry in suspension during storage. Also, the tank and agitator design must achieve the required turbulence at minimum cost. Slurry storage tanks with a capacity of 480,000 U.S. gallons (approx. 11,500 barrels) are used in Tasmania where the solids specific gravity is five times that of water. These tanks based on a similar design used with the Ohio Coal pipeline, will be dwarfed by the 4,000,000 U.S. gallon capacity (95,000 barrels) tanks to be utilized in conjunction with the Arizona Coal pipeline.

Automation

According to Koch (Ref. 62) practically all present pipeline installations - some with as many as six substations - are operated by remote control. Smith and Wasp (Ref. 55) feel that the independence of pipeline from inflationary labor cost is one of the major assets of this mode of transportation. Halvorsen (Ref. 63) on the basis of one year of trouble free operation of Cadiz, reports that the operation of slurry pipeline can be accomplished with the same push button ease characterizing oil and gas pipelines. Equipping the Cadiz pipeline for remote control permitted a single plant operator to operate the entire line in addition to running the slurry preparation plant which screened, dewatered, crushed, and blended the slurry.

Section 4

DESCRIPTION AND DISCUSSION OF DESIGN PROCEDURE

This section describes and discusses the use of the design procedure recommended by this study.

As previously stated, a homogeneous model describes the behavior of fly ash, digested sludge, and fly ash/sludge mixtures flowing in pipes. The use of this model as a hydraulic design procedure involves the following steps:

1. Approximate "effective" values of the coefficient of rigidity (η) and the yield stress (τ_o) of the subject material should be established by means of laboratory viscometry measurements for the range of shear stresses to be encountered commercially.

2. The critical velocity for the system may be calculated from the rheology data using the Hedstrom procedure described in Section 3.

3. For any pipe velocity greater than the Hedstrom critical velocity (i.e., for any velocity in the turbulent regime), a Reynolds Number is calculated as follows:

$$N_{Re} = \frac{DV\rho}{\eta}$$

4. From standard friction factor/Reynolds Number charts, the Fanning friction factor for the given Reynolds Number and pipe roughness can now be found.

5. Hence, pipe friction losses can be calculated from the Fanning friction factor, which is defined as:

$$f = (\Delta p \ D/4 L) / (\rho V^2 / 2g_c)$$

The homogeneous model assumes that a constant viscosity exists in the turbulent regime, and that this constant viscosity is equal to the coefficient of rigidity of the material.

Investigators in the field of slurry hydraulics tend to attempt the determination of the "correct" rheological model that will predict turbulent as well as laminar friction losses. As discussed in Section 3, the question of the "correct" viscosity has been the subject of considerable controversy and many well-known correlation procedures employ viscosities that have no physical significance in turbulent flow. However, when the aims in selecting a rheological model are clearly defined, this question is of academic importance only. It must be appreciated that there is no unique fitting of a model to a given set of data. An infinite number of functions can be fitted to any given set of rheological data, and the successful projection of any one of these functions to predict laminar or turbulent friction losses in pipes, in effect, only defines a "necessary" condition that is the correct function. It is not a "sufficient" condition.

This study takes a practical approach to the question of the correct viscosity to be used, in that it ascertains whether or not the rheological data were obtained in the same shear stress range over which the pipeline will operate. The greatest fallacy which can be committed with any rheological model is to use it to extrapolate a shear stress/shear rate relationship to a value higher than the range covered by the rheological data. Avoidance of this error should be considered a fundamental axiom in slurry work. There is no a priori reason why viscosities measured in the laminar flow field should be the same viscosities that exist in turbulent field since the actual shear stresses which exist in a turbulent pipe flow are unknown. However, Oldroyd (Ref. 29) and others have established that slurry systems usually exhibit a limiting viscosity at high shear rates. More recently, the work of Thomas (Ref. 43) and Eissenberg (Ref. 45) has demonstrated the usefulness of this viscosity.

Eissenberg (Ref. 45) has made a significant but simple observation in this connection. For thoria slurries, which exhibit Bingham plastic characteristics, Eissenberg was able to show two important facts: the first is that the coefficient of rigidity of the Bingham plastic became the viscosity of the Newtonian slurry when the yield structure was destroyed by the addition of a powerful dispersant; the second is that this Newtonian viscosity obtained after the yield structure was destroyed gave good correlation of the data.

The implied result of Eissenberg's findings is, therefore, that the yield structure of the slurry is destroyed in the turbulent field; hence, the viscosity of the slurry is the coefficient of rigidity.

In order to emphasize the basis for the use of the coefficient of rigidity to correlate turbulent data, reference is made to Figures 9-1 and 9-4. Figure 9-1 is a rheological curve for a sludge/fly ash mixture which exhibits a linear response of shear stress with rate of shearing strain. The constant viscosity here is, of course, the coefficient of rigidity of this material. Figure 9-4 shows the friction loss/velocity data for the same material flowing in 12-inch and 16-inch diameter pipes.

The line drawn on the turbulent flow data points is the prediction of the turbulent friction losses for the system, using the constant viscosity (obtained from Figure 9-1) in conjunction with the design procedure outlined above. The predicted line is in excellent agreement with the measured data for a velocity range of 2.3 to 9.0 feet per second, which encompasses a change of more than a decade in pipe-wall shear stress (0.032 to 0.380 lb_f/ft^2). The close agreement of the measured data and the predicted head loss shows that the two viscosities (i.e., the coefficient of rigidity and the effective turbulent pipe viscosity) are the same.

A final point should be made here regarding the treatment of rotational viscometry data, such as are shown in Figure 9-1. It will be noted that at the lower shear rates (0 to 100 $\sec^{-1}$), the data tend to dip below the linear response exhibited at higher shears. (This effect is shown more clearly in data given in Sections 7.2 and 8.2.) This curvature of the data is partly due to the geometry of the measuring system. The definition of viscosity, i.e.,

$$\mu = \frac{\text{shear stress}}{\text{rate of shearing strain}}$$

is formulated as the basis of flow between parallel plates. The conversion of this to the integrated form, applicable to a Couette-type viscometer, involves a logarithmic expression in terms of the cup radius (R_c) and the spindle radius (R_s). This accounts for the curvature of the data curve.

Since the deviation of the data occurs outside the range of shears of commercial interest, it in no way affects the choice of coefficient of rigidity. However, in evaluating the yield stress of the material, a correction must be applied as follows: Extrapolation of the straight portion of the curve to the vertical axis gives an accurately determined point. This is then corrected down to the true yield value by the factor K, where

$$K = \frac{1 - \left(\frac{R_s}{R_c}\right)}{\ln\left(\frac{R_c}{R_s}\right)}$$

For the viscometer system used in this study, K is equal to 0.947.

Section 5

HYDRAULIC TEST EQUIPMENT

5.1 TEST PROCEDURES

The purpose of the test program, as stated previously, was to develop a procedure by which the friction losses for the pipe flow of waste materials could be predicted from basic laboratory data.

The procedure adopted involved the use of a large diameter pipe test loop, shown in Figure 5.1, and the laboratory equipment described in Section 6.0. The friction losses of a material flowing in the 12 and 16-inch pipes were measured by means of Dp cells, and samples of the material were taken directly from the pipe. The samples were tested in the laboratory for viscosity, yield stress and solids concentration. From these laboratory data, a prediction of the pipe friction loss was made, and the prediction was compared with the measured friction loss.

For each slurry tested, the test loop system was filled after sufficient agitation produced a uniform slurry in the mixer tank. All instruments were checked for zero readings. During the test runs the flow was adjusted to the desired rate, and the slurry was circulated through the loop until stable conditions were reached. Values of friction loss and system pressure and temperature were then recorded, and samples were obtained for laboratory analysis. The flow was then adjusted for the next data point. Table 5-1 is a list of tests performed in this program.

TABLE 5-1

LIST OF LARGE DIAMETER PIPE TESTS

Date	Run Number	Material	Percent Solids	Description
10/28/68	W-1-H	Water		Initial water run
11/1/68	DS-1-H	Sludge	3.5	Hydraulic run
11/2/68	FS-1-H	Fly Ash/Sludge	11.0	Hydraulic run
11/2/68	FS-2-H	Fly Ash/Sludge	22.0	Hydraulic run
11/4/68	FS-1-O	Fly Ash/Sludge	22.0	Start-up test
11/5/68	FS-3-H	Fly Ash/Sludge	38.0	Hydraulic run
11/14/68	W-2-H	Water		Check run
11/16/68	FW-1-H	Fly Ash Slurry	53.2	Hydraulic run
11/18/68	FW-1-O	Fly Ash Slurry	53.2	Start-up test
11/23/68	W-3-H	Water		Check run
11/24/68	DS-2-H	Sludge	3.0	Hydraulic run
11/24/68	DS-3-H	Sludge	2.5	Hydraulic run
11/26/68	W-4-H	Water		Check run
12/4/68	W-5-H	Water		Check run
12/5/68	FW-4-H	Fly Ash Slurry	57.4	Hydraulic run - velocity profiles taken.
12/7/68	FW-5-H	Fly Ash Slurry	55-58	Hydraulic run - with addition of Orzan AL-50.
12/8/68	W-6-H	Water		Check run

In order to obtain as wide a range of data as possible, similar tests were performed in a small (1/2-inch) pipe test system, as described later.

5.1.1 Sludge Tests

Digested sludge used in these tests was obtained from the Southerly Sewage Treatment Plant in Cleveland, Ohio. It was loaded via centrifugal pumps into 5500 gallon tank trailers and hauled by road approximately 105 miles to the test site. The rheology of the first shipment was closely checked before loading and after transit to the test site. No change was detected. At the test site it was unloaded directly into the mixer tank. Approximately 16,000 gallons were used for each test run. Two attempts to concentrate 16,000 gallons of sludge to a heavier solids concentration by settling failed. One batch was held for seven days, during which time very gentle agitation was applied intermittently in an attempt to settle the solids. The other batch was held approximately three days under quiescent conditions.

After the test runs, the sludge was disposed of upon land selected by the coal company. It was trucked from the test facility to the various dyked locations. Odor at these locations was negligible, even during or immediately after dumping.

5.1.2 Fly Ash Tests

Fly ash for these tests was obtained from electrostatic precipitators at the Sammis Plant of Ohio Edison Company, located at Sutton, Ohio. It was hauled to the test site and unloaded directly into the mixer tank by pneumatic trailers. The approximate weight of solids to the tank was checked by weighing the vehicle at various times during unloading. Final solids percentage was determined by laboratory analysis. The abrasive effect of the fly ash slurries and the resultant change in pipe roughness is discussed in detail in Appendix A.

5.2 TEST LOOP

A test loop containing 12-inch and 16-inch diameter pipe was made available for hydraulic tests in this study by Hanna Coal Company, a Division of Consolidation Coal Co. The loop is located at Cadiz, Ohio. Figure 5-1 is a schematic of the facilities and Table 5-2 is a list providing brief descriptions of the major components. The volume of the loop piping was 7,500 gallons.

Two centrifugal pumps were used during the test: a Hazelton 14-inch pump and a Morris 8-inch pump. Mechanical problems with the large pump necessitated its replacement midway through the tests with the 8-inch pump. Flushing seal water was required on the fly ash runs to protect the packing from the abrasive action of the fly ash.

In all cases, the test slurries were stored and circulated through a conical-bottom mixing tank. Water was also added at this point for dilution or flushing. The tank was agitated to ensure that the slurry was uniformly suspended.

A maximum flow of approximately 3500 gpm was available from either centrifugal pump. Velocity was controlled by manually adjusting a plug valve upstream of the sample splitter. A maximum velocity of 6.0 feet per second in the 16-inch loop and 10.0 feet per second in the 12-inch loop could be obtained. Sample points were located at the top and in the middle of the 12-inch and 16-inch lines, and at the sample splitter.

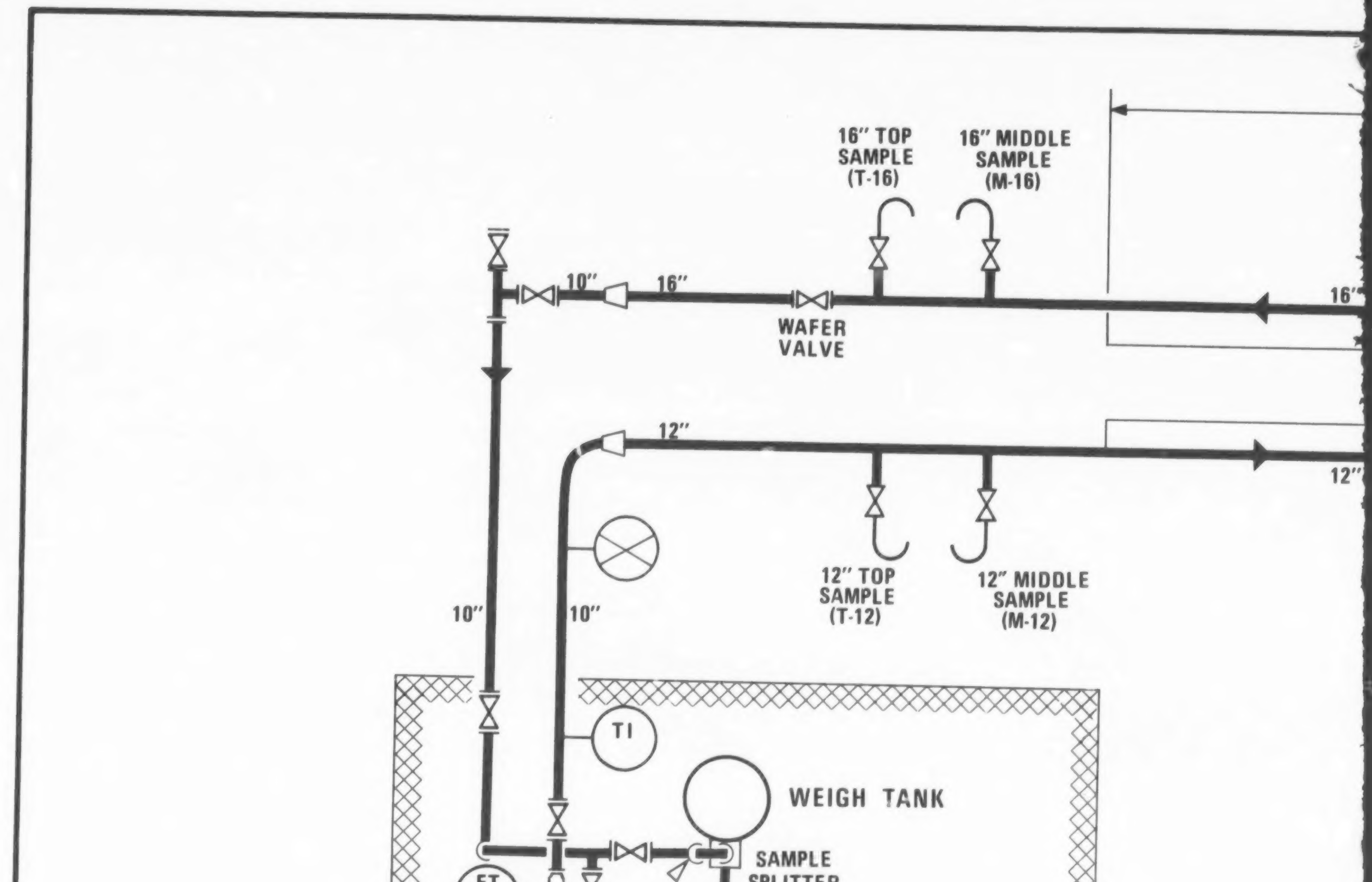
16" TOP
SAMPLE
(T-16)
16" MIDDLE
SAMPLE
(M-16)
10"
16"
WAFER
VALVE
16"
12"
12"
12" TOP
SAMPLE
(T-12)
12" MIDDLE
SAMPLE
(M-12)
10"
10"
TI
WEIGH TANK
SAMPLE
SPLITTER
FT
2" DRAIN
10"
TANK 3
24,000 GALS.
14"
TEST PUMP

A

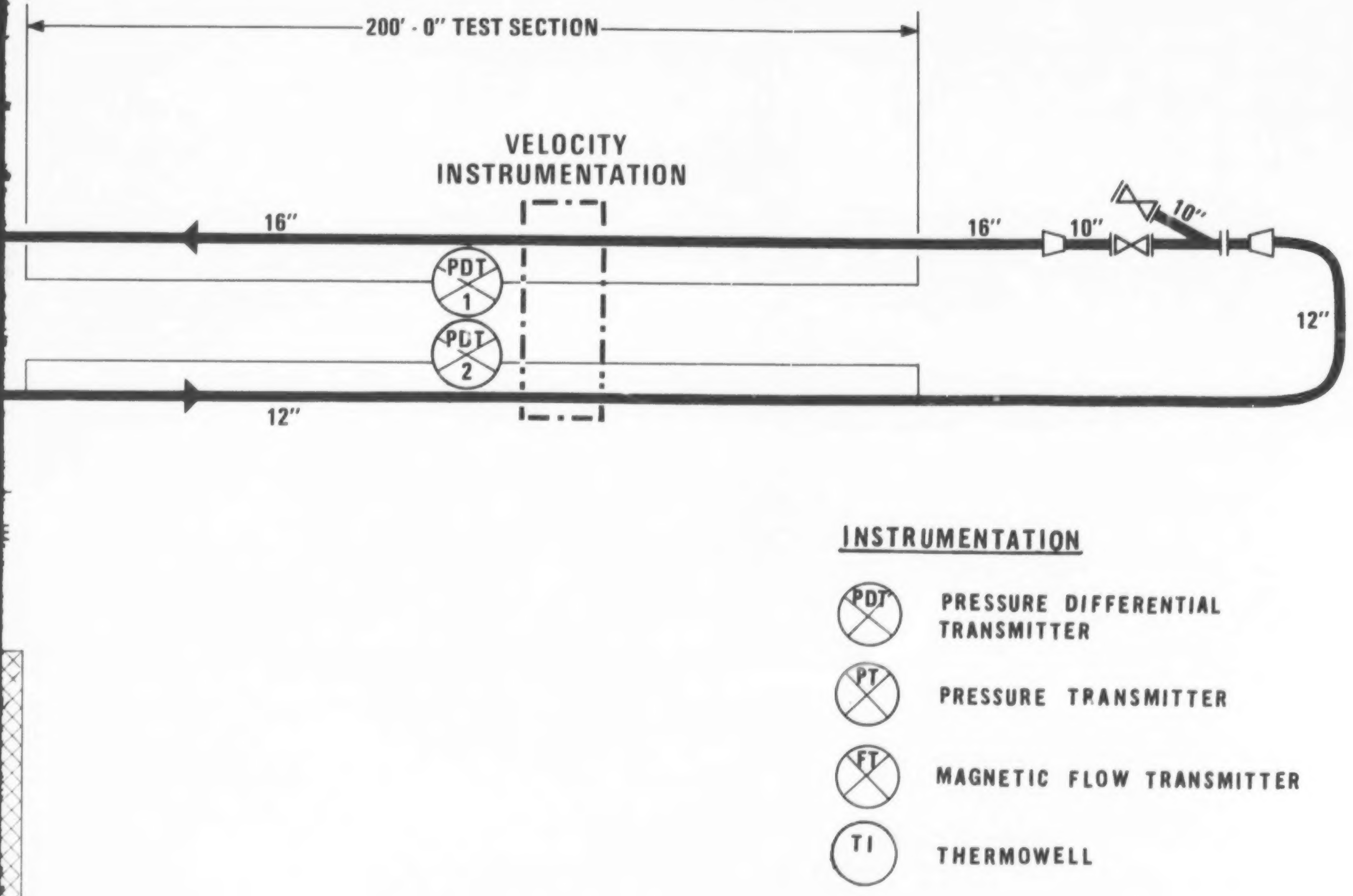
200' - 0" TEST SECTION
VELOCITY INSTRUMENTATION
16"
16"
10"
10"
12"
PDT 1
PDT 2
12"
INSTRUMENTATION
PDT
PRESSURE DIFFERENTIAL TRANSMITTER
PT
PRESSURE TRANSMITTER
FT
MAGNETIC FLOW TRANSMITTER
TI
THERMOWELL

FIGURE 5-1
WASTE MANAGEMENT STUDY
HYDRAULIC TEST PROGRAM

LARGE DIAMETER LOOP FLOW DIAGRAM

AT CADIZ, OHIO

B

FIGURE 5-2

WASTE MANAGEMENT STUDY HYDRAULIC TEST PROGRAM
SMALL PIPE TEST APPARATUS

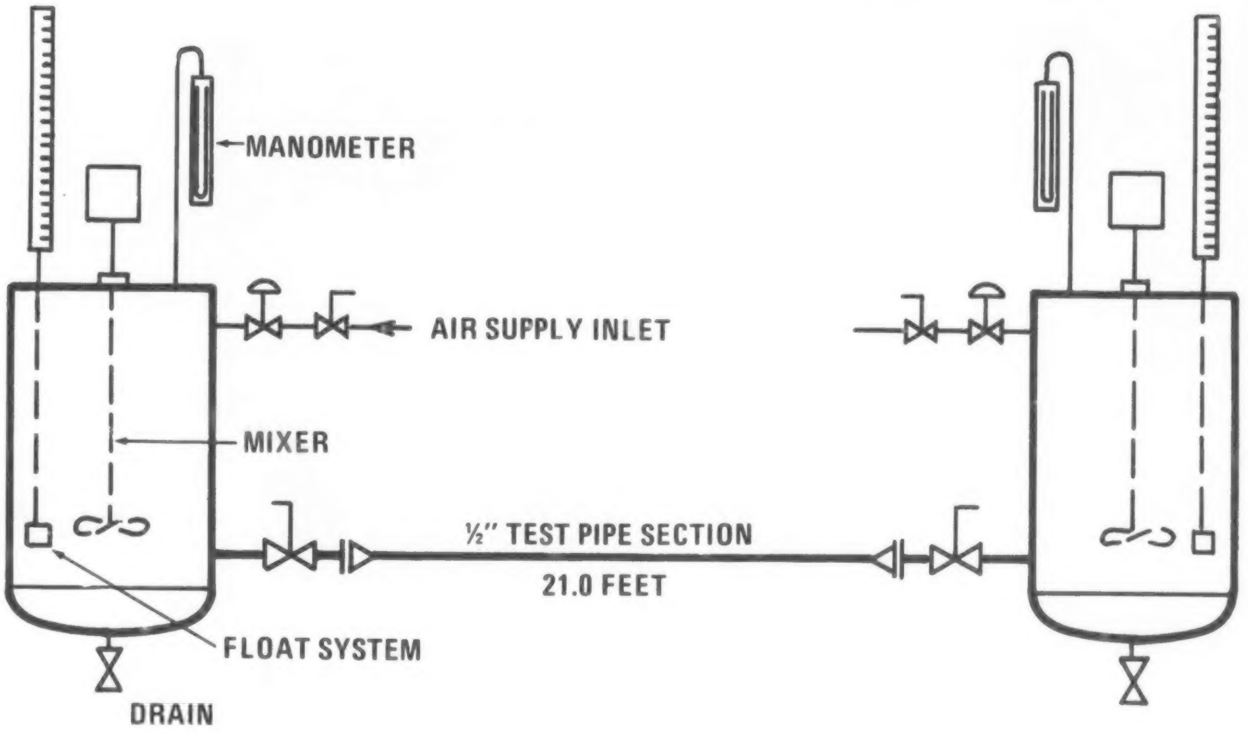
MANOMETER
AIR SUPPLY INLET
MIXER
½" TEST PIPE SECTION
21.0 FEET
FLOAT SYSTEM
DRAIN

CAPACITY (EACH VESSEL) = 20 GALLONS

TABLE 5-2
DESCRIPTION OF TEST EQUIPMENT

Item	Description
Pipe (test sections)	12.750 inch O.D. and 16.000 inch O.D. x 0.375 inch wall API 5L Grade B seamless.
Pump	14 inch Type CB Barrett Haentzens and Co. single stage centrifugal pump rated at 4500 gpm @ 450 rpm, 30 feet of head and 42 horsepower. Measured rpm was 715.
Pump	8 inch Morris Machine Works dredge pump, 8 inch x 8 inch, Model DRG, Type 8GAF-30, 3500 gpm at 580 rpm 60% efficiency and 60 feet of 1.0 specific gravity fluid.
Motor	Westinghouse 200 horsepower constant speed electric motor, style 23N6247, serial No. 1-S-61, 1180 rpm.
Flow metering system	Foxboro magnetic flow transmitter, 10 inch 150# USAS flanged, standard neoprene lining, output of 0.001021 mv/gpm. Foxboro Dyanlog recorder with 12 inch circular chart, 0-5000 gpm range.

TABLE 5-2 (Cont.)

Item	Description
Flow Metering System (cont.)	Check flows with 2025 gallon conical weigh tank equipped with electric diversion valve and digital timer.
Sample storage	28,000 gallon conical bottom tank equipped with 20 horsepower vertical mixer. Inlet is discharge from splitter box and outlet is direct to inlet of pump. Volume of contents determined by measuring outage and reading gallons from a chart.
Pressure Drop Measurement	Foxboro pneumatic differential pressure transducers Model M13A/MK 2 delivering a 3-15 psi signal to Foxboro 2 pen recorder Model M40R-P.
Temperature Measurement	Sight readings of a mercury thermometer with 1 degree graduations inserted in a liquid filled thermowell.
System Pressure	Foxboro pressure recorder Model 12R single pen 0-60 psi range.
Manometers	Meriam well type manometers using either #2 blue fluid or #3 red fluid

TABLE 5-2 (Cont.)

Item	Description
Manometers (cont.)	with corresponding scales graduated directly in inches of water.
Velocity Profile	Mechanical adjustable pitot tube operated through appropriate stuffing box to permit calibrated positioning at any point across the stream. Vertical travel. Static pressure measured from a side tap on the line at the location of the pitot tube.
Stream Sample Points	Piping installed to sample the flowing stream at the top and middle of the stream. Control through manually operated 1 inch and 1-1/4 inch plug valves.

The test sections were removed prior to the tests and internally cleaned. Water runs made after each slurry test provided instrument calibration and a check on pipe roughness.

5.3 INSTRUMENTATION

Flow through the system was determined by a 10-inch recording magnetic flow meter. Range was 0 to 5000 gallons per minute (gpm) and normal operating range was 500 to 3300 gpm. Because of the series configuration of the loop, the flow rate was used for determining the bulk velocity in each diameter leg. The meter was calibrated by a factory technician and a crosscheck was made at various flow rates by timing the diversion into a weigh tank.

Pneumatic differential pressure transducers were installed on each test section with recorders located in the control room. Manometers were installed across these transducers to provide a visual check on their performance. The pressure connections to the test pipe were through traps that allowed solids to settle to the bottom of the bottle and minimized plugging of the gauge lines. During the latter part of the tests, low ambient temperatures prevailed and the gauge lines were filled with a 25 percent glycol solution. Corrections were applied for the different specific gravities where required. Transducers and manometers were enclosed in a heated area to minimize temperature variations on the measuring devices. Initial calibration of the transducers was provided by a factory technician. Temperature was taken from a thermometer in a liquid-filled well downstream of the flow meter. Static pressure was also recorded at this point.

5.4 SMALL PIPE TEST APPARATUS

To permit analysis of a wider range of pipe sizes and to present data that would have widest possible use, a small pipe test apparatus was constructed.

The apparatus consists of two identical pressure vessels of 120 gallon capacity. Each was equipped with a mixer capable of maintaining a uniform slurry for delivery into the pipe test section. Each vessel was also equipped with a variable pressure air supply and an indicating liquid level float. Flow into the test section was controlled by a manually operated valve located on the vessel containing the slurry. Figure 5-2 is a sketch of the equipment.

During testing, the slurry was forced to flow from one vessel to the other by air pressure. The actual operating range used for slurries under test was 0 to 20 psi. The rate of increase in liquid level was timed in the receiving vessel in order to determine the actual pipe velocity. Temperatures were determined by submerging a thermometer in the slurry. From these observations, the variation of pipe wall shear stress with velocity was calculated.

Section 6
LABORATORY DATA

This section presents the methods used to generate basic data for waste materials. Data for the materials tested at Cadiz, Ohio are shown, together with data for other waste materials which may be of interest to the study as a whole.

6.1 TESTING METHODS

6.1.1 Rheology

The rheology of the various materials was established using a Contraves rotational viscometer. The testing procedure adopted was to record shear stress for increasing values of shear rate for a well mixed sample. Then the sample was remixed and shear stress for decreasing values of shear rate was recorded. This was repeated, and average values of shear stress for ascending and descending shear rates were obtained. This minimizes the effects of solids settling in the viscometer cup.

A plot of shear stress versus shear rate gives the values of yield, τ_0, and coefficient of rigidity, η, for the material under investigation.

In order to relate the values of η from the viscometer to those relevant to pipeline operating temperatures, the measured value is reduced on the basis of the viscosity of the suspending medium at the same temperature, μ. This reduced viscosity, η/μ, can then be converted into the viscosity at pipeline temperatures by multiplying by the value of μ at the particular pipe temperature. The validity of this correction is shown later.

6.1.2 Corrosion/Erosion Rates

A test apparatus similar to the one used by Bomberger (Ref. 57) employing a laboratory corrosion probe was used to evaluate the corrosion/erosion rates to be expected from pipelining various waste materials. The apparatus is shown in Figure 6-1.

Table 3-2, given in the State of the Art Section, shows corrosion rates measured for coal slurry using this technique, and compares these rates to the rates actually measured in a commercially operating coal slurry pipeline. It can be seen that the method gives excellent correlation of pipeline corrosion/erosion conditions.

6.1.3 Settling Rate

The settling rate of solids in a slurry gives an indication not only of how fast a material will settle in the pipeline but also of the terminal settled concentration of solids and the nature of settled solids.

A well mixed sample is charged to a 1,000 milliliter graduated cylinder, and the position of the solid/liquid interface with respect to time is recorded. The terminal settled concentration is noted, and the nature of the settled material is checked with a glass rod (in terms of it being packed, gritty, or fluid).

FIGURE 6-1

CORROSION TEST EQUIPMENT (CORROSOMETER)

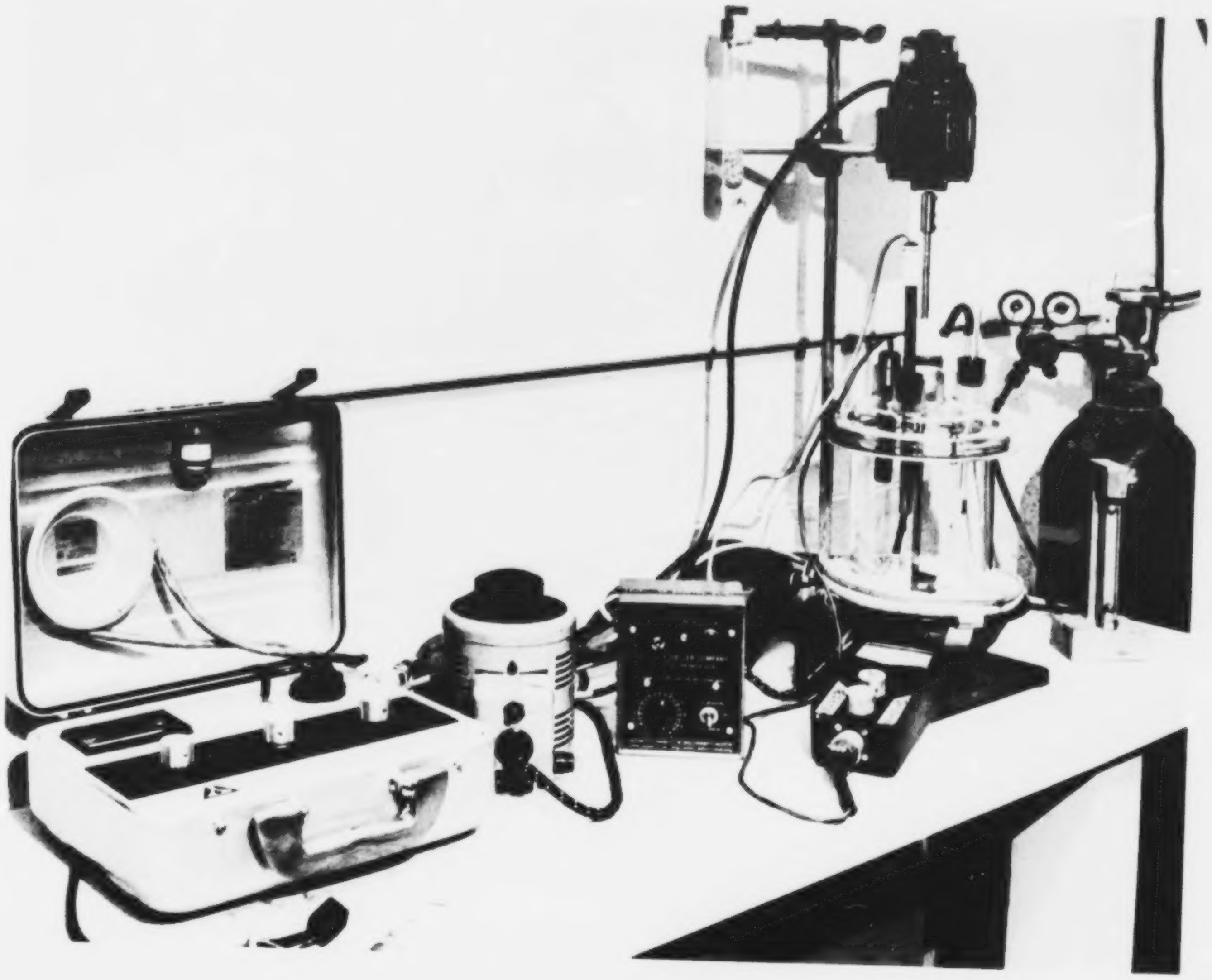

LEFT TO RIGHT: CORROSOMETER, TEMP. CONTROL, EROSION (MIXING) SPEED CONTROL
OXYGEN METER, CORROSION POT.

6.2 DIGESTED SLUDGE

6.2.1 Rheology

Prior to the Cadiz tests, the rheologies of samples of Southerly Digested Sludge were evaluated. Figure 6-2 shows the variation of reduced viscosity with concentration for sludges as received sludge, and for sludges which had been heat treated at different temperatures.

The data show that heat treatment has little or no effect on the basic viscosity of the sludge. Figure 6-3 is a plot of yield stress versus concentration for the same material. These data show that treatment at 76°C does result in a slight decrease in yield, but temperature at 70°C has no effect on the sludge.

Figures 6-2 and 6-3 also show η/μ and τ_o values for various concentrations of sludge solids for the materials tested in the Cadiz pipeline loop. It can be seen that the bulk samples were very similar to the laboratory samples examined prior to the full scale tests.

Figures 6-4 and 6-5 show the effect of temperature on the rheology of digested sludge. It can be seen that over the range of temperatures to be expected in a pipeline, the yield stress is independent of temperature. Also, the variation of viscosity with temperature can be adequately described by the reduced viscosity correction as shown in Figure 6-4.

The rheology of the Cadiz test samples is compared with the rheologies of sludges from various sources in Table 6.1.

6.2.2 Settling Tests

A satisfactory settling test could not be achieved with digested

TABLE 6.1

COMPARISON OF PROPERTIES OF VARIOUS SLUDGES TESTED

Sludge Source	Solids S. G.	Properties at 3.5% Solids	
		Reduced Viscosity (η/μ)	Yield Stress τ_o(Dynes/cm^2)
Field Sample			
Cadiz Sample	1.84	7.1	6.0
Laboratory Samples			
1. Washington Water Pollution Control Plant	1.77	5.8	2.5
2. Washington Water Pollution Control Plant (Special Process Sample)	1.56	5.1	1.35
3. Cleveland Southerly Plant	1.84	5.9	4.2

FIGURE 6-2
REDUCED VISCOSITY vs. SOLIDS CONCENTRATION
DIGESTED SLUDGE

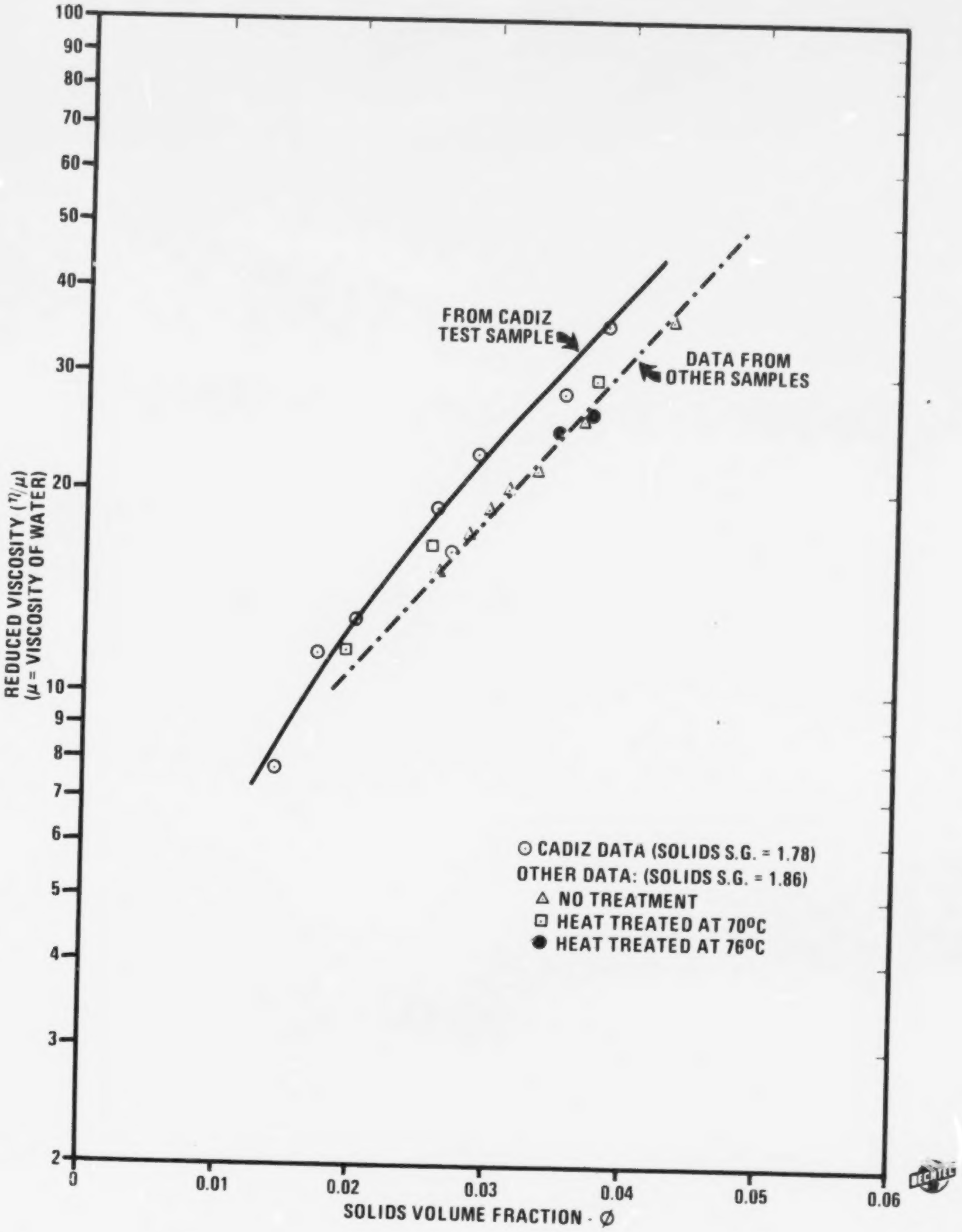

FIGURE 6-3

YIELD STRESS vs. SOLIDS CONCENTRATION
SOUTHERLY DIGESTED SLUDGE

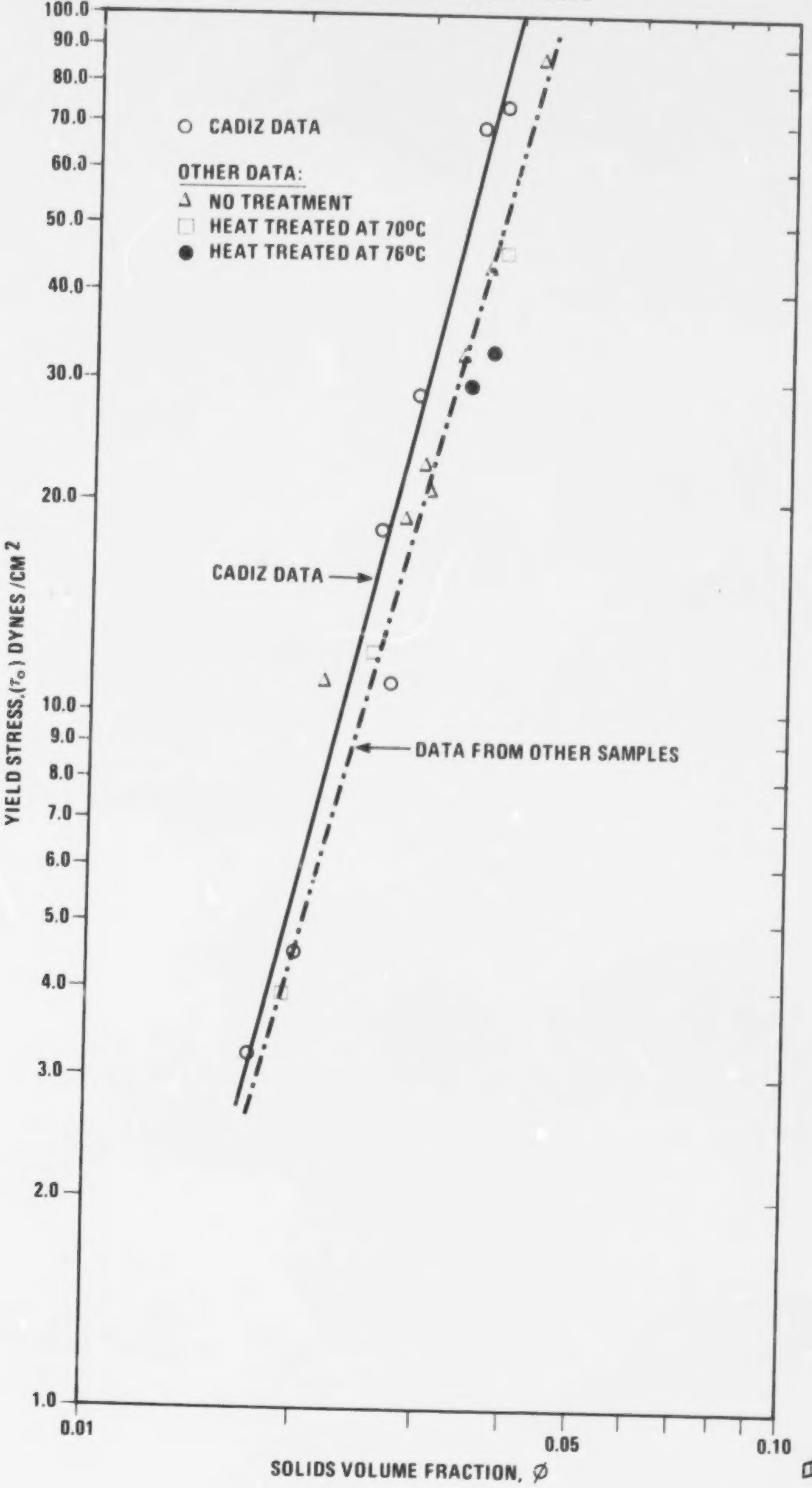

FIGURE 6-4

VARIATION OF VISCOSITY WITH TEMPERATURE DIGESTED SLUDGE

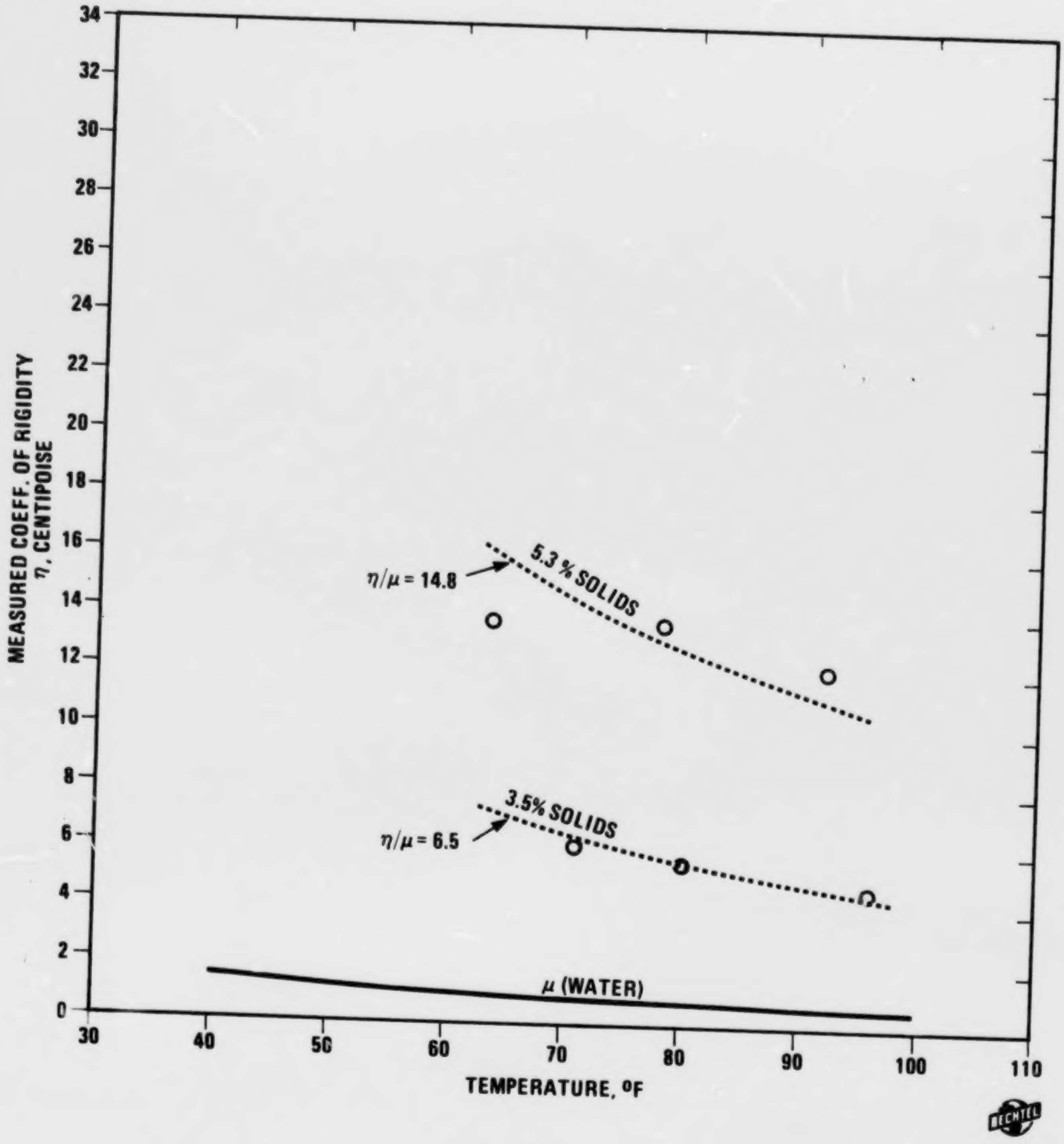

FIGURE 6-5

VARIATION OF YIELD STRESS
WITH TEMPERATURE

DIGESTED SLUDGE

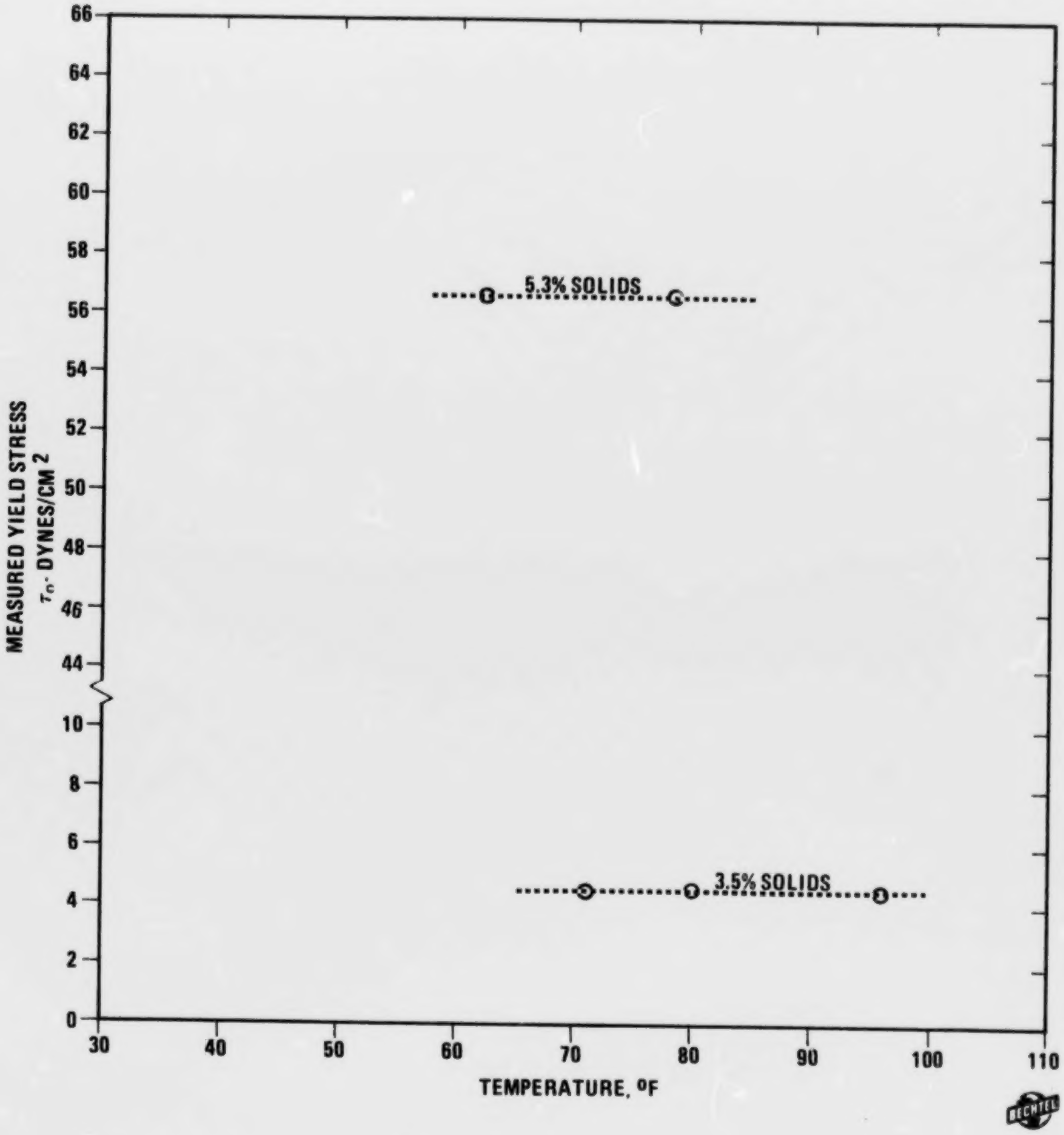

sludge. The nature of suspended solids is such that very low settling rates are realized, and this tendency is increased due to the production of gas in the material which prevents the solids from settling.

In tests performed on sludge, a stratified effect was noticed in which alternate bands of solids and clear supernatant occurred in the settling cylinder.

6.2.3 General Properties

The sludge solids used in the Cadiz tests had an average specific gravity of 1.78. The average volatile matter in the solids was 48 percent by weight.

6.3 FLY ASH

6.3.1 Rheology

The rheology of slurries of Sammis fly ash in water was measured both prior to and during the Cadiz test runs. Figures 6-6 and 6-7 show the variation of viscosity and yield stress with concentration. Measurement of the properties of slurries containing less that 45 percent solids by weight was not possible due to high rate of settling in the viscometer cup. For the purpose of comparison, the viscosity data for suspensions of true spheres are also shown.

Figures 6-8 and 6-9 show the effect of elevated temperatures on viscosity and yield stress respectively.

It can be seen that the reduced viscosity is constant with respect to temperature for both concentration levels. However, the increased

FIGURE 6-6

REDUCED VISCOSITY vs. SOLIDS CONCENTRATION SUSPENSIONS OF FLY ASH IN WATER AND IN DIGESTED SLUDGE

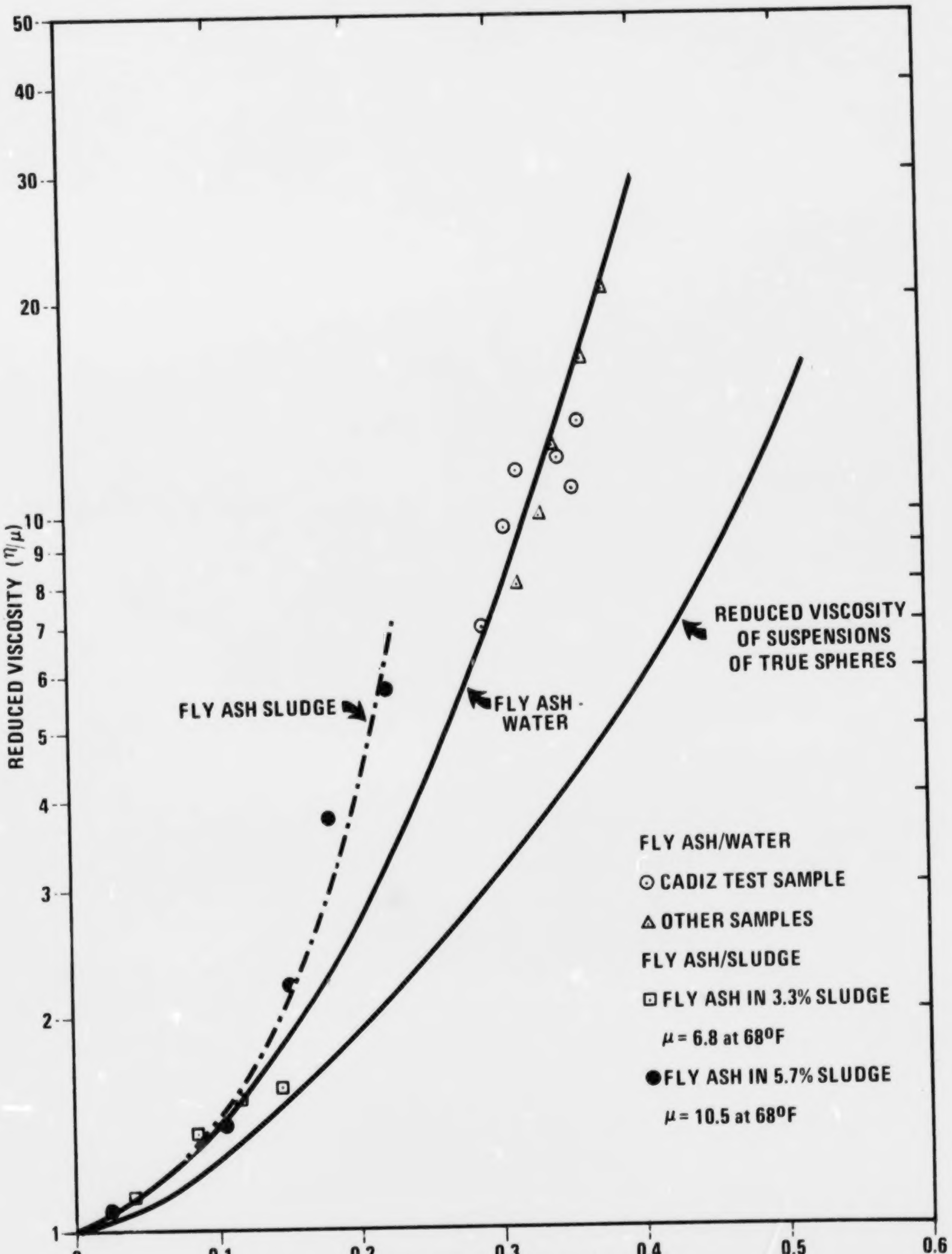

FIGURE 6-7
YIELD STRESS vs. SOLIDS CONCENTRATION
SUSPENSIONS OF FLY ASH IN WATER

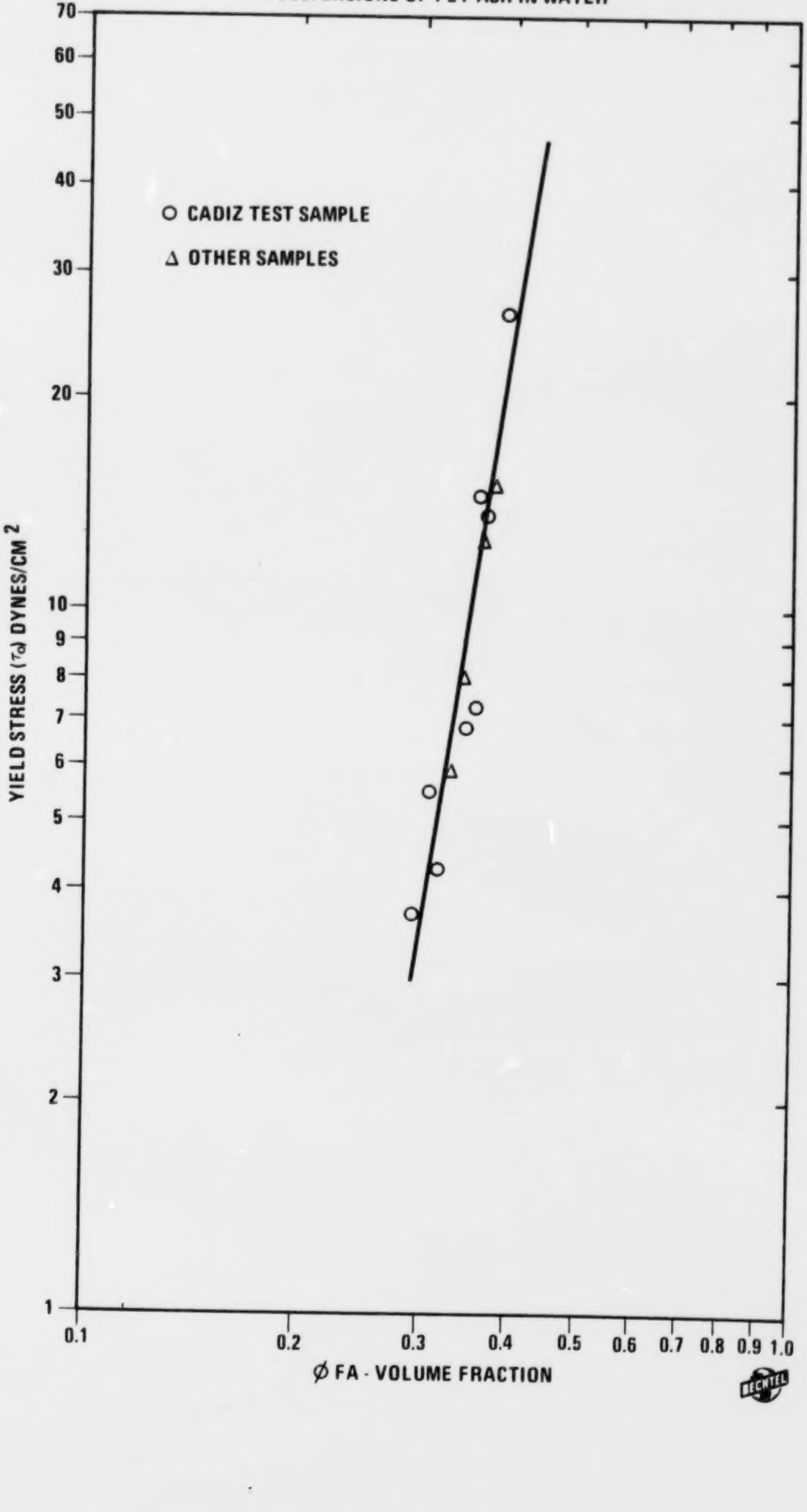

FIGURE 6-8

VARIATION OF VISCOSITY WITH TEMPERATURE SUSPENSIONS OF FLY ASH IN WATER

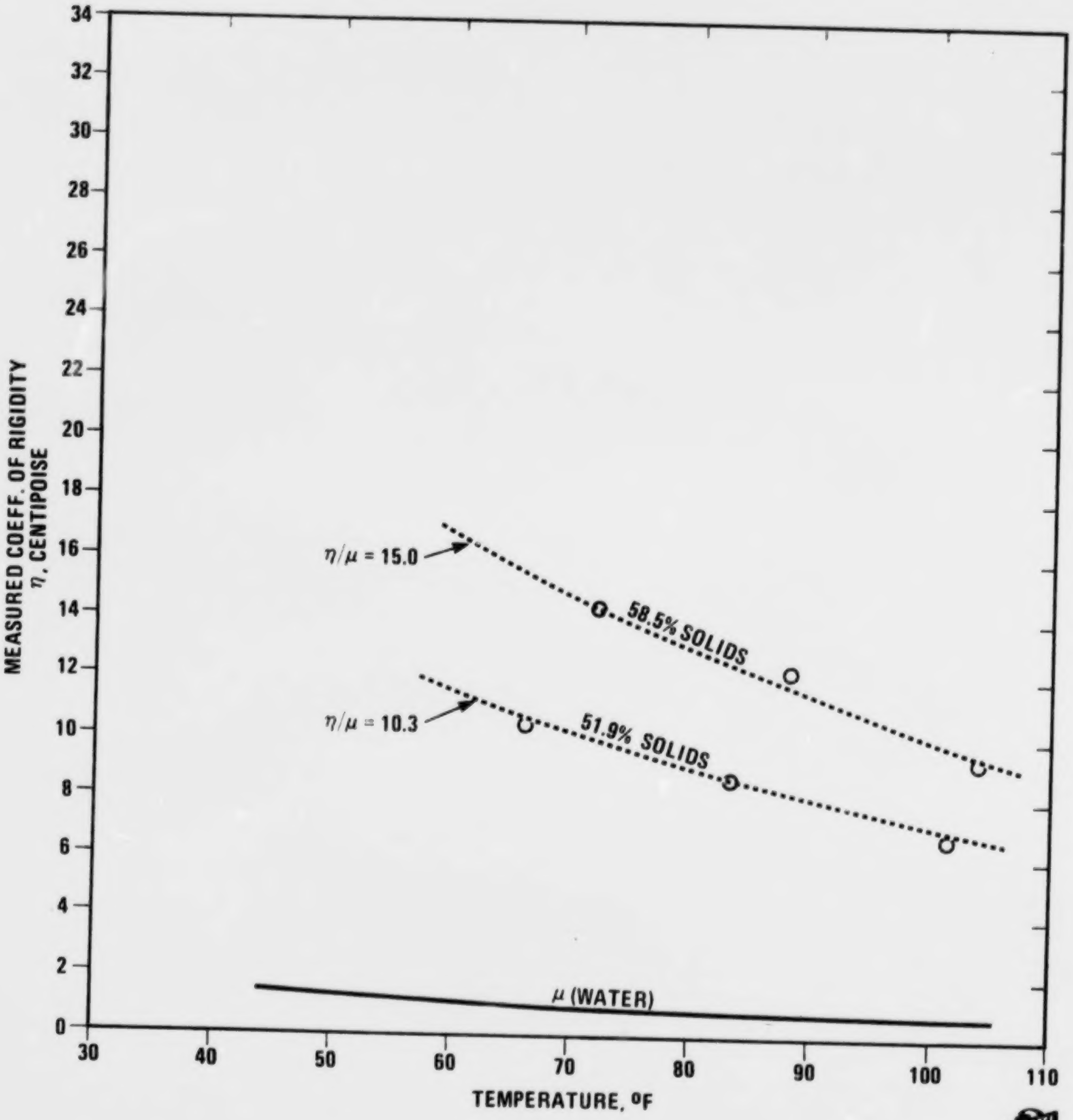

FIGURE 6-9

VARIATION OF YIELD STRESS
WITH TEMPERATURE
SUSPENSIONS OF FLY ASH IN WATER

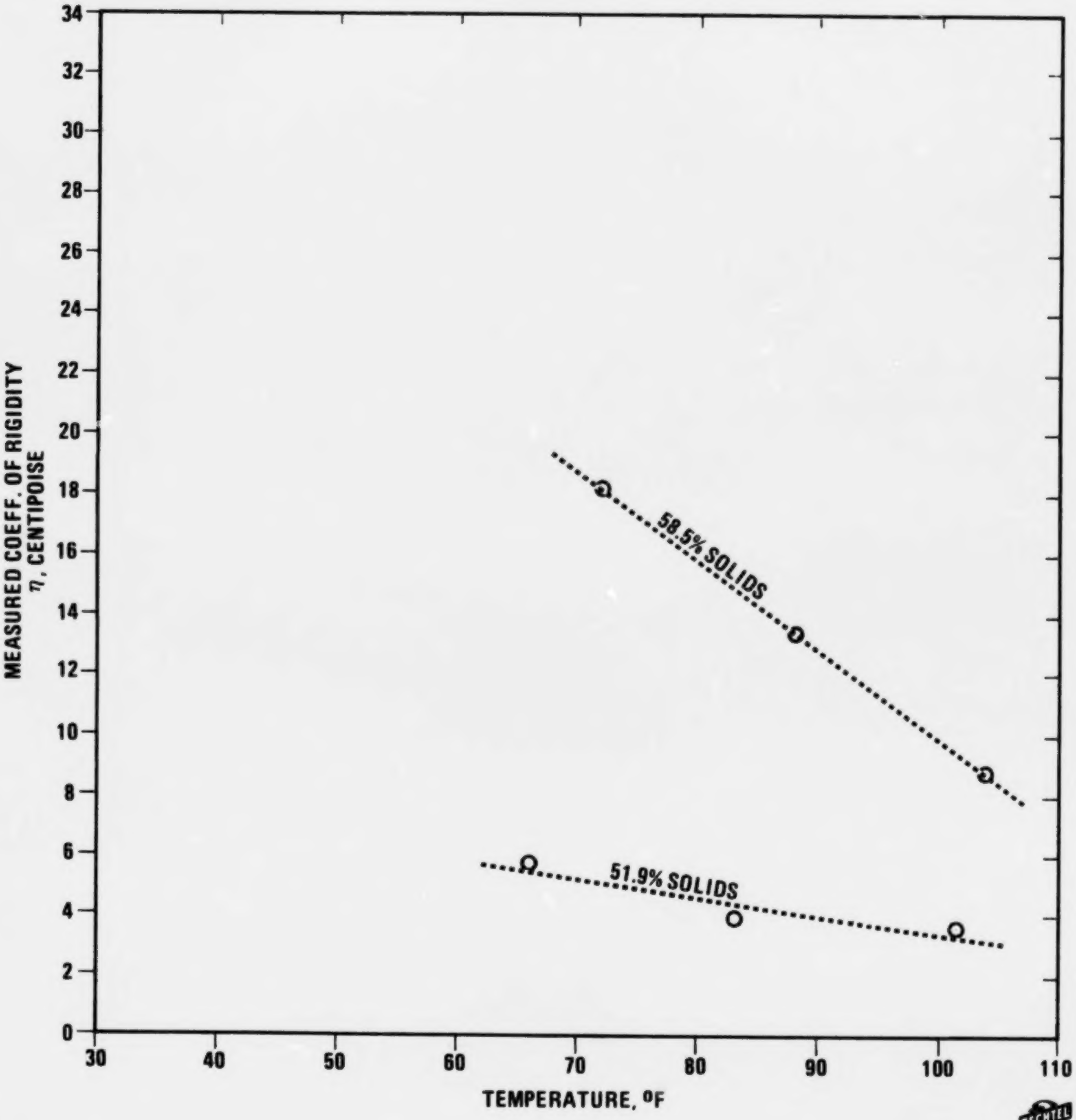

temperature has a noticeable effect of decreasing the value of the yield stress.

6.3.2 Settling Test

Figure 6-10 shows the settling characteristics of a 50 weight percent fly ash slurry. Terminal settled concentration was reached in less than six hours, and the settled slurry was relatively fluid in nature. However, it was noted that vibration caused the settled slurry to pack.

6.3.3 Slide Angle

A well mixed fly ash/water slurry containing 53 percent solids by weight was allowed to settle in a tube which was set at an angle of 10 percent slope.

The final configuration of the settled solids was such that, at the low point, the whole cross-section of the tube was filled with settled material.

This slumping of the settled material at a moderate slope is an indication that, in the settled state, fly ash does not exhibit a prohibitive yield stress. The measurements of the rheology of settled slurry given in Section 9.4 confirm this, and it can be concluded from these tests that the settled fly ash resulting from a pipeline shutdown can be successfully resuspended on startup.

FIGURE 6-10

SETTLING OF FLY ASH SLURRY

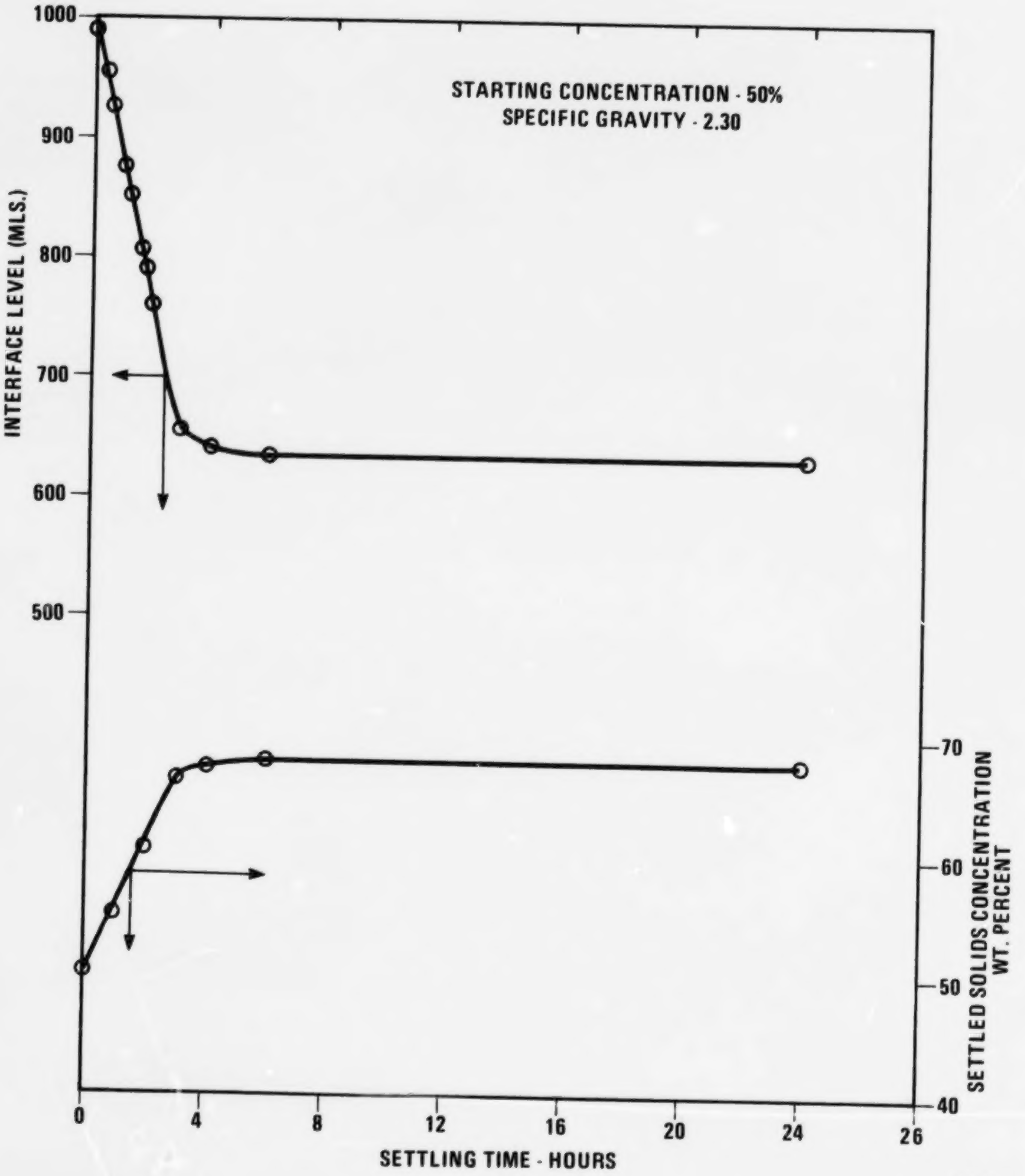

6.3.4 General Properties

The fly ash used in the Cadiz tests had an average specific gravity of 2.56. The size consist was as follows:

Tyler Mesh	Percent Retained
+ 14	Trace
14 X 28	0.14
28 X 48	1.8
48 X 100	3.5
100 X 100	2.8
200 X 325	12.6
- 325	71.9
	100.0

6.4 SLUDGE/FLY ASH MIXTURES

6.4.1 Rheology

Figure 6-6 shows the variation of reduced viscosity of fly ash/sludge mixtures versus concentration of fly ash. The viscosity of the mixture is reduced on the basis of the viscosity of sludge at the measurement temperature.

It is interesting to note that at low concentrations these data, reduced in this manner, are in the same region that dilute fly ash/water slurries would be expected to be. However, as the concentration of fly ash is increased, the data diverge from the fly ash/water data.

Figure 6-11 shows the variation of yield stress with concentration of fly ash.

The data are plotted in the form of a reduced yield stress $(\tau_o)_m / (\tau_o)_s$ where $(\tau_o)_m$ is the actual measured yield stress for the mixture and $(\tau_o)_s$ is the yield stress of the suspending medium (digested sludge).

Figure 6-11 shows that data for sludges of 3.3 and 5.7 percent solids containing fly ash are represented by a single line. This line is asymptotic to the fly ash/water slurry data line.

Hence, the data for any sludge containing fly ash can be generalized according to Figure 6-11.

6.5 MAINTENANCE DREDGINGS

6.5.1 Rheology

Figures 6-13 and 6-14 show the variation of viscosity and yield stress with solids concentration for samples of Cleveland Harbor dredgings. The reduced viscosity is extremely sensitive to changes in concentration as indicated in Figure 6-13.

6.5.2 Corrosion

Tests on two dredgings samples show that both initial and residual corrosion rates are nil.

FIGURE 6-11

REDUCED YIELD STRESS vs. FLY ASH CONCENTRATION
SLUDGE/FLY ASH MIXTURE

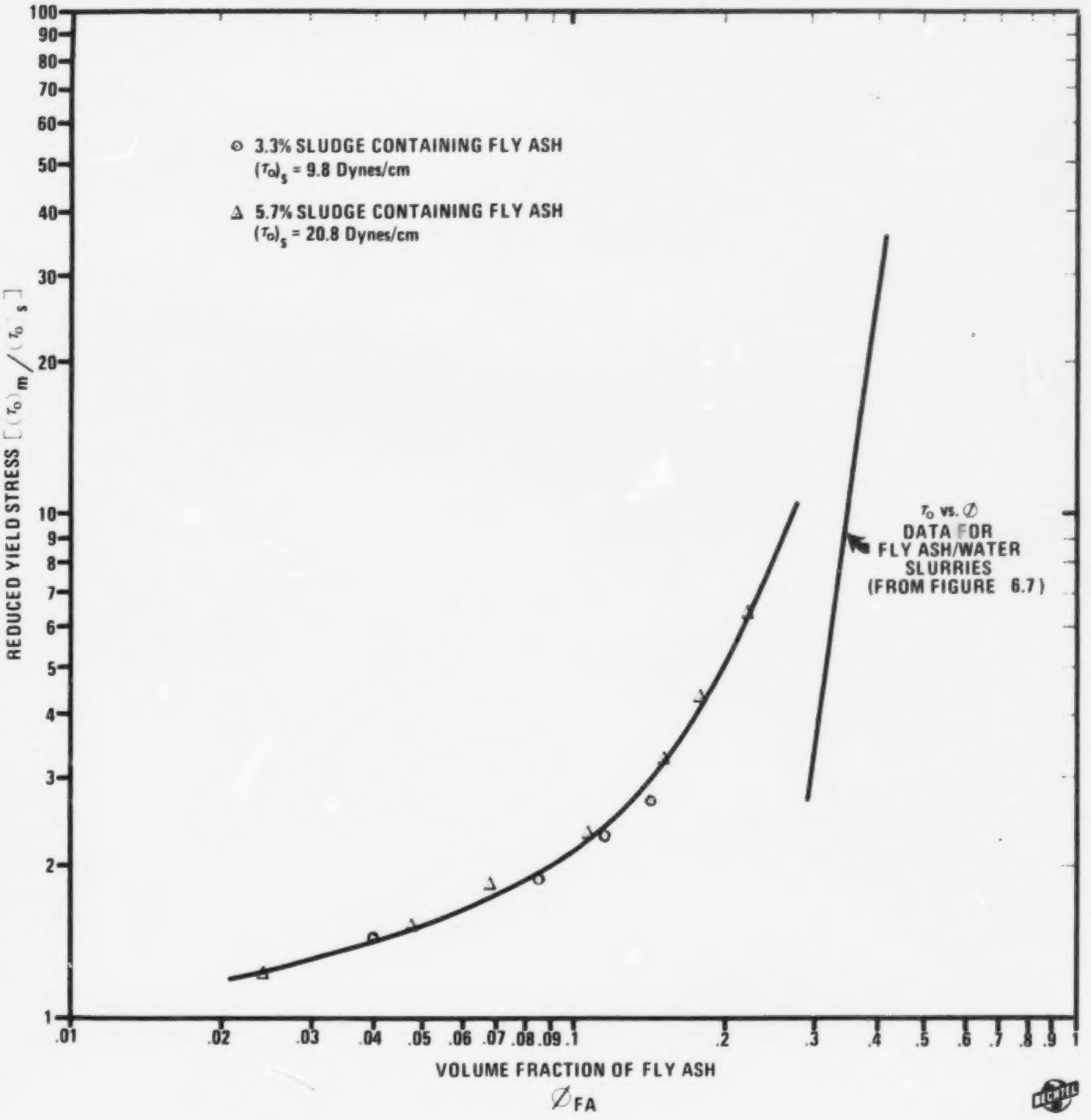

τ_o vs. $\varnothing$
DATA FOR
FLY ASH/WATER
SLURRIES
(FROM FIGURE 6.7)

FIGURE 6-12

SETTLING TEST
SLUDGE/FLY ASH MIXTURE

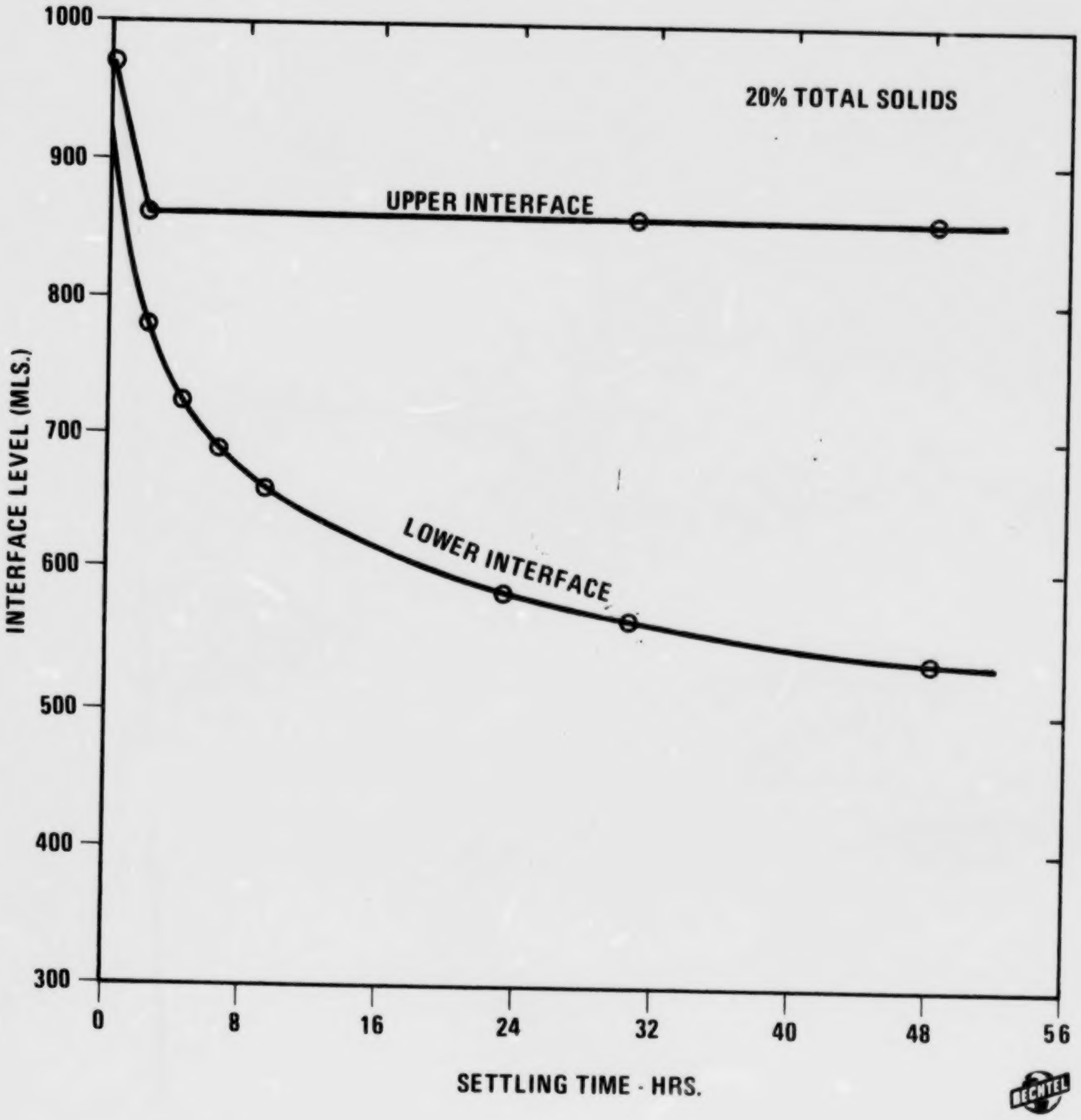

FIGURE 6-13

REDUCED VISCOSITY vs. SOLIDS CONCENTRATION CLEVELAND HARBOR DREDGINGS

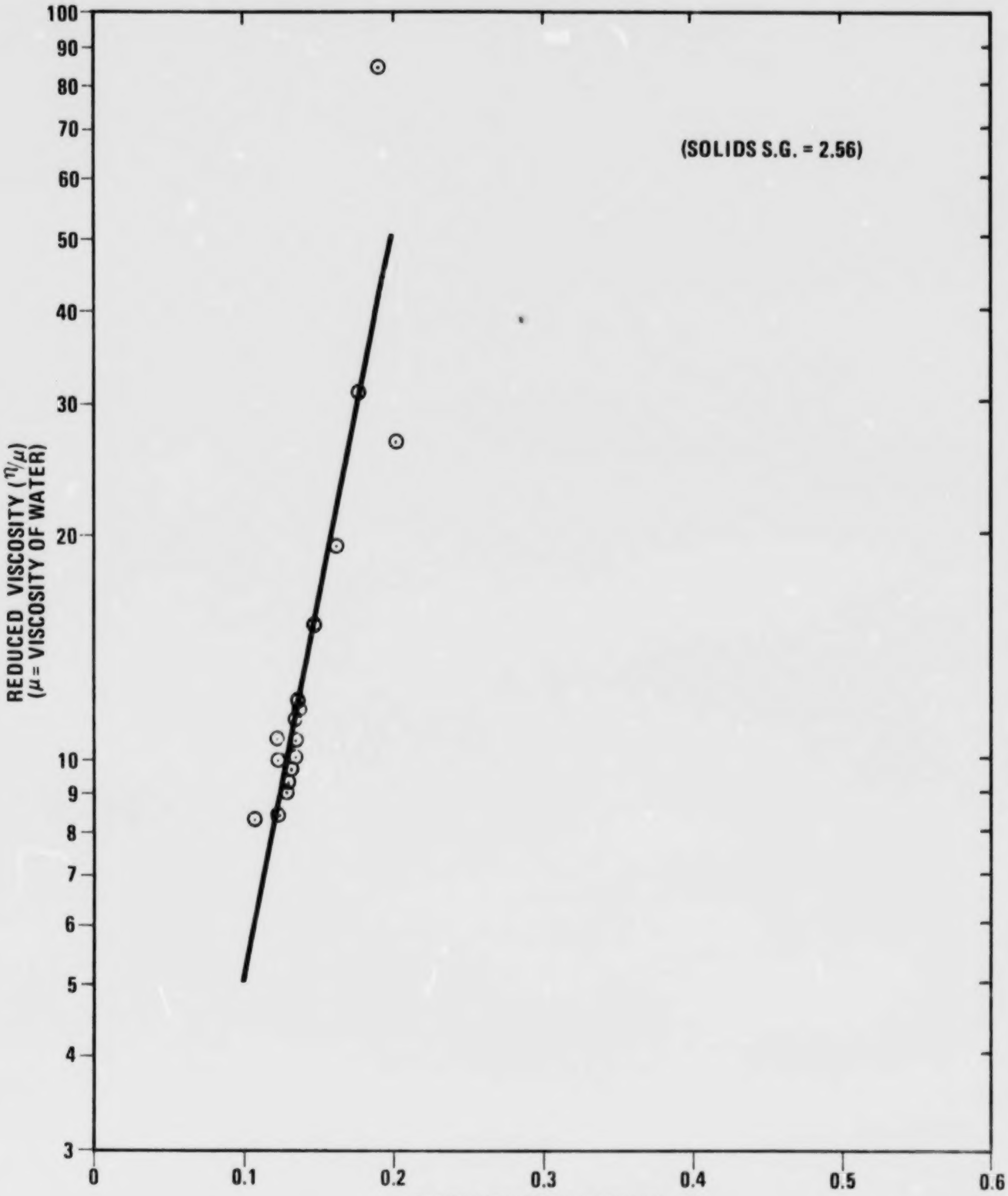

FIGURE 6-14

YIELD STRESS vs. SOLIDS CONCENTRATION
CLEVELAND HARBOR DREDGINGS

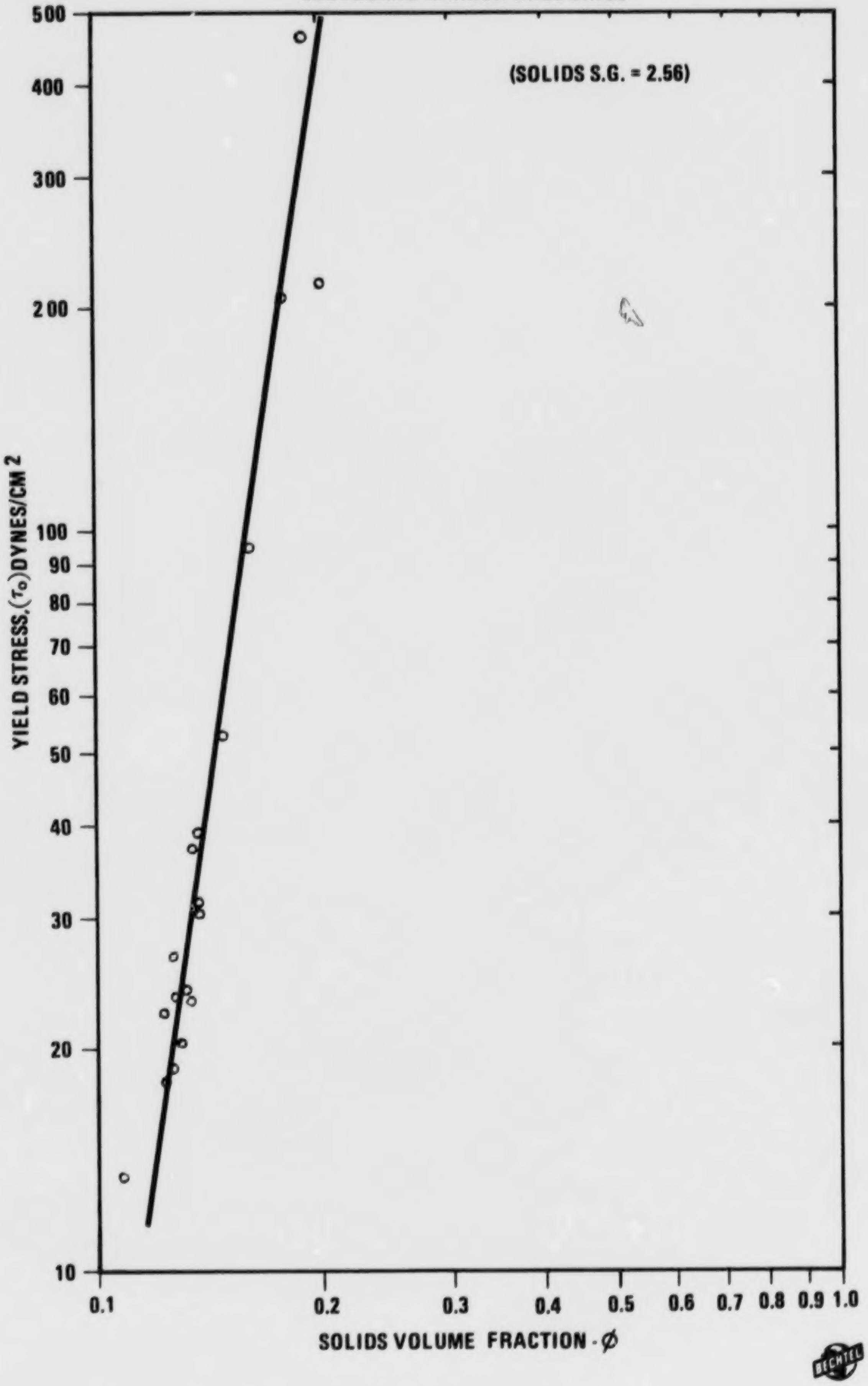

FIGURE 6-15

REDUCED VISCOSITY vs. SOLIDS CONCENTRATION
DIGESTED SLUDGE/DREDGINGS MIXTURES

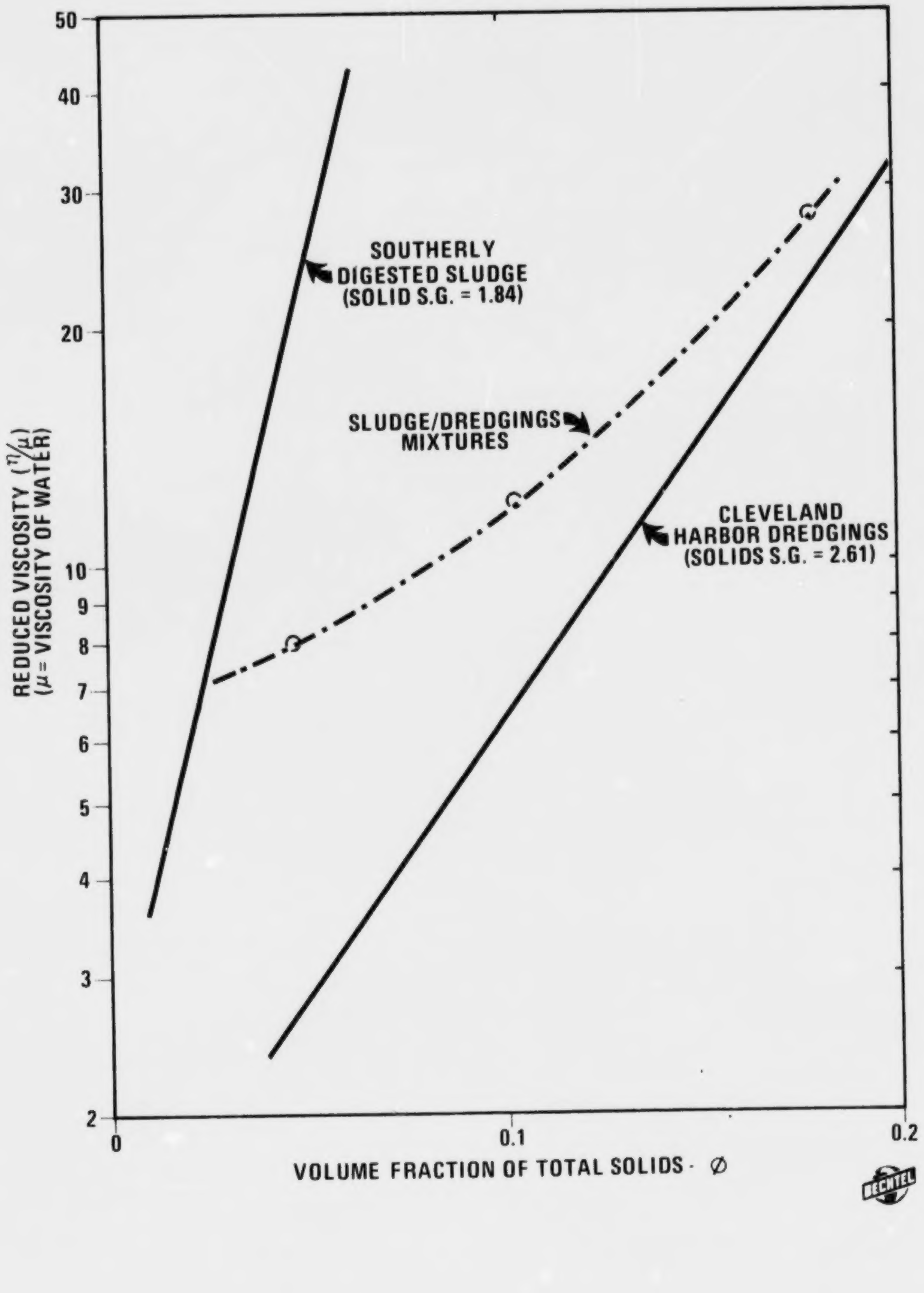

From these tests it can be concluded that cross-country pipelining of dredgings would present no major corrosion problems, although an inhibitor or oxygen scavenger may be needed for the first portion of the line.

6.5.3 Settling Rate

A 70-hour settling test on dredgings showed that in spite of the relatively high solids gravity (2.6), very little settling occurred over the period of the test (the settled solids increased to 26 percent solids from the initial concentration of 22.8 percent).

Large amounts of gas were generated during the test, such that the sample volume expanded by some 10 percent, which would explain the low settling rate achieved.

6.5.4 Temperature Effects

Rheology tests were performed on dredgings which had been stored at 37°F and dredgings which had been stored at room temperature.

Tests after storage times of 2, 7, and 28 days showed that in neither case did the rheological characteristics of the material change significantly with time.

6.6 SLUDGE/DREDGINGS MIXTURES

6.6.1 Rheology

Figures 6-15 and 6-16 show the variation of reduced viscosity and yield stress with total solids concentration. The relationships for sludge and dredgings are shown also.

It can be seen that the properties of the mixture on a total solids basis tend towards those for dredgings as the amount of dredgings in the mixture is increased.

6.7 WATER TREATMENT PLANT SLUDGE

6.7.1 Rheology

Figures 6-17 and 6-18 show the variation of the rheological properties of water treatment plant sludge with solids concentration. Also shown on the curves is the rheology of digested sewage sludge.

It can be seen that the properties of water treatment plant sludge are similar to those of digested sludge, and it would appear that transportation of water treatment plant sludge as a low-volume additive to digested sludge would present no problems.

FIGURE 6-16

YIELD STRESS vs. SOLIDS CONCENTRATION
DREDGINGS/SLUDGE MIXTURES

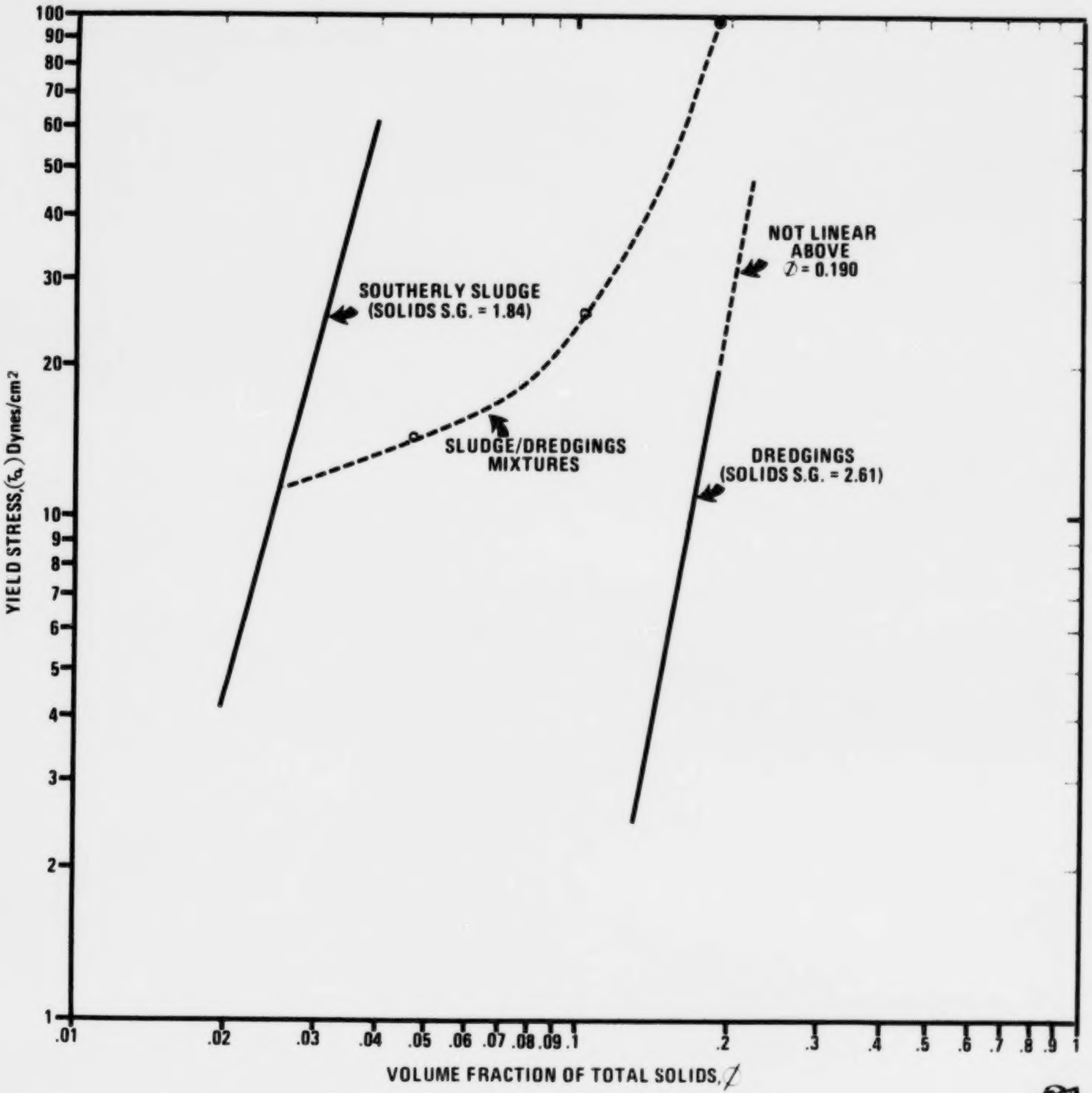

FIGURE 6-17

REDUCED VISCOSITY vs. SOLIDS CONCENTRATION
WATER TREATMENT PLANT SLUDGE

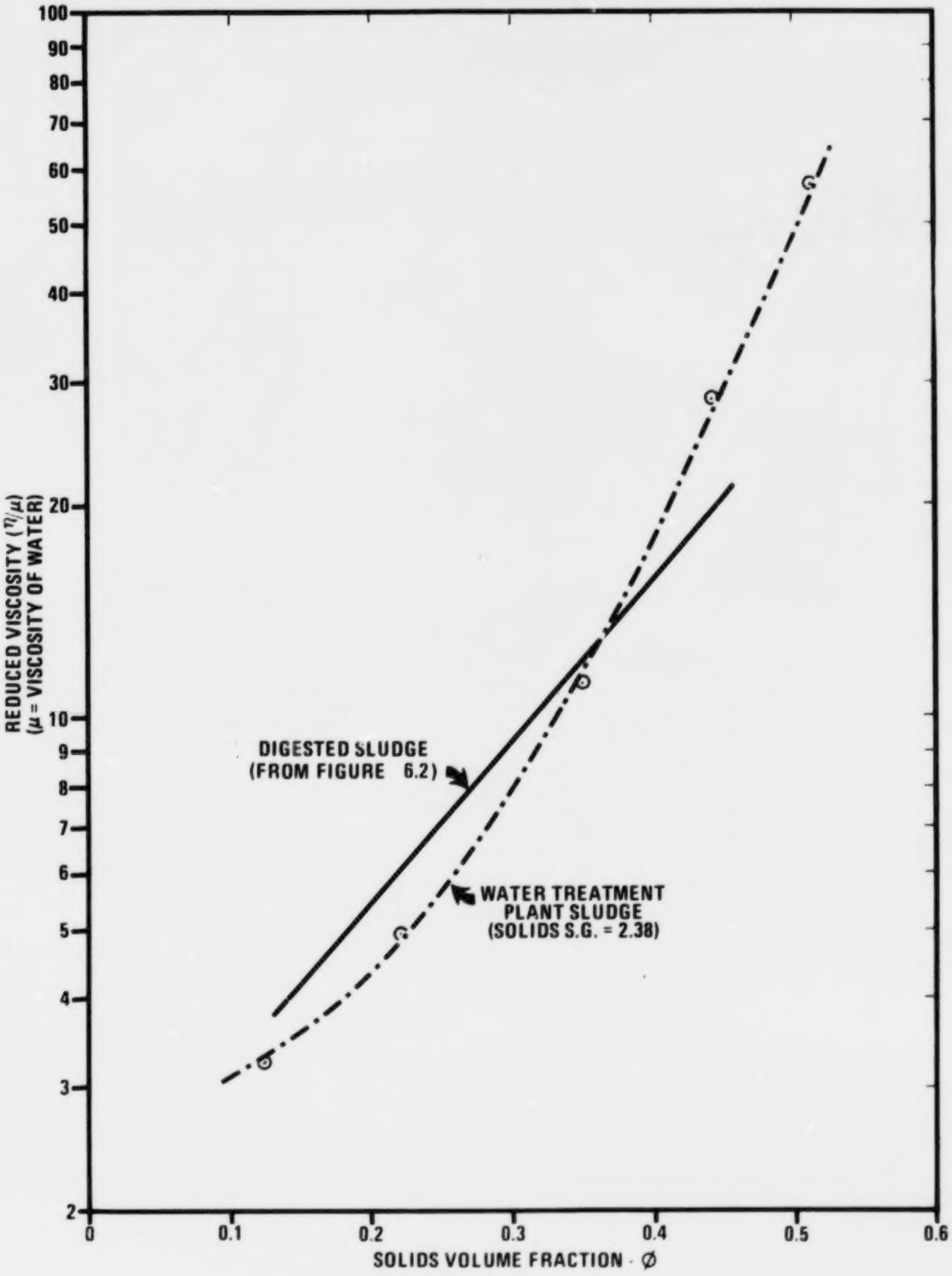

FIGURE 6-18

YIELD STRESS vs. SOLIDS CONCENTRATION WATER TREATMENT PLANT SLUDGE

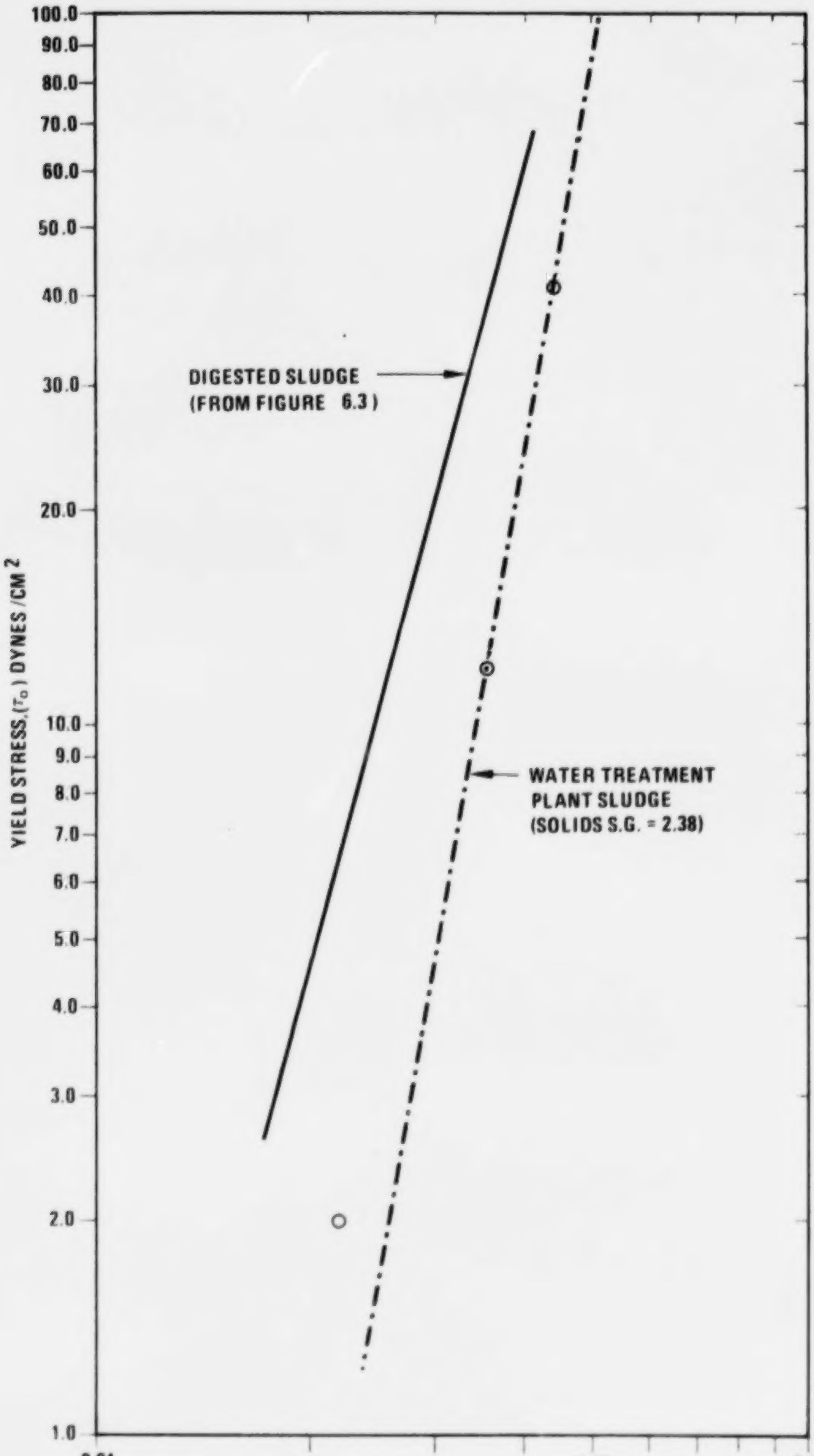

Section 7

PIPE TESTS ON DIGESTED SLUDGE

7.1 PIPELINING OF DIGESTED SLUDGE

Tests were performed on sludges of various solids concentrations for a wide range of pipe diameters. Table 7-1 is a list of these tests, which are discussed in detail below.

7.1.1 Hydrodynamics

The data show conclusively that the turbulent friction losses encountered in a digested sludge pipeline are accurately predicted from a knowledge of the rheology of the system.

Once established, the rheology can be incorporated into various design procedures in order to predict turbulent flow characteristics. As will be seen in the following paragraphs, a simple homogeneous model gives excellent prediction of measured data for widely varying conditions of velocity, concentration, and pipe diameter, and is eminently suitable as a design procedure for commercial pipelines. Other correlation procedures are applied to the data, of which the power-law model due to Dodge and Metzner also gives good correlation of the data.

Since, from a practical standpoint, only the turbulent flow regime is of importance for the transportation of digested sludge, it is necessary to be able to predict the transition point from laminar

Table 7-1

HYDRAULIC TESTS ON DIGESTED SLUDGE

Run Number	Solids Concentration (percent by weight)	Pipe I. D. (Inches)
DS-1-H	3.5	12.0 & 15.25
DS-2-H	3.0	12.0 & 15.25
DS-3-H	2.5	12.0 & 15.25
DS-4-H	4.7	0.622
DS-5-H	8.8	0.622
DS-6-H	12.1	0.622

flow to turbulent flow. It is herein found that the Hedstrom criterion for turbulent/laminar transition gives an excellent correlation of the observed transition velocities, over the whole range of flow conditions.

The tests establish that the homogeneous model can be confidently used to design commercial pipelines provided that the pipeline operates at velocities in excess of the Hedstrom-predicted critical. As outlined in Section 3, the use of this design model hinges on an accurate evaluation of the system rheology. A viscometer, such as the one used in this study, can provide such data. The rheology relevant to each run is discussed in detail in the following paragraphs and general considerations of the rheology of digested sludge are given in Section 6.

7.1.2 Operability

The fact that digested sludge, even at concentrations of 12 percent solids, is essentially a fluid and does not tend to pack in a static condition ensures that startup and shutdown of a sludge pipeline will present no operational difficulties.

7.1.3 Corrosion

Laboratory tests described in Section 6 show that only moderate corrosion rates can be expected in sludge pipelines. The initial corrosion rate of 3.5 mils per year decreases with time, and the residual corrosion rate is practically nil.

The use of an inhibitor or oxygen scavenger for the first portion of the pipeline should prevent any serious metal losses due to the initial more severe condition.

7.2 RHEOLOGY

The rheological parameters of yield stress (τ_o) and coefficient of rigidity (η) of digested sludge were established using a rotational viscometer, as described in Section 6.

Figures 7 1 to 7-8 show typical examples of rheograms obtained from samples taken from the pipe systems. Over the range of expected commercial pipe shear stresses, the shear stress/shear rate characteristic is essentially a straight line, and in this range of shear, digested sludge can be characterized as a Bingham plastic.

The laboratory rheology measurements were invariably performed at a different temperature from that at which the pipe loop was operating. To correct for this in data correlation, the measured viscosity (η) was reduced by the viscosity of water (μ) at the same temperature. This reduced viscosity (η / μ) was then converted to the viscosity at pipe test conditions by multiplying by the viscosity of water at the flowing temperature. Due to errors in sampling and measurements the values of η / μ for a given sludge show slight variations during any one pipe test (see relevant run sheets in Appendix A). An average value was used for correlation purposes.

In order to evaluate possible effects of sludge degradation in

FIGURE 7-1
ROTATIONAL VISCOMETER RHEOGRAM
SOUTHERLY DIGESTED SLUDGE

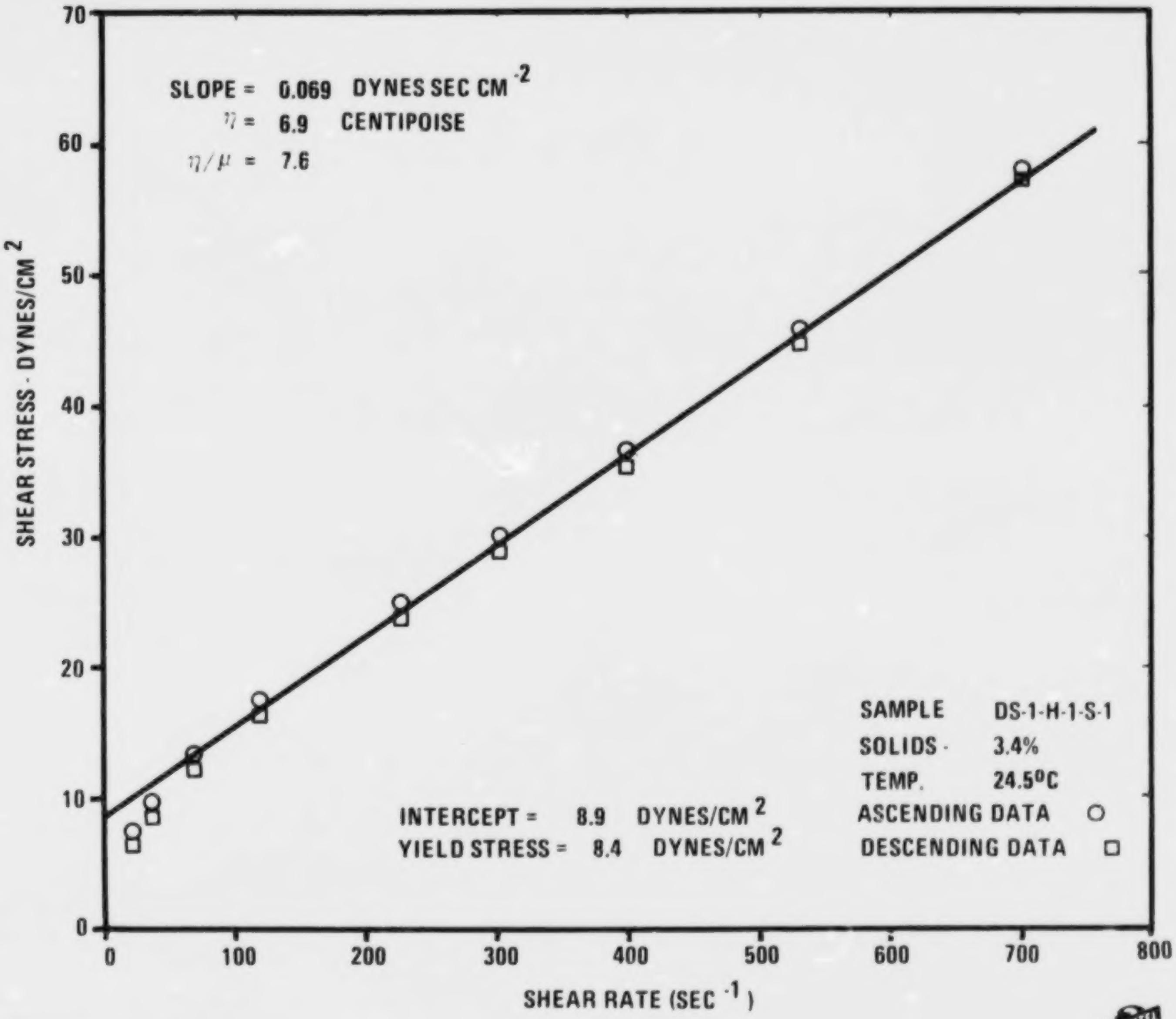

FIGURE 7-2
ROTATIONAL VISCOMETER RHEOGRAM
SOUTHERLY DIGESTED SLUDGE

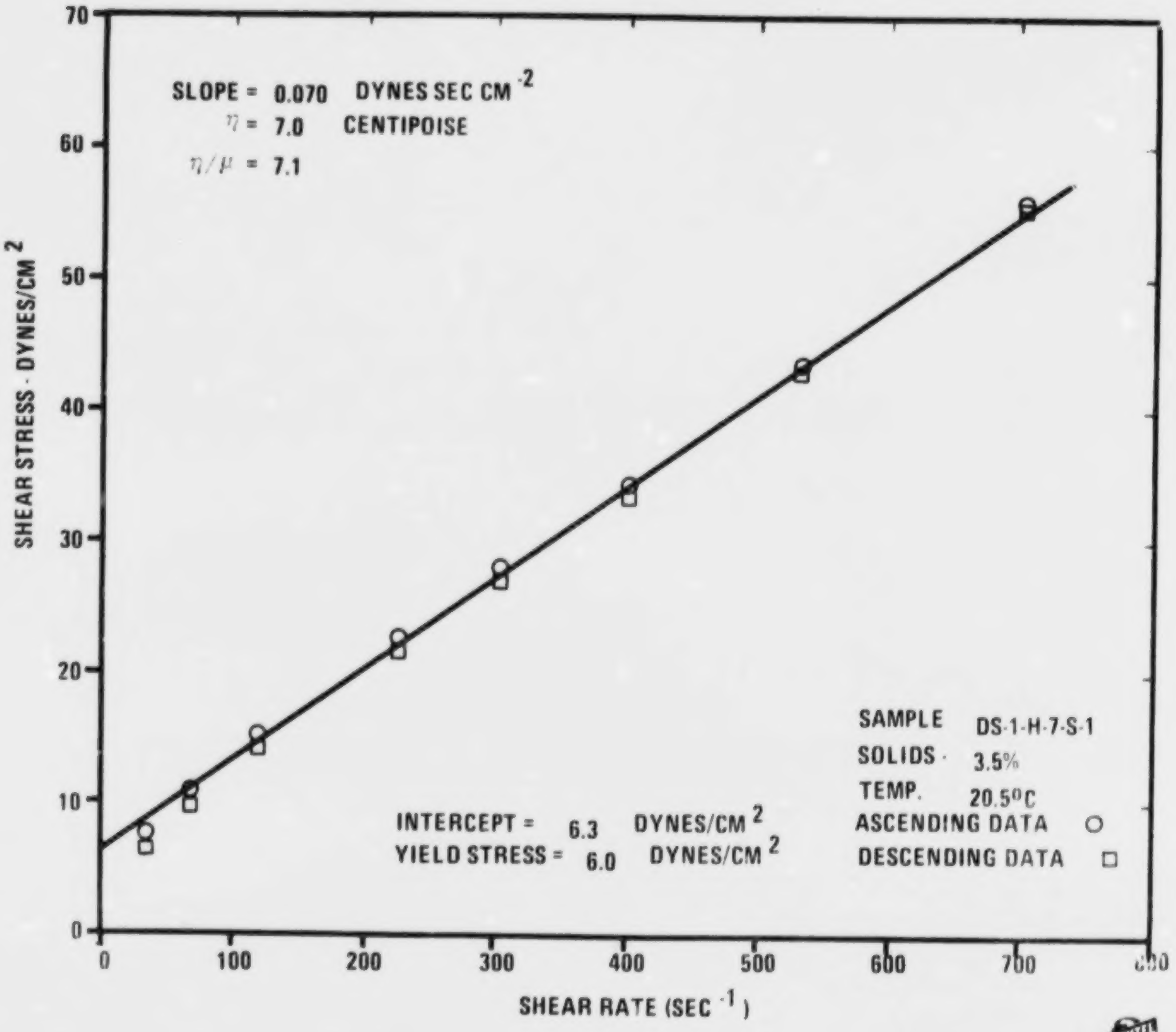

FIGURE 7-3
ROTATIONAL VISCOMETER RHEOGRAM
SOUTHERLY DIGESTED SLUDGE

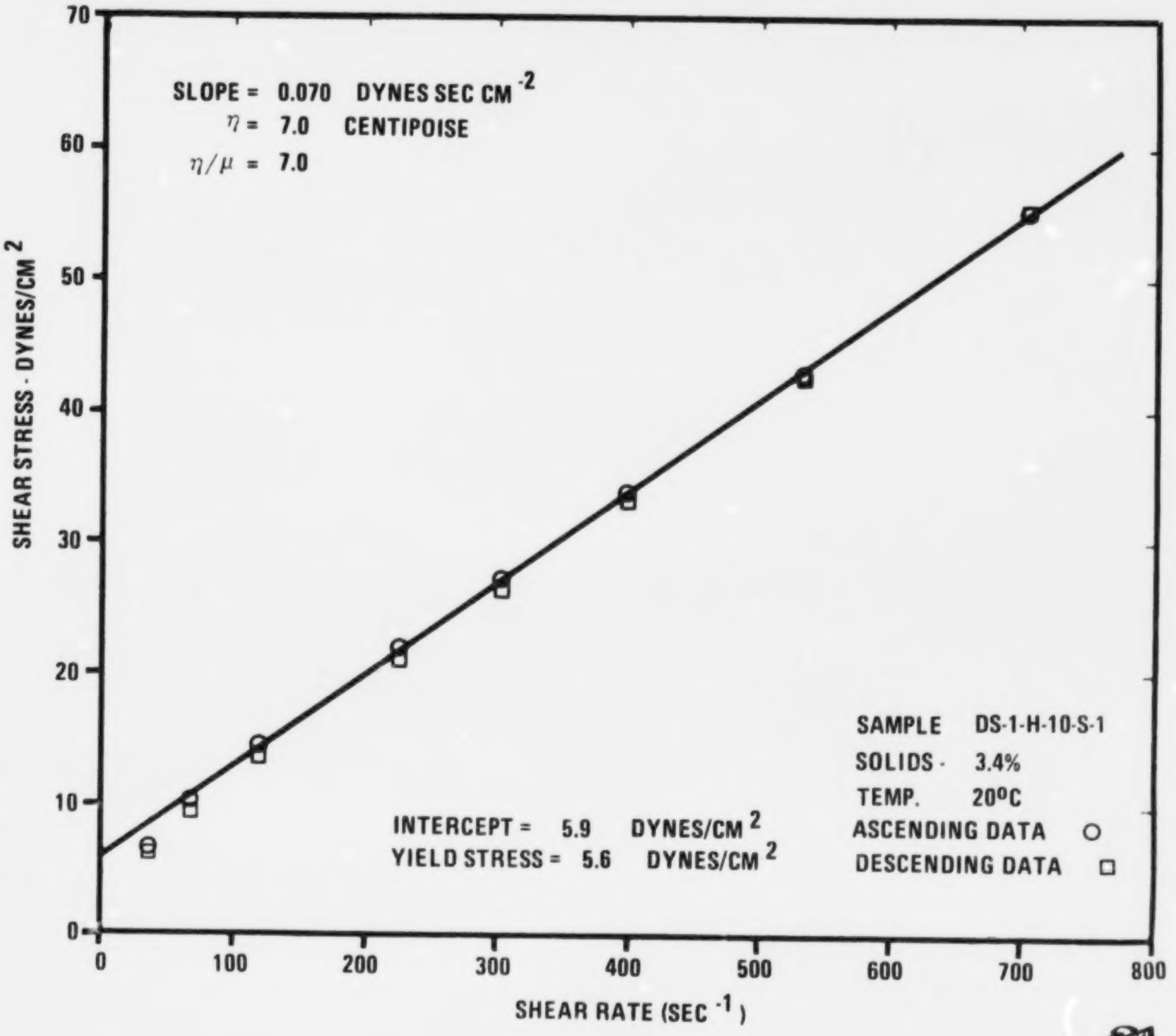

FIGURE 7-4
REDUCED VISCOSITY & YIELD STRESS
VS.
PUMPING TIME
SOUTHERLY SLUDGE

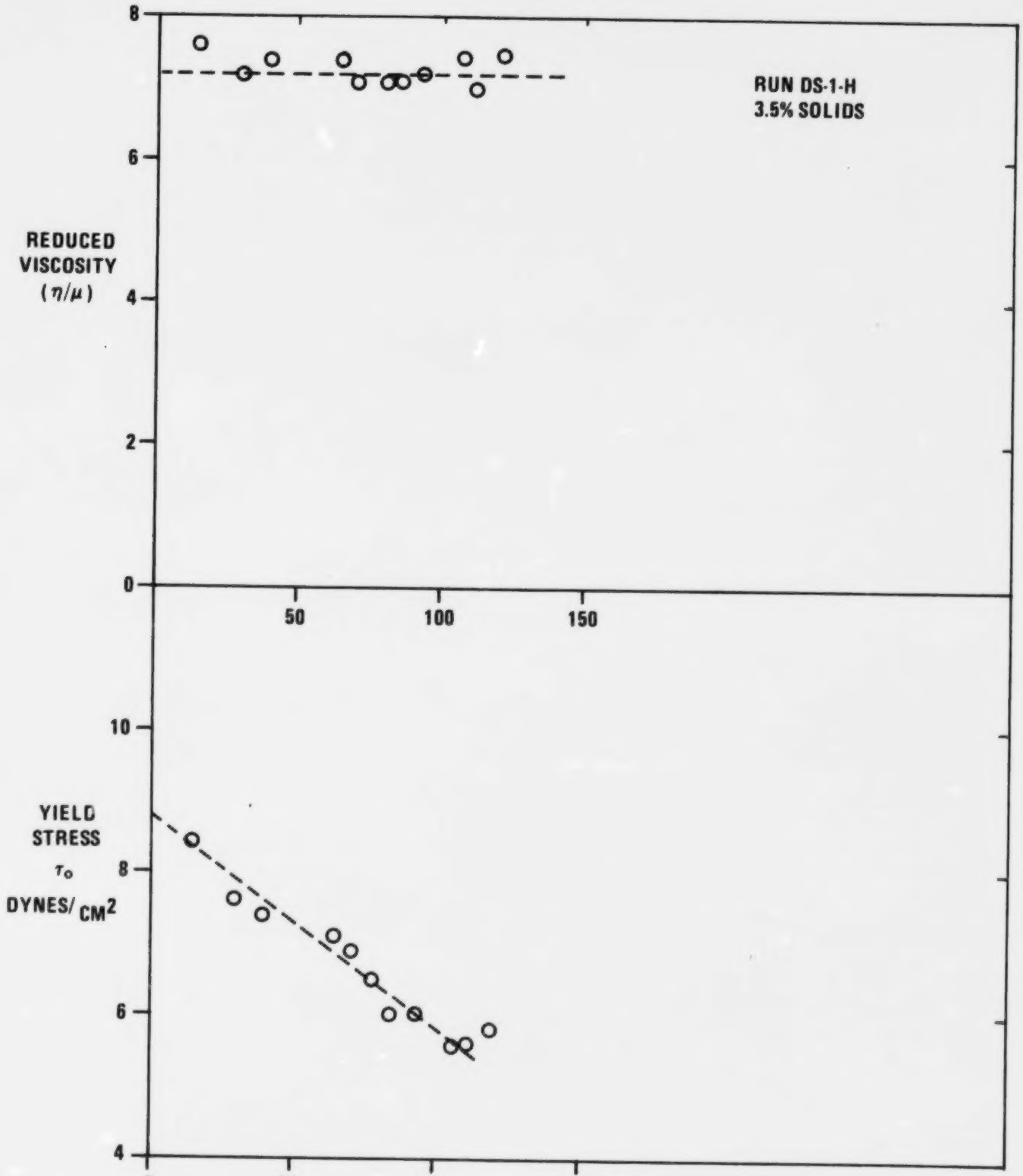

FIGURE 7-5
ROTATIONAL VISCOMETER RHEOGRAM
SOUTHERLY DIGESTED SLUDGE

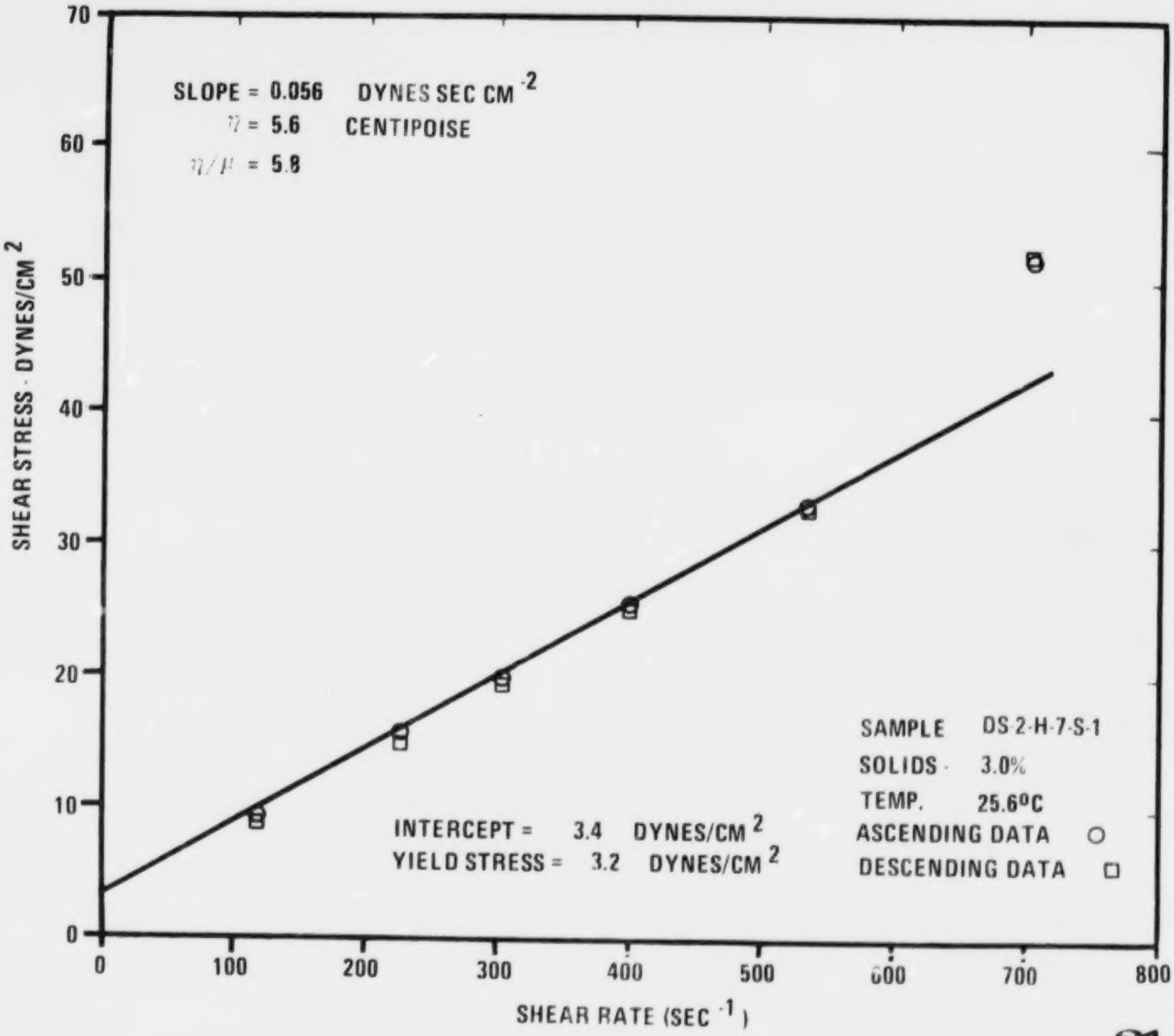

FIGURE 7-6
ROTATIONAL VISCOMETER RHEOGRAM
SOUTHERLY DIGESTED SLUDGE

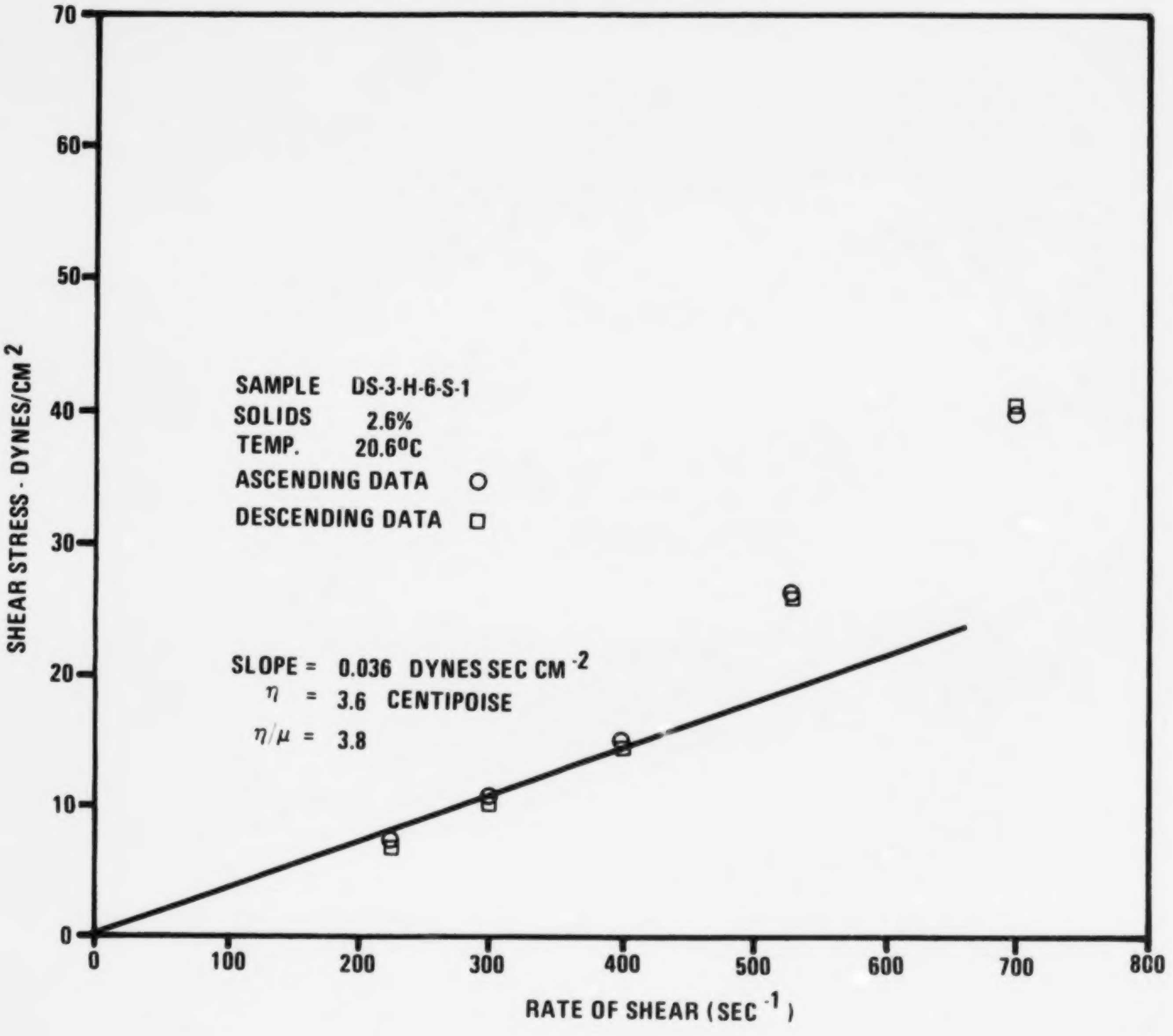

FIGURE 7-7

ROTATIONAL VISCOMETER RHEOGRAM
SOUTHERLY DIGESTED SLUDGE

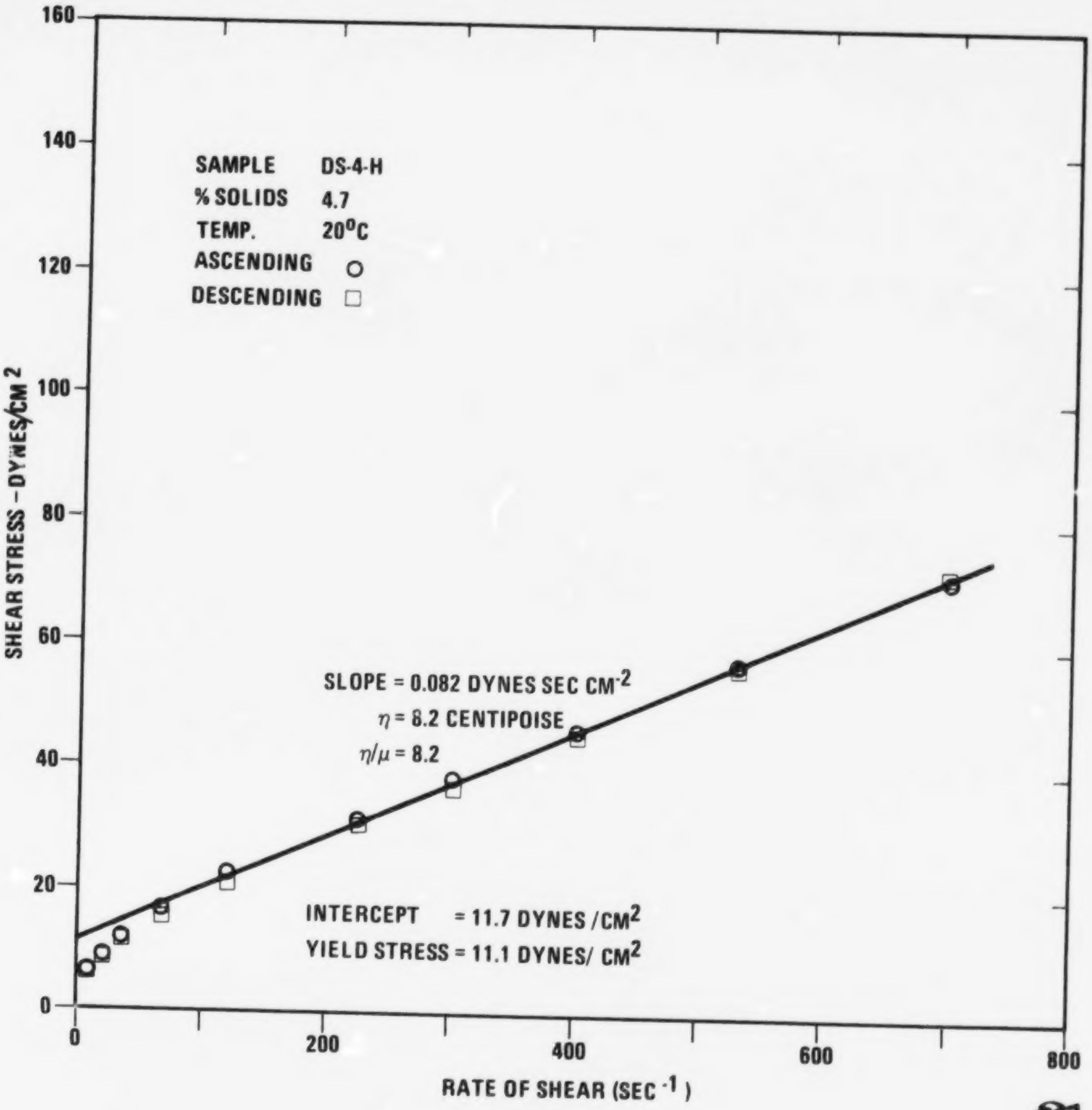

FIGURE 7-8

ROTATIONAL VISCOMETER RHEOGRAM
SOUTHERLY DIGESTED SLUDGE

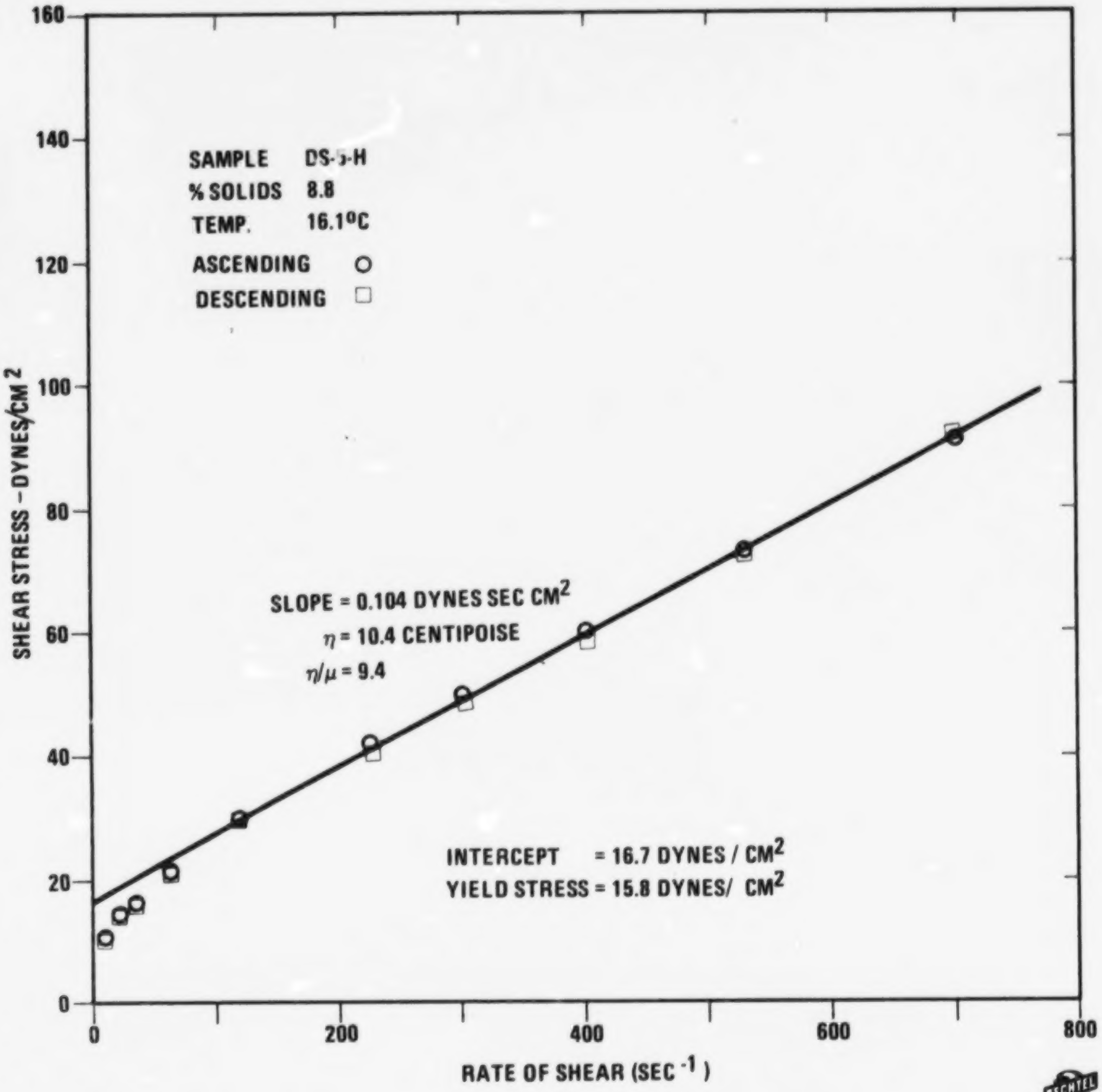

the test loop, samples were taken throughout the runs, and the variation of sludge rheology was carefully followed. Figures 7-1 to 7-3 show rheograms taken at three different times during Run DS-1-H which was conducted at 3.5 percent solids. The figures clearly show a decrease in yield stress with pumping time. Figure 7-4 is a plot of η/μ and τ_0 as a function of pumping time for this run. It can be seen that the reduced viscosity data have a certain degree of scatter, but that the viscosity was constant throughout the run.

On the other hand, measured values of yield stress show a definite decreasing trend with running time. This degradation effect agrees with the findings of Babbitt and Caldwell (Ref. 59), who subjected various sludges to severe agitation and found that a lower yield stress resulted, while no change was detected in the plastic viscosity.

Examination of Figure 7-4 shows that the yield stress could possibly be approaching a terminal value towards the end of the run, as very little change was detected over the last 35 minutes.

Run DS-2-H, at 3.0 percent solids, was performed on the sludge batch from DS-1-H, diluted with water. No degradation was detected during the run, possibly because the sludge had been fully degraded by the prior test. Figure 7-5 is a typical rheogram for the sludge used in Run DS-2-H. It can be seen that at higher shears the data diverge from the straight line characteristic. This deviation is due to the onset of turbulence in the viscometer, and such data points were ignored in establishing values of yield stress and coefficient of rigidity.

Figure 7-6 shows a typical rheogram for a sludge at 2.5 percent solids (Run DS-3-H). Again, the data show the onset of turbulence at higher shears, and in addition, the extrapolation of the valid data to zero shear shows that at this concentration digested sludge exhibits no yield structure and behaves as a Newtonian fluid.

Figures 7-7, 7-8 and 7-9 show rheograms for the thicker sludges (4.7, 8.8 and 12.1 percent solids) used in the small pipe tests. Up to 8.8 percent solids, sludge behaves in a similar manner to the dilute cases discussed previously. In the case of the 12.1 percent sludge, a distinct change in the nature of the material can be seen in that the simple treatment applied to the data for the dilute sludges does not apply in this case. Hence, it is necessary to resort to a more complex rheological model. Figure 7-9 shows a plot of the rheology data for this run (DS-6-H) on the basis of a Casson Model.

The Casson Model may be stated as:

$$\sqrt{\tau} = \frac{1}{\sqrt{\eta}}\sqrt{G} + \sqrt{\tau_0}$$

where τ is the shear stress and G is the shear rate. Figure 7-9 shows that the Casson Model represents the data fairly well.

FIGURE 7-9

ROTATIONAL VISCOMETER RHEOGRAM (CASSON - TYPE)
SOUTHERLY DIGESTED SLUDGE

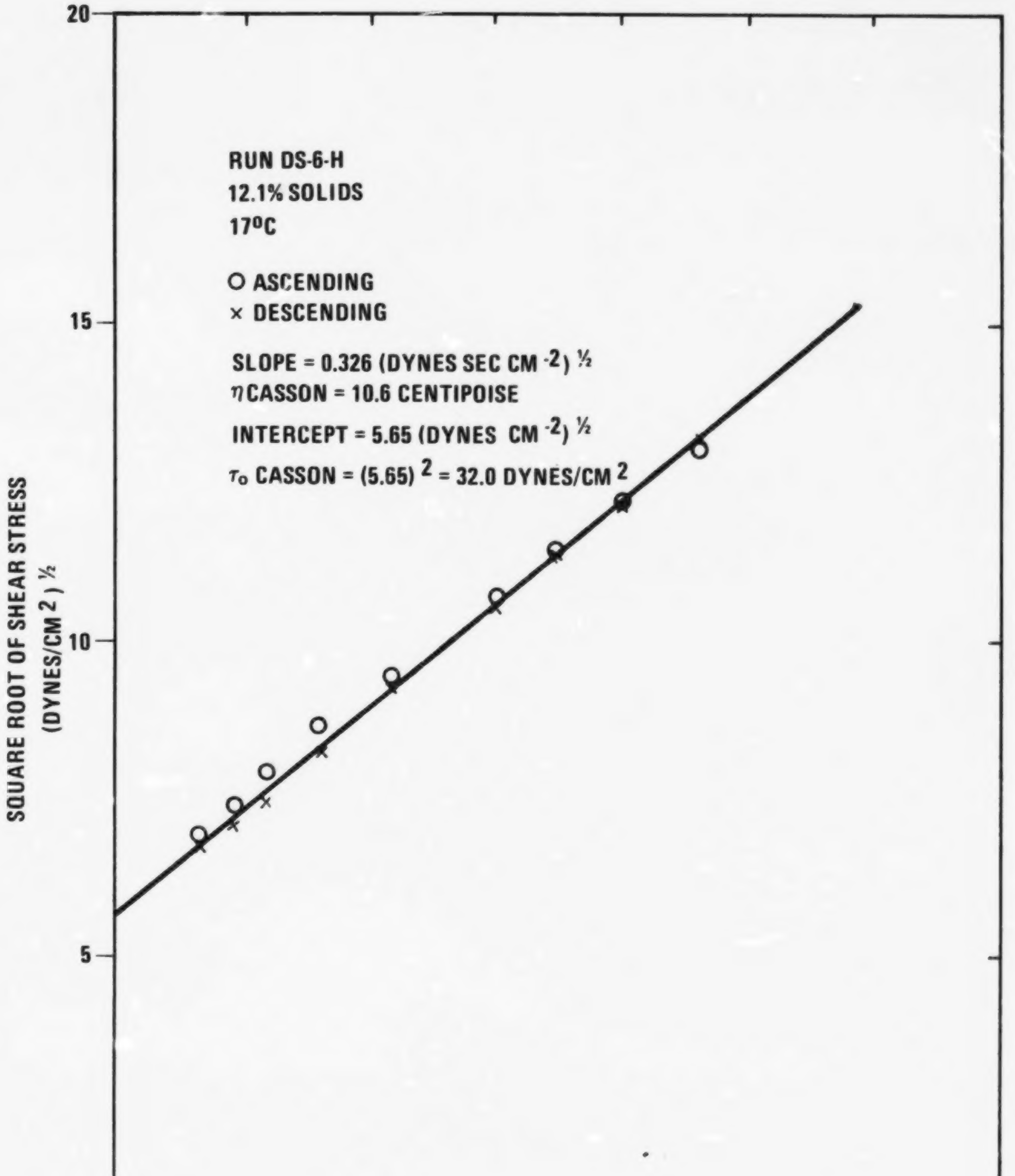

7.3 HYDRAULIC DATA

The hydraulic data from pipe tests on digested sewage sludge are presented in Figures 7-10 to 7-26. Complete run sheets for the large diameter pipe tests are given in Tables A-1 to A-3 in Appendix A.

7.3.1 Laminar Regime and Transition Velocity

Figure 7-10 shows a plot of pipewall shear stress versus velocity for 12-inch and 16-inch pipe data for Run DS-1-H (3.5 percent solids). The data show that in the lower velocity range, the pipe flow was in the laminar regime. Also shown is the shear stress/velocity curve predicted by the Buckingham equation for Bingham plastics, which is given in Section 3, Equation 3, as

$$\frac{8V}{D} = \frac{\tau_w g_c}{\eta}\left[1-\frac{4}{3}\left(\frac{\tau_o}{\tau_w}\right)+\frac{1}{3}\left(\frac{\tau_o}{\tau_w}\right)\right]^4$$

It can be seen that the predicted shear stresses in the laminar regime are some 20 to 30 percent lower than the observed values.

The transition from turbulent flow to laminar flow for this system can be identified from the data as taking place at 2.2 ft/sec. The use of the correlation proposed by Hedstrom (Ref. 18), modified as described in Section 3, results in a prediction of 2.2 ft/sec for the critical velocity, which is in agreement with the observed critical. The intersection of the predicted curve for the laminar regime with the predicted curve for the turbulent regime (discussed

FIGURE 7-10

SHEAR STRESS vs. VELOCITY
SOUTHERLY DIGESTED SLUDGE

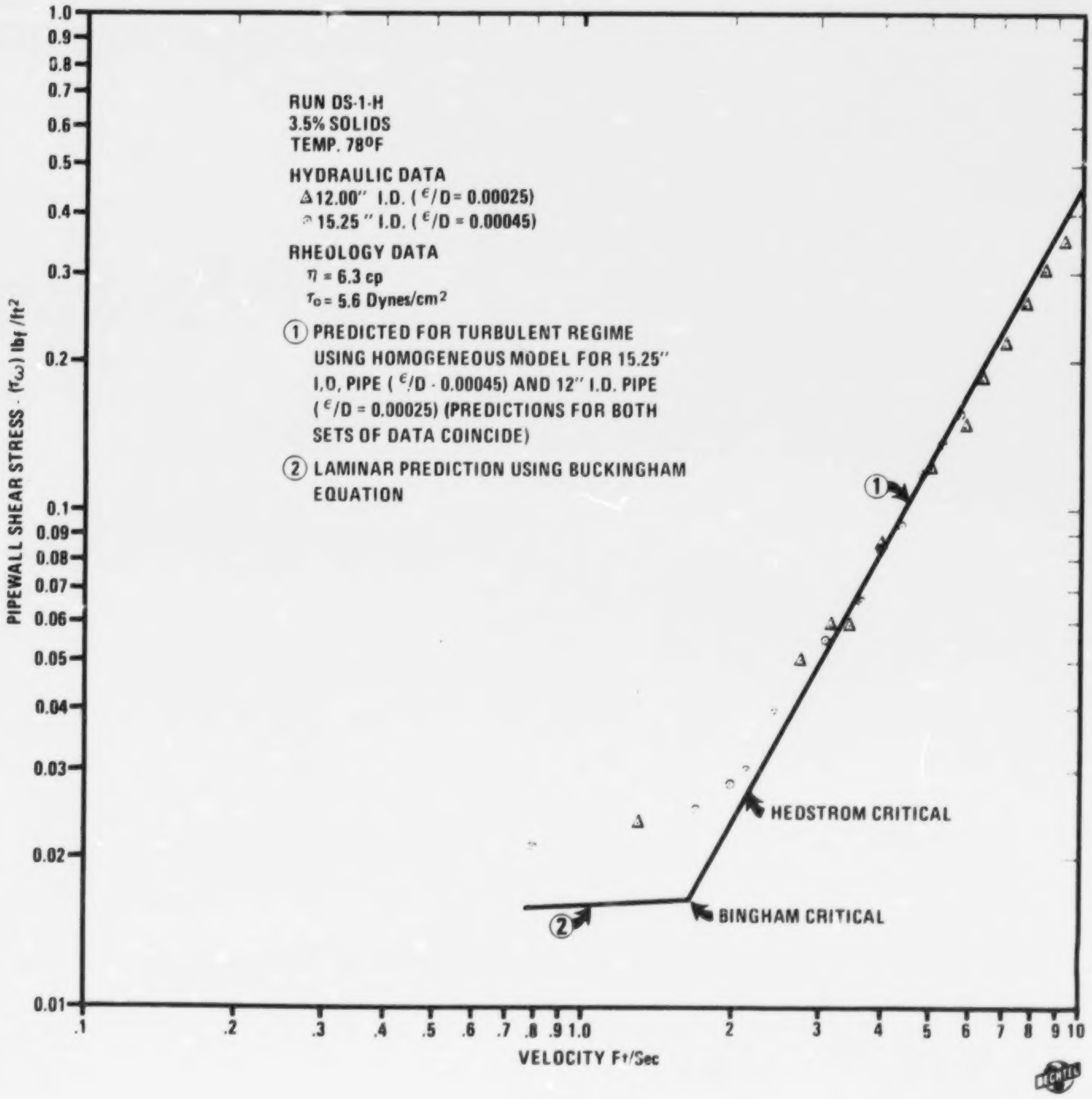

FIGURE 7-11

FRICTION FACTOR vs. REYNOLDS NUMBER
SOUTHERLY DIGESTED SLUDGE

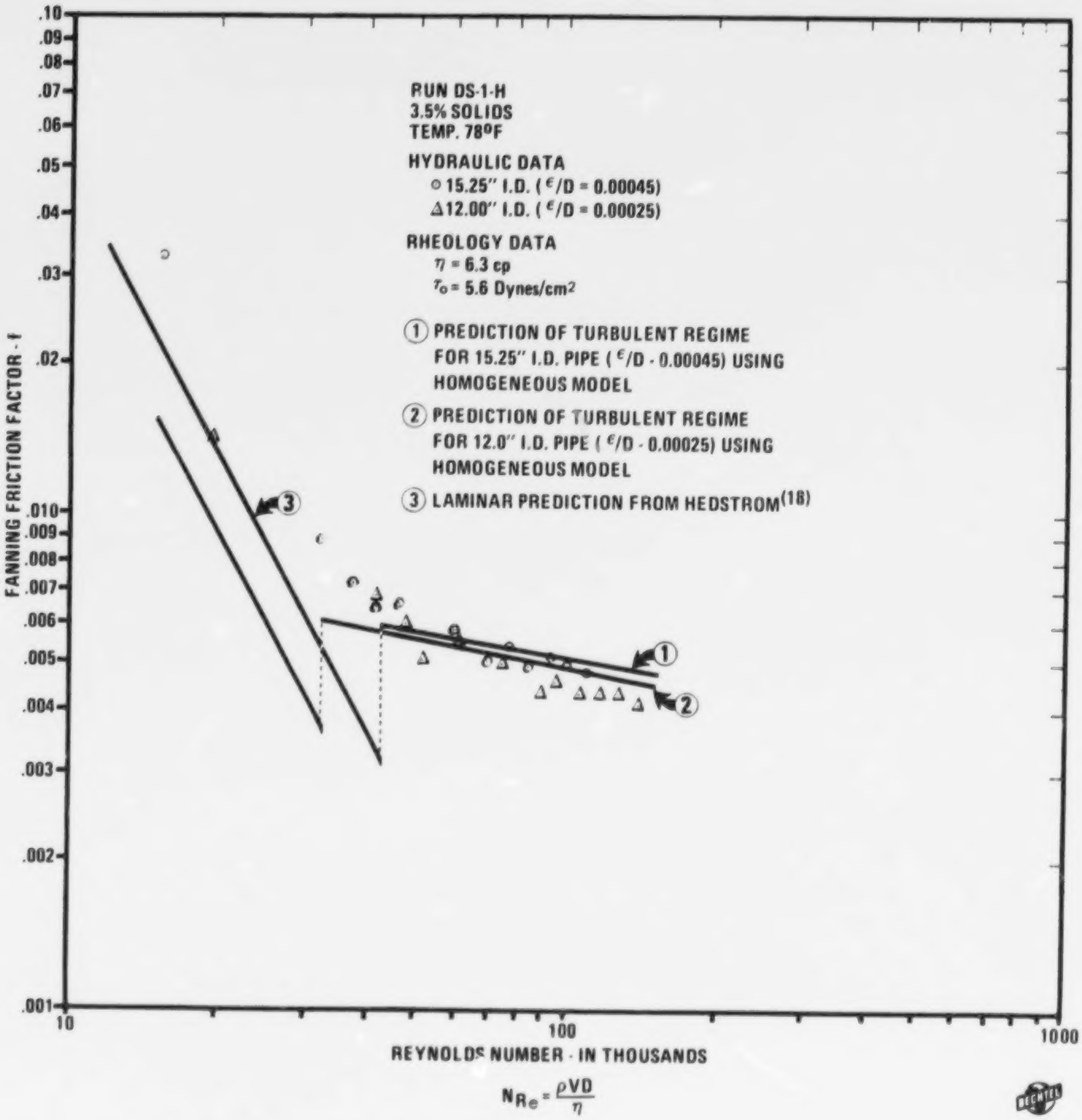

FIGURE 7-12

FRICTION FACTOR vs. REYNOLDS NUMBER
SOUTHERLY DIGESTED SLUDGE

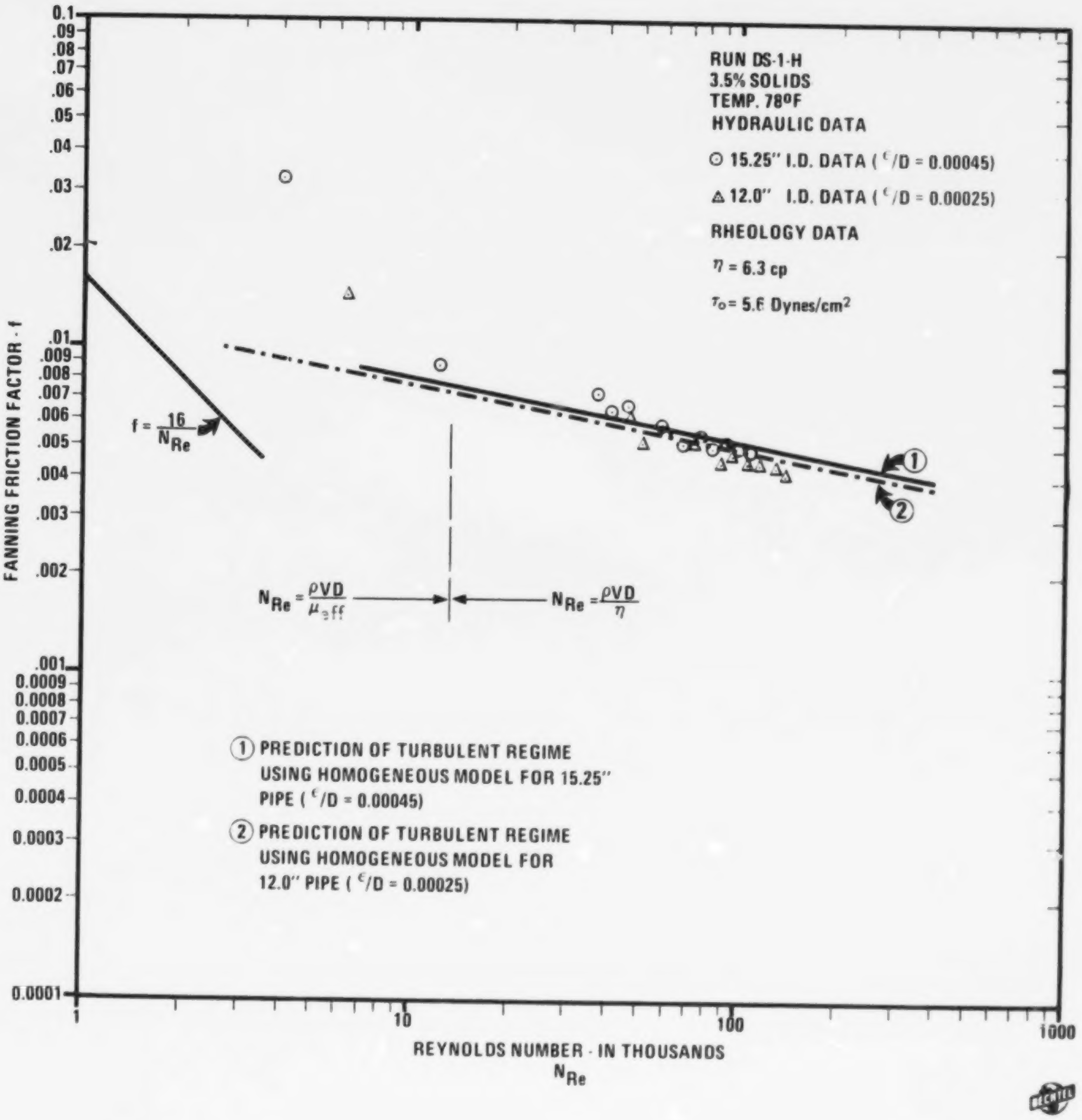

FIGURE 7-13

FRICTION FACTOR vs. REYNOLDS NUMBER
SOUTHERLY DIGESTED SLUDGE

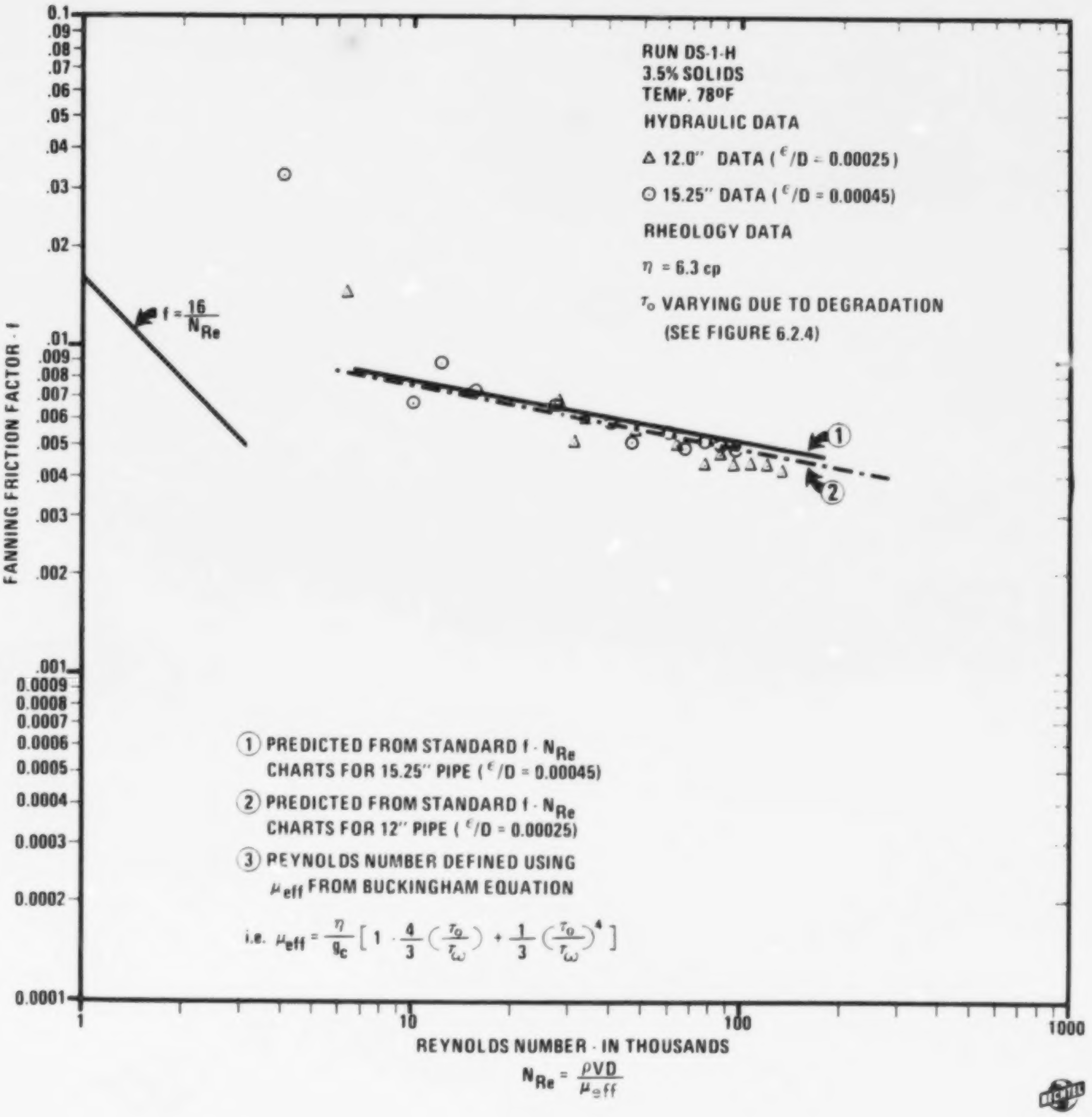

FIGURE 7-14

SHEAR STRESS vs. VELOCITY
SOUTHERLY DIGESTED SLUDGE

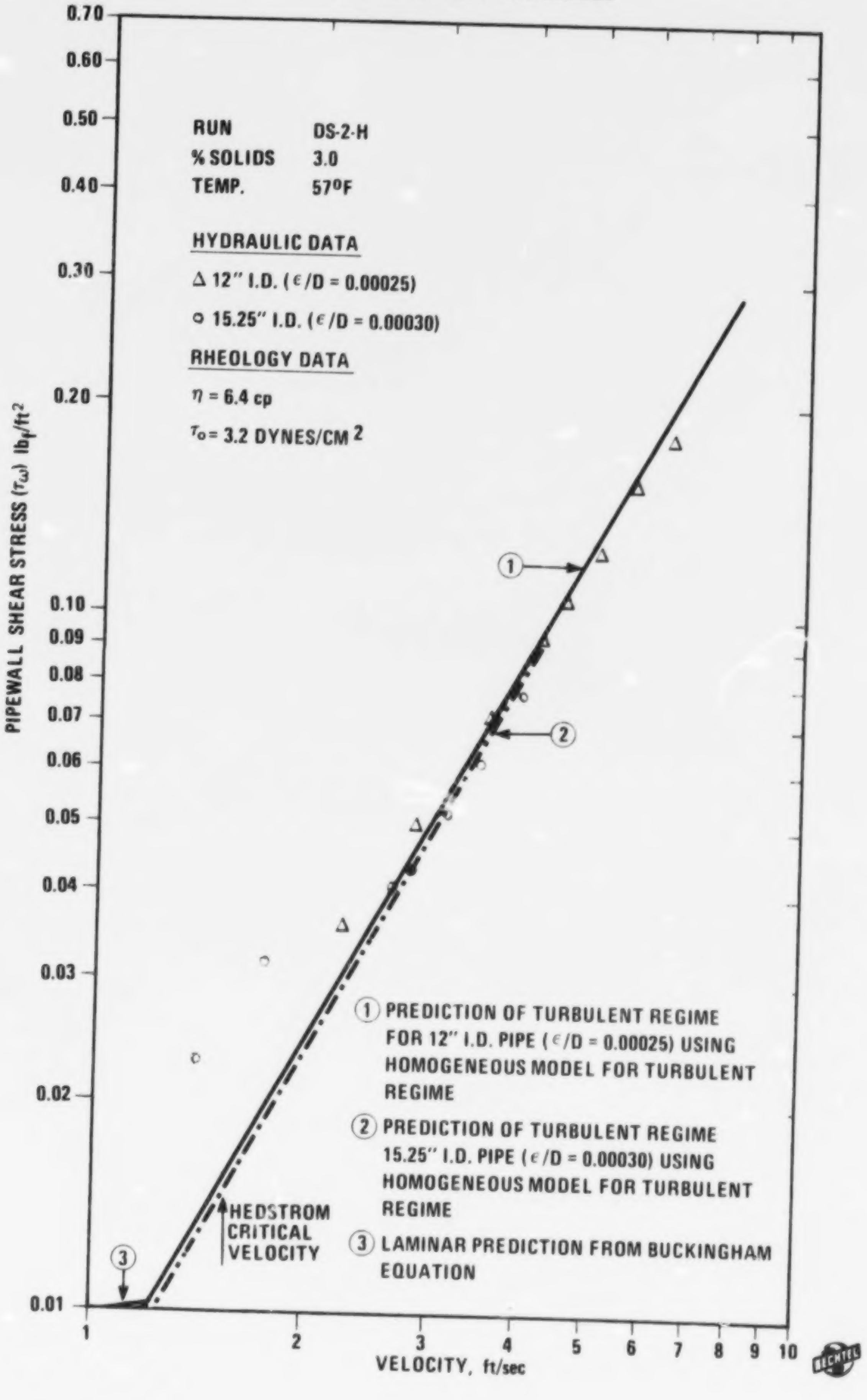

FIGURE 7-15

FRICTION FACTOR vs. REYNOLDS NUMBER
SOUTHERLY DIGESTED SLUDGE

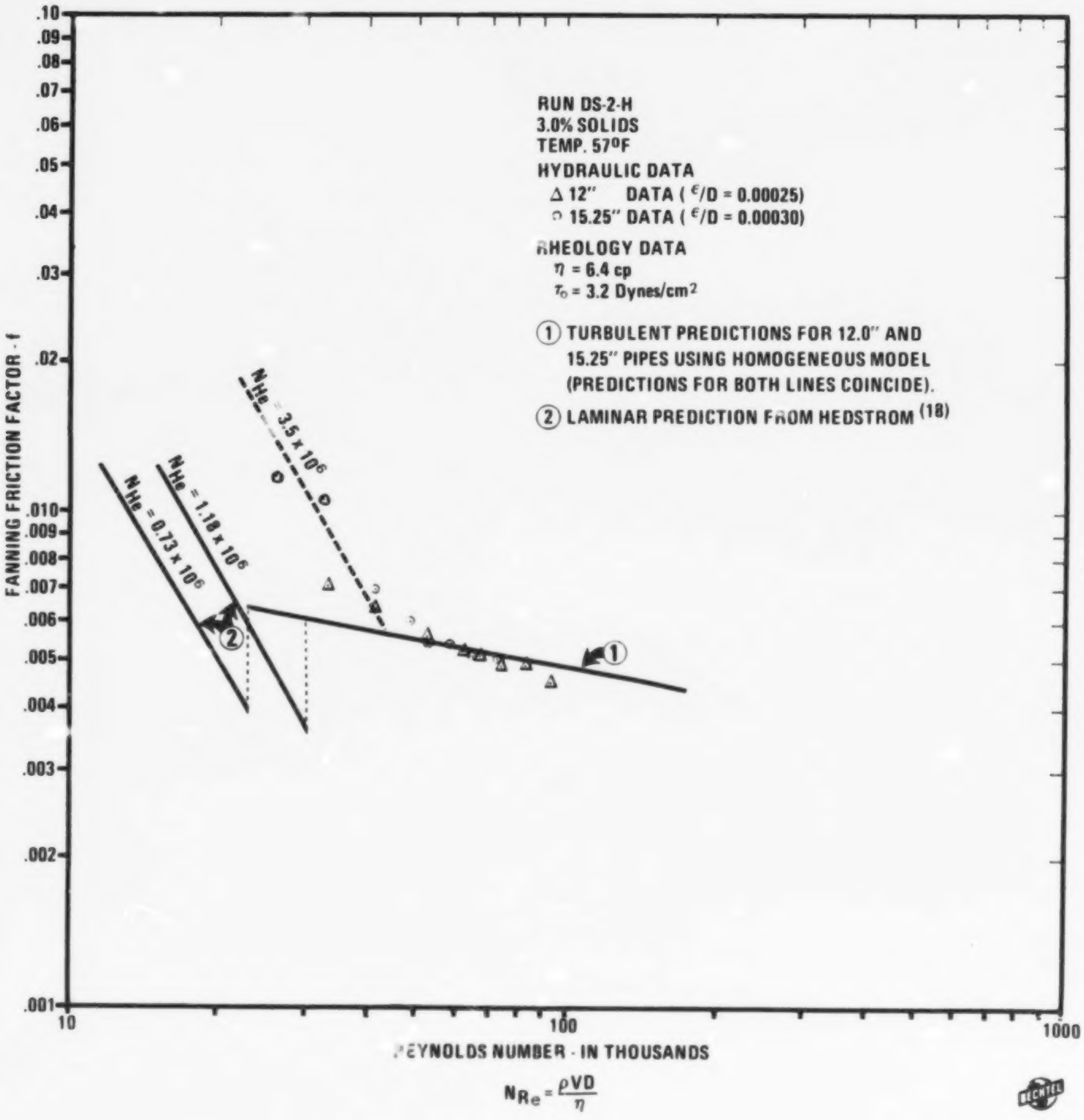

FIGURE 7-16

ROTATIONAL VISCOMETER RHEOGRAM FOR
PSEUDOPLASTIC PARAMETERS

SOUTHERLY DIGESTED SLUDGE

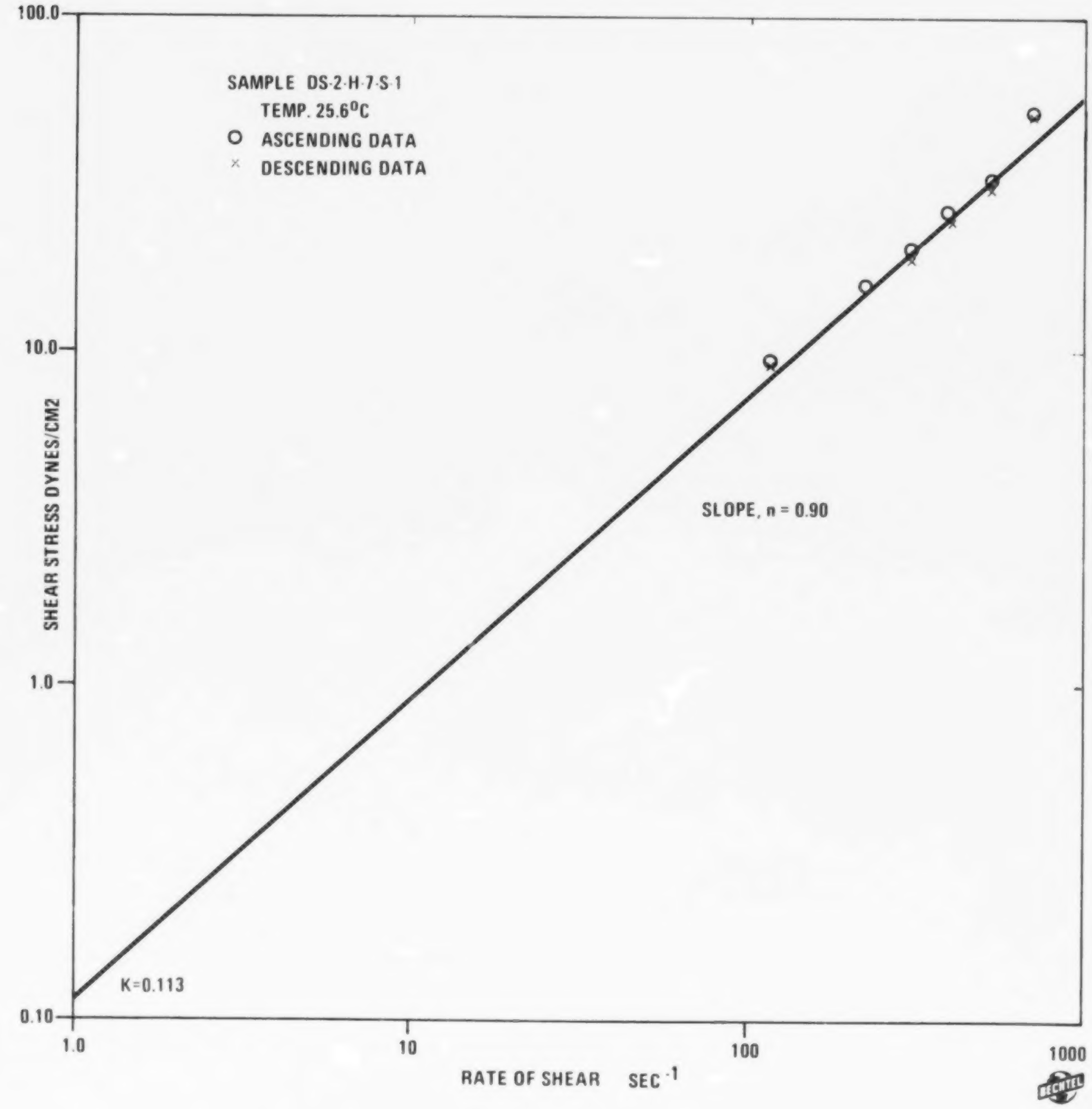

FIGURE 7-17

SHEAR STRESS vs. VELOCITY

SOUTHERLY DIGESTED SLUDGE

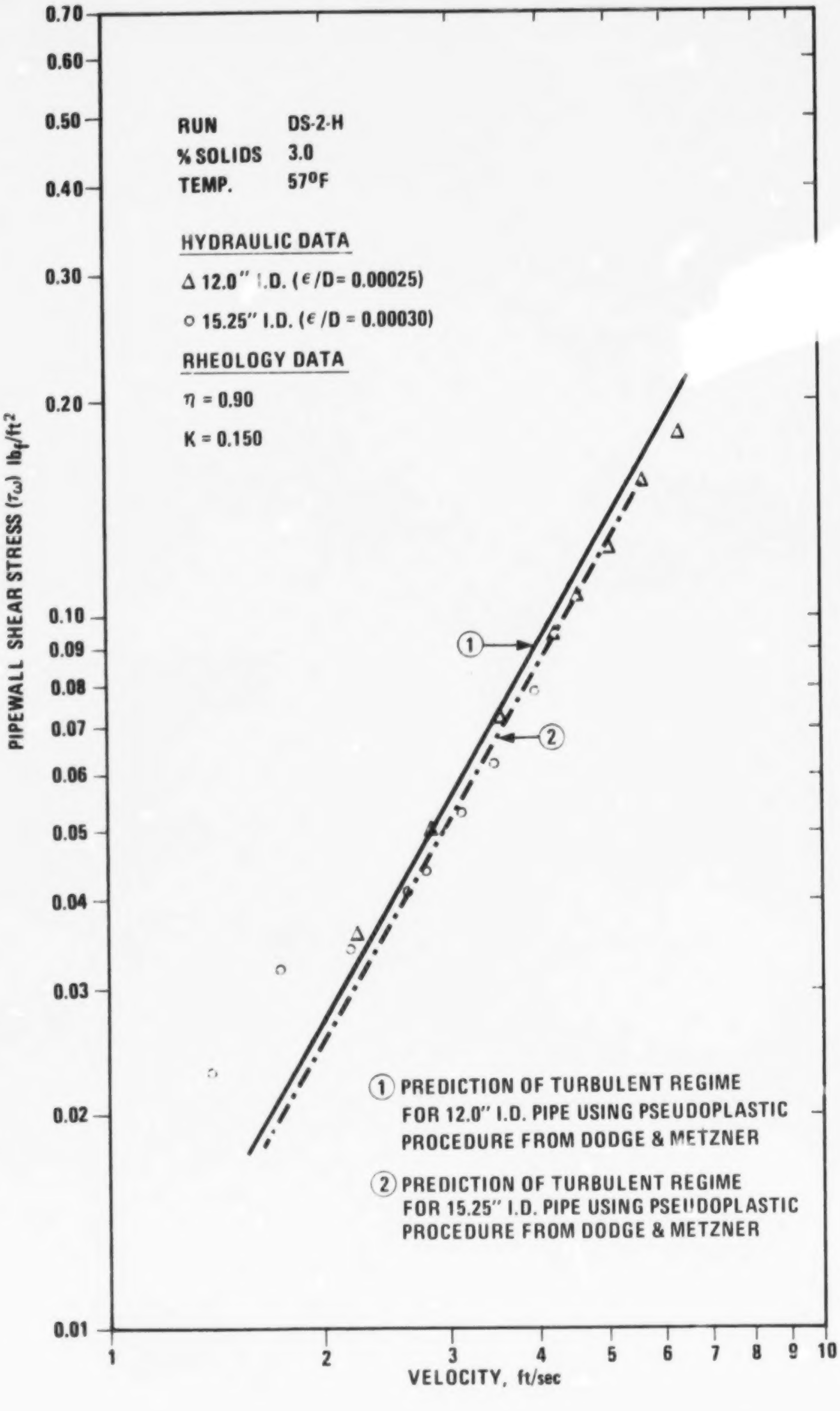

FIGURE 7-18
SHEAR STRESS vs. VELOCITY
SOUTHERLY DIGESTED SLUDGE

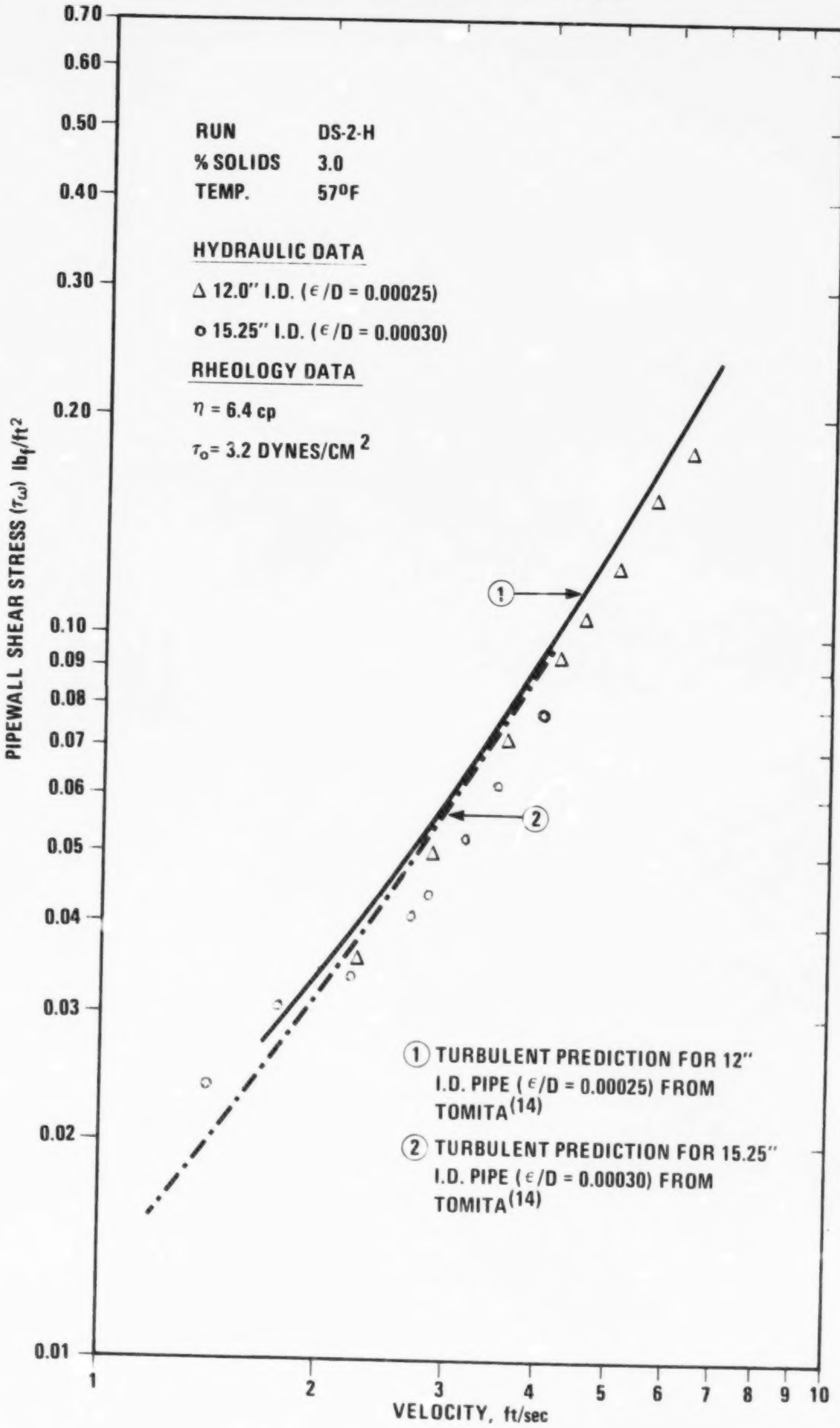

FIGURE 7-19
SHEAR STRESS vs. VELOCITY
SOUTHERLY DIGESTED SLUDGE

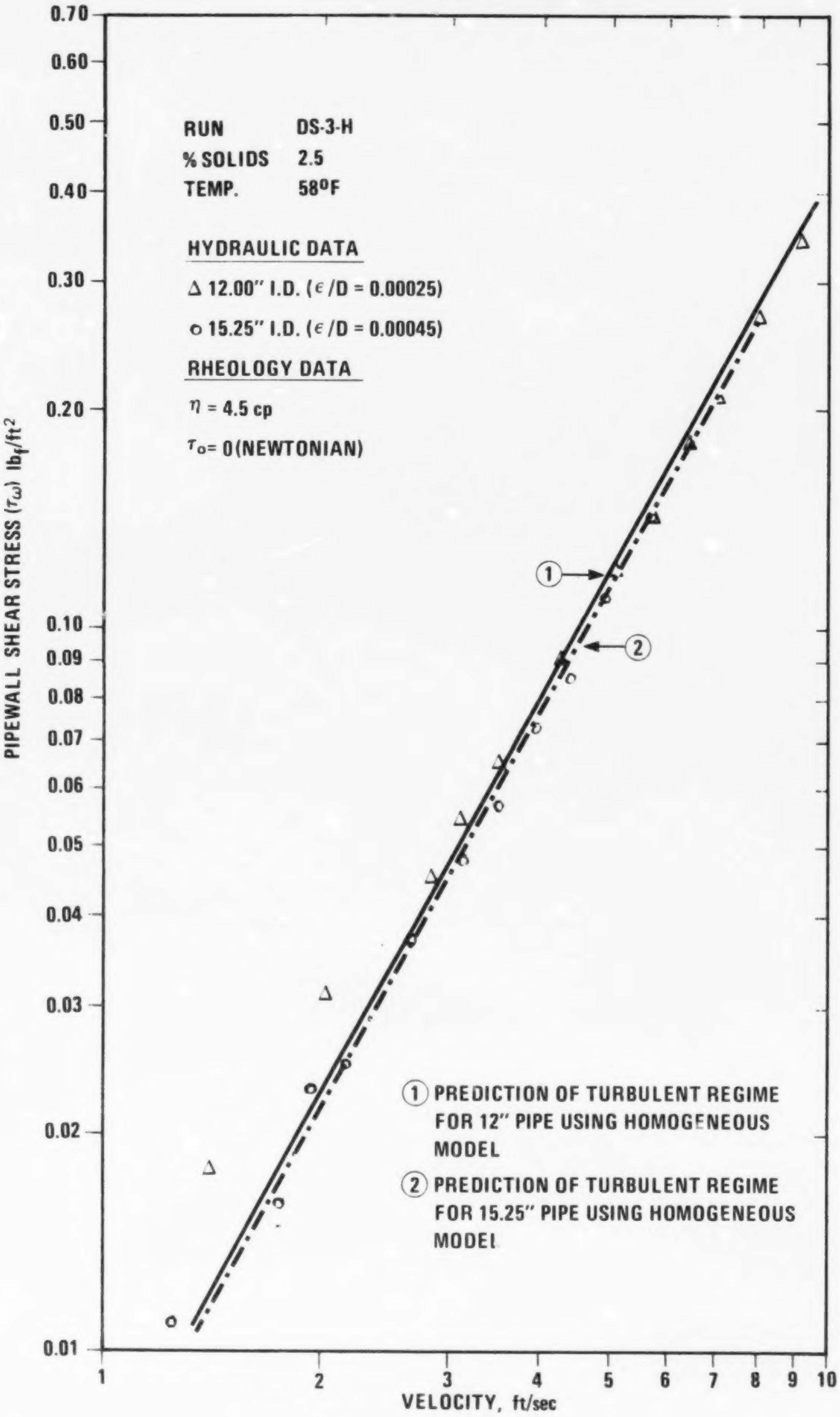

FIGURE 7-20

FRICTION FACTOR vs. REYNOLDS NUMBER
SOUTHERLY DIGESTED SLUDGE

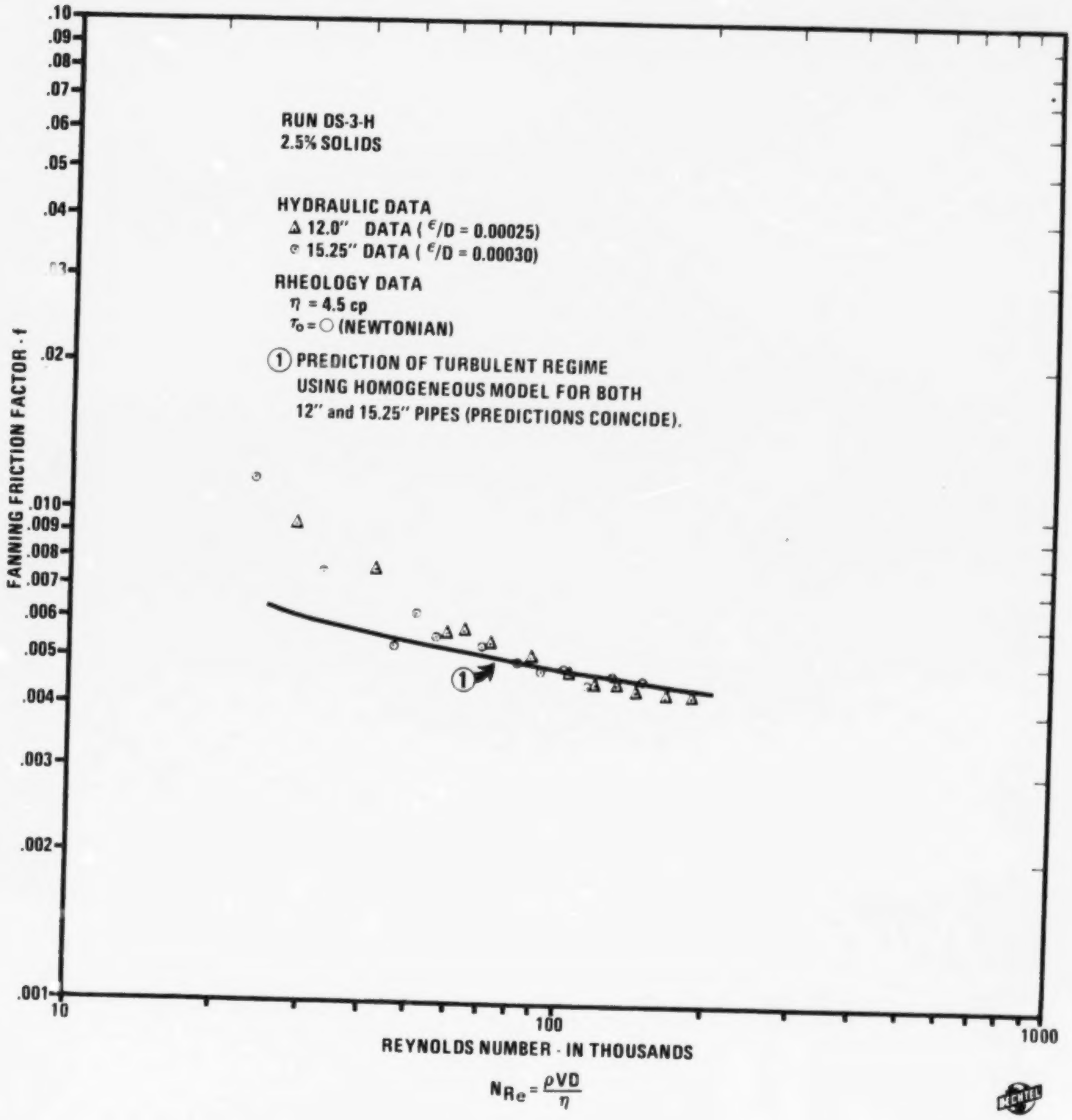

FIGURE 7-21

SHEAR STRESS vs. VELOCITY
DIGESTED SLUDGE

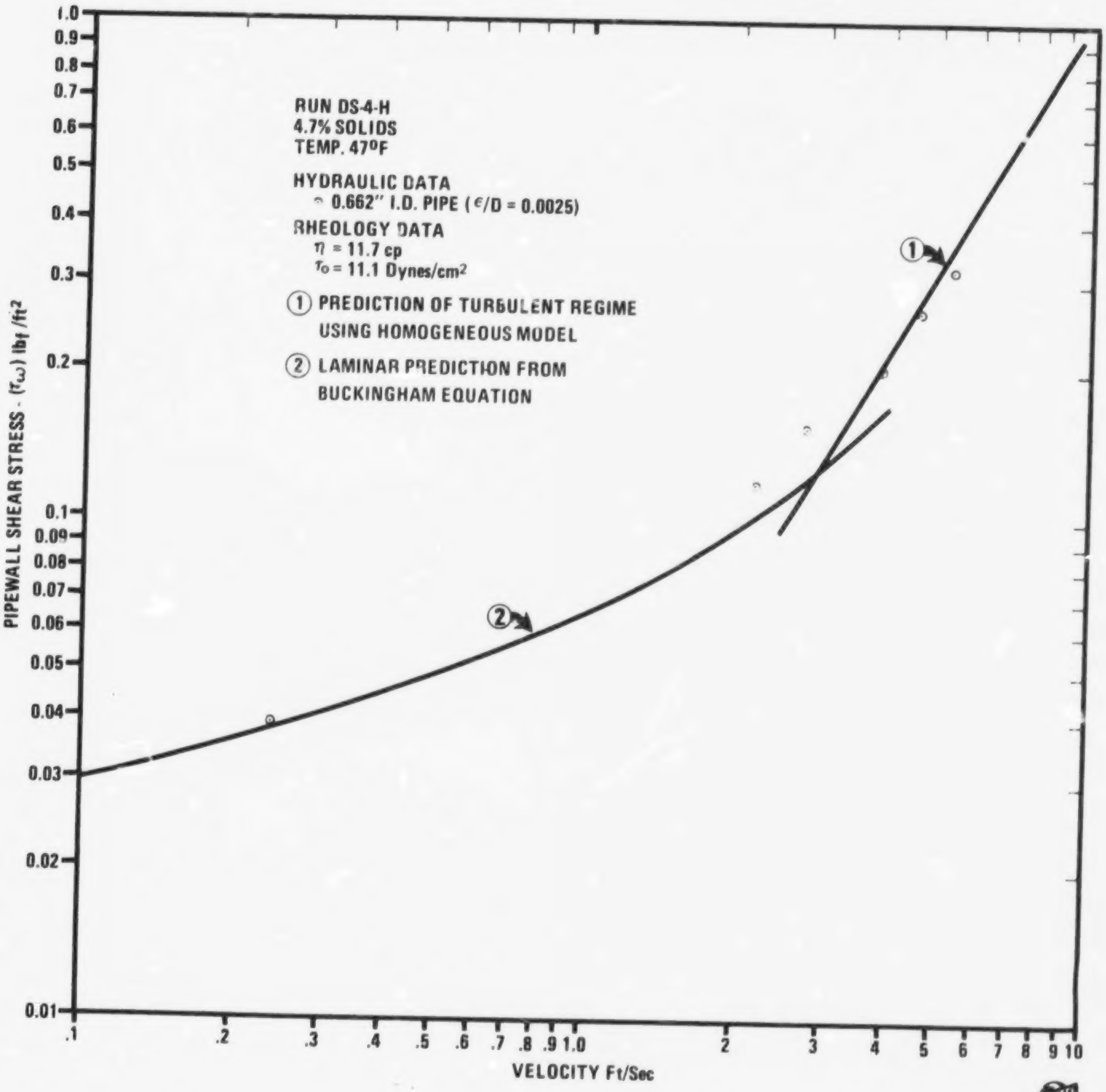

FIGURE 7-22
FRICTIONFACTOR vs. REYNOLDS NUMBER
DIGESTED SLUDGE

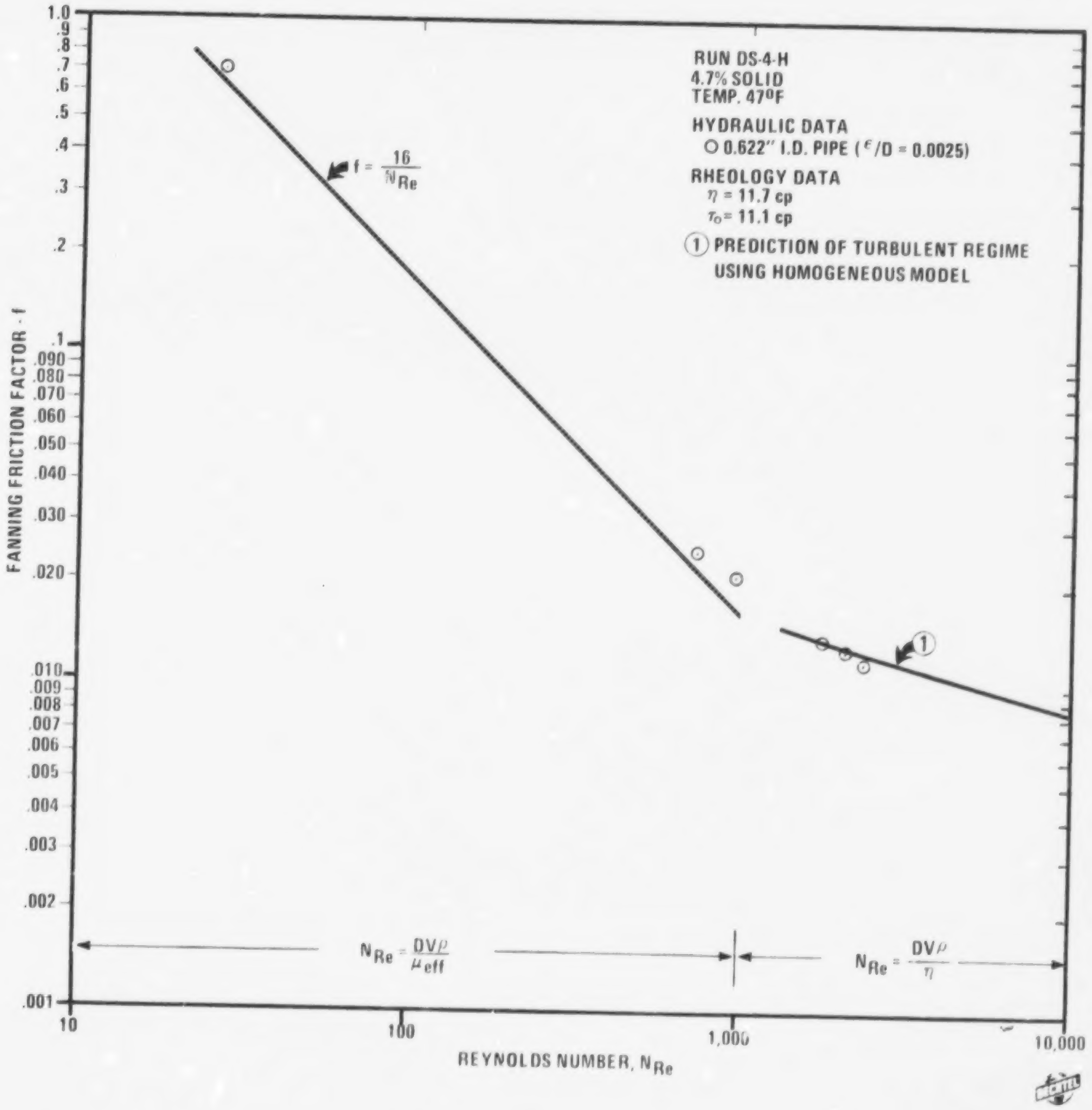

FIGURE 7-23
FRICTION FACTOR vs. REYNOLDS NUMBER
DIGESTED SLUDGE

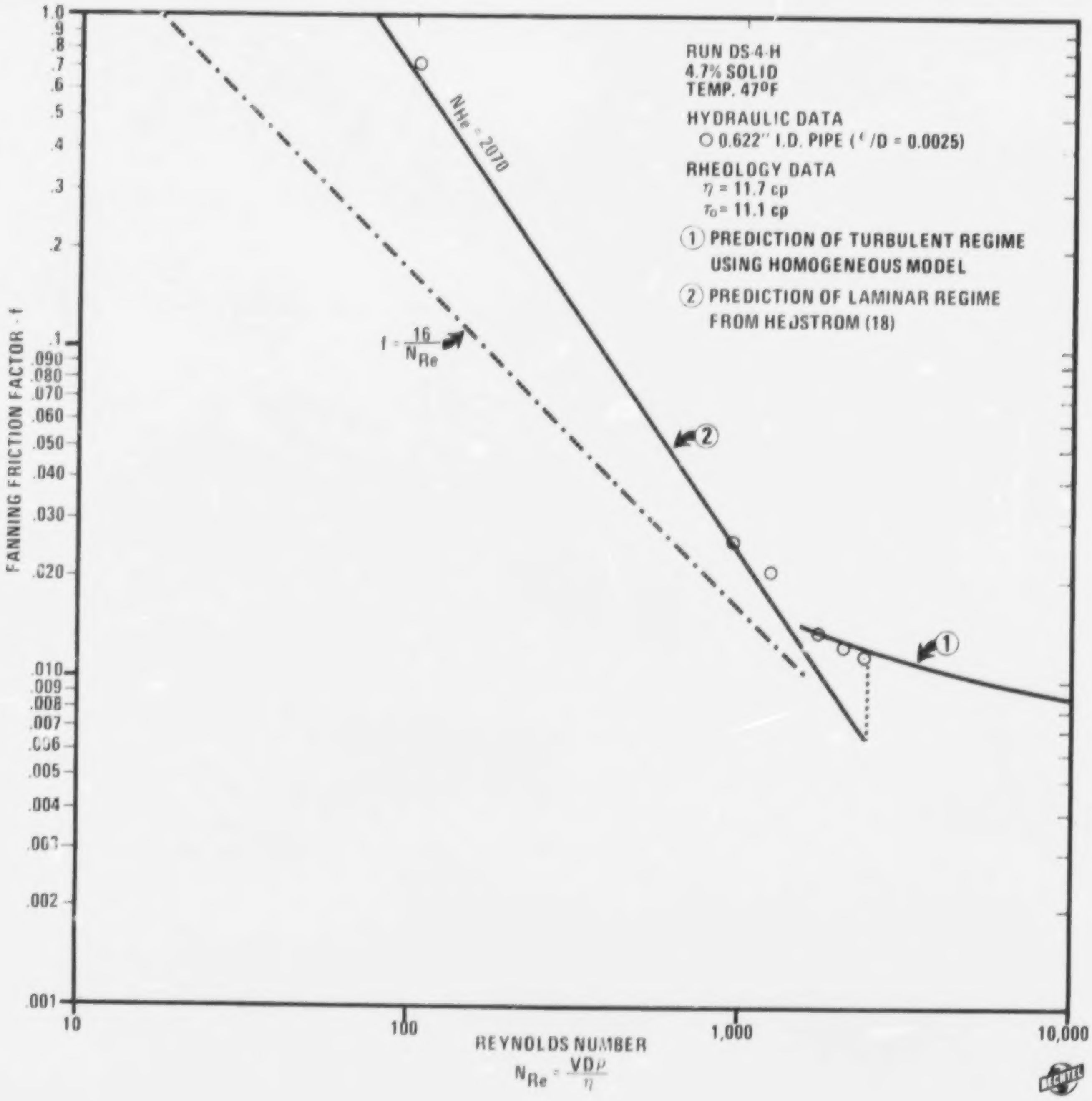

FIGURE 7-24

SHEAR STRESS vs. VELOCITY
DIGESTED SLUDGE

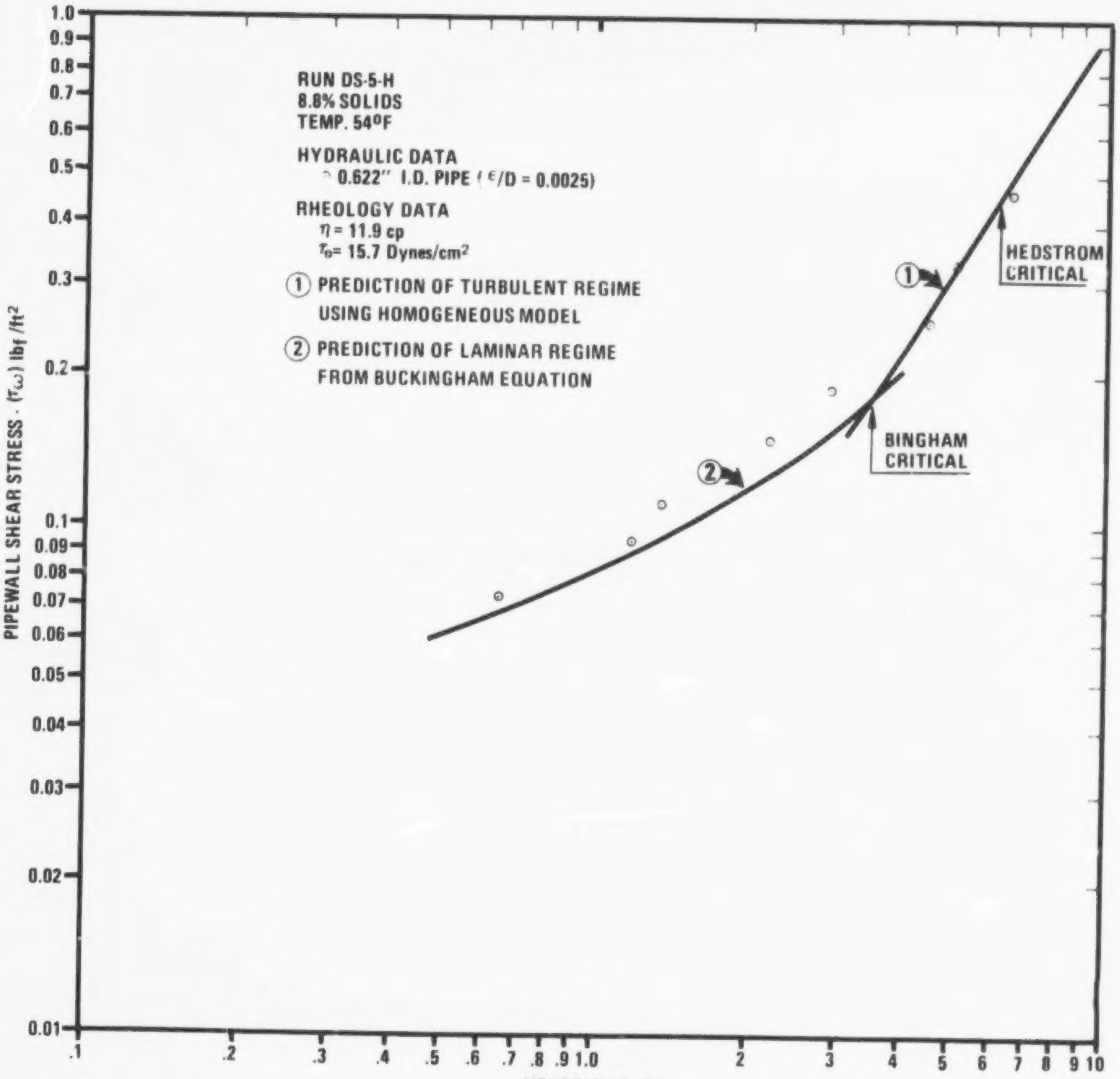

FIGURE 7-25
FRICTION FACTOR VS REYNOLDS NUMBER
DIGESTED SLUDGE

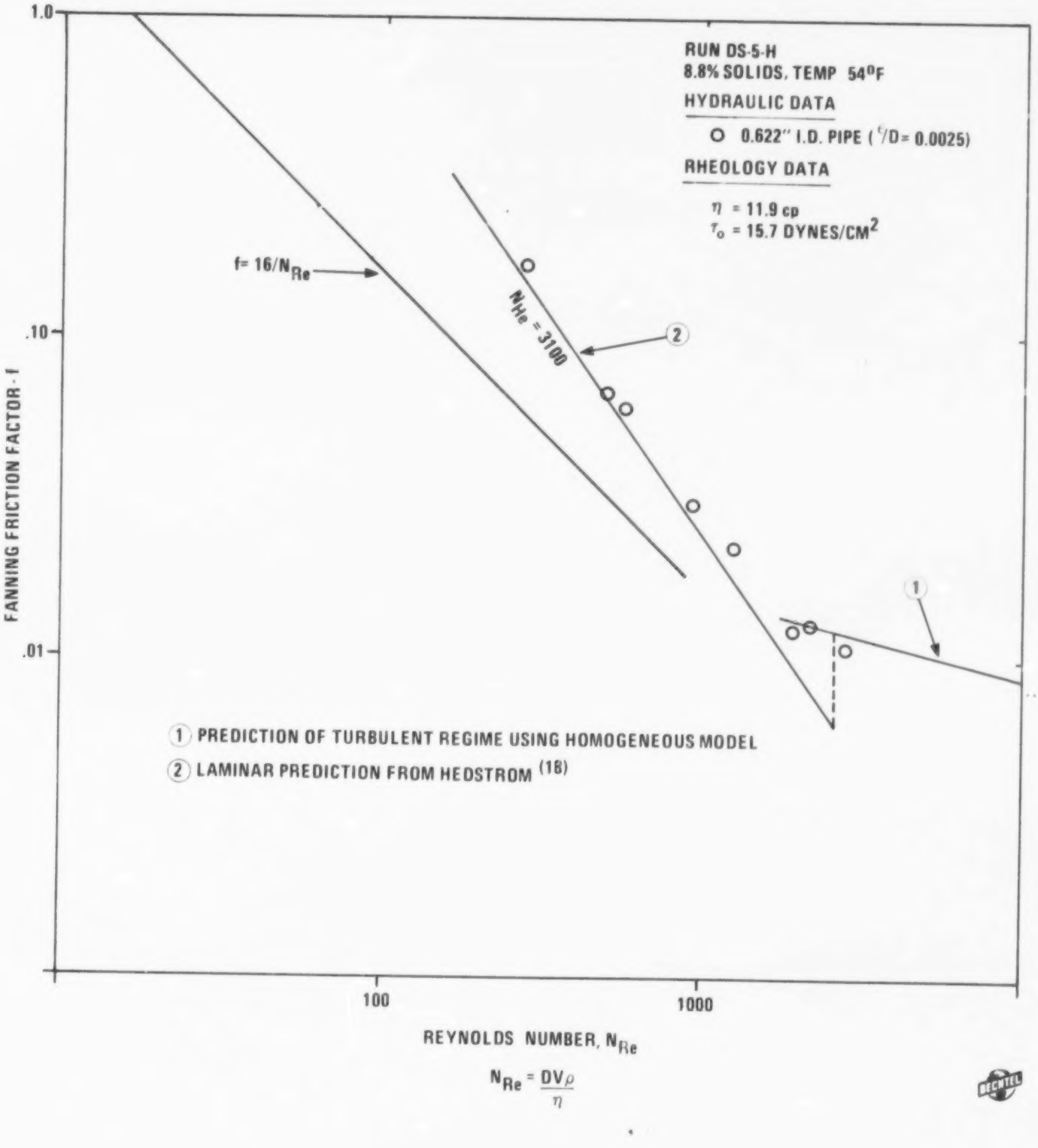

FIGURE 7-26

SHEAR STRESS vs. VELOCITY
DIGESTED SLUDGE

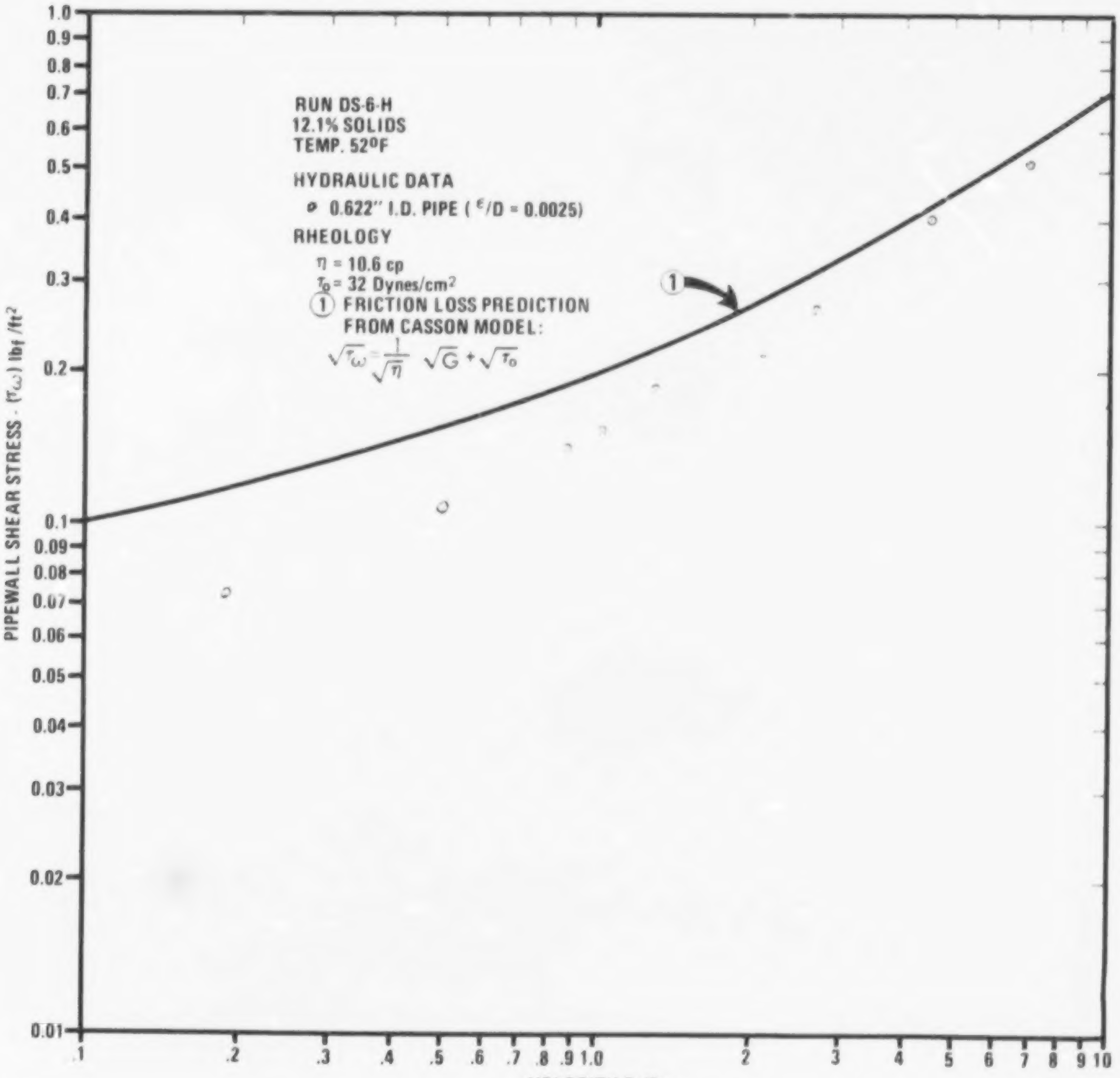

later), also yields a calculated critical velocity (which will be referred to here as the Bingham critical velocity). The predicted Bingham critical can be seen from Figure 7-10 to be at 1.65 ft/sec. The advantage of the Hedstrom correlation for the prediction of transition is clearly seen. The following table shows that for each of the sludges tested the critical velocity as predicted by the Hedstrom correlation was more conservative than the Bingham critical.

Run No.	Solids Concentration (Percent)	Critical Velocity (ft/sec) Observed	Hedstrom	Bingham
DS-1-H	3.5	2.2	2.2	1.65
DS-2-H	3.0	2.0	1.6	1.25
DS-3-H	2.5	Newtonian	-	-
DS-4-H	4.7	3.7	5.7	2.90
DS-5-H	8.8	5.1	6.2	3.40

Figure 7-26 shows the 1/2-inch pipe data for Run DS-6-H (12.1 percent solids). The pipewall shear stress/velocity curve was predicted using the Casson half-power model:

$$\sqrt{\tau_w} = \frac{1}{\sqrt{\eta}} \sqrt{G} + \sqrt{\tau_o}$$

The Casson correlation gives good prediction of the data in higher velocities, but is unsatisfactory at velocities less than 1.0 ft/sec.

It is possible that thick sludges are not best represented by a half-power Casson, but by a different power function. This could be highly variable for different sludges, and any particular case should be thoroughly examined to determine the correct rheological model.

Figures 7-11 and 7-12 show the data for Run DS-1-H plotted as Fanning friction factor versus Reynolds Number, and from these curves, a comparison of predictions of the laminar data using both the Bingham and Hedstrom correlations can be obtained. From the Buckingham equation, an effective laminar viscosity can be obtained, as follows:

$$\mu_{eff} = \frac{\tau_w}{(8V/D)} = \frac{\eta}{g_c}\left[1 - \frac{4}{3}\left(\frac{\tau_o}{\tau_w}\right) + \frac{1}{3}\left(\frac{\tau_o}{\tau_w}\right)^4\right]$$

By definition, when the Reynolds Number is defined using μ_{eff}, the laminar data should fall on the usual Newtonian line, $f = 16/N_{Re}$. As shown in Figure 7-12, this correlation was not achieved. The Hedstrom correlation (Figure 7-11) is a much closer representation of the measured data. The discontinuity between laminar and turbulent predictions shown in Figure 7-11 is due to the empirical modification (described in Section 3) to the Hedstrom correlation.

Friction factor/Reynolds Number curves are included for the other runs. Figures 7-23 and 7-25 show excellent correlation of laminar data for thicker sludges (4.7 and 8.8 weight percent solids) using the Hedstrom procedure.

7.3.2 Turbulent Regime

The homogeneous model described in Section 4 gives excellent correlation of turbulent flow data for a wide range of concentrations and pipe diameters.

Reference to Figure 7-10 shows that both the 12-inch and 16-inch pipe data are correlated by a single line. Normally a τ_w versus velocity plot would show a diameter effect; namely, for the same velocity the smaller diameter pipe would exhibit a larger shear stress. However, in this case, the 16-inch pipe was considerably rougher than the 12-inch pipe (ϵ/D of 0.00045 vs ϵ/D of 0.00025). The increased roughness resulted in pressure drops which obliterate the diameter effect.

It should be noted that the pipe roughness affects the friction losses in a non-Newtonian pipe system just as in a Newtonian system. In applying the homogeneous model to the data, the pipe roughnesses (as given by water runs) were accounted for using the conventional friction factor Reynolds Number charts.

A comparison between Figures 7-10 and 7-11 clarifies this point. It should be pointed out that between these two runs tests were made with fly ash slurry. The abrasive nature of this slurry caused a significant decrease in the roughness of the 16-inch test section (See Appendix A). For Run DS-2-H, the relative roughness of the 16-inch section was 0.00030, much closer to that of the 12-inch section than in DS-1-H. As discussed earlier, the higher roughness in the

16-inch pipe caused the 12 and 16-inch data for Run DS-1-H to fall on a single line. The homogeneous model duplicates this effect. From Figure 7-11, it can be seen that due to the decrease in roughness in the 16-inch section, for Run DS-2-H there is a spread between the 16-inch and 12-inch data. Again the homogeneous model predicts this effect.

The pipewall shear stress-velocity data show that in the turbulent regime, the data fall on a straight line, indicating a constant turbulent viscosity. In Figure 7-12, once turbulent flow is established (by the Hedstrom critical velocity), the Reynolds Number is redefined as $N_{Re} = \rho VD/\eta$, as opposed to the laminar Reynolds Number of $\rho VD/\mu_{eff}$. Excellent correlation of turbulent data is achieved using the constant viscosity. Figure 7-13 is included for illustrative purposes, and shows the effect of using a varying effective viscosity μ_{eff} to define Reynolds Number in the turbulent regime. Much poorer correlation is obtained by this definition of viscosity, and the advantage of using the coefficient of rigidity as a constant turbulent viscosity is clearly shown.

Friction factor /Reynolds Number plots are given for the other runs. It should be noted that a single prediction curve correlates both the 16 and 12-inch data for Runs DS-2-H and DS-3-H (Figures 7-15 and 7-20) due to the closeness of the pipe roughnesses.

For the purpose of comparison with the homogeneous design procedure proposed in this report, two other well known correlation mechanisms have been applied to the data for Run DS-2-H (3.0 percent solids).

Figure 7-17 shows a data correlation using the pseudoplastic model, based on the Ostwald-de Waele equation

$$\tau = K \left(\frac{dU}{dr} \right)^n$$

The rheological parameters of consistency, K, and flow index, η are established by a plot of the rotational viscometer data as shown in Figure 7-16. The consistency factor is temperature corrected to the flowing conditions as follows:

$$K \text{ (pipe)} = K \text{ (viscometer)} \times \frac{\mu \text{ (at pipe temperature)}}{\mu \text{ (viscometer temperature)}}$$

where μ is the viscosity of water.

Figure 7-17 shows that this correlation also gives good prediction of the data. Reference to Table 7-3 will show that although the method results in larger deviations from the observed data than does the homogeneous method, the pseudoplastic model shows a more uniform deviation from reality. That is, it is a slightly better representation of the slope of the friction loss/velocity curve than the homogeneous model.

However, the method is rather clumsy inasmuch as the flow parameters have no immediate physical significance and because accounting for pipe roughness is more of the nature of the estimation. This latter point is illustrated by the larger spread in the 12-inch and 16-inch correlation lines in Figure 7-17 as compared to Figure 7-14.

Figure 7-18 is a correlation of Run DS-2-H using the procedure proposed by Tomita (Ref. 14) (See Section 3). The method predicts high values of shear stress, but as can be seen from Table 7-3, the correlation is an excellent representation of the shape of the friction loss/velocity curve. However, Tomita's correlation exhibits a diameter effect since the correlation of the 16-inch data is much worse than that of the 12-inch data.

In the use of the homogeneous model, it has been assumed there are no turbulence damping effects in this system, and this assumption is borne out by the results. It can be said that at velocities greater than the Hedstrom critical, the homogeneous model is wholly adequate as a commercial pipeline design procedure.

Tables 7-2, 7-3 and 7-4 show comparison of friction losses predicted by all three procedures and the measured values.

The small pipe tests were conducted mainly in the laminar regime, but the homogeneous model is in good agreement with the turbulent and transition data (See Figures 7-21 and 7-24).

Table 7-2

TURBULENT CORRELATION OF DS-1-H USING HOMOGENEOUS MODEL

Line No.	Velocity ft/sec	ΔpObs (psi/200')	τ_wObs (lb/ft^2)	τ_wCalc (lb/ft)	Percent Deviation
12 Inch Data					
1	3.45	0.33	0.059	0.063	+ 6.8
2	5.90	0.83	0.149	0.168	+12.7
3	7.10	1.20	0.216	0.236	+ 9.3
4	8.50	1.70	0.306	0.328	+ 7.2
5	9.30	1.93	0.347	0.387	+11.5
6	7.80	1.45	0.261	0.280	+ 7.3
7	6.40	1.03	0.185	0.195	+ 5.4
8	5.00	0.68	0.122	0.124	+ 1.6
9	4.00	0.48	0.086	0.082	- 4.7
10	2.75	0.28	0.050	0.042	-16.0
11	1.30	0.13	0.023	Laminar Regime	
12	3.18	0.33	0.059	0.055	- 6.8
16 Inch Data					
1	2.15	0.13	0.030	0.027	-10.0
2	3.65	0.29	0.066	0.070	+ 6.1
3	4.40	0.41	0.094	0.098	+ 4.1
4	5.30	0.60	0.137	0.137	0.0
5	5.75	0.68	0.156	0.156	0.0
6	4.85	0.52	0.119	0.117	- 1.7
7	4.00	0.37	0.085	0.083	- 2.4
8	3.10	0.24	0.055	0.051	- 7.9
9	2.45	0.17	0.039	0.034	-12.8
10	1.70	0.11	0.025	Laminar Regime	
11	0.86	0.09	0.021	Laminar Regime	
12	1.96	0.12	0.027	Laminar Regime	

Table 7-3

TURBULENT CORRELATION OF DS-2

Line No.	Velocity (ft/sec)	τ_w Obs (lb/ft^2)	HOMOGENEOUS		PSEU
			τ_w Calc (lb/ft)	Percent Deviation	τ_w Ca (lb/ft
12 Inch Data					
1	5.7	0.155	0.158	+ 1.9	0.167
2	4.25	0.094	0.094	0.0	0.100
3	2.85	0.050	0.046	- 8.0	0.050
4	5.1	0.124	0.130	+ 4.8	0.137
5	6.4	0.180	0.196	+ 8.9	0.205
6	3.6	0.072	0.070	- 2.9	0.074
7	2.25	0.036	0.030	- 16.6	0.032
8	4.6	0.106	0.108	+ 1.9	0.114
16 Inch Data					
1	3.5	0.062	0.064	+ 3.2	0.066
2	2.65	0.041	0.039	- 4.9	0.041
3	1.75	0.032	0.019	Transition Zone	0.020
4	3.15	0.053	0.053	0.0	0.055
5	4.0	0.078	0.082	+ 5.1	0.083
6	2.2	0.034	0.028	- 17.7	0.030
7	1.4	0.023	0.013	Transition Zone	0.014
8	7.8	0.044	0.044	0.0	0.045

A

Table 7-3

CORRELATION OF DS-2-H

EOUS	PSEUDOPLASTIC		TOMITA	
Percent Deviation	τ_w Calc (lb/ft^2)	Percent Deviation	τ_w Calc (lb/ft^2)	Percent Deviation
+ 1.9	0.167	+ 7.7	0.170	+ 9.7
0.0	0.100	+ 6.4	0.103	+ 9.6
- 8.0	0.050	0.0	0.054	+ 8.0
+ 4.8	0.137	+ 10.5	0.140	+ 12.7
+ 8.9	0.205	+ 13.9	0.208	+ 15.6
- 2.9	0.074	+ 2.9	0.080	+ 11.1
- 16.6	0.032	- 11.1	0.040	+ 11,1
+ 1.9	0.114	+ 7.6	0.118	+ 11.3
+ 3.2	0.066	+ 6.5	0.074	+ 19.4
- 4.9	0.041	0.0	0.048	+ 17.1
Transition Zone	0.020	Transition Zone	0.027	Transition Zone
0.0	0.055	+ 3.8	0.063	+ 18.9
+ 5.1	0.083	+ 6.4	0.092	+ 12.2
- 17.7	0.030	- 11.8	0.037	+ 32.2
Transition Zone	0.014	Transition Zone	0.020	Transition Zone
0.0	0.045	+ 2.3	0.052	+ 19.1

B

Table 7-4

TURBULENT CORRELATION OF RUN DS-3-H USING HOMOGENEOUS MODEL

Line No.	Velocity (fps)	τ_w Observed (lb/ft^2)	τ_w Calculated (lb/ft^2)	Percent Deviation
12 Inch Data				
1	7.0	0.209	0.220	+5.3
2	5.7	0.142	0.149	+5.1
3	4.25	0.090	0.087	-3.3
4	2.85	0.045	0.042	-6.7
5	2.03	0.031	0.023	-25.8
6	3.50	0.065	0.063	-3.1
7	5.10	0.121	0.122	+0.8
8	6.4	0.180	0.188	+4.4
9	8.0	0.266	0.274	+3.0
10	9.1	0.344	0.357	+3.8
11	3.1	0.054	0.050	-7.4
12	1.4	0.018	0.012	Transition Zone
16 Inch Data				
1	4.4	0.085	0.093	+9.4
2	3.5	0.057	0.060	+5.3
3	2.65	0.037	0.036	-2.7
4	1.75	0.016	0.017	+6.2
5	1.25	0.011	0.009	-18.2
6	2.15	0.025	0.025	0.0
7	3.15	0.048	0.049	+2.1
8	3.95	0.073	0.071	-2.7
9	4.90	0.110	0.113	+2.7
10	5.65	0.142	0.143	+0.7
11	1.94	0.023	0.020	-13.1
12	0.90	0.009	0.005	Transition Zone

Section 8
PIPE TESTS ON FLY ASH SLURRIES

8.1 PIPELINING OF FLY ASH SLURRIES

The tests performed on fly ash slurries are listed in Table 8-1 and are discussed in detail in the following paragraphs.

8.1.1 Hydrodynamics

The hydraulic data for fly ash slurries can be represented by a homogeneous model subject to certain limitations. The data from these tests show that the presence of the solid particles results in damping of turbulence in the system; hence, a true Newtonian prediction gives high values of friction losses. However, for the thicker slurries tested, this damping was of the order of five percent in the range of Reynolds Numbers of interest to commercial pipelining. Data for a 53 percent slurry show a deviation of some 13 percent between predicted and observed friction factors. However, this large deviation is due more to dilution of the slurry because of solids settling in the line than to turbulent dampening. Previous data (Ref. 43) has shown that damping of turbulence is increased as solids concentration increases.

Also, the minimum transport velocity for the dilute slurry is controlled by sedimentation (Durand critical) rather than laminar turbulent (Reynolds) transition. This precludes the use of the Hedstrom criterion for prediction of critical velocity. On this basis, the use of the homogeneous model is not recommended for slurries of less than 57 percent by weight of solids.

Table 8-1

LIST OF TESTS ON FLY ASH SLURRIES

RUN NO.	SOLIDS CONC (percent by weight)	PIPE I.D. (Inches)
FW-1-H	52.8	15.25, 12.0, 0.622
FW-4-H	57.4	15.25, 12.0
FW-5-H*	57.0	15.25, 12.0
FW-1-O**	52.8	15.25, 12.0

* With the addition of thinning agent, Orzan AL-50.

** Operability Test.

The addition of a thinning agent results in a lower system viscosity, and hence lower friction losses. As an order of magnitude comparison, the addition of Orzan reduced the friction losses for a 57 percent slurry to the level measured for a 53 percent slurry.

8.1.2 Operability

Data are shown in paragraph 8.4 for a startup test performed on 53 percent fly ash slurry. It should be noted that due to operational difficulties immediately prior to shutdown, the loop was run at very low velocities (1 to 2 feet per second) for some 90 minutes and so the startup test cannot be considered representative.

As can be seen from the data, the solids were not re-suspended during the operability test. This was probably due to the fact that during the low velocity period the coarser solids settled in the pipe, forming a tightly packed bed. However, this situation would not be encountered in a commercial shutdown situation, where operating velocities of 5 to 6 feet per second would be used.

Laboratory data given in Paragraph 8.4 indicate that the nature of equilibrium settled fly ash slurries is such that a fly ash slurry pipeline can be successfully restarted following a shutdown. This is supported by the fact that several fly ash lines have operated successfully for a number of years (Ref. 60).

8.1.3 Corrosion/Erosion

Tests on fly ash water slurries indicate that extremely low corrosion rates (less than 1.0 mil per year), are to be expected in fly ash slurry pipelines. When mixed with water, fly ash has a rather low pH (4.0) and would be expected to be moderately corrosive. However, the pH changes rapidly with time, and in a matter of minutes has increased to a steady value of 11 or so. This appears to be due to neutralization of acids, which initially cause the low pH, by lime and other basic materials after a brief exposure to a water environment.

This high pH condition is, of course, highly desirable from a pipeline corrosion viewpoint, and explains the low rates observed.

Operating experience has been reported on two short lines transporting fly ash located in Pennsylvania (Ref. 60). One of the lines, during 10 years of operation at about 5 feet per second, has experienced no difficulty due to corrosion or wear in the pipeline. The other, operating for 7 years at about 7 feet per second, developed considerable wear in the lower portion of the pipe. However, this slurry was very dilute (of the order of 10 percent solids), and in all probability a large portion of the solids were transported as a bed in the lower half of the pipe. For thicker slurries in the homogeneous regime, this problem would not be encountered.

8.2 RHEOLOGY

Figures 8-1 to 8-3 show rotational viscometer data for the fly ash slurries used in the hydraulic tests.

By comparison with the rheology data for digested sludge (Paragraph 7.2), it can be seen that the fly ash data show a larger spread between the data taken at ascending shear rates and those taken at descending shear rates. This larger deviation between sets of data is due to the fly ash settling out in the viscometer cup. In analyzing the rheology data for fly ash, the emphasis was placed on the ascending data at low shears, and the descending data at high shears, provided that the latter were in the laminar regime. By this approach, inaccuracies in measurements arising from fly ash settling out were minimized.

Examination of Figures 8-2 and 8-3 shows the effect of a dispersant on the rheological behavior of a fly ash slurry. The addition of Orzan AL-50, in the amount of 0.09 percent by weight of total solids, causes a drastic reduction in yield stress and a 20 percent decrease in the coefficient of rigidity. The effect of this on pipe flow is discussed later.

It should be noted that in Figures 8-1 to 8-3 the data at the highest shear rates were ignored since they are clearly in the turbulent flow regime in the viscometer. For a complete listing of the rheology data relevant to a given pipe test, see Tables A-4, A-7 and A-9 in Appendix A. General considerations of the properties of fly ash slurries are given in Paragraph 6.3.

FIGURE 8-1

ROTATIONAL VISCOMETER RHEOGRAM

FLY ASH

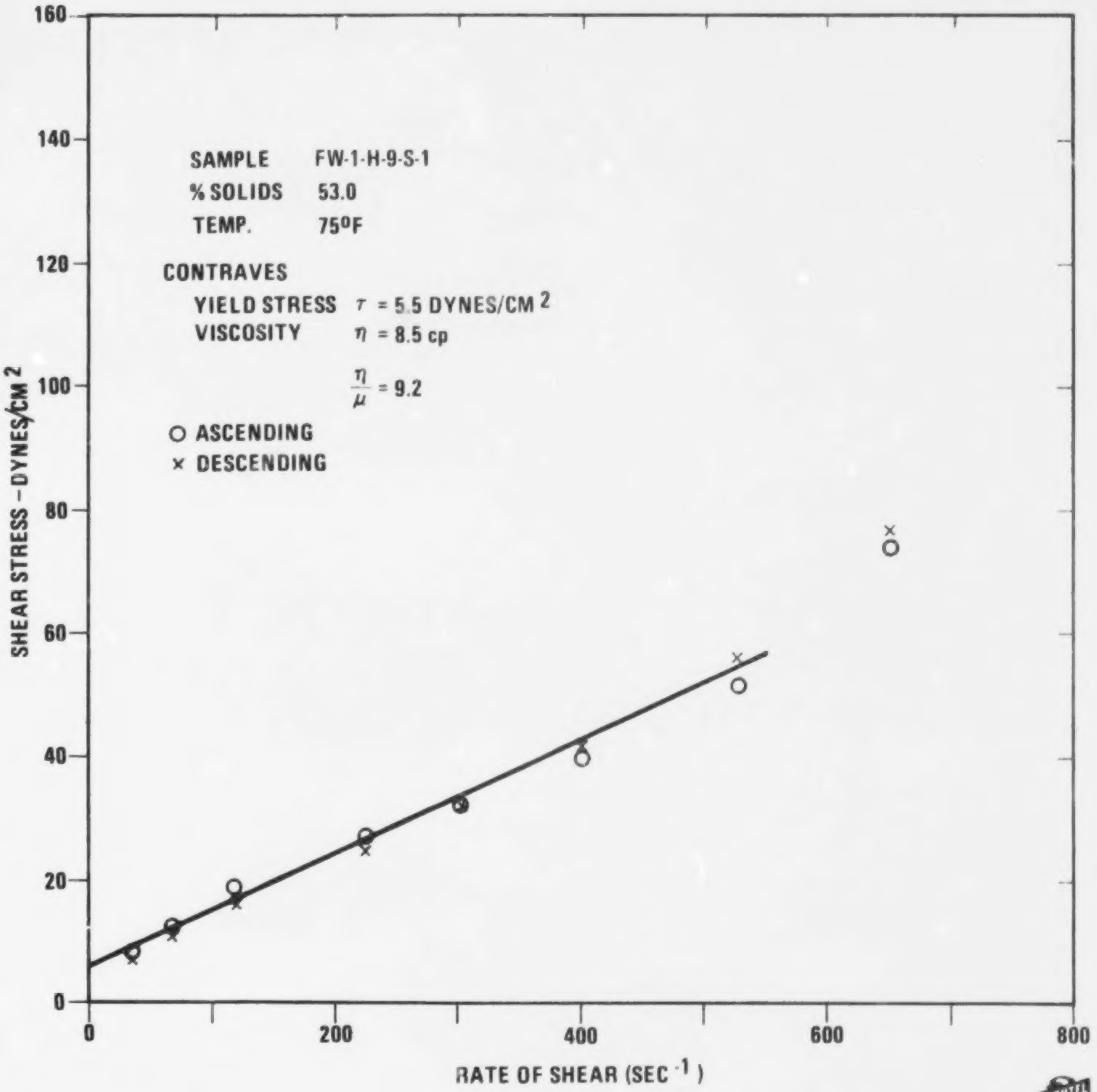

FIGURE 8-2

ROTATIONAL VISCOMETER RHEOGRAM
FLY ASH

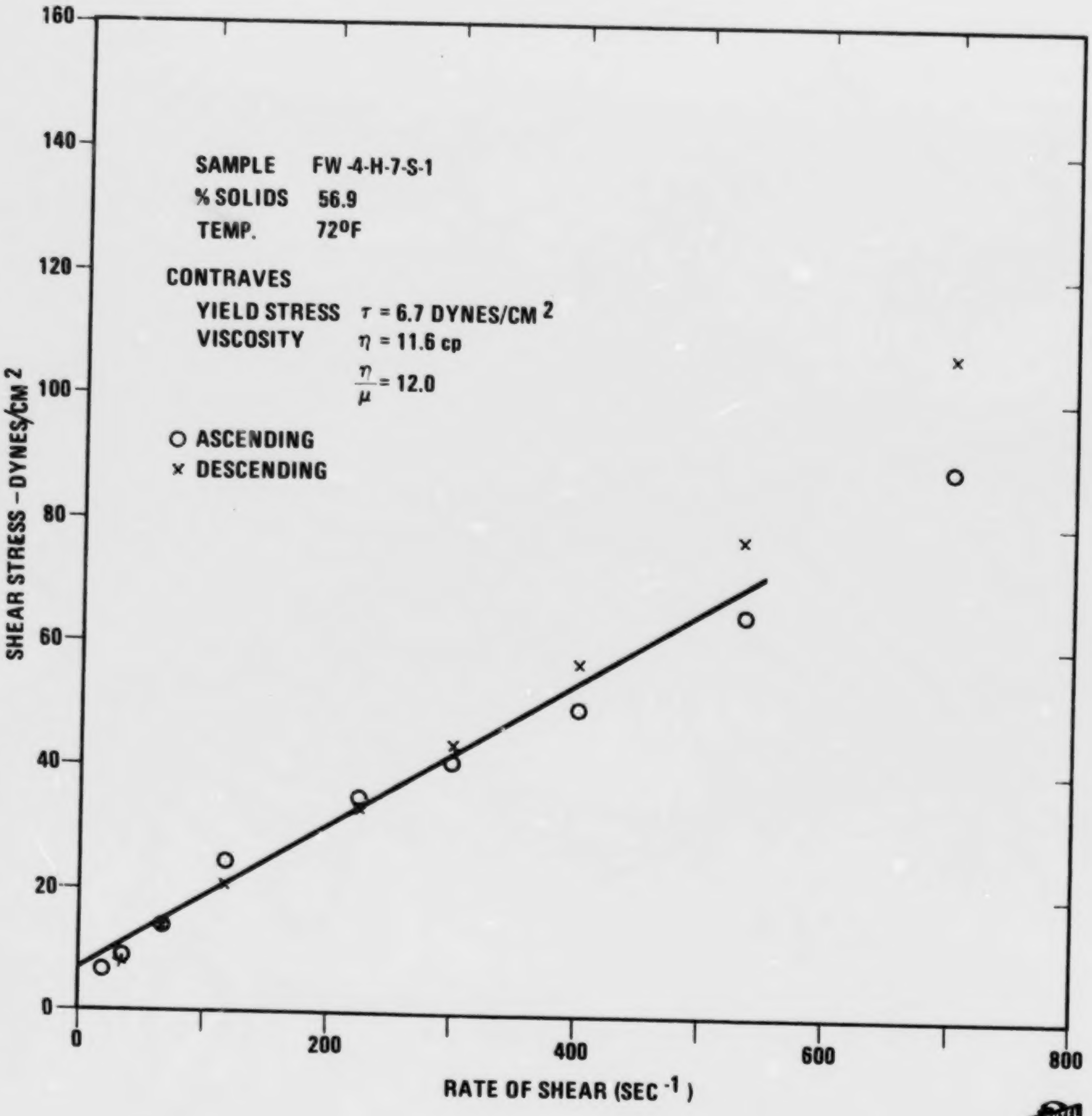

FIGURE 8-3

ROTATIONAL VISCOMETER RHEOGRAM
FLY ASH WITH 0.09% ORZAN

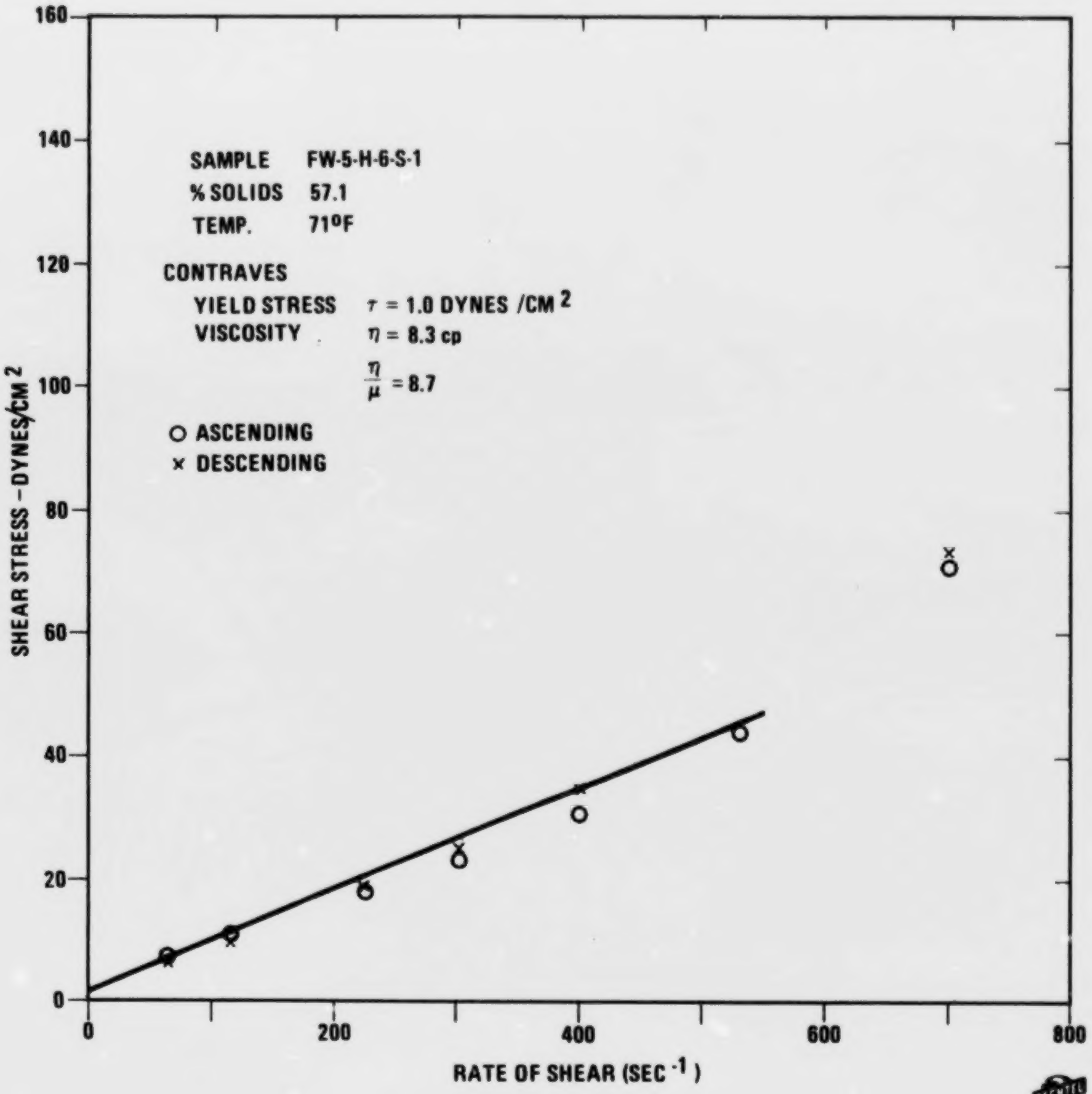

8.3 HYDRAULIC DATA

The hydraulic data from pipe tests on fly ash slurries are presented in Figures 8-4 to 8-15. Complete run sheets and relevant sample analysis are given in Paragraph A-3 of Appendix A.

8.3.1 Transition Velocity

Unlike digested sludge, which behaves as a homogeneous fluid over the whole range of commercial pipeline conditions, the behavior of fly ash slurries can be either homogeneous or heterogeneous, depending on slurry concentration and pipe velocity.

Figure 8-4 shows a plot of the wall shear stress/velocity data for the most dilute fly ash tested (Run FW-1-H - 53 percent solids). For the 16-inch pipe, there is a distinct hooking of the data at velocities lower than 2.2 feet per second. The Hedstrom prediction of critical velocity for this system is 1.6 feet per second.

This significant disagreement is due to the solids settling out in the pipe; that is, the system is in the heterogeneous flow regime at the lower velocities. Hence, the critical velocity for this system is not a laminar/turbulent transition velocity, but a minimum transport velocity, below which solids begin to settle in the pipe.

Thomas (Ref. 43) has reported on minimum transport velocities for kaolin and thorium oxide suspensions. His data show that for dilute suspensions (characterized by low yield stress) the minimum transport velocity is essentially constant for any given suspension, and that this velocity is appreciably greater than the laminar/turbulent transition velocity. As concentration increases, so does the minimum transport velocity, but it does not increase as rapidly as the transition

FIGURE 8-4

SHEAR STRESS vs. VELOCITY
FLY ASH SLURRY

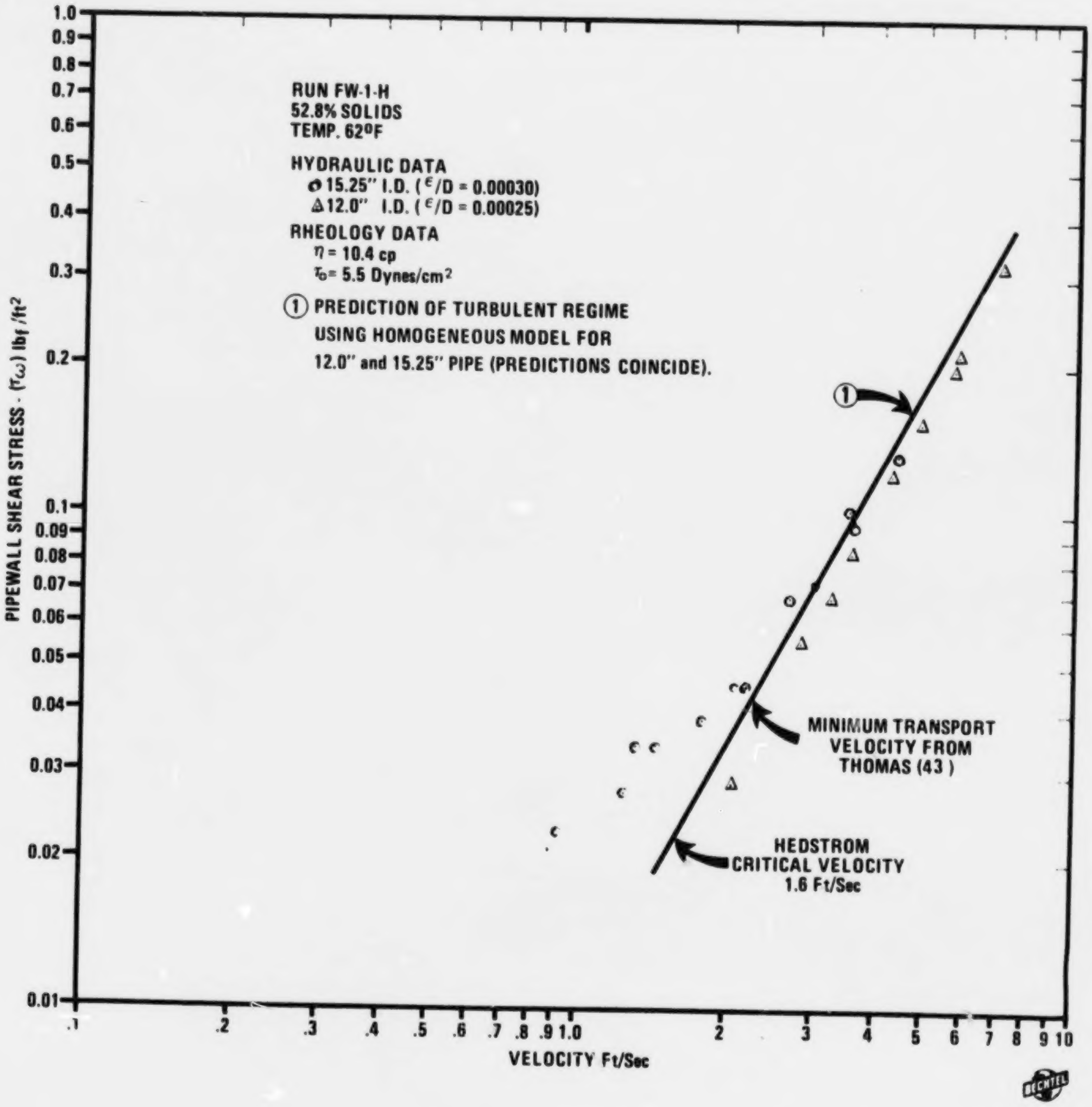

FIGURE 8-5

FRICTION FACTOR vs. REYNOLDS NUMBER
FLY ASH SLURRY

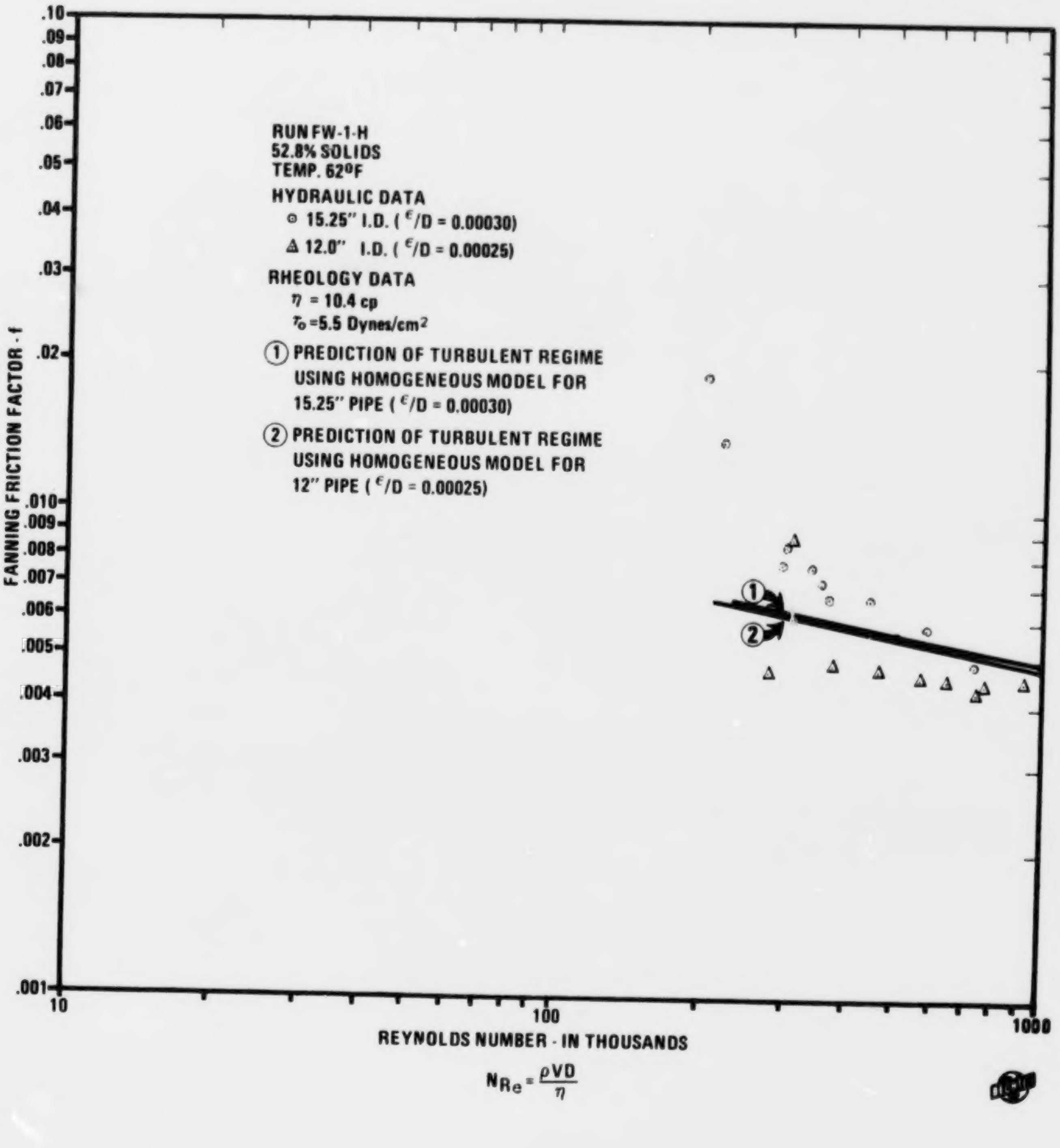

FIGURE 8-6

SHEAR STRESS vs. VELOCITY

FLY ASH SLURRY

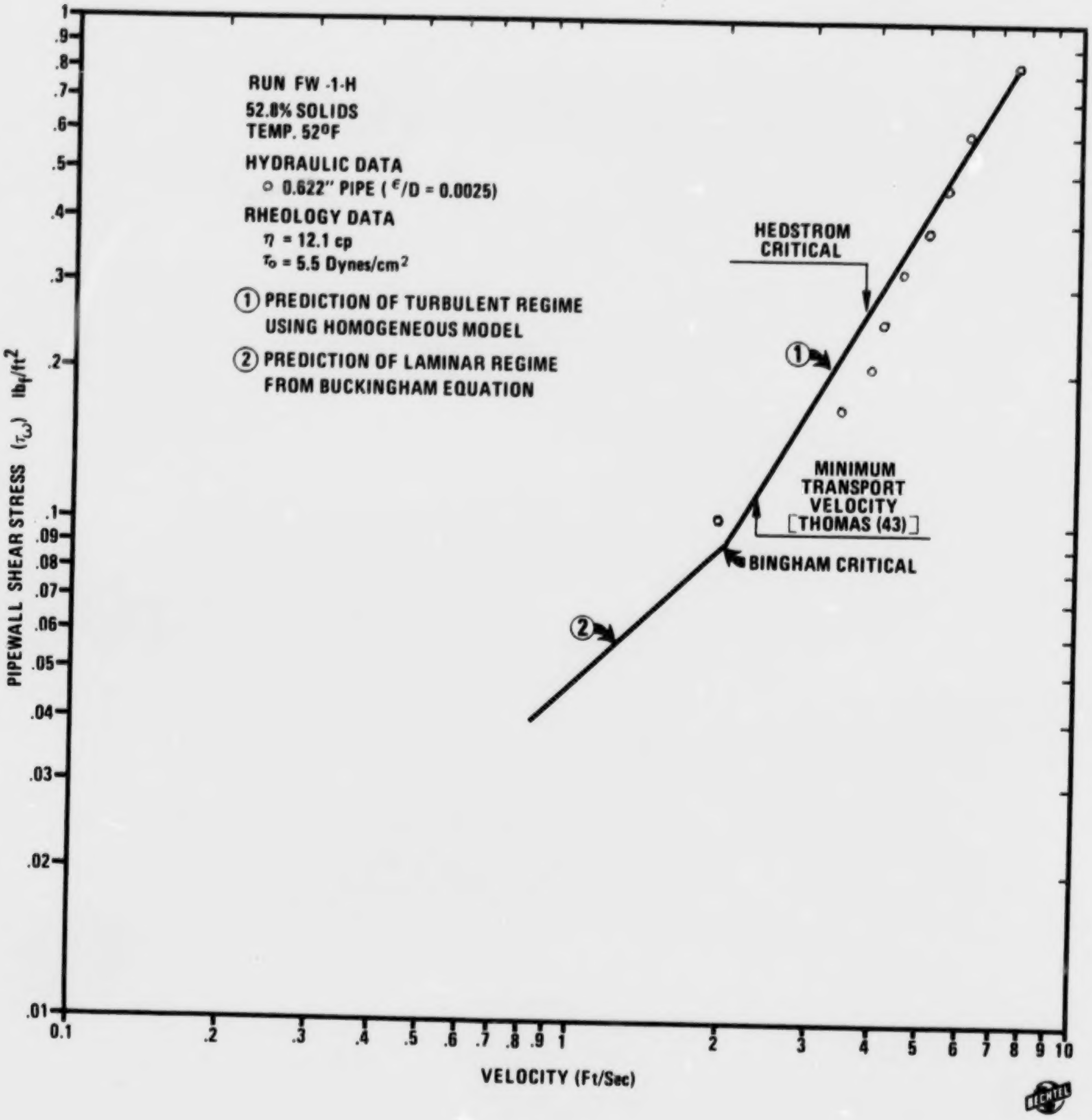

FIGURE 8-7

FRICTION FACTOR vs. REYNOLDS NUMBER
FLY ASH SLURRY

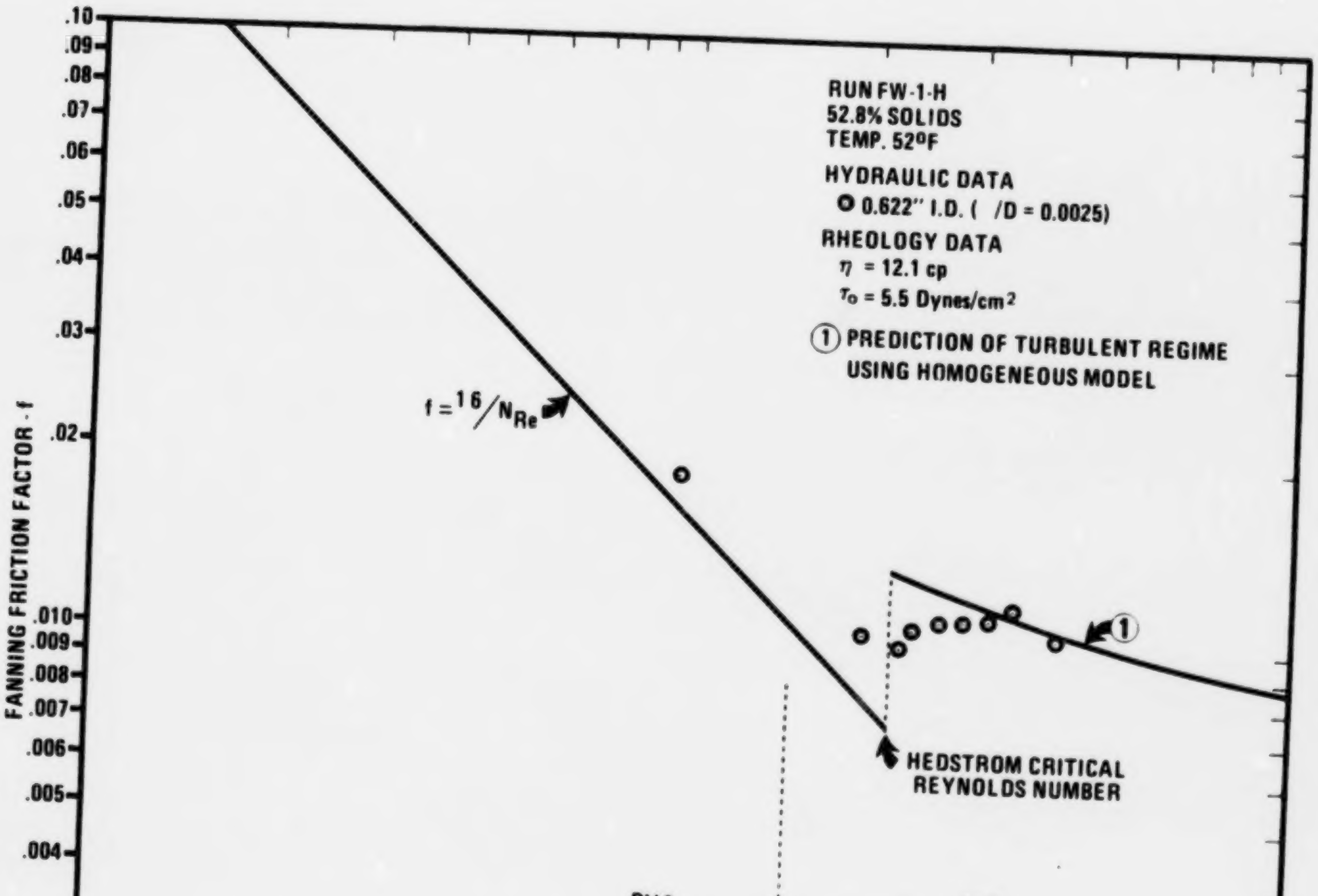

FIGURE 8-8
SHEAR STRESS vs. VELOCITY
FLY ASH

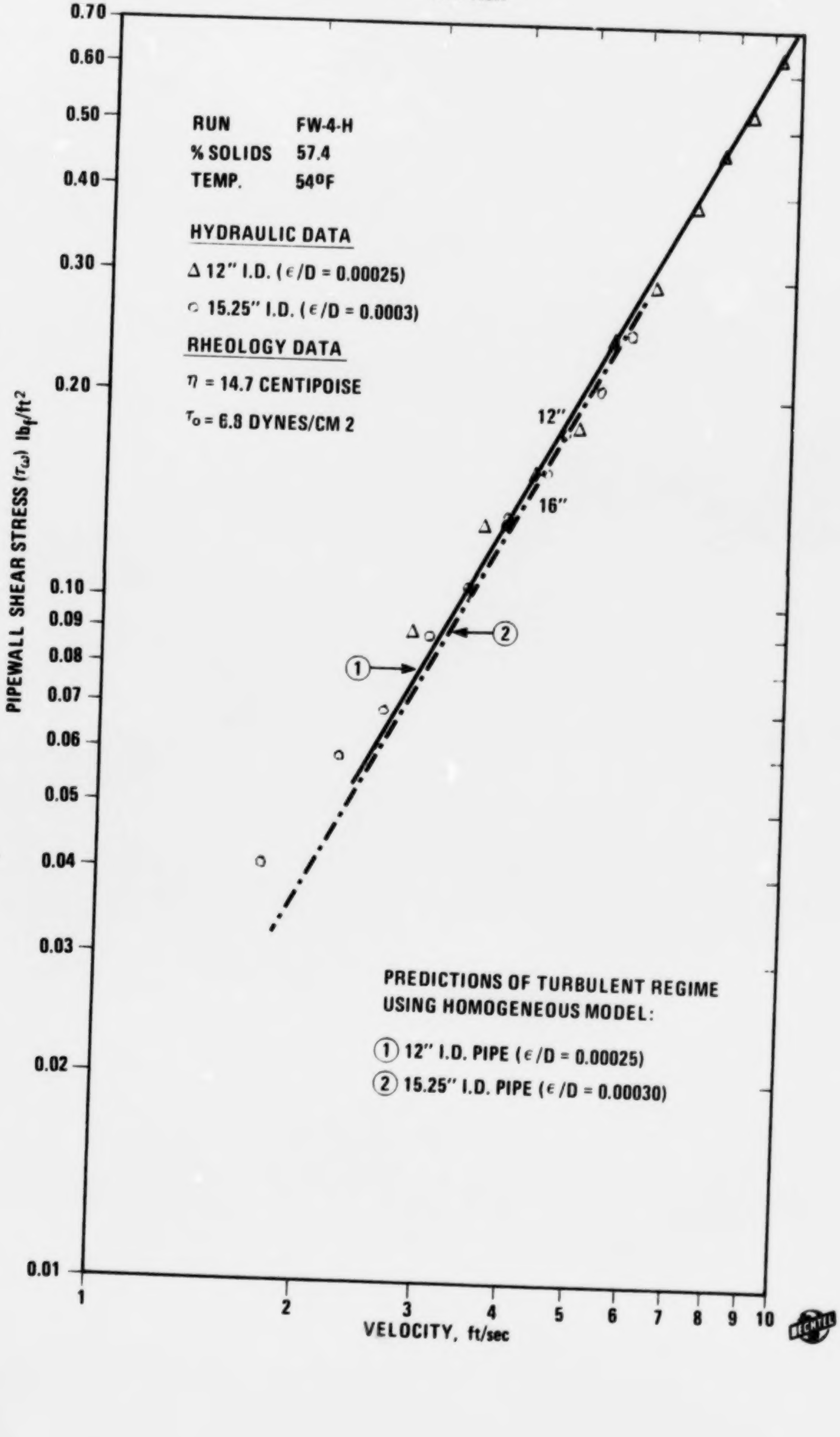

FIGURE 8-9

FRICTION FACTOR vs. REYNOLDS NUMBER
FLY ASH

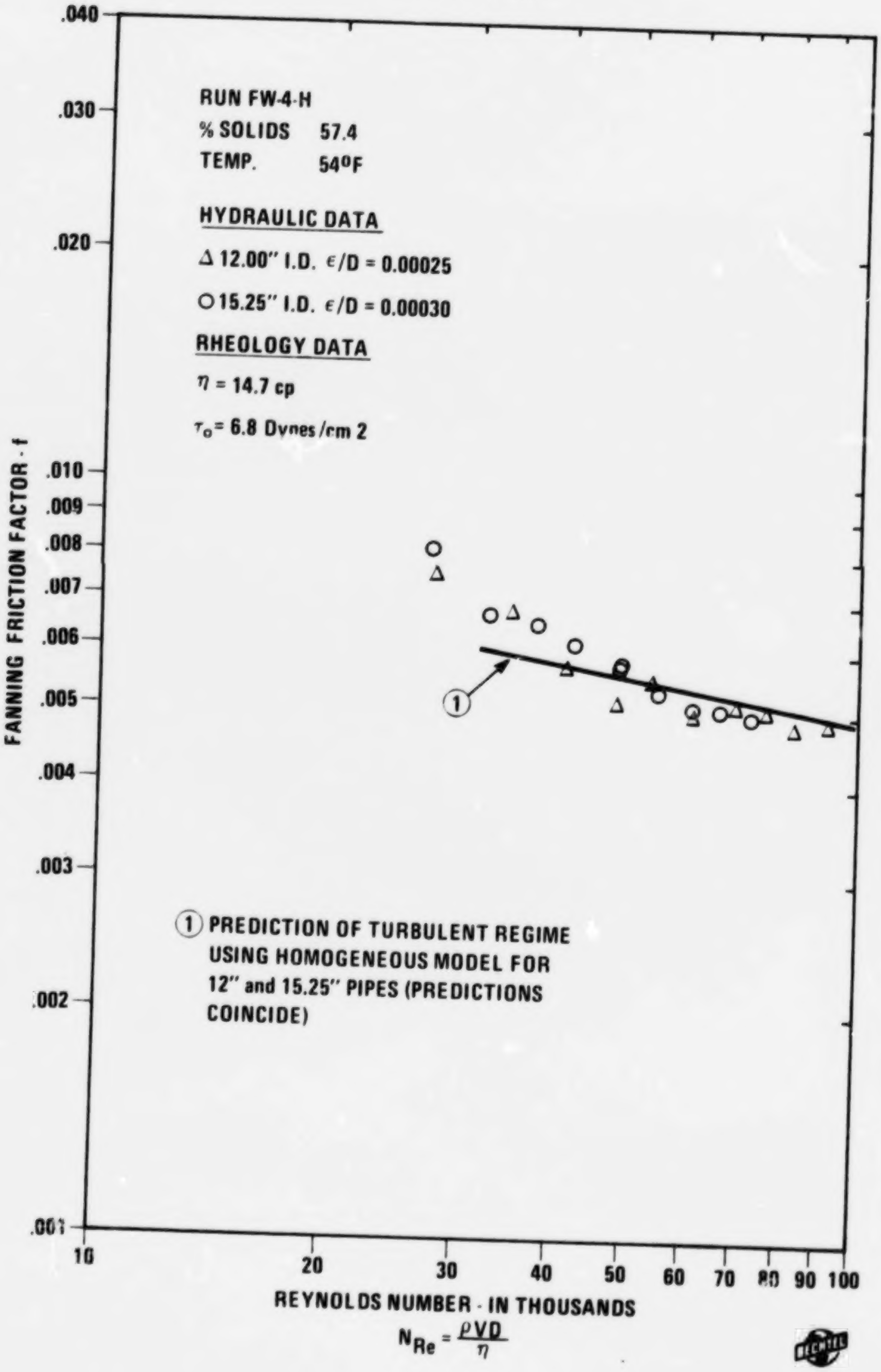

FIGURE 8-10
PSEUDOPLASTIC RHEOGRAM

FLY ASH SLURRY

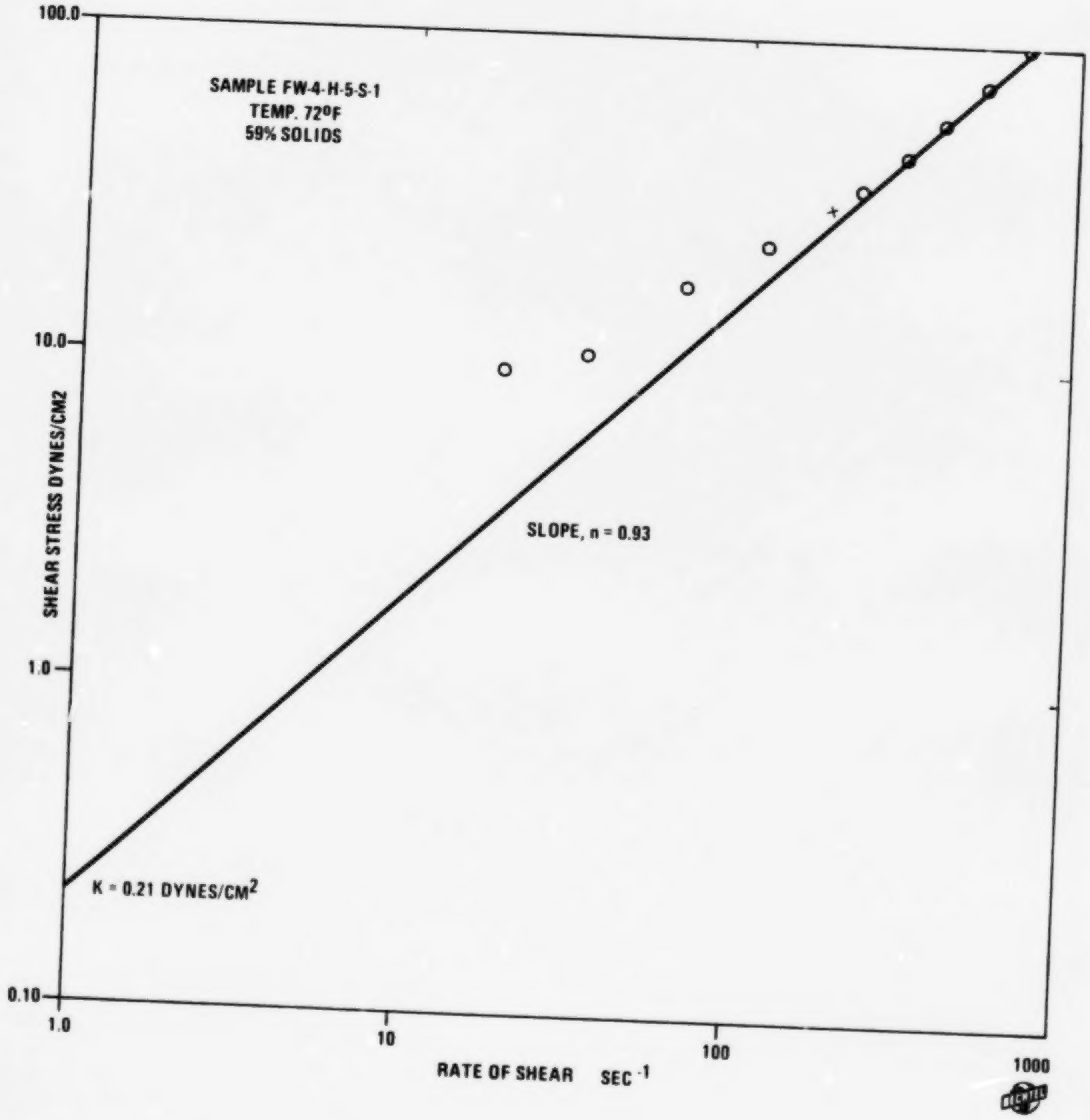

FIGURE 8-11

SHEAR STRESS vs. VELOCITY
FLY ASH

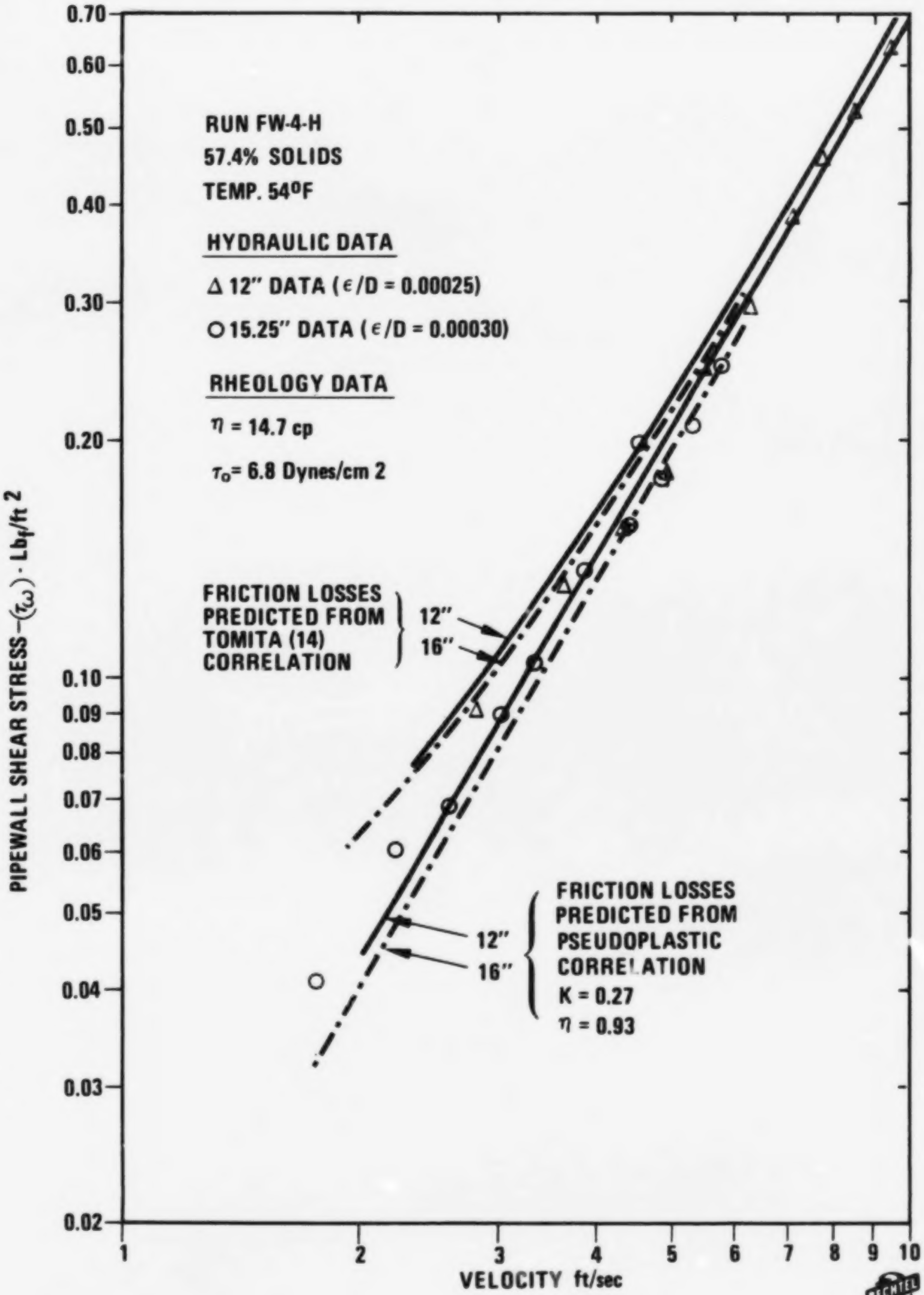

FIGURE 8-12
SHEAR STRESS vs. VELOCITY
FLY ASH WITH 0.09% ORZAN

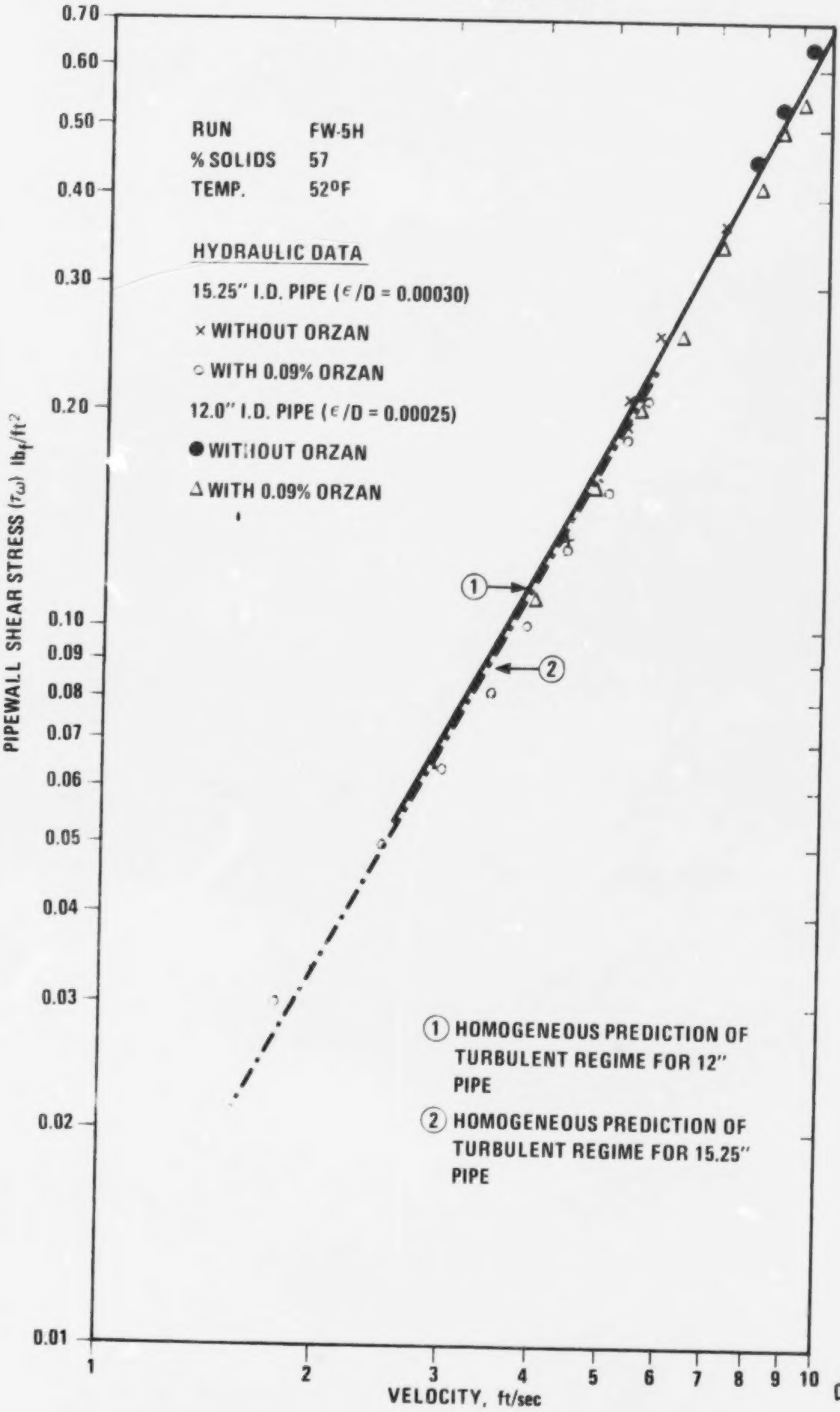

FIGURE 8-13

FANNING FRICTION FACTOR vs. REYNOLDS NUMBER

FLY ASH WITH 0.09% ORZAN

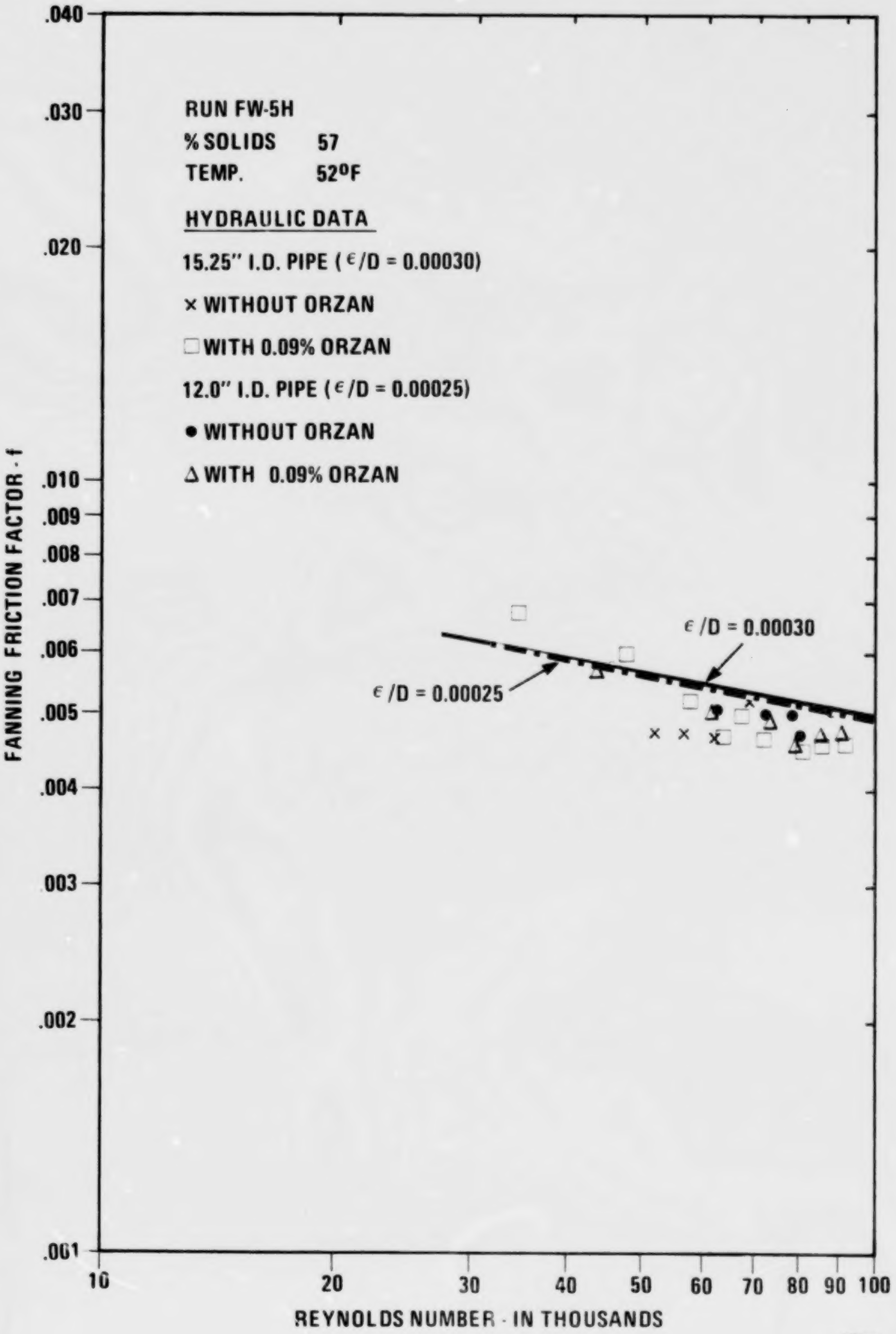

FIGURE 8-14
VELOCITY PROFILE IN 16" PIPE WITH 57% FLY ASH
RUN FW - 5-H-4

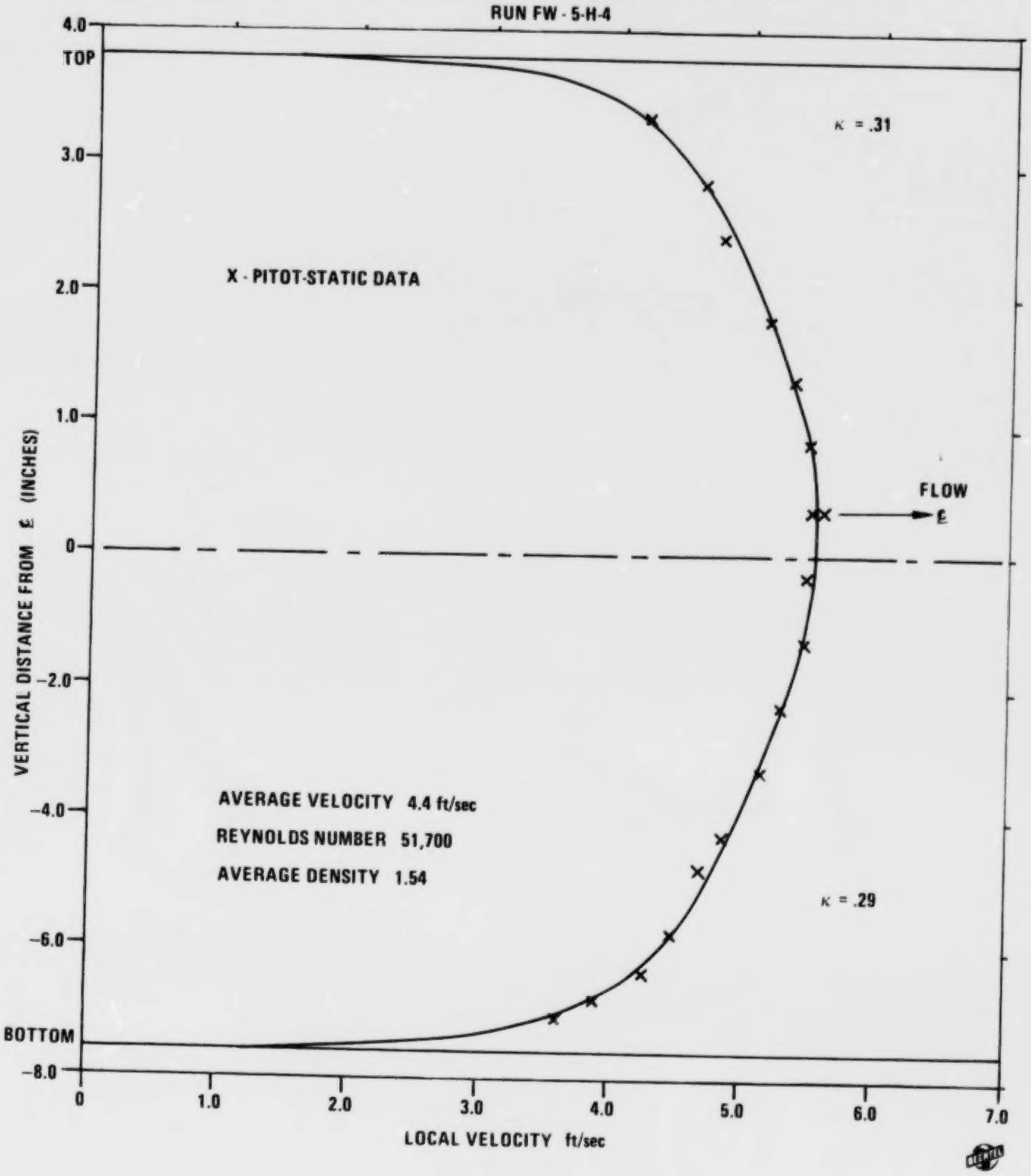

AVERAGE VELOCITY 4.4 ft/sec
REYNOLDS NUMBER 51,700
AVERAGE DENSITY 1.54

FIGURE 8-15

VELOCITY PROFILE IN 16" PIPE WITH 57% FLY ASH

RUN FW - 5-H-5

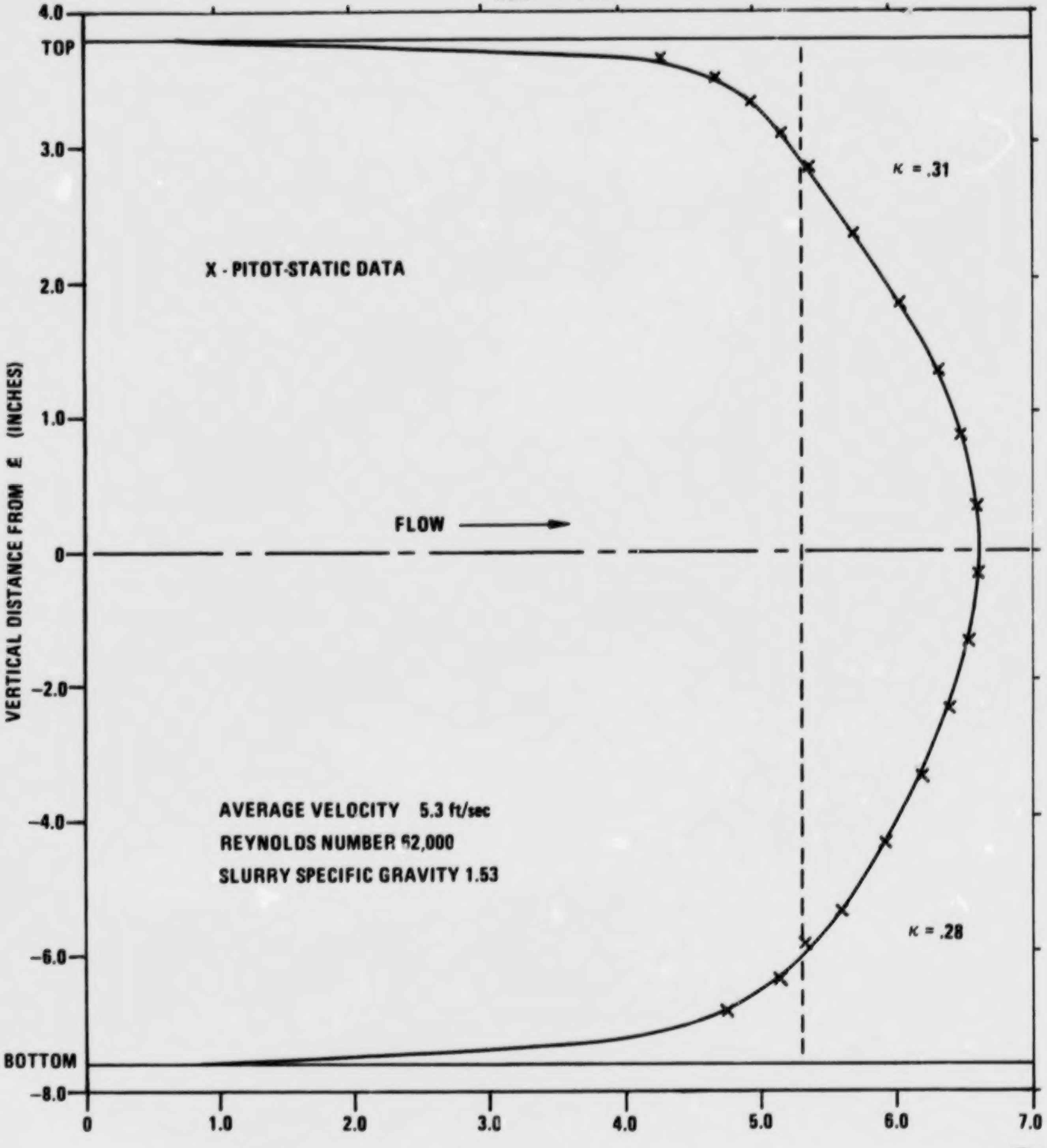

velocity, so that eventually the two coincide. Thus for higher concentration the flow is homogeneous and the minimum transport velocity is essentially the velocity at transition.

From Thomas' data, a minimum transport velocity of 2.3 feet per second is predicted for this slurry.

Figure 8-8 shows the hydraulic data for run FW-4-H which was performed on a slurry containing 57.4 percent fly ash by weight. At about 2.2 feet per second the data begin to show a slight deviation from the homogeneous model prediction, indicating a transition zone. The Hedstrom predicted critical velocity is 2 feet per second, which is in good agreement with the observed critical velocity.

Hence, it appears that at this concentration, the transition velocity of the suspension is essentially controlled by the Reynolds Number effect rather than the settling (Durand) effect. Sedimentation of solids in the lines was not detected, as indicated by the analysis of samples taken from the top and middle of each line (see Paragraph A-2, Appendix A.).

It can be concluded from the data cited above that the use of the Hedstrom procedure for the prediction of transition velocity is limited to fly ash slurries of concentrations of 57 percent solids and greater.

8.3.2 Turbulent Regime

With the exception of the large diameter pipe tests on 53 percent fly ash slurry (Run FW-1-H) the tests show that the flyash/water system is well represented by the homogeneous model.

As previously stated, during Run FW-1-H a quantity of solids was deposited in the 16-inch pipe section. The effect of this deposition on hydraulic correlation is shown in Figure 8-5, which is a plot of the data in the form of friction factor versus Reynolds Number. The 16-inch data diverge from the homogeneous prediction due to the bed deposited in the pipe at low velocities. This solids deposition resulted in dilution of the bulk of the slurry at the lower velocities. Consequently, at low Reynolds Numbers the observed data are much lower than the homogeneous prediction, as seen in Figure 8-5. It should be noted that for this run both the 12-inch and 16-inch data are correlated by a single line at velocities greater than 4 feet per second. Below this velocity, the data diverge significantly, as shown in Figure 8-4.

Figures 8-8 and 8-9 show the hydraulic data and the homogeneous model predictions for Run FW-4-H (57.4 percent solids).

In the turbulent regime, the model gives fair correlation of the data, but the prediction is generally higher than the measured data (see Figure 8-9). This suppression is due to the damping of turbulence by the solid particles. It can be seen that the degree of damping is not constant but varies with the Reynolds Number. In fact, the data tend toward the homogeneous prediction at high Reynolds Numbers. These findings are in general agreement with the published data of D. G. Thomas (Ref. 43). In the range of commercial pipe velocities the turbulent damping amounts to 5 percent on friction loss, almost within the limits of experimental error.

Figure 8-10 shows a rheogram used to establish the rheological parameters for the power law model of Dodge and Metzner. When corrected for temperature, the power law also gives good correlation of this run, as shown in Figure 8-11.

The Tomita correlation for Bingham plastics is shown in Figure 8-12. This method, although well representing the shape of the flow curve, predicts consistently high.

Table 8-2 is a numerical comparison of all three methods with the observed data.

Figures 8-12 and 8-13 show data for Run FW-5-H, which was performed on a slurry of 57 percent solids to which a dispersant, Orzan AL-50, was added.

It can be seen that the addition of Orzan results in lower friction losses. (It should be noted that the decrease in head loss is partially attributable to a dilution of the inventory due to the addition of seal water at the pump.)

Figure 8-13 shows that the suppression of data from the homogeneous prediction follows the same trend as before; that is, the data tend towards the Newtonian line at higher Reynolds Numbers. Comparing this run with Run FW-4-H, which was performed at approximately the same conditions of solids concentration, we can see that the degree of turbulence damping is slightly larger due to the addition of Orzan (amounting to about 7 percent on friction losses in the range of probably commercial Reynolds Numbers).

In an effort to obtain an independent check on the turbulence damping effect, velocity profiles across the 16-inch pipe section were performed at two bulk velocity levels, prior to the addition of Orzan.

Velocity profile data for a fluid allows calculation of the Von Karman coefficient of turbulent exchange. Once this coefficient is obtained, the dampening effect in the system can be evaluated by comparison with the Von Karman coefficient for a Newtonian fluid

Table 8-2

COMPARISON OF TURBULENT CORRELATIONS - RUN FW-4-H

			Homogeneous		Pseudoplastic		Tomita	
Line No.	Velocity (ft/sec)	τ_w Obs (lb/ft^2)	τ_w Calc (lb/ft^2)	Percent Deviation	τ_w Calc (lb/ft^2)	Percent Deviation	τ_w Calc (lb/ft^2)	Percent Deviation
12 Inch Data								
1	9.4	0.635	0.650	+ 2.4	0.631	- 0.6	0.671	+ 5.7
2	7.8	0.457	0.466	+ 2.0	0.451	- 1.3	0.485	+ 6.1
3	6.3	0.293	0.312	+ 6.5	0.312	+ 6.5	0.336	+ 14.7
4	4.9	0.184	0.200	+ 8.7	0.202	+ 9.8	0.224	+ 21.8
5	8.5	0.524	0.549	+ 4.8	0.524	0.0	0.562	+ 7.3
6	7.1	0.382	0.393	+ 2.9	0.384	+ 0.5	0.413	+ 8.1
7	5.5	0.247	0.247	0.0	0.247	0.0	0.266	+ 7.7
8	4.3	0.155	0.154	- 0.7	0.162	+ 4.5	0.175	+ 12.9
9	2.85	0.090	0.075	- 16.7	0.077	- 14.5	0.098	+ 8.9
10	3.6	0.130	0.114	- 12.3	0.118	- 9.2	0.137	+ 5.4
16 Inch Data								
1	5.8	0.249	0.262	+ 5.2	0.262	+ 5.2	0.280	+ 12.5
2	4.8	0.178	0.188	+ 5.6	0.182	+ 2.3	0.212	+ 19.1
3	3.9	0.133	0.128	- 3.8	0.126	- 6.8	0.150	+ 12.8
4	3.0	0.089	0.081	- 9.0	0.080	- 10.1	0.104	+ 16.8
5	5.3	0.211	0.222	+ 5.2	0.215	+ 1.9	0.242	+ 14.7
6	4.4	0.156	0.159	+ 1.9	0.156	0.0	0.180	+ 15.4
7	3.4	0.105	0.098	- 6.7	0.099	- 5.7	0.122	+ 16.2
8	2.62	0.069	0.062	- 10.1	0.063	- 8.7	0.089	+ 29.0
9	1.76	0.041			Transition Zone			
10	2.21	0.60	0.046	- 23.4	0.047	- 21.7	0.071	+ 18.3

(which is equal to 0.38).

The application of the Prandtl concept of velocity defect ($^U/U^*$) to velocity profile data allows calculation of the Von Karman coefficient according to the following equation:

$$\frac{U}{U^*} = A + \frac{2.303}{\kappa} \log \frac{r_d U}{\nu}$$

where U is the measured velocity at point r_d
ν is the kinematic viscosity of the fluid
U^* is the friction velocity ($=\sqrt{\tau_w/\rho}$)
and κ is the Von Karman coefficient.

A measurement of the velocity profile across a pipe gives the data necessary to evaluate $^U/U^*$ as a function of local Reynolds Number, which gives a straight line, the slope of which yields a value of the Von Karman coefficient.

Figure 8-14 shows a velocity profile for a bulk velocity of 5.3 feet per second. The measured friction factor for this velocity is lower than the Newtonian prediction by some 12.5 percent, i.e.,

$$\frac{f_{obs}}{f_{calc}} = 0.875$$

Now, the von Karman coefficient of turbulent exchange, κ , is related to the friction factor as follows:

$$f \propto \kappa^2$$

Therefore, since the value of κ for a Newtonian fluid is 0.38, the friction loss data indicate a von Karman factor of

$$\kappa = 0.38 \sqrt{0.875} = 0.36$$

The profile data in Figure 8-14 show an "observed" von Karman coefficient of 0.31 in the upper portion of the pipe.

The same situation is found in Figure 8-15, which is a velocity profile at a bulk velocity of 4.4 feet per second. The friction loss data indicate Von Karman coefficient of 0.34, as opposed to 0.31 measured by velocity profile in the upper portion of the pipe.

The agreement between the two is not good, and further work in this direction is indicated.

The application of the unmodified friction loss prediction to these data gives fairly good correlation as seen in Figure 8-12 and can be used as a slightly conservative method of pipeline design.

8.4 PIPELINE OPERABILITY

In an attempt to establish the operability of a fly ash slurry pipeline, the test loop was shut down for a period of 38 hours following Run FW-1-H (53 percent solids).

However, the portion of run FW-1-H immediately prior to shutdown was conducted at very low velocities. This is not a true representation of pipeline shutdown conditions inasmuch as low velocity operation results in classified settling of the solids, so that a bed of coarse particles is laid down in the pipe. A commercial pipeline would be shut down at a steady condition of 5 to 6 feet per second, that is, in the homogeneous flow regime.

The data obtained from the start-up run are shown in Figures 8-16 and 8-17 and they reflect the effects of this nonrepresentative shutdown. Figure 8-16 shows a plot of pipewall shear stress with running time for both test sections. It can be seen that after 25 minutes of operation both sections were exhibiting friction losses which were much greater than would be anticipated from run FW-1-H at the same velocities.

The 16-inch data (at 5.1 feet per second) show that a steady condition was achieved after 7 minutes, and this is confirmed by the data shown in Figure 8-17. Figure 8-17 is a plot of C/C_A versus running time for the coarsest solids fractions, where C/C_A is defined as:

$$\frac{C}{C_A} = \frac{\text{Volumetric Solids concentration at top of pipe}}{\text{Volumetric Solids concentration at middle of pipe}}$$

A C/C_A of 1.0 would mean that the slurry is uniformly suspended throughout the cross-section of the pipe. For the 16-inch data this

FIGURE 8-16

SHEAR/STRESS vs. TIME
RUN FW-1-0
FLY ASH OPERABILITY TEST

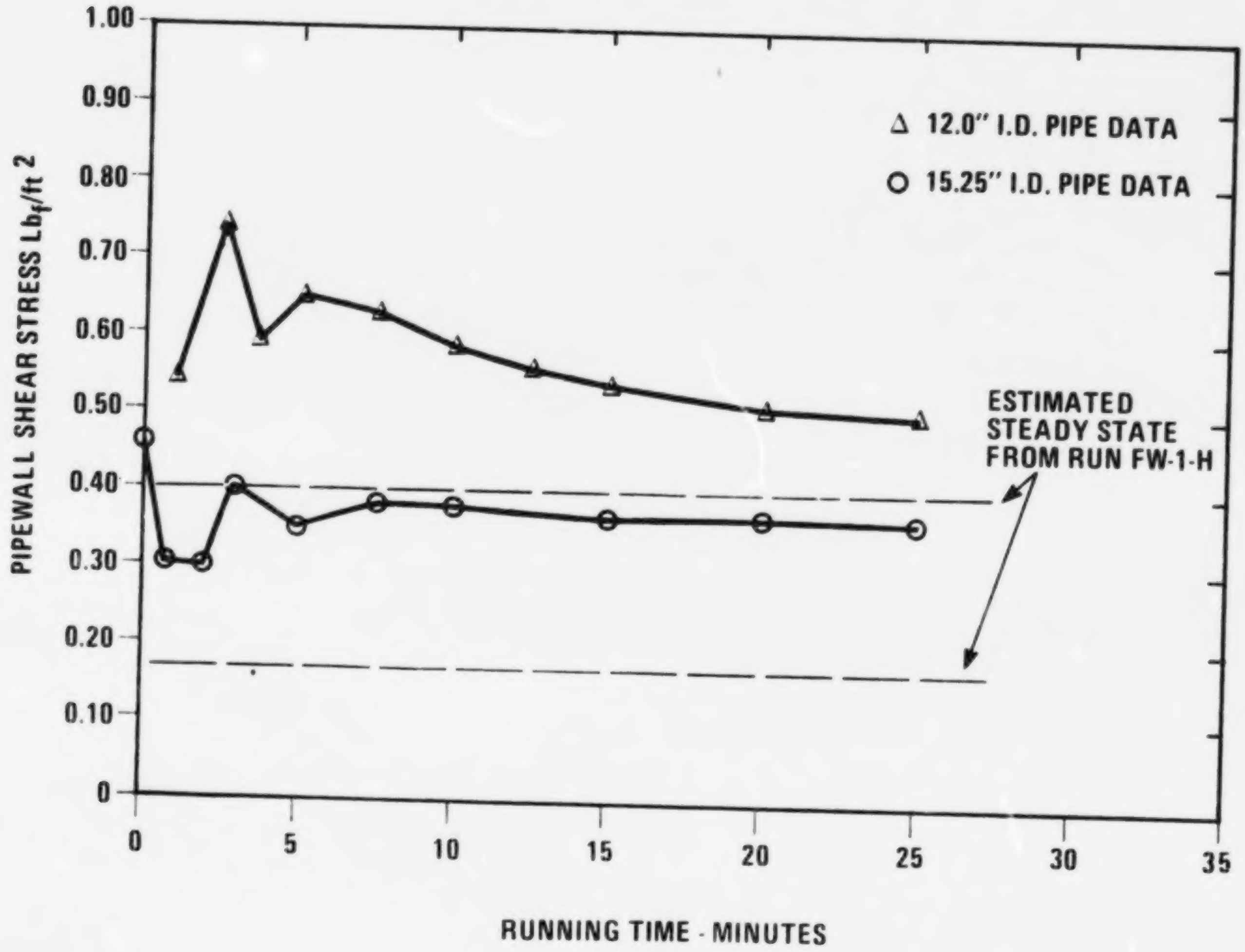

FIGURE 8-17

C/C_A vs. TIME
RUN FW-1-0 – FLY ASH OPERABILITY TEST

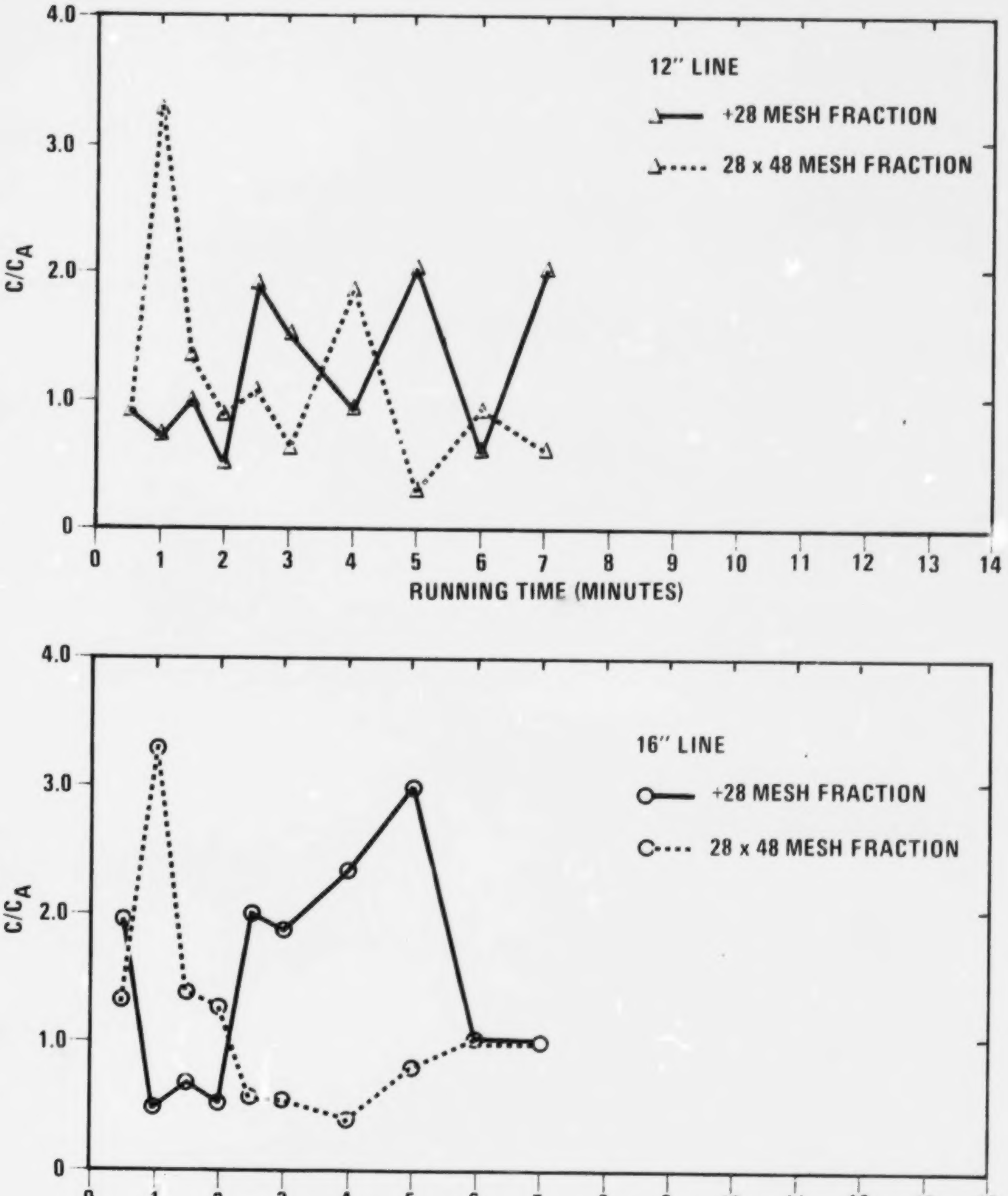

was achieved after 6 minutes operation as shown by analysis of samples taken from the top and the middle of the test section (Figure 8-17).

The 12-inch data (at 8.2 feet per second) show that the higher velocity tended to sweep-out the 12-inch section for about 20 minutes, after which the friction loss stabilized at a higher value than would be expected in steady state operation.

It is evident that the bed deposited in the pipes prior to and during shutdown was not resuspended, resulting in restriction of the pipe area, and consequent increase in velocity and friction loss. On the basis of the steady state friction losses achieved, it would require the deposition of a bed of such magnitude that the bulk of the slurry would be diluted from 53 percent solids to approximately 50 percent solids. This dilution effect was found from bulk samples of the slurry (see Table A-11). The bulk slurry samples obtained during the last three minutes of sampling held a steady solids level of 50 to 51 percent.

However, this resuspension difficulty and consequent system overpressure is entirely due to the manner in which the system was shut down. Closer scrutiny of the properties of terminally settled fly ash slurries shows that in the equilibrium settled condition (73 percent solids) the slurry is still fluid, and therefore, the settled slurry resulting from a true pipeline shutdown can be resuspended on startup.

Therefore, it can be concluded from other sources that a fly ash slurry pipeline normally operating in the turbulent homogeneous flow regime can be shutdown and restarted, although time did not permit another large scale pipe test to demonstrate this.

FIGURE 8-18

ROTATIONAL VISCOMETER RHEOGRAM
TERMINAL SETTLED FLY ASH SLURRY

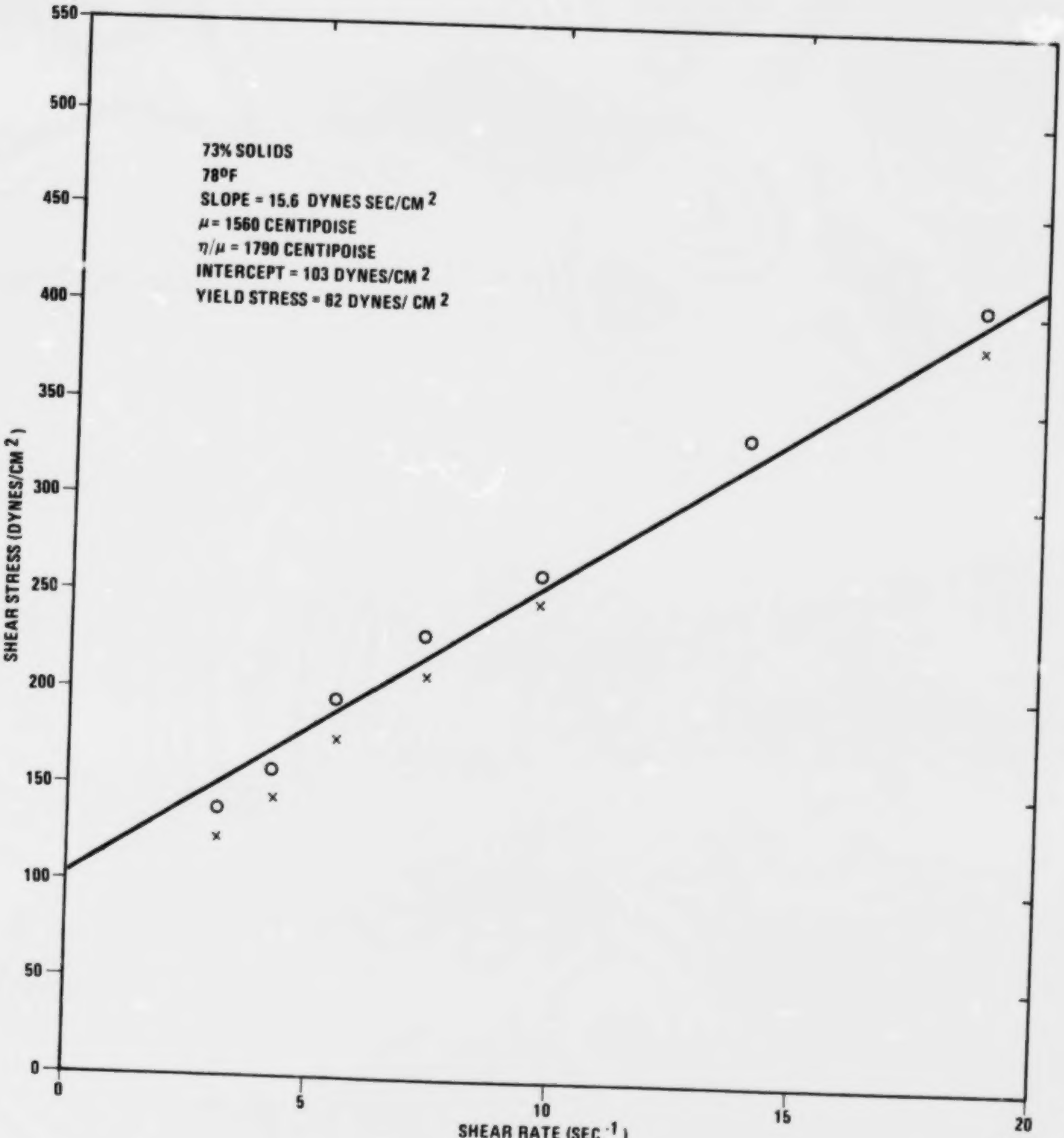

Section 9

PIPE TESTS ON SLUDGE/FLY ASH MIXTURES

9.1 PIPELINING OF SLUDGE/FLY ASH MIXTURES

The tests performed on sludge/fly ash mixtures are listed in Table 9-1 and are discussed in detail in the following paragraphs.

9.1.1 Hydrodynamics

As with the digested sludge, the data show that pipeline friction losses for these systems can be accurately predicted from laboratory measurements of rheology.

The homogeneous model gave excellent correlation of turbulent data for a wide range of solids concentrations in both 12-inch and 16-inch pipe sections. The Hedstrom prediction of transition velocity was in very good agreement with the observed values.

The fact that this procedure is in good agreement with data for digested sludge, fly ash, and digested sludge/fly ash mixtures establishes the prediction ability of the model, not only for a wide range of pipe diameters and concentrations but also for different materials.

9.1.2 Operability

An operability test was performed on a fly ash/sludge mixture of 20 percent total solids by weight, and is discussed in paragraph 9.4. This run indicates that the startup and shutdown of commercial pipelines will present no operational difficulties.

Table 9-1

HYDRAULIC TESTS ON FLY ASH/SLUDGE MIXTURES

Run No.	Solids Concentration (percent by weight)	Pipe I. D. (inches)
FS-1-H	11	12.0 & 15.25
FS-2-H	20	12.0 & 15.25
FS-3-H	35	12.0 & 15.25
FS 1-0	20	15.25*

* Operability Test

9.2 RHEOLOGY

Figures 9-1 to 9-3 show typical rheology data for the three fly ash/sludge mixtures tested. As in paragraph 6.4, the system is treated as a suspension of fly ash solids in a homogeneous conveying medium (digested sludge).

Hence, in obtaining a reduced viscosity, η/μ, μ is taken as the viscosity of digested sludge at the same temperature. For each of the runs, the digested sludge contained 3.5 percent solids by weight, and its properties are given for Run DS-1-H, paragraph 7.2.

Examination of Figures 9-1 to 9-3 shows that as the quantity of fly ash is increased, both the yield stress and coefficient of rigidity of the mixture increase.

Although these pipe tests were performed using only one sludge, the laboratory data given in Section 6 show that when the rheology data are reduced on the basis of the sludge properties, the design procedure can be applied to mixtures of fly ash and sludge, for any sludge concentration. Figure 6-6 shows that if the reduced viscosity is plotted against volume concentration of fly ash the data fall on the lower portion of the curve for fly ash/water slurries. That is, the reduced viscosity is dependent only upon the solids concentration, and not upon the nature of the suspending medium. Hence, the generalized curve in Figure 6-6 can be applied to mixtures of fly ash and sludge, for any sludge concentration.

FIGURE 9-1

ROTATIONAL VISCOMETER RHEOGRAM
FLY ASH/SLUDGE MIXTURE

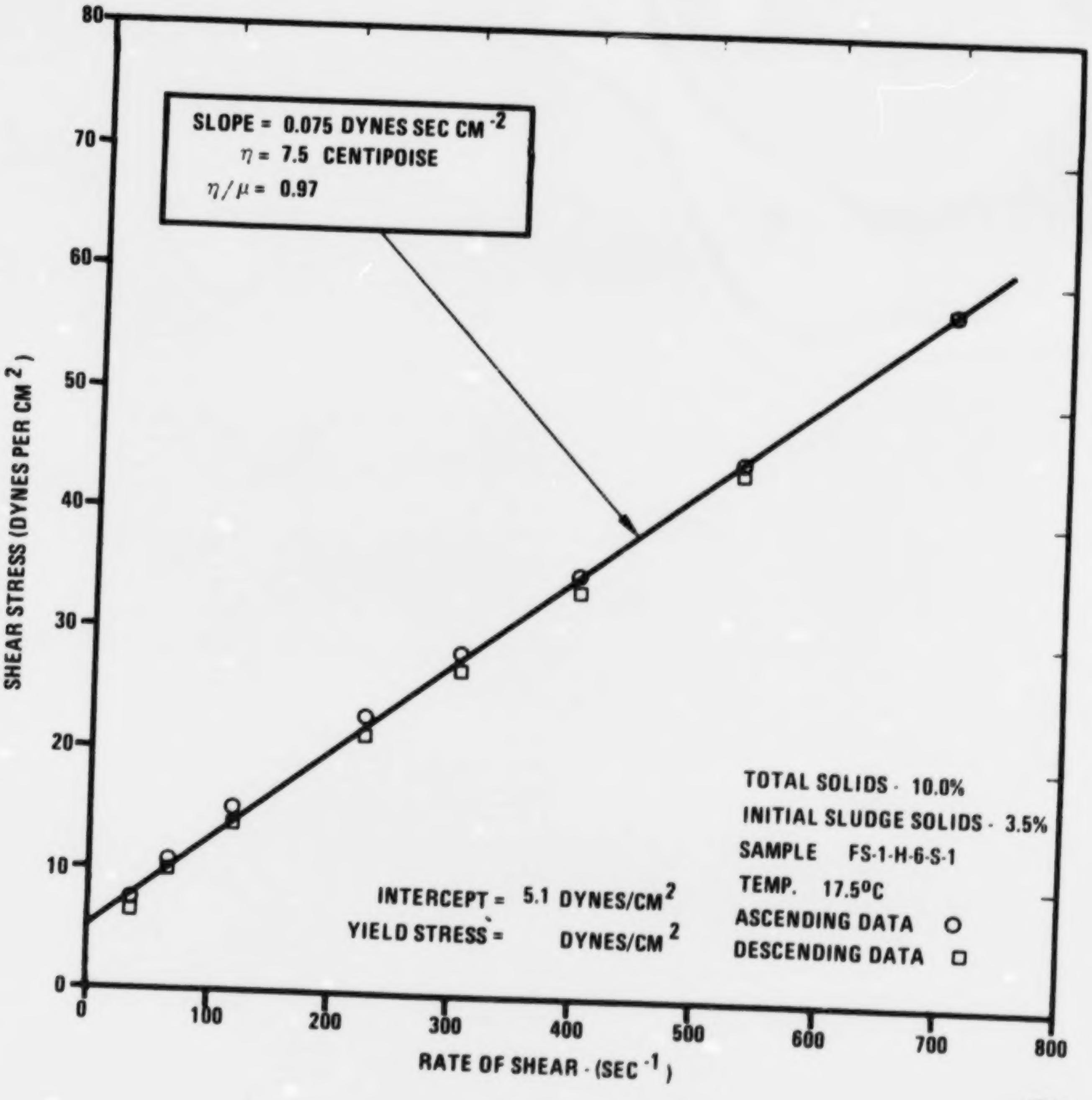

FIGURE 9-2

ROTATIONAL VISCOMETER RHEOGRAM
FLY ASH/SLUDGE MIXTURE

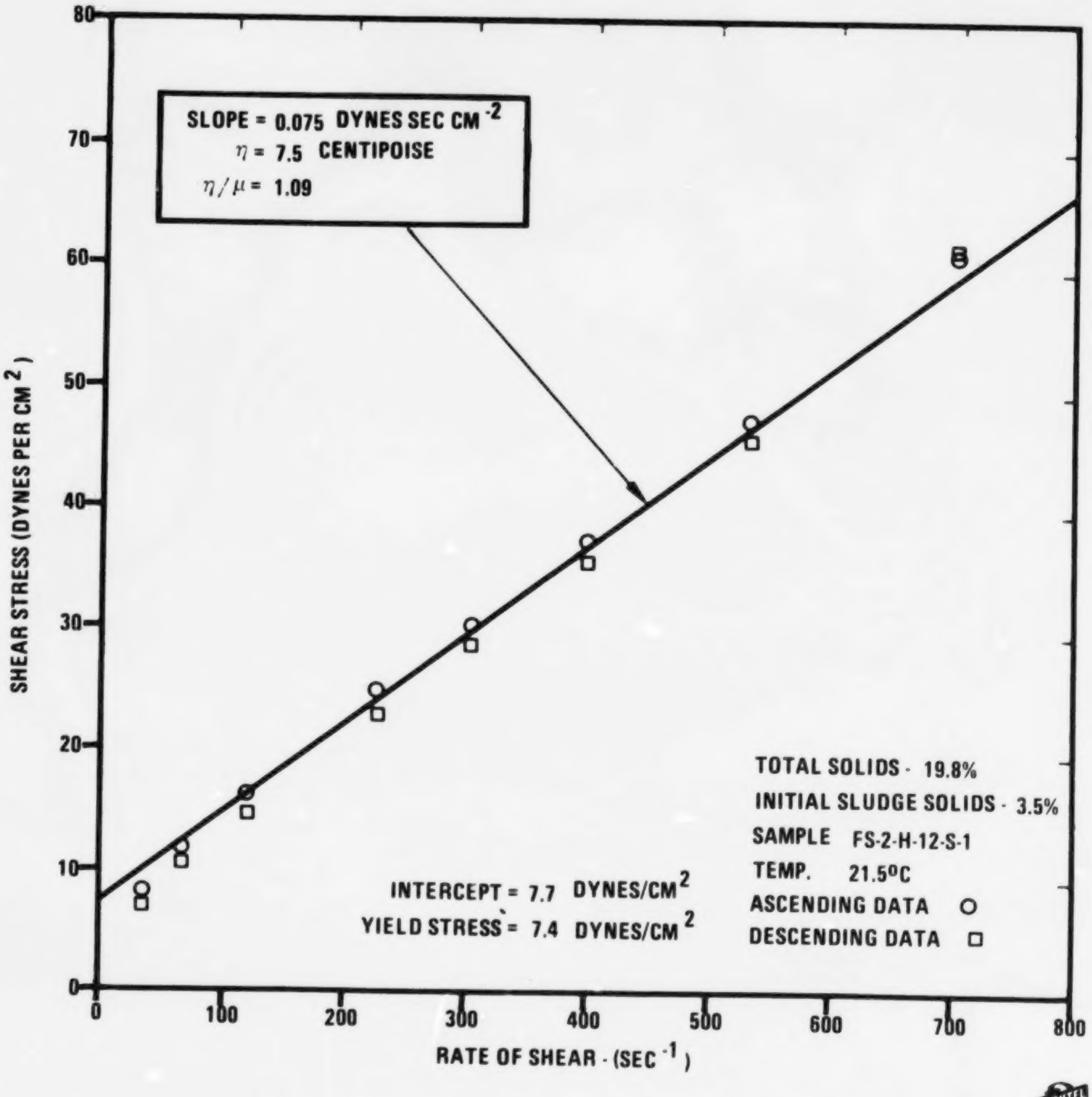

FIGURE 9-3

ROTATIONAL VISCOMETER RHEOGRAM
FLY ASH/SLUDGE MIXTURE

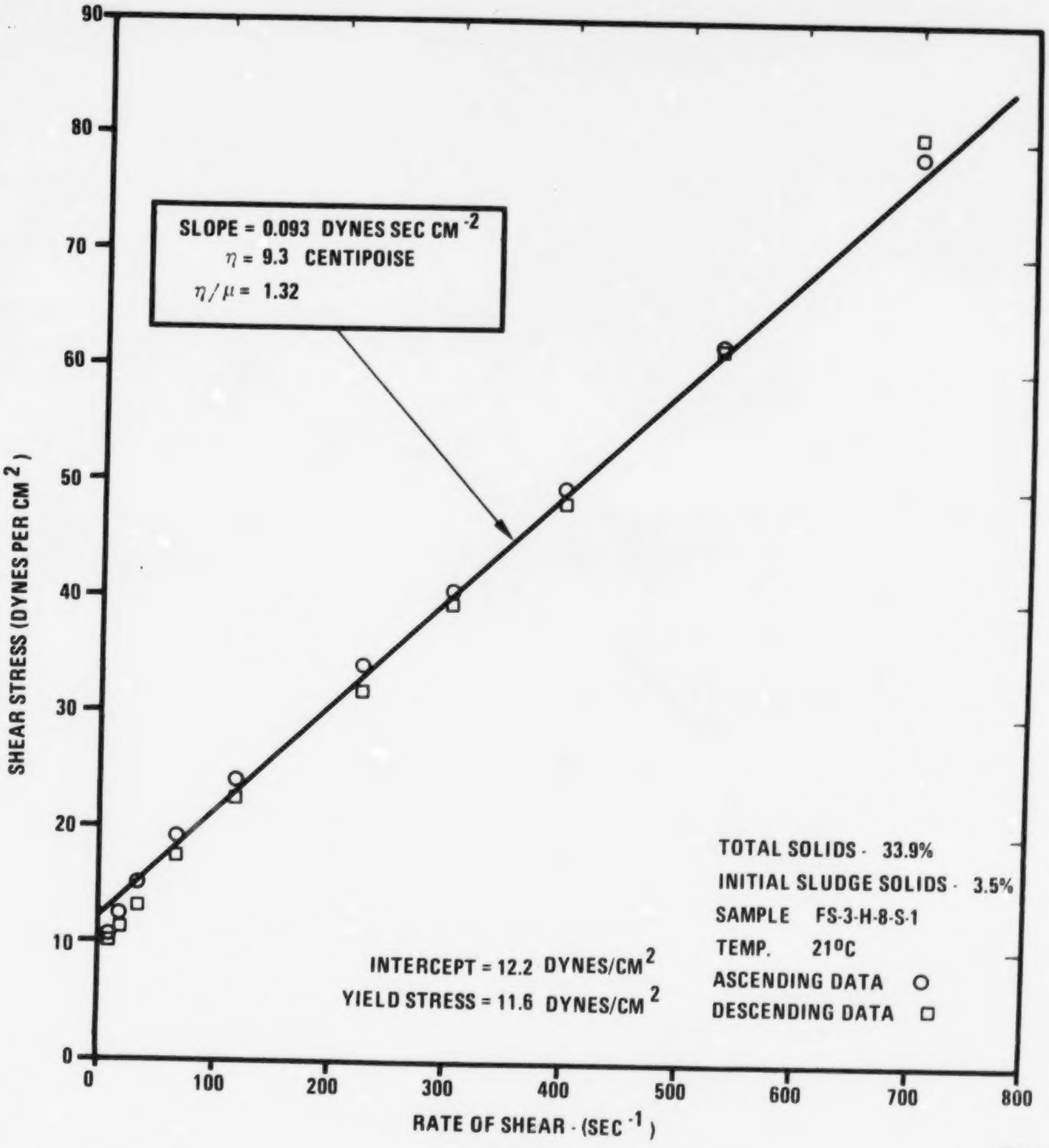

Similarly, yield stress can be reduced on the basis shown in Figure 6-11, **where** $(\tau_o)_m$ is the measured yield stress of the mixture and $(\tau_o)_s$ is the yield stress of the sludge. It can be seen in Figure 6-11 that data for 3.3 percent sludge and 5.7 percent sludge, both containing fly ash solids, are represented by a single line when reduced on this basis.

The reduced viscosity of 0.97 shown in Figure 9-1 indicates that the addition of fly ash to sludge resulted in a reduction in viscosity. This may in fact be the case, due to an interaction between the two materials, but it is more likely that the viscosity increased slightly, and the low η/μ, Figure 9-1, is due to experimental error.

9.3 HYDRAULIC DATA

The hydraulic data for 3.5 percent sludge containing three concentrations of fly ash are shown in Figures 9-4 to 9-9. Complete run sheets are given in paragraph A.4 of Appendix A.

The figures show that the homogeneous model gives excellent prediction of the observed data in the turbulent regime. The transition velocities are accurately predicted by the Hedstrom procedure for the full range of concentration.

9.3.1 Transition Velocity

Figure 9-4 shows a plot of shear stress versus velocity for measured data points from Run FS-1-H (11 percent total solids). The

FIGURE 9-4

SHEAR STRESS vs. VELOCITY
FLY ASH/SLUDGE MIXTURE

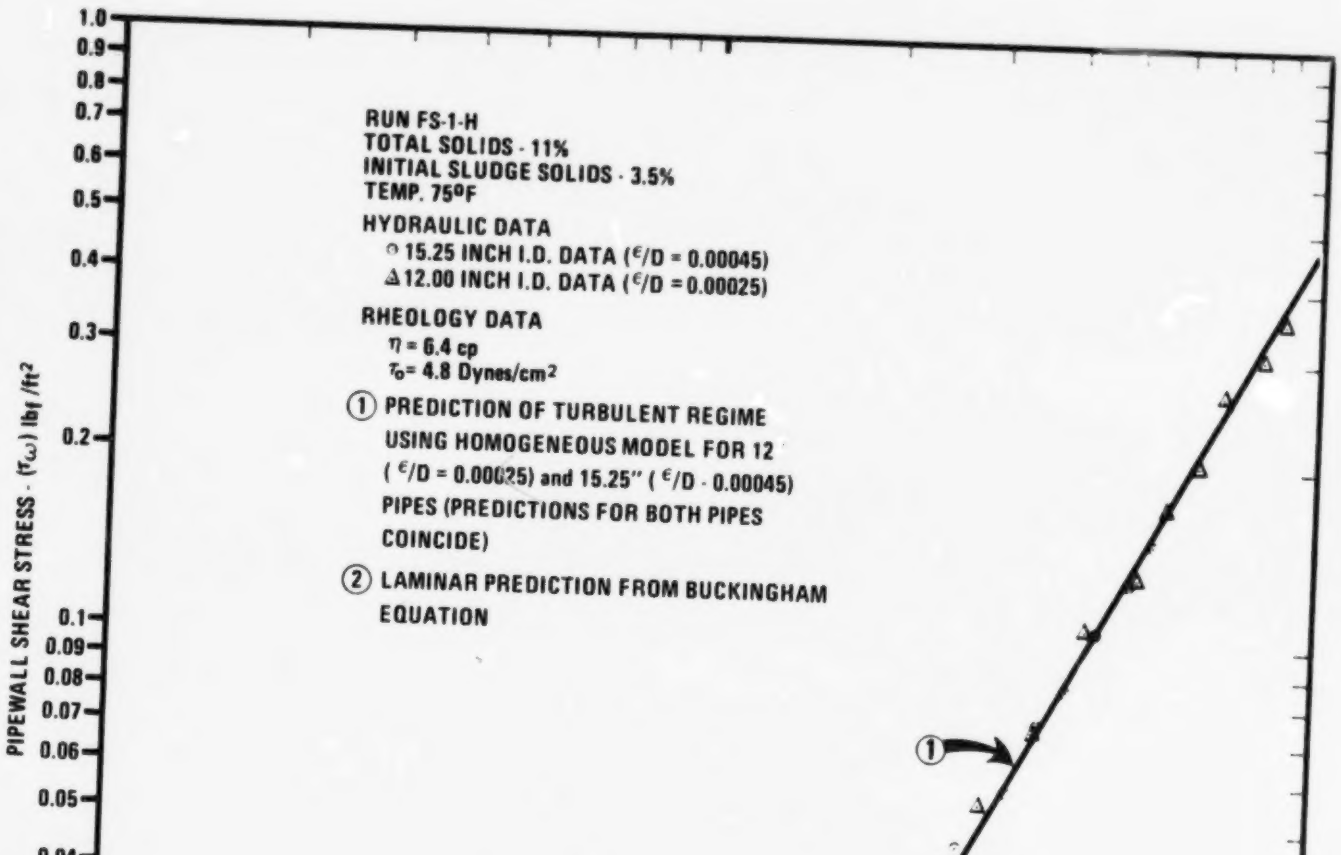

laminar correlation is calculated from the Bingham model, and fails to predict the transition velocity (V_c = 1.5 feet per second).

Figure 9.5 shows the same data on the basis of friction factor versus Reynolds Number. The laminar correlation is in the form of a Hedstrom plot, and although the laminar predictions are low excellent correlation of transition is obtained (V_c of 2.0 feet per second versus 2.1 feet per second observed).

Figures 9-6 to 9-9 show the data for runs FS-2-H and FS-3-H (20 and 35 percent total solids respectively). In each case the Bingham critical is lower than the observed value, while the Hedstrom procedure gives excellent correlation of transition velocity. The following table compares the observed transition velocities with predicted values.

		Critical Velocity		
Run No.	Total Solids (percent by weight)	Observed	Bingham Prediction	Hedstrom Prediction
FS-1-H	11.0	2.1	1.5	2.0
FS-2-H	20.0	2.4	1.9	2.5
FS-3-H	35.0	2.7	2.1	2.7

9.3.2 Turbulent Regime

The shear stress/velocity data are closely correlated by the homogeneous model. The difference in roughness of the 12 and 16-inch pipes obliterates any diameter effect (as discussed in paragraph 7.3) and the data are correlated by a single line (see Figures 9-4, 9-6 and 9-8).

FIGURE 9-5

FRICTION FACTOR vs. REYNOLDS NUMBER
FLY ASH/SLUDGE MIXTURE

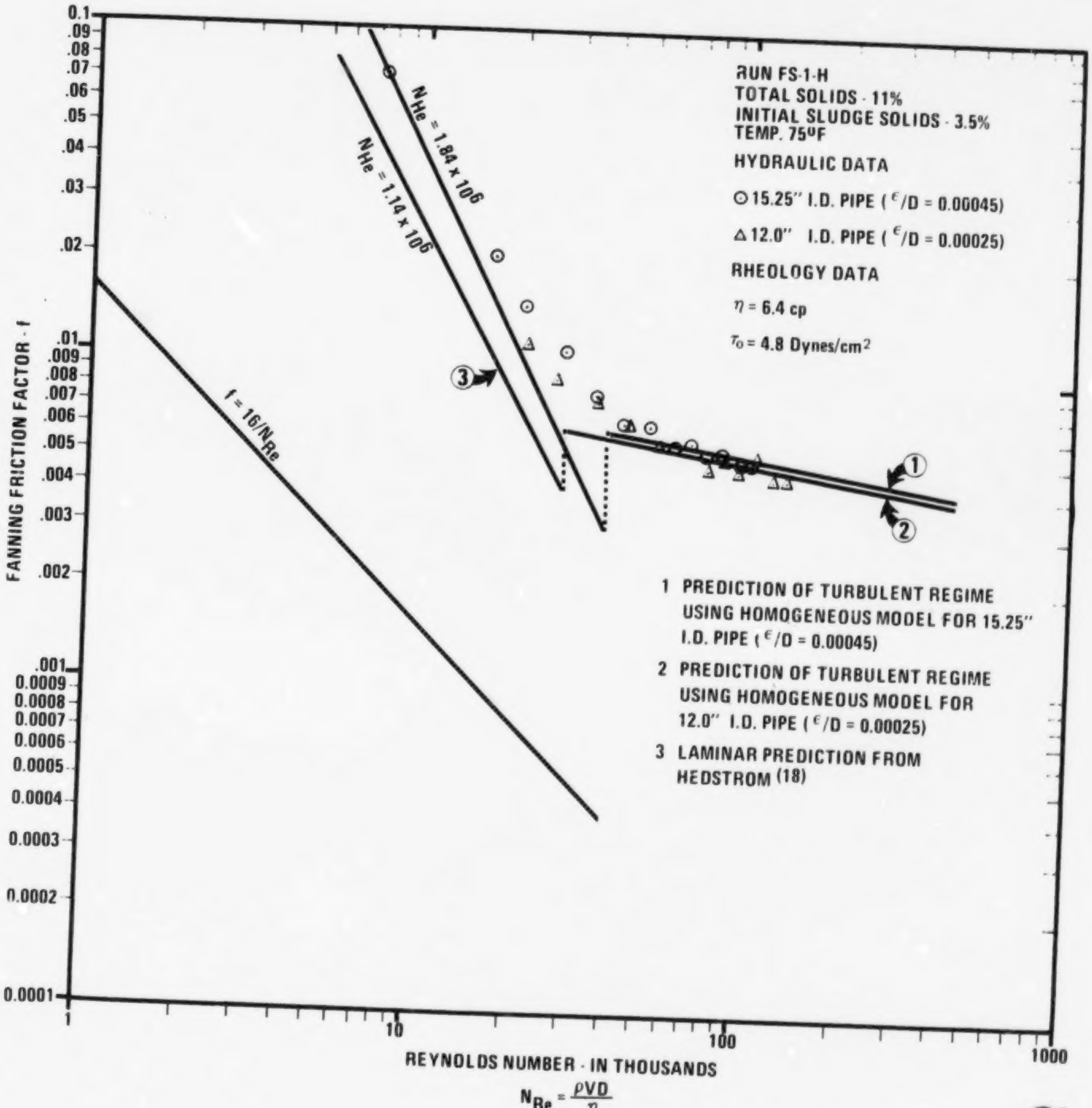

FIGURE 9-6

SHEAR STRESS vs. VELOCITY
FLY ASH/SLUDGE MIXTURE

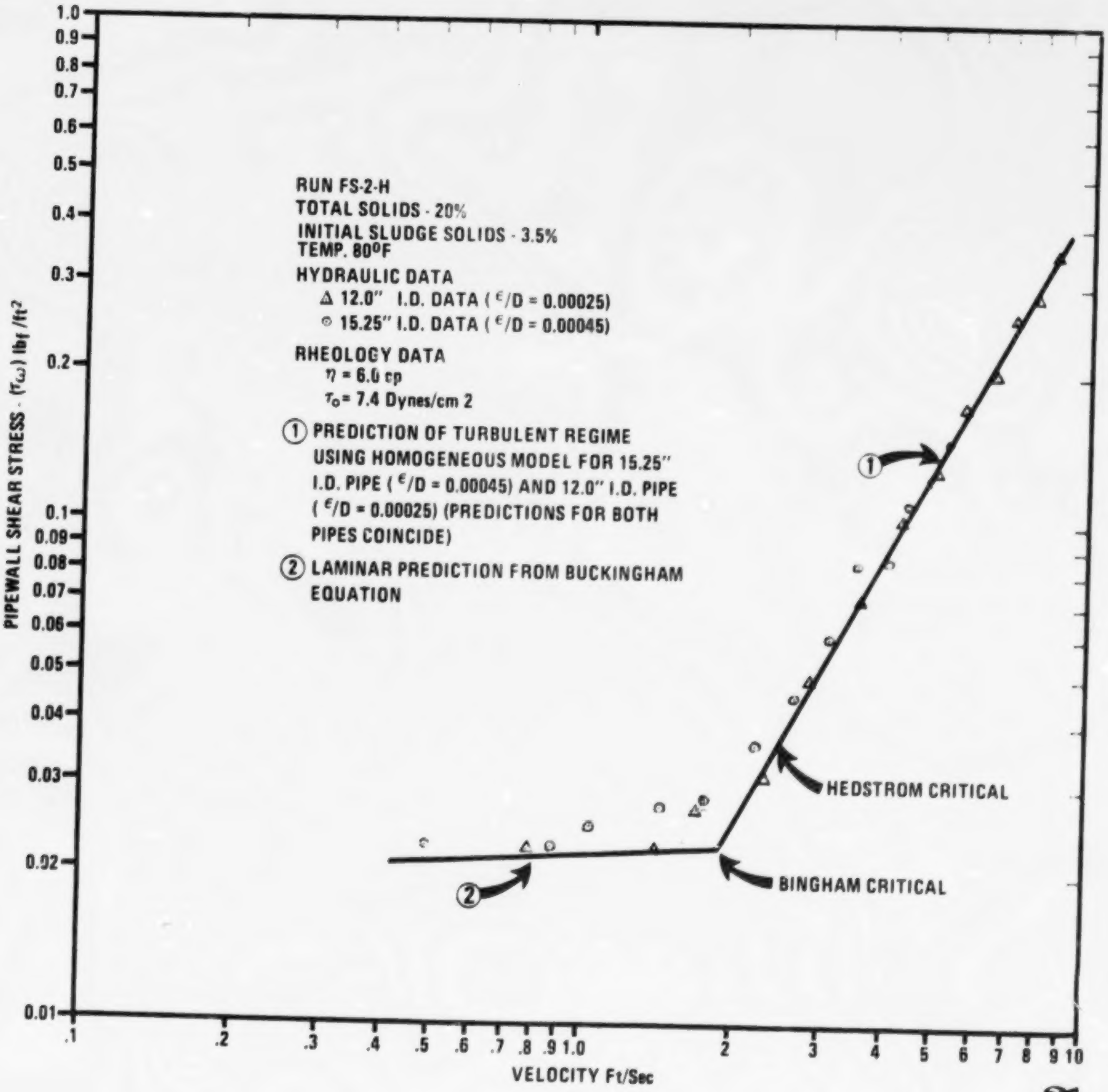

FIGURE 9-7

FRICTION FACTOR vs. REYNOLDS NUMBER
FLY ASH/SLUDGE MIXTURE

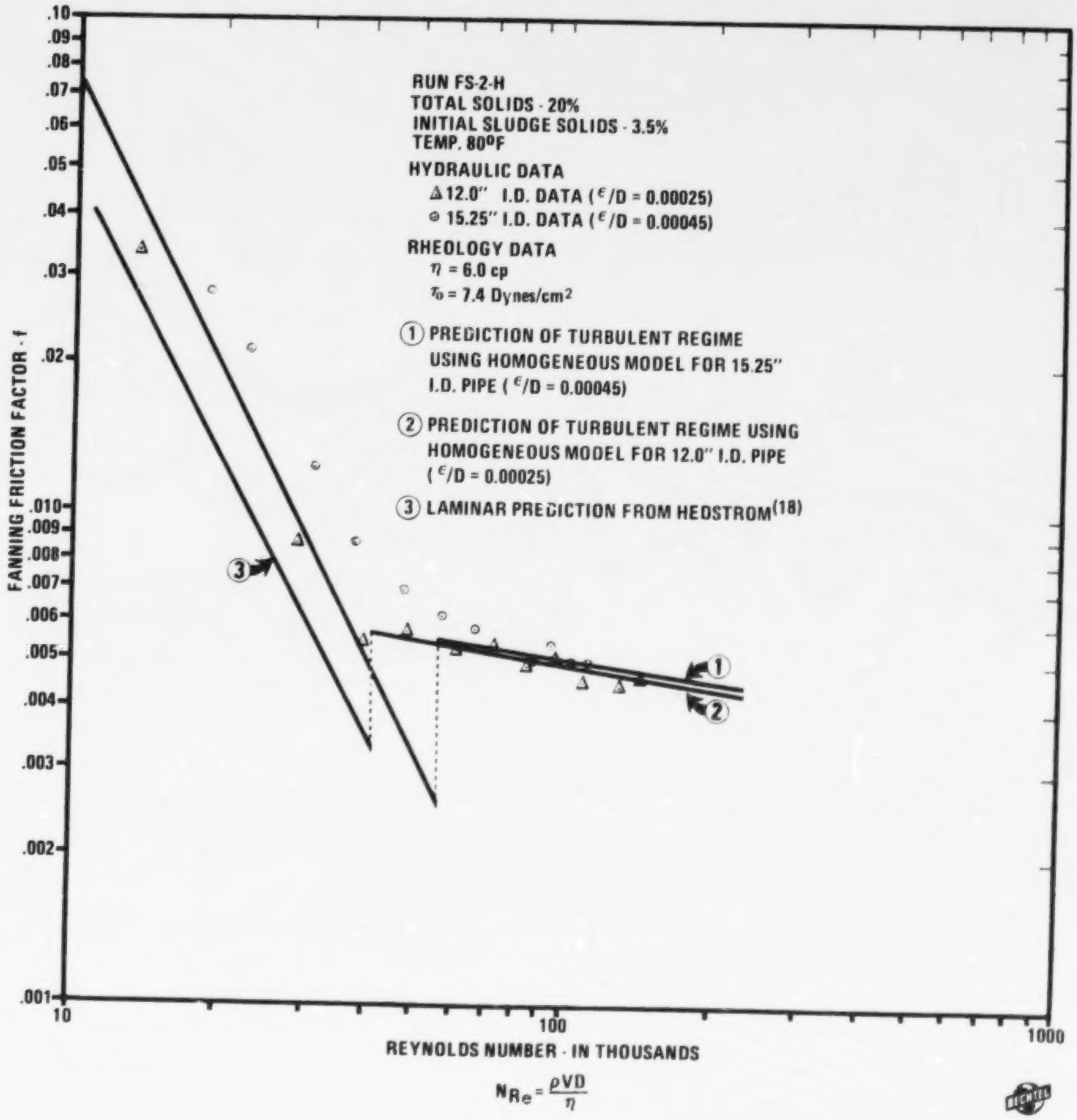

FIGURE 9-8

SHEAR STRESS vs. VELOCITY
FLY ASH/SLUDGE MIXTURE

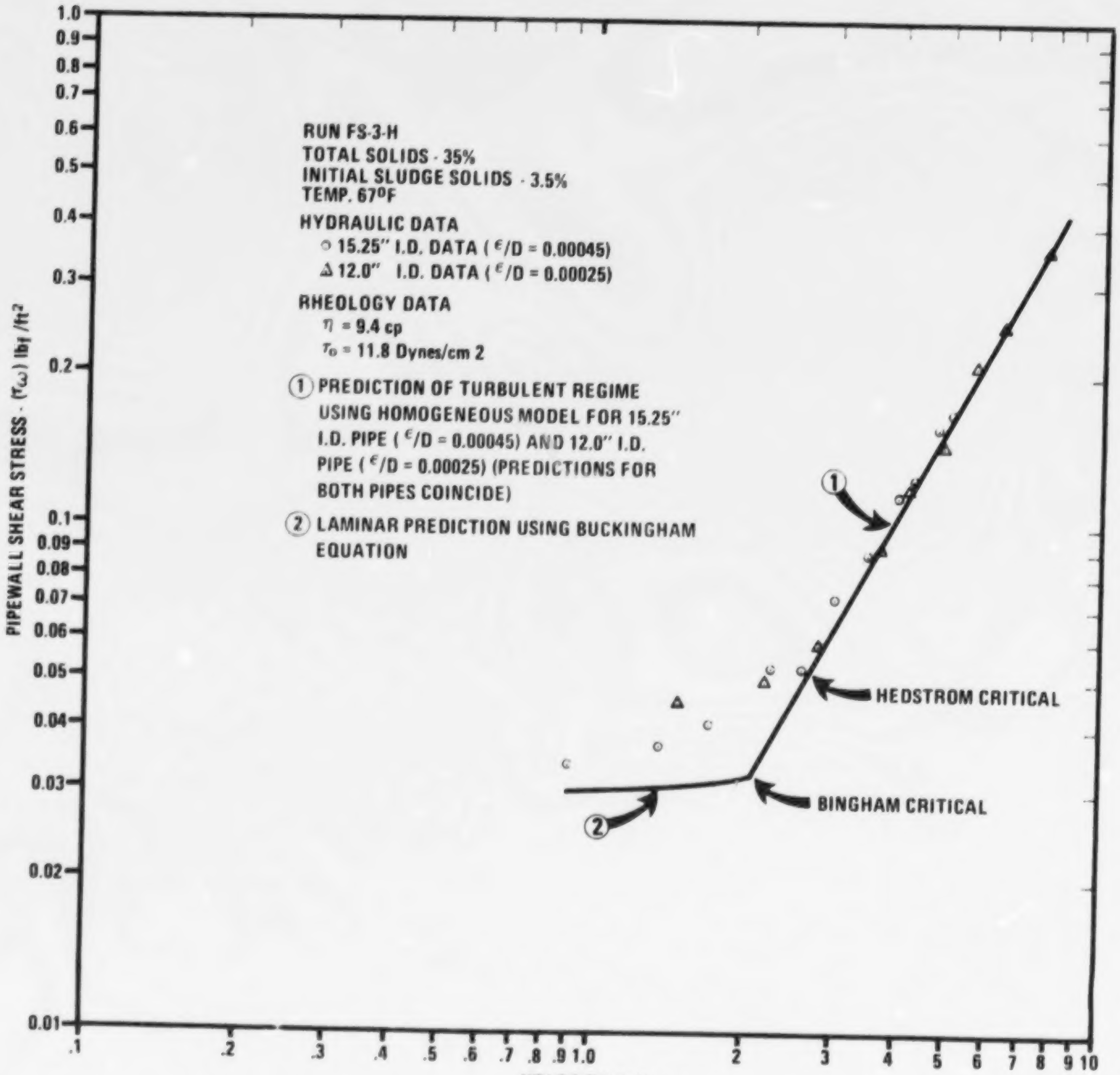

FIGURE 9-9

FRICTION FACTOR vs. REYNOLDS NUMBER
FLY ASH/SLUDGE MIXTURE

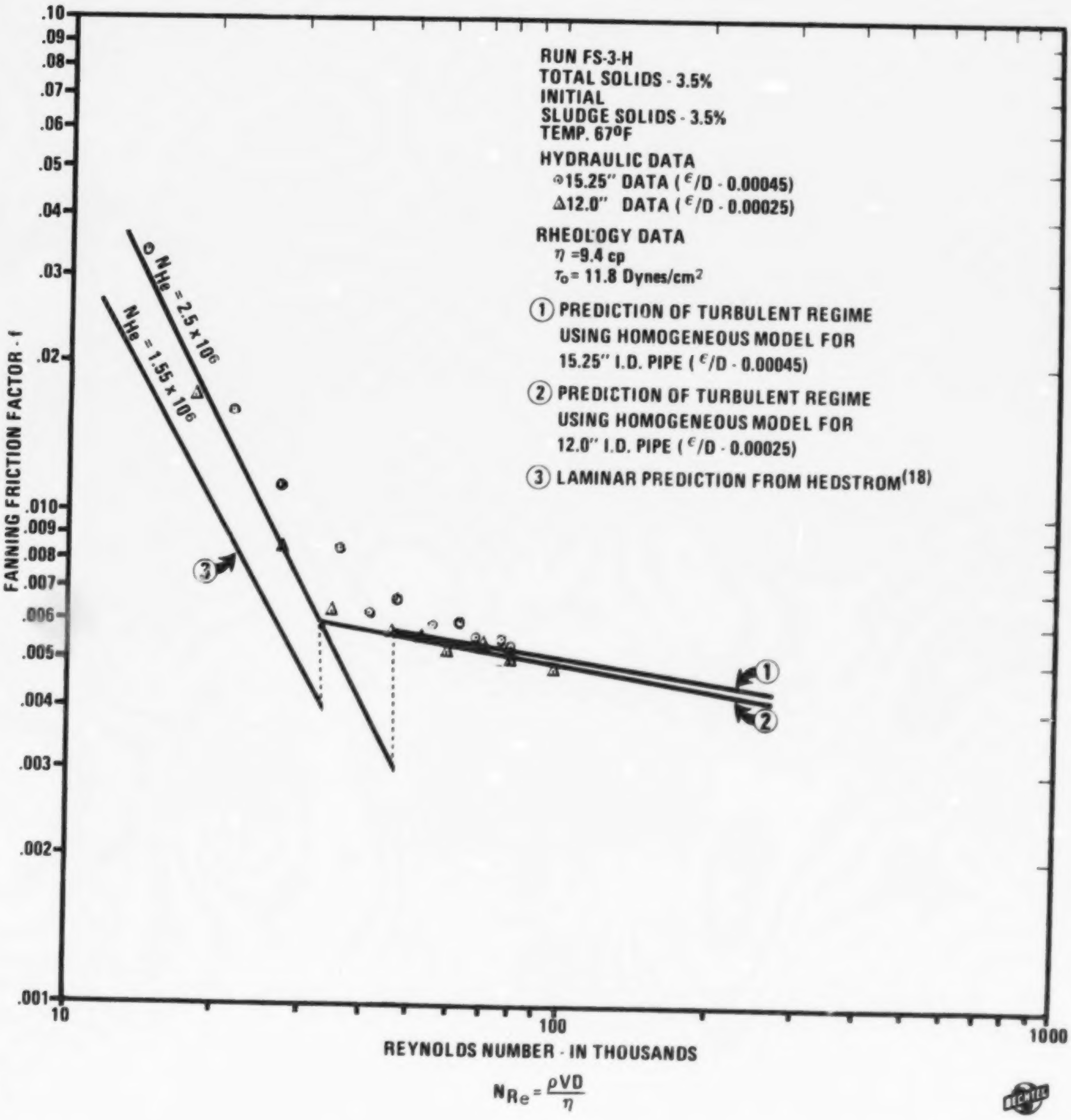

The difference in pipe roughness is clearly shown in the friction factor/Reynolds Number plots (Figures 9-5, 9-7 and 9-9), where two distinct correlation curves are applied. There is no significant damping of turbulence in this system.

Tables 9-2, 9-3, and 9-4 show the wall shear stresses calculated using the homogeneous model, and compare the calculated values with the observed data.

9.4 PIPELINE OPERABILITY

For the purpose of establishing the operability of a fly ash/sludge pipeline, the test loop was shut down for a period of about 39 hours following run FS-2-H (20 percent solids).

The loop was then restarted and, as can be seen from Figure 9-10, within 3 minutes of startup the system was back to approximately normal operation. Figure 9-10 is a comparison of conditions following startup at 3.3 feet per second with steady conditions at 3.1 feet per second prior to shutdown.

The wall shear stress reached a steady value of 0.073 lb_f/ft^2 compared with 0.060 lb_f/ft^2 before shutdown. The difference is a result of the slightly higher startup velocity, and the fact that startup was performed a temperature of some 15°F lower than the steady condition prior to shutdown, thus giving an increased viscosity. A plot of friction factor versus running time is given in Figure 9-10. This smooths out the effects of initial velocity fluctuations, and shows that

Table 9-2

CORRELATION OF FS-1-H USING HOMOGENEOUS MODEL

Line No.	Velocity (fps)	τ_w Observed (lb/ft^2)	τ_w Calculated (lb/ft^2)	Percent Deviation
12 Inch Data				
1	8.9	0.351	0.372	+6.0
2	7.2	0.265	0.253	-4.5
3	5.8	0.171	0.170	-0.6
4	4.3	0.106	0.100	-5.7
5	2.9	0.054	0.048	-11.1
6	1.42	0.023	---	Transition Zone
7	0.64	0.018	---	Transition Zone
8	1.76	0.027	---	Transition Zone
9	2.36	0.036	0.033	-8.3
10	3.6	0.072	0.071	-1.4
11	5.2	0.130	0.139	+6.9
12	8.2	0.302	0.323	+7.0
13	6.5	0.202	0.209	+3.5
16 Inch Data				
1	5.5	0.149	0.154	+3.4
2	4.4	0.105	0.103	-1.9
3	3.6	0.073	0.070	-4.1
4	2.68	0.046	0.041	-10.9
5	1.79	0.025	---	Transition Zone
6	0.88	0.016	---	Transition Zone
7	0.40	0.011	---	Transition Zone
8	1.09	0.017	---	Transition Zone
9	1.46	0.023	---	Transition Zone
10	2.20	0.032	0.030	-6.3
11	3.2	0.057	0.057	0.0
12	5.1	0.128	0.134	+4.7
13	4.0	0.085	0.086	+1.3

Table 9-3

CORRELATION OF FS-2-H USING HOMOGENEOUS MODEL

Line No.	Velocity (fps)	τ_w Observed (lb/ft^2)	τ_w Calculated (lb/ft^2)	Percent Deviation
12 Inch Data				
1	8.5	0.356	0.354	-0.6
2	7.1	0.265	0.257	-3.0
3	5.7	0.175	0.169	-3.4
4	4.3	0.104	0.100	-3.8
5	2.84	0.050	0.048	-4.0
6	1.42	0.023	---	Transition Zone
7	0.80	0.023	---	Transition Zone
8	1.70	0.027	---	Transition Zone
9	2.33	0.032	---	Transition Zone
10	3.6	0.072	0.072	0.0
11	5.0	0.130	0.133	+2.3
12	6.5	0.203	0.215	+5.9
13	7.8	0.292	0.300	+2.7
16 Inch Data				
1	5.3	0.149	0.148	-0.7
2	4.4	0.112	0.105	-6.2
3	3.5	0.085	0.068	-20.0
4	2.64	0.046	0.043	-6.5
5	1.76	0.029	---	Transition Zone
6	0.88	0.023	---	Transition Zone
7	0.49	0.023	---	Transition Zone
8	1.05	0.025	---	Transition Zone
9	1.44	0.027	---	Transition Zone
10	2.21	0.037	---	Transition Zone
11	3.1	0.060	0.056	-6.7
12	4.0	0.087	0.088	+1.5
13	4.9	0.126	0.128	+1.6

Table 9-4

CORRELATION OF RUN FS-3-H USING HOMOGENEOUS MODEL

Line No.	Velocity (fps)	τ_w Observed (lb/ft^2)	τ_w Calculated (lb/ft^2)	Percent Deviation
12 Inch Data				
1	5.7	0.212	0.202	-4.7
2	4.2	0.121	0.119	-1.7
3	2.78	0.059	0.055	-6.8
4	1.48	0.045	---	Transition Zone
5	2.21	0.050	---	Transition Zone
6	3.7	0.092	0.093	+1.1
7	4.8	0.148	0.151	+2.0
8	6.4	0.252	0.255	+1.2
9	7.8	0.360	0.365	+1.4
16 Inch Data				
1	5.1	0.172	0.166	-3.5
2	4.3	0.126	0.121	-4.1
3	3.5	0.089	0.083	-6.7
4	2.62	0.053	---	Transition Zone
5	1.72	0.041	---	Transition Zone
6	0.91	0.034	---	Transition Zone
7	1.37	0.037	---	Transition Zone
8	2.27	0.053	---	Transition Zone
9	3.0	0.073	0.062	-15.0
10	4.0	0.117	0.106	-9.4
11	4.9	0.160	0.152	-5.0

FIGURE 9-10

OPERABILITY TEST RUN
RUN FS-1-0
FLY ASH/SLUDGE - 20% SOLIDS

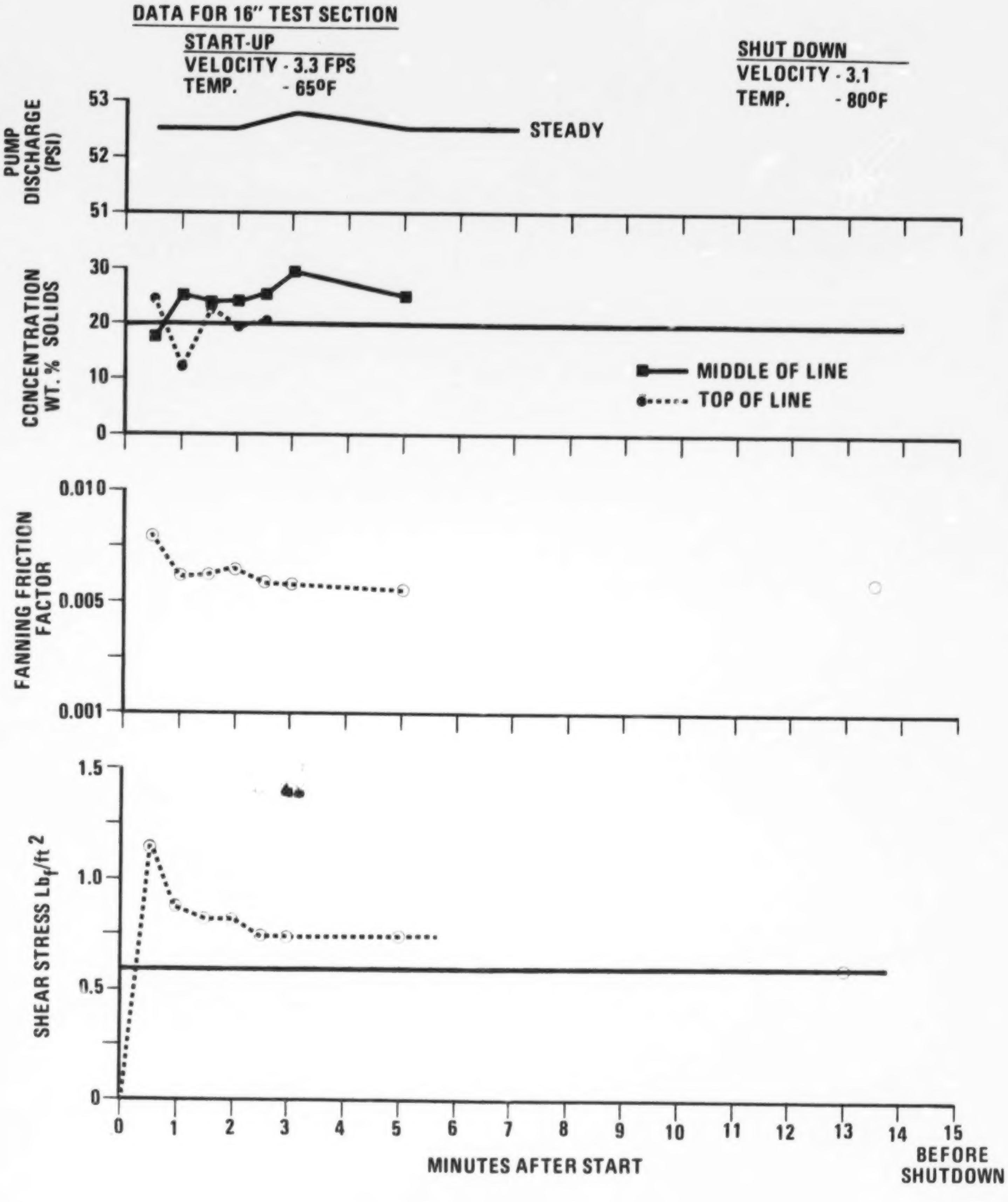

after the initial surge on startup, the system rapidly approached steady conditions.

Samples of slurry were taken from the top and the middle of the 16-inch section during startup, as shown in Figure 9-10, and these show that the system is tending towards complete resuspension after 5 minutes.

It must be pointed out that the conditions of the startup test (3.3 feet per second) were rather harsh, since a Hedstrom critical of 2.5 feet per second could be expected for this system. The test has shown that a sludge/fly ash system can easily be restarted at a velocity close to critical, and therefore in commercial operation such a pipeline can be safely shutdown and restarted.

Appendix A

SUPPLEMENTARY DATA

A-1 WATER RUNS

Figures A-1 and A-2 show the data for six water runs performed in the loop for the purpose of establishing pipe roughnesses.

Throughout the tests, the 12-inch section maintained a constant relative roughness (ϵ/D) of 0.00025 as shown in Figure A-1, except when the fly ash and sludge mixture was in the loop. During this run, a coating effect took place on the pipe wall; however, the deposit was removed when fly ash slurries were used in the loop.

Figure A-2 shows the water data for the 16-inch test section. It can be clearly seen that the relative roughness is significantly reduced following the first fly ash run. This is attributed to a sand blasting effect (in fact large pieces of scale were recovered from the line following this run), which reduced the ϵ/D value from 0.00045 to 0.00030.

Figure A-3 is a check on the velocity profile equipment used in the tests, from which a von Karman coefficient for water of 0.38 was calculated. This is in excellent agreement with the classical value of the coefficient. The pitot tube was checked against a hot-film anemometer, kindly loaned by the D.I.S.A. Company; as Figure A-3 shows, good agreement was obtained between the two.

Figure A-4 explains the identification code used for the test runs.

FIGURE A-1

FANNING FRICTION FACTOR vs. REYNOLDS NUMBER FOR
12″ PIPE USING WATER

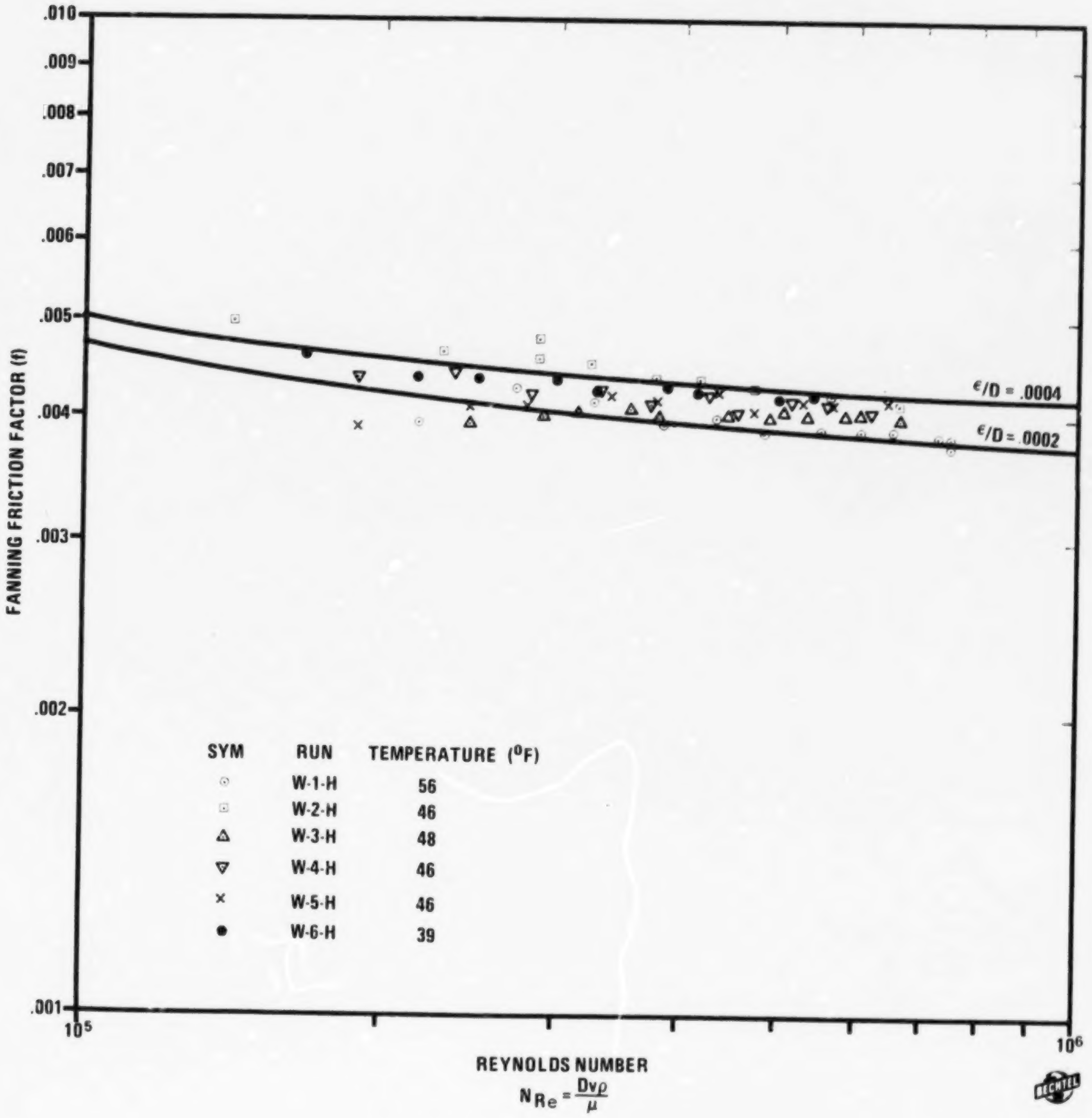

FIGURE A-2

FANNING FRICTION FACTOR vs. REYNOLDS NUMBER FOR
15.25" PIPE USING WATER

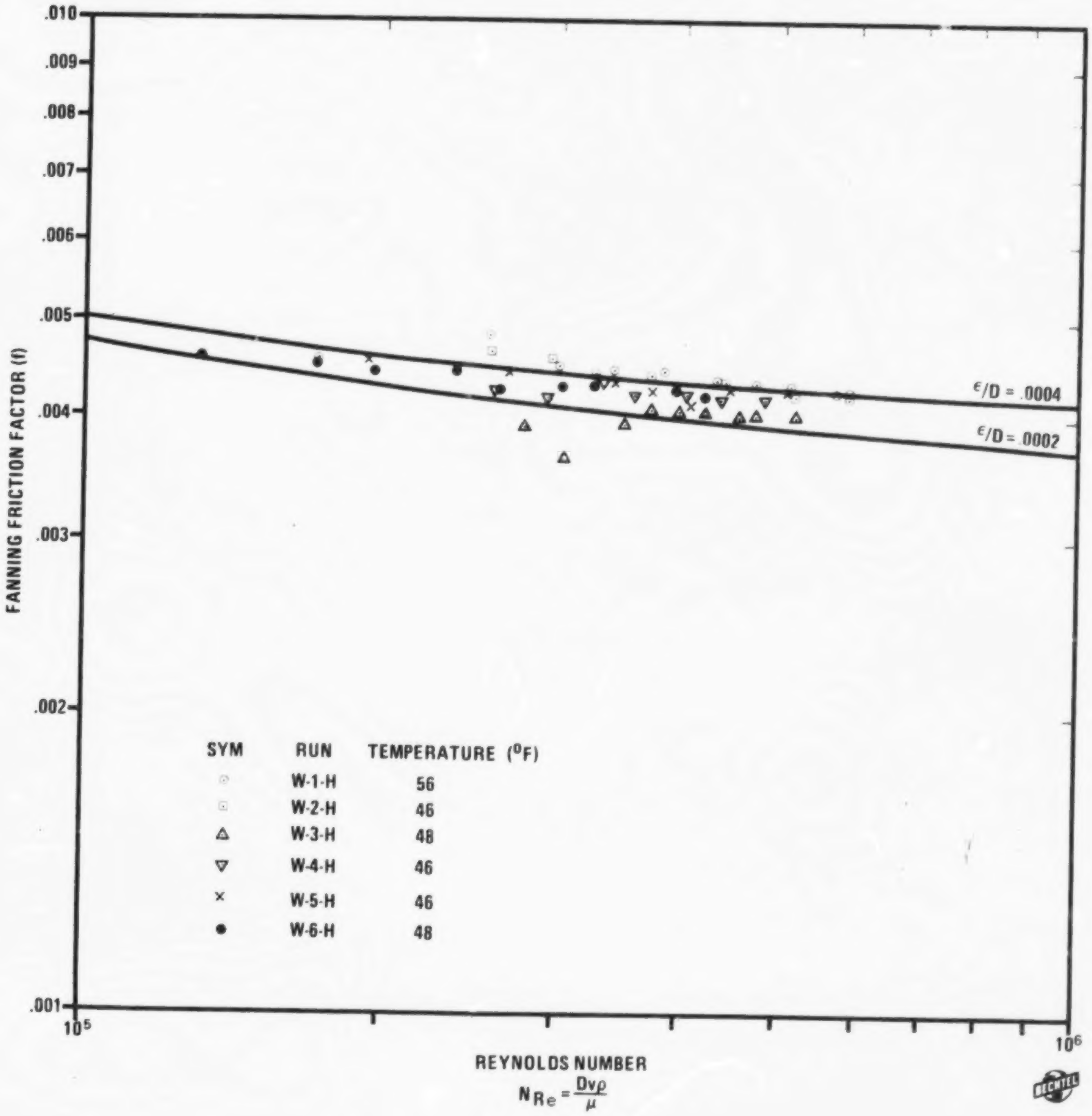

FIGURE A-3

VELOCITY PROFILE IN 16" PIPE WITH WATER

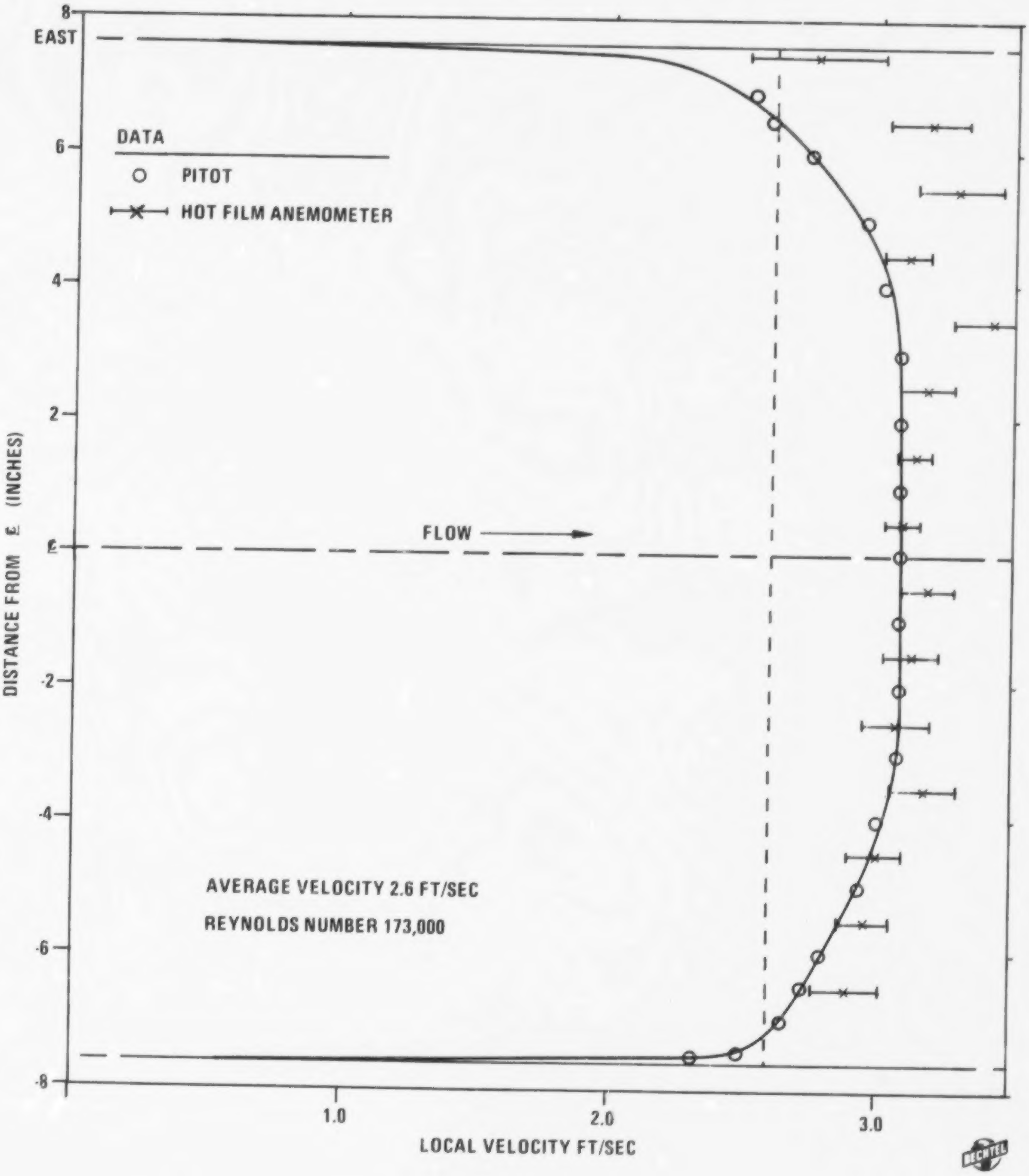

FIGURE A-4

SAMPLE IDENTIFICATION

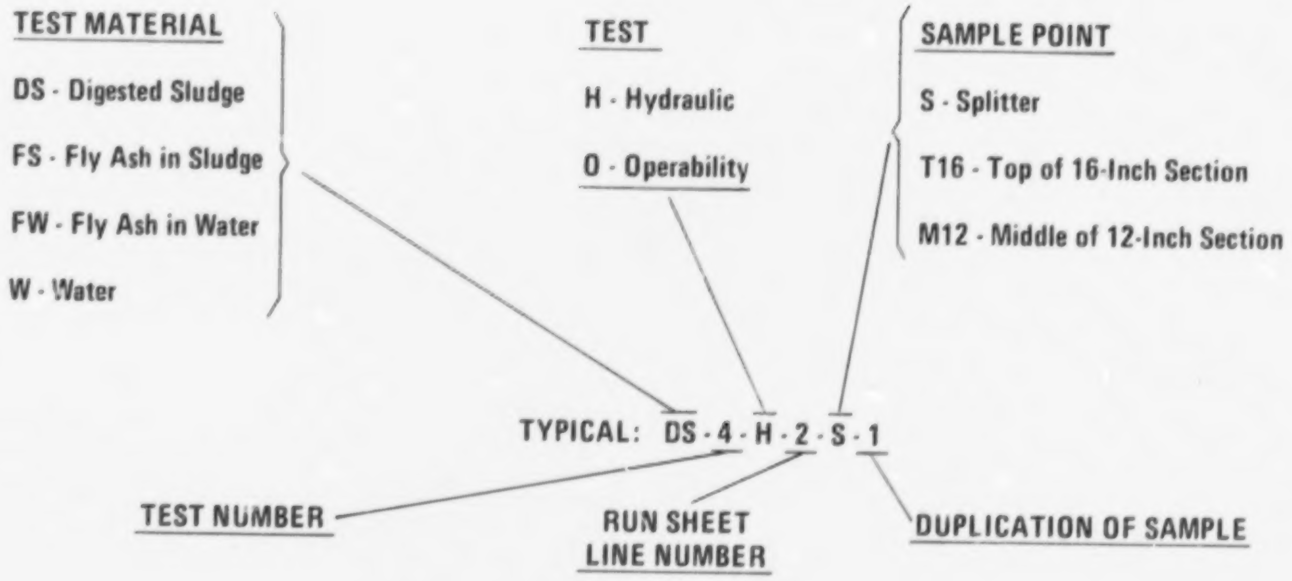
TEST MATERIAL
DS - Digested Sludge
FS - Fly Ash in Sludge
FW - Fly Ash in Water
W - Water
TEST
H - Hydraulic
O - Operability
SAMPLE POINT
S - Splitter
T16 - Top of 16-Inch Section
M12 - Middle of 12-Inch Section
TYPICAL: DS - 4 - H - 2 - S - 1
TEST NUMBER
RUN SHEET LINE NUMBER
DUPLICATION OF SAMPLE

A-2 DIGESTED SLUDGE RUNS

Tables A-1 to A-3 present the data gathered from pipe tests on digested sludge.

TABLE A-1

RUN NO.: DS-1-H
MATERIAL: Digested Sludge
SOLIDS CONCENTRATION: 3.5% Wt.
GRAVITY (AVE): 1.01 = 63.0 lbs/ft^3
RHEOLOGY (AVE): η = 6.3 cP, τ_o - as shown
TEMPERATURE: 78°F
DATE: 11/1/68

Line No.	Time (hr:min)	Temp (°F)	Pressure (psi)	Specific Gravity	Solids Concentration (Wt%)	Flow (gpm)	Velocity	
							12 Inch (fps)	16 Inch (fps)
Start	15:00							
1	15:15	77.	50.	1.01	3.4	1220	3.45	2.15
2	15:30	77.5	47.5	—	3.4	2070	5.90	3.65
3	15:40	77.5	44.	1.01	3.6	2500	7.10	4.40
4	16:05	77.5	36.5	—	3.8	3000	8.50	5.30
5	16:12	77.5	35.6	—	4.2	3260	9.30	5.75
6	16:18	77.5	38.5	—	3.0	2750	7.80	4.85
7	16:25	78.5	42.9	1.01	3.5	2260	6.40	4.00
8	16:33	78.5	45.5	—	3.2	1750	5.00	3.10
9	16:46	79.	47.5	—	3.3	1400	4.00	2.45
10	16:50	79.	49.1	—	3.4	970	2.75	1.70
11	17:00	79.5	51.0	—	3.9	460	1.30	0.80
12	17:11	—	50.5	—	—	1120	3.18	1.96

A

ocity		Pressure Drop		Rheology		Reynolds No.		Shear Stress		Friction Factor	
h	16 Inch (fps)	12 Inch (psi/200)	16 Inch (psi/200)	η/μ	τ_o (dynes/cm^2)	12 Inch ($\times 10^{-4}$)	16 Inch ($\times 10^{-4}$)	12 Inch (lbs/ft^2)	16 Inch (lbs/ft^2)	12 Inch ($\times 10^3$)	16 Inch ($\times 10^3$)
	2.15	0.33	0.13	7.6	8.4	5.13	4.07	.059	.030	5.10	6.58
	3.65	0.83	0.29	7.2	7.6	8.78	6.90	.149	.066	4.39	5.09
	4.40	1.20	0.41	7.4	7.4	10.56	8.32	.216	.094	4.38	4.95
	5.30	1.70	0.60	7.4	7.1	12.65	10.02	.306	.137	4.33	4.99
	5.75	1.93	0.68	7.1	6.9	13.84	10.87	.347	.156	4.11	4.81
	4.85	1.45	0.52	7.1	6.5	11.80	9.17	.261	.119	4.39	5.17
	4.00	1.03	0.37	7.1	6.0	9.52	7.56	.185	.085	4.63	5.41
	3.10	0.68	0.24	7.2	6.0	7.44	5.86	.122	.055	5.00	5.84
	2.45	0.48	0.17	7.4	5.6	5.95	4.63	.086	.039	5.52	6.62
	1.70	0.28	0.11	7.0	5.6	4.09	3.21	.050	.025	6.81	8.90
	0.80	0.13	0.09	7.5	5.8	1.93	1.51	.023	.021	14.15	32.9
	1.96	0.33	0.12	—	—	4.73	3.71	.059	.027	6.00	7.3

B

TABLE A-2

RUN NO.: DS 2-H
MATERIAL: Digested Sludge
SOLIDS CONCENTRATION: 3.0 Wt%
GRAVITY (AVE): = 63.0 lb/ft^3
RHEOLOGY (AVE): η = 6.4 cp, τ_o = 3.1 dynes/cm^2
TEMPERATURE: 57^{o}F
DATE: 11/24/68

Line No.	Time hr:min	Temp. ^{o}F	Pressure psi	Solids Concentration Wt%	Flow gpm	Velocity		Pressure
						12 Inch fps	16 Inch fps	12 Inch psi/200
Start	9:47							
1	10:20	56	—	2.9	2000	5.7	3.5	0.86
2	10:47	—	—	2.6	1500	4.25	2.65	0.52
3	11:00	56	—	2.9	1000	2.85	1.75	0.28
4	11:10	56	—	2.7	1790	5.1	3.15	0.69
5	11:19	—	—	3.2	2250	6.4	4.0	1.00
6	11:29	58	—	3.3	1275	3.6	2.2	0.40
7	11:35	59	—	3.3	800	2.25	1.4	0.20
8	11:44	60	—	3.3	1620	4.6	2.8	0.59

A

Pressure Drop		Rheology		Reynolds No.		Shear Stress		Friction Factor	
2 Inch psi/200	16 Inch psi/200	η / μ	τ_o dynes/cm^2	12 Inch x10^{-4}	16 Inch x10^{-4}	12 Inch lbs/ft^2	16 Inch lbs/ft^2	12 Inch x10^3	16 Inch x10
0.86	0.27	4.4	3.1	8.34	6.51	0.155	0.062	4.87	5.15
0.52	0.18	5.6	2.2	6.22	4.93	0.094	0.041	5.30	5.99
0.28	0.14	5.1	2.6	4.17	3.26	0.050	0.032	6.34	10.69
0.69	0.23	5.5	2.0	7.47	5.86	0.124	0.053	4.88	5.42
1.00	0.34	5.6	3.7	9.37	7.45	0.180	0.078	4.49	4.97
0.40	0.15	6.0	3.7	5.27	4.10	0.072	0.034	5.68	7.25
0.20	0.10	5.4	4.5	3.30	2.61	0.036	0.023	7.27	11.93
0.59	0.19	6.0	3.5	6.74	5.21	0.106	0.043	5.13	5.67

B

1

TABLE A-3

RUN NO: DS 3-H
MATERIAL: Digested Sludge
SOLIDS CONCENTRATION: 2.5 Wt%
GRAVITY (AVE): 1.010 = 63.0 lb/ft^3
RHEOLOGY (AVE): η = 4.5 cp τ_o = ~0 dynes/cm^2
TEMPERATURE: 58°F
DATE: 11/24/68

Line No.	Time hr:min	Temp. °F	Pressure psi	Solids Concentration Wt%	Flow gpm	Velocity		Pressure D	
						12 Inch fps	16 Inch fps	12 Inch psi/200'	16 In ps
Start	14:51								
1	15:02	—	—	2.8	2490	7.0	4.4	1.16	0
2	15:07	—	—	2.7	2000	5.7	3.4	0.79	0
3	15:13	56	—	1.9	1500	4.25	2.65	0.50	0
4	15:18	56	—	2.2	1000	2.85	1.75	0.25	0
5	15:24	58	—	2.7	720	2.03	1.25	0.17	0
6	15:30	58	—	2.6	1225	3.5	2.15	0.36	0.
7	15:36	58	—	2.7	1790	5.10	3.15	0.67	0
8	15:40	58	—	2.5	2250	6.40	3.95	1.00	0
9	15:47	58	—	2.2	2800	8.0	4.9	1.48	0
10	15:53	59	—	2.6	3200	9.1	5.65	1.91	0
11	16:00	60	—	3.2	1100	3.1	1.94	0.30	0.
12	16:04	—	—	—	500	1.4	0.90	0.10	0.

A

Pressure Drop		Rheology		Reynolds No.		Shear Stress		Friction Factor	
12 Inch psi/200'	16 Inch psi/200'	η / μ	τ_o dynes/cm^2	12 Inch x10^{-4}	16 Inch x10^{-4}	12 Inch lbs/ft^2	16 Inch lbs/ft^2	12 Inch x10^3	16 Inch x10^3
1.16	0.37	3.2	~0	14.58	11.65	0.209	.085	4.36	4.46
0.79	0.25	3.5	~0	11.87	9.27	0.142	.057	4.47	4.77
0.50	0.16	—	—	8.85	7.02	0.090	.037	5.09	5.32
0.25	0.07	3.7	~0	5.94	4.63	0.045	.016	5.66	5.34
0.17	0.05	3.9	~0	4.23	3.31	0.031	.011	7.59	7.48
0.36	0.11	3.9	~0	7.29	5.69	0.065	.025	5.41	5.56
0.67	0.21	4.2	~0	10.62	8.33	0.121	.048	4.74	4.95
1.00	0.32	3.8	~0	13.33	10.46	0.18	.073	4.49	4.80
1.48	0.48	4.1	~0	16.67	12.94	0.266	.110	4.26	4.67
1.91	0.62	3.9	~0	18.96	14.96	0.344	.142	4.24	4.54
0.30	0.10	4.1	~0	6.45	5.14	0.054	.023	5.74	6.21
0.10	0.04	—	—	2.92	2.38	0.018	.009	9.39	11.55

B

A-3 FLY ASH RUNS

Tables A-4 to A-11 present the data gathered from pipe tests on fly ash/water slurries.

TABLF A-4

RUN NO.: FW-1-H
MATERIAL: Fly Ash
SOLIDS CONCENTRATION: 52.8% Wt.
GRAVITY (AVE): 1.47 = 91.7 lbs/ft^3
RHEOLOGY (AVE): η = 10.4 cP, τ_o = 5.5 dynes/cm^2
TEMPERATURE: 62°F
DATE: 11-16-68

Line No.	Time hr:min	Temp °F	Pressure psi	Specific Gravity	Solids Concentration Wt %	Flow gpm	Velocity		F
							12 Inch fps	16 Inch fps	1 ps
Start	16:05	-	60+						
1	16:20	-	↓	1.470	52.0	1200	3.40	2.11	0
2	16:32	60		—	51.6	750	2.13	1.32	0
3	16.42	60		1.451	52.9	1020	2.89	1.79	0
4	16:50	-		1.480	53.0	1520	4.31	2.67	0
5	16:55	60		1.466	53.2	2000	5.67	3.51	1
6	17:01	60		1.490	53.2	2490	7.06	4.37	1
7	17:14	61		1.472	53.8	1725	4.89	3.03	0
8	17:21	61		1.480	53.0	1250	3.55	2.20	0
9	17:30	62		1.460	53.0	1000	2.84	1.76	0
10	17:40	63		1.472	53.8	720	2.04	1.26	0
11	18:00	64		1.445	51.2	1150	3.26	2.02	0
12	18:25	64		1.462	52.2	2050	5.82	3.60	1
13	18:55	-		—	—	525	1.49	0.92	0
14	19:25	67		—	—	730	2.07	1.28	0
15	19:50	67		—	—	825	2.34	1.45	0

A

ity	Pressure Drop		Rheology		Reynolds No.		Shear Stress		Friction Factor	
16 Inch fps	12 Inch psi/200'	16 Inch psi/200'	η / μ	dynes/cm^2 τ_o	12 Inch $\times 10^{-4}$	16 Inch $\times 10^{-4}$	12 Inch lbs/ft^2	16 Inch lbs/ft^2	12 Inch x10^3	16 Inch x10^3
2.11	0.37	0.20	10.4	5.7	4.46	3.51	.066	.045	4.04	7.23
1.32	0.14	0.15	8.9	5.5	2.78	2.19	.025	.034	3.90	13.88
1.79	0.29	0.17	10.5	5.5	3.79	2.98	.052	.038	4.37	8.51
2.67	0.675	0.30	-	-	5.64	4.44	.121	.068	4.59	6.76
3.51	1.10	0.45	11.9	5.5	7.43	5.84	.198	.102	4.32	5.86
4.37	1.78	0.58	8.6	3.7	9.24	7.28	.320	.132	4.51	4.87
3.03	0.86	0.32	10.2	5.5	6.41	5.04	.154	.073	4.54	5.60
2.20	0.47	0.20	8.5	3.8	4.64	3.65	.084	.045	4.73	6.66
1.76	0.31	0.15	9.2	5.5	3.71	2.92	.055	.034	4.87	7.81
1.26	0.14	0.12	8.7	4.7	2.67	2.10	.025	.027	4.24	12.05
2.02	0.38	0.20	9.3	4.7	4.27	3.36	.068	.045	4.51	7.87
3.60	1.19	0.42	9.4	3.2	7.61	5.99	.214	.096	4.45	5.20
0.92	0.057	0.10	-	-	1.95	1.53	.010	.022	3.25	18.89
1.28	0.16	0.11	-	-	2.71	2.13	.028	.025	4.72	10.75
1.45	0.38	0.15	-	-	3.06	2.41	.068	.034	8.77	11.48

B

TABLE A-5

SCREEN ANALYSIS
RUN FW-1-H

SAMPLE NO.	PERCENT RETAINED ON TYLER MESH							PERCENT SOLIDS
	+14	14x28	28x48	48x100	100x200	200x325	-325	
FW-1-H-1-S-1	0.1	0.3	0.8	2.4	8.2	14.3	73.9	52.0
FW-1-H-1-M16-1	trace	0.3	0.7	1.9	6.1	10.8	80.2	50.5
FW-1-H-1-T16-1	trace	0.2	0.7	1.8	5.6	11.0	80.7	50.7
FW-1-H-1-M12-1	trace	0.3	1.0	2.0	6.5	12.0	78.2	52.3
FW-1-H-1-T12-1	trace	0.4	0.8	2.2	6.0	11.6	79.0	52.5
FW-1-H-2-S-1	trace	0.2	0.6	1.9	5.7	11.8	79.8	51.6
FW-1-H-3-S-1	trace	0.3	0.9	1.9	6.2	11.3	79.4	52.9
FW-1-H-3-M16-1	0.3	3.2	3.8	5.7	12.5	9.1	65.4	38.0
FW-1-H-3-T16-1	trace	0.2	0.8	1.9	5.8	11.4	79.9	49.8
FW-1-H-3-M12-1	↓	0.5	1.2	3.0	8.9	11.2	75.2	49.3
FW-1-H-3-T12-1		0.3	0.9	1.9	5.7	11.8	79.4	52.2
FW-1-H-4-S-1		0.3	0.7	2.0	6.6	11.9	78.5	53.0
FW-1-H-5-S-1		0.2	0.9	2.2	6.0	12.0	78.7	53.2
FW-1-H-6-S-1		0.3	0.6	2.3	6.6	13.0	77.2	53.2
FW-1-H-7-S-1		0.3	0.9	2.3	7.0	12.3	77.2	53.8
FW-1-H-8-S-1		0.2	0.8	2.1	6.6	11.7	78.6	53.0
FW-1-H-9-S-1		0.2	0.8	1.9	6.1	12.3	78.7	53.0
FW-1-H-10-S-1		0.1	0.4	1.8	5.8	10.3	81.6	53.8
FW-1-H-11-S-1		0.2	0.4	2.0	6.4	11.3	79.7	51.2
FW-1-H-11-M16-1		0.4	0.6	2.2	6.4	11.0	79.4	50.9
FW-1-H-11-T16-1		0.2	0.6	2.0	5.5	10.8	80.9	51.1
FW-1-H-11-M12-1		0.3	0.7	1.9	6.3	11.1	79.7	51.6
FW-1-H-11-T12-1		0.2	0.8	1.8	5.7	11.0	80.5	52.9
FW-1-H-12-S-1		0.1	0.9	1.5	6.1	10.7	80.7	52.2

TABLE A-6

FW-1-H FLY ASH

1/2 INCH SMALL TUBE

SOLIDS CONCENTRATION = 52.8 percent by weight
PLASTIC VISCOSITY = 12.1 centipoise
YIELD STRESS = 5.5 dynes/cm^2
SLURRY DENSITY = 91.7 lbs/ft^3
PIPE I.D. = 0.622 inches
PIPE LENGTH = 21.83 ft
TEMPERATURE = 52°F

Flow gpm	Pressure Drop psi	Velocity ft/sec	Shear Stress lbs/ft^2	Reynolds Number	Fanning Friction Factor
4.75	4.6	5.02	0.393	2924.	0.0110
4.3	3.75	4.54	0.320	2647.	0.0109
3.68	2.5	3.89	0.213	2265.	0.0099
3.9	3	4.12	0.256	2401.	0.01062
3.21	1.97	3.39	0.168	1976.	0.01029
5.2	5.55	5.49	0.474	3201.	0.0111
5.74	7.1	6.06	0.606	3534.	0.0116
7.1	9.75	7.50	0.833	4371.	0.0104
1.85	1.19	1.95	0.102	1139.	0.0187
0.85	1.05	0.90	0.090	523.	0.0783

TABLE A-7

RUN NO.: FW-4-H
MATERIAL: Fly Ash
SOLIDS CONCENTRATION: 57.4% Wt
GRAVITY (AVE): 1.55 = 96.7 lbs/ft^3
RHEOLOGY (AVE): η = 14.7 cP, τ_o = 6.8 dynes/cm^2
TEMPERATURE: 54°F
DATE: 1/15/69

Line No.	Time hr:min	Temp °F	Pressure psi	Specific Gravity	Solids Concentration Wt %	Flow gpm	Velocity		Pr
							12 Inch fps	16 Inch fps	12 In psi/
Start	14:25								
1	14:40	52	Not recorded	1.57	57.2	3300	9.36	5.80	3.
2	15:00	53		1.58	57.0	2750	7.80	4.83	2.
3	16:30	54		1.53	56.5	2220	6.30	3.90	1.
4	16:45	54		1.57	59.1	1725	4.89	3.03	1.
5	17:20	54		1.56	58.4	3000	8.51	5.27	2.
6	17:35	54		1.56	56.9	2500	7.09	4.39	2.
7	18:00	54		1.55	57.2	1930	5.47	3.39	1.
8	18:20	54		1.55	57.5	1490	4.23	2.62	0.
9	18:42	54		1.52	56.5	1000	2.84	1.76	0.
10	18:52	54		1.51	53.4	1260	3.57	2.21	0.

A

locity		Pressure Drop		Rheology		Reynolds No.		Shear Stress		Friction Factor	
h	16 Inch fps	12 Inch psi/200'	16 Inch psi/200'	η/μ	τ_o dynes/cm^2	12 Inch x10^{-4}	16 Inch x10^{-4}	12 Inch lbs/ft^2	16 Inch lbs/ft^2	12 Inch x10^3	16 Inch x10^3
6	5.80	3.53	1.09	12.6	6.3	9.14	7.19	0.635	0.249	4.83	4.94
0	4.83	2.54	0.78	-	-	7.62	6.00	0.457	0.178	5.00	5.09
0	3.90	1.63	0.58	12.0	6.5	6.15	4.84	0.293	0.133	4.93	5.81
9	3.03	1.02	0.39	13.5	7.4	4.79	3.76	0.184	0.089	5.11	6.47
1	5.27	2.91	0.92	13.2	6.9	8.31	6.54	0.524	0.210	4.82	5.05
9	4.39	2.12	0.68	12.0	6.7	6.93	5.45	0.382	0.156	5.05	5.37
7	3.39	1.37	0.46	-	-	5.35	4.21	0.247	0.105	5.47	6.09
3	2.62	0.86	0.30	11.9	6.7	4.13	3.25	0.155	0.068	5.77	6.67
4	1.76	0.50	0.18	10.2	6.7	2.77	2.18	0.090	0.041	7.45	8.89
7	2.21	0.72	0.26	9.3	5.6	3.49	2.75	0.129	0.059	6.75	8.09

B

TABLE A-8

SCREEN ANALYSES
RUN FW-4-H

SAMPLE NO.	PERCENT RETAINED ON TYLER MESH							PERCENT SOLIDS
	+14	14x28	28x48	48x100	100x200	200x325	-325	
FW-4-H-1-S-1	trace	0.2	1.2	2.9	8.4	13.1	74.2	57.2
FW-4-H-2-S-1		0.3	1.2	2.8	8.6	12.9	74.2	57.0
FW-4-H-3-S-1		0.3	1.2	3.0	8.4	12.7	74.4	60.1
FW-4-H-3-M16-1		0.1	1.5	3.1	8.6	13.0	72.7	57.3
FW-4-H-3-T16-1		0.2	1.2	3.2	9.5	14.5	71.4	54.0
FW-4-H-3-M12-1		0.1	1.1	3.0	7.8	14.6	72.4	57.3
FW-4-H-3-T12-1		0.1	1.2	3.0	8.3	14.0	73.4	56.5
FW-4-H-4-S-1		0.2	1.1	2.8	8.3	13.1	74.5	56.5
FW-4-H-5-S-1		0.2	0.9	2.8	7.9	13.4	74.8	59.1
FW-4-H-5-M16-1		0.2	1.0	3.0	8.6	13.2	74.0	53.8
FW-4-H-5-T16-1		0.1	1.6	3.0	8.5	13.2	73.6	56.7
FW-4-H-5-M12-1		0.1	1.3	3.0	8.5	13.6	73.5	56.2
FW-4-H-5-T12-1		0.1	1.4	3.3	9.3	14.7	70.2	50.6
FW-4-H-6-S-1		0.2	1.0	2.8	8.3	13.0	74.7	57.4
FW-4-H-7-S-1		0.2	1.0	2.7	8.3	12.9	74.9	56.9
FW-4-H-7-M16-1		0.2	1.2	3.0	8.5	13.5	73.6	48.7
FW-4-H-7-T16-1		0.2	1.5	3.2	9.3	14.8	71.0	54.7
FW-4-H-7-M12-1		0.2	1.5	3.9	9.3	13.8	78.1	52.5
FW-4-H-7-T12-1		0.1	1.5	3.2	10.0	15.9	69.3	56.0
FW-4-H-8-S-1		0.1	1.0	2.9	8.2	12.9	74.9	57.2
FW-4-H-8-M16-1		0.2	1.2	3.2	7.5	13.0	74.9	54.1
FW-4-H-8-T16-1		0.2	1.4	3.9	8.8	14.5	71.2	52.0
FW-4-H-8-M12-1		0.2	1.3	2.9	8.2	12.8	73.6	57.2
FW-4-H-8-T12-1		0.2	1.1	3.1	6.9	13.9	72.1	57.0
FW-4-H-9-S-1		0.2	1.1	2.8	8.0	12.8	75.1	57.5
FW-4-H-10-S-1		0.1	1.0	2.9	7.3	12.4	76.3	56.5
FW-4-H-10-M16-1		0.1	1.3	2.7	7.8	13.8	73.3	48.8
FW-4-H-10-T16-1		0.1	1.1	2.3	7.3	11.4	77.8	54.9
FW-4-H-10-M12-1		0.1	1.3	2.9	8.3	12.7	74.7	55.0
FW-4-H-10-T12-1		0.2	1.4	2.8	8.1	12.0	75.5	54.7
FW-4-H-11-S-1		0.1	1.0	2.9	8.3	12.6	75.1	53.4

TABLE A-9

RUN NO.: FW-5-H
MATERIAL: Fly Ash (with Orzan added)
SOLIDS CONCENTRATION: 57 % Wt.
GRAVITY (AVE): As shown
RHEOLOGY (AVE): η = As shown cP, τ_o = as shown
TEMPERATURE: 52°F
DATE: 12/7/68

Line No.	Time hr:min	Temp °F	Pressure psi	Specific Gravity		Solids Concentration Wt %		Flow gpm	Velocity		Pre
									12 Inch fps	16 Inch fps	12 In psi/2
Start	12:20										
1	13:10	42	-	1.551	1.54	60.6	58.5	3300	9.36	5.80	3.6
2	13:24	43	59	1.546		58.5		3000	8.51	5.27	2.9
3	13:38	43	63	1.545		59.4		2740	7.77	4.81	2.5
4	13:54	45	70	1.538		58.5		2500	7.09	4.39	2.0
5	15:20	50	52	1.530		58.7		3000	8.51	5.27	2.8
	16:30	Added 0.09% Orzan AL-50									
6	16:55	50	49	1.506	1.50	57.1	57.0	3000	8.51	5.27	2.7
7	17:10	51	62	1.501		57.0		2490	7.06	4.37	1.9
8	17:37	52	-	-		-		2800	7.94	4.92	2.3
9	17:50	53	44	1.469		57.3		3200	9.08	5.62	3.0
10	18:04	53	66	1.495		57.5		2200	6.24	3.86	1.4
11	18:18	53	70	1.491	1.47	57.7	55.0	1950	5.53	3.43	1.13
12	18:38	54	74	1.471		56.0		1680	4.77	2.95	0.88
13	19:00	54	77	1.468		55.5		1390	3.94	2.44	0.61
14	19:15	54	80	1.453		53.4		1000	2.84	1.76	0.36

A

Velocity		Pressure Drop		Rheology		Reynolds No.		Shear Stress		Friction Factor	
ch	16 Inch fps	12 Inch psi/200'	16 Inch psi/200'	η / μ	τ_o dynes/ cm^2	12 Inch $x10^{-4}$	16 Inch $x10^{-4}$	12 Inch lbs/ft^2	16 Inch lbs/ft^2	12 Inch $x10^3$	16 Inch $x10^3$
36	5.80	3.60	1.13	10.9 ↑	7.3 ↑	8.67	6.83	.648	.258	5.00	5.19
51	5.27	2.98	.91	10.4	7.3	7.89	6.20	.536	.208	5.00	5.06
77	4.81	2.5	.71	10.8 — 10.8	7.1 — 7.3	7.20	5.67	.450	.162	5.03	4.73
09	4.39	2.04	.59	-	-	6.57	5.17	.367	.135	4.93	4.72
51	5.27	2.82	.84	9.7 ↓	6.7 ↓	7.88	6.21	.504	.192	4.70	4.67
51	5.27	2.73	.81	8.7 ↑	1.1 ↑	10.84	8.53	.494	.185	4.67	4.60
06	4.37	1.90	.56	8.7	1.9	8.99	7.08	.342	.128	4.72	4.61
94	4.92	2.35	.68	- — 8.7	-	10.11	7.96	.423	.155	4.62	4.43
08	5.62	3.02	.91	-	-	11.56	9.10	.544	.208	4.54	4.54
24	3.86	1.43	.44	8.6 ↓	1.00 — 1.0	7.95	6.25	.257	.101	4.55	4.64
53	3.43	1.13	.36	7.3 ↑	2.2	8.47	6.67	.203	.082	4.66	4.92
77	2.95	0.88	.28	7.6 — 7.3	1.3	7.29	5.74	.158	.064	4.89	5.16
94	2.44	0.61	.22	6.6	1.0	6.04	4.75	.110	.050	4.95	5.93
34	1.76	0.36	.13	7.1 ↓	1.0 ↓	4.34	3.42	.065	.030	5.65	6.76

B

TABLE A-10

SCREEN ANALYSES
RUN FW-5-H

SAMPLE NO.	PERCENT RETAINED ON TYLER MESH							PERCENT SOLIDS
	+14	14x28	28x48	48x100	100x200	200x325	-325	
FW-5-H-1-S-1	trace	0.3	1.9	4.0	9.1	12.4	72.3	58.0
FW-5-H-2-S-1		0.2	1.7	4.0	8.6	12.5	73.0	58.8
FW-5-H-3-S-1		0.3	2.3	4.0	8.7	12.4	72.3	58.0
FW-5-H-4-S-1		0.5	2.1	3.7	7.9	12.1	73.7	58.1
FW-5-H-4-M16-1		0.2	1.9	4.2	9.5	16.0	68.0	55.8
FW-5-H-4-T16-1		0.1	2.0	4.7	9.5	12.2	71.5	56.4
FW-5-H-5-S-1	trace	0.2	1.7	3.7	8.6	12.0	73.8	57.2
FW-5-H-5-M16-1		0.2	1.9	3.7	9.2	13.6	72.4	57.8
FW-5-H-5-T16-1		0.2	1.5	4.0	8.8	15.4	70.1	54.9
FW-5-H-6-S-1	trace	0.3	2.1	3.9	8.0	12.4	73.3	55.3
FW-5-H-7-S-1		0.2	1.6	3.4	8.7	12.8	73.3	54.5
FW-5-H-7-M16-1		0.2	2.3	4.1	8.9	16.1	66.2	69.0
FW-5-H-7-T16-1		0.2	1.6	3.6	8.1	12.1	74.4	54.4
FW-5-H-7-M12-1		0.2	1.4	3.5	7.9	12.6	74.4	54.3
FW-5-H-7-T12-1		0.2	1.4	3.3	6.7	12.4	76.0	54.9
FW-5-H-9-S-1	trace	0.3	1.2	3.7	7.6	11.8	75.4	58.0
FW-5-H-10-S-1		0.3	1.5	3.3	9.1	12.1	73.7	54.0
FW-5-H-10-M16-1		0.2	1.5	3.3	7.5	11.6	75.9	53.9
FW-5-H-10-T16-1		0.2	1.4	3.0	8.0	10.6	76.8	54.1
FW-5-H-10-M12-1		0.2	1.5	3.3	7.6	11.8	75.6	54.1
FW-5-H- 10-T12-1		0.2	1.7	3.5	6.6	11.7	76.3	54.0
FW-5-H-11-S-1		0.3	1.7	4.0	8.1	11.6	74.3	54.0
FW-5-H-12-S-1		0.2	2.0	3.3	8.6	11.5	74.4	-
FW-5-H-12-M16-1		0.2	1.3	3.0	8.3	12.5	74.7	52.3
FW-5-H-12-T16-1		0.2	1.5	3.2	8.0	11.8	75.3	53.2
FW-5-H-12-M12-1		0.2	1.8	3.3	7.8	10.5	76.4	53.4
FW-5-H-12-T12-1		0.2	1.8	3.3	8.3	11.7	75.2	54.0

BECHTEL

TABLE A-10 (continued)

SCREEN ANALYSES
RUN FW-5-H

SAMPLE NO.	PERCENT RETAINED ON TYLER MESH							PERCENT SOLIDS
	+14	14x28	28x48	48x100	100x200	200x325	-325	
FW-5-H-13-S-1	trace	0.3	2.2	3.1	7.8	11.6	75.0	53.0
FW-5-H-13-M16-1		0.3	0.8	3.3	7.3	10.6	77.7	53.0
FW-5-H-13-T16-1		0.4	1.4	3.2	7.2	11.4	76.4	52.4
FW-5-H-13-M12-1		0.3	1.2	3.4	7.6	11.2	76.4	51.4
FW-5-H-13-T12-1		0.3	0.8	3.7	8.4	11.4	75.4	52.1
FW-5-H-14-S-1	trace	0.3	1.9	3.1	7.5	10.5	76.7	52.2
FW-5-H-14-M16-1		0.2	1.2	2.2	7.5	10.8	78.1	53.5
FW-5-H-14-T16-1		0.3	1.1	2.7	7.2	10.8	77.9	50.7
FW-5-H-14-M12-1		0.3	1.0	4.0	7.0	10.0	77.7	52.0
FW-5-H-14-T12-1		0.3	1.4	3.2	7.9	10.6	76.6	51.8

TABLE A-11

RUN FW-1-0
SCREEN ANALYSES

SAMPLE NO.	PERCENT RETAINED ON TYLER MESH							PERCENT SOLIDS
	+14	14x28	28x48	48x100	100x200	200x325	-325	
FW-1-0-1-S-1	trace	0.1	0.7	2.0	5.9	11.5	79.8	56.8
1-M16-1		0.1	0.4	1.4	6.6	10.8	80.7	51.8
1-T16-1		0.2	0.6	1.7	5.6	11.4	80.5	51.0
1-M12-1		0.2	1.1	2.4	6.3	12.1	77.9	70.5
1-T12-1		0.2	1.1	2.5	5.9	11.3	79.0	67.2
FW-1-0-2-S-1		0.1	0.6	1.9	6.3	10.7	80.4	51.8
2-M16-1		0.2	0.8	1.9	6.2	11.2	79.7	60.7
2-T16-1		0.2	0.6	2.1	5.6	11.4	80.1	55.3
2-M12-1		0.1	1.0	2.9	6.8	11.4	77.8	70.0
2-T12-1		0.2	1.2	2.8	6.1	11.6	78.1	65.4
FW-1-0-3-S-1		0.1	0.8	2.2	5.6	11.2	80.1	59.3
3-M16-1		0.2	0.9	1.6	6.3	11.7	79.3	41.8
3-T16-1		0.1	0.8	1.5	6.0	11.3	80.3	52.7
3-M12-1		0.2	0.5	2.0	6.2	10.7	80.4	47.7
3-T12-1		0.2	0.6	2.0	5.2	10.6	81.4	47.7
FW-1-0-4-S-1		0.1	0.6	1.4	6.3	11.8	79.8	41.4
4-M16-1		0.2	1.1	2.8	6.8	11.1	78.0	68.0
4-T16-1		0.1	1.2	2.5	5.8	11.3	79.1	69.8
4-M12-1		0.2	1.0	1.6	6.1	10.7	80.4	48.8
4-T12-1		0.1	0.8	1.7	5.5	11.2	80.7	48.3
FW-1-0-5-S-1		0.1	1.0	1.6	6.0	11.8	79.5	53.7
5-M16-1		0.1	1.0	1.7	6.0	11.2	80.0	47.3
5-T16-1		0.2	0.7	2.0	5.9	10.6	80.6	47.3
5-M12-1		0.1	0.8	1.9	6.1	10.8	80.3	56.4
5-T12-1		0.2	1.0	1.9	5.2	11.7	80.0	54.8
FW-1-0-6-S-1		0.1	0.9	1.7	6.2	11.1	80.0	48.5
6-M16-1		0.1	1.0	2.0	6.4	10.8	79.7	52.8
6-T16-1		0.2	0.7	1.9	5.4	11.3	80.5	50.7
6-M12-1		0.2	1.0	1.8	6.5	11.1	79.4	50.8
6-T12-1		0.3	0.8	1.7	5.7	11.1	80.4	51.0

TABLE A-11 (continued)

RUN FW-1-0
SCREEN ANALYSES

SAMPLE NO.	PERCENT RETAINED ON TYLER MESH							PERCENT SOLIDS
	+14	14x28	28x48	48x100	100x200	200x325	-325	
FW-1-0-7-S-1	trace	0.1	1.2	1.9	5.9	11.6	79.3	57.6
7-M16-1		0.2	0.7	2.0	6.1	10.3	80.7	57.3
7-T16-1		0.5	0.7	1.8	6.3	11.5	79.2	55.0
7-M12-1		0.3	0.5	1.6	5.9	10.5	81.2	52.1
7-T12-1		0.3	0.7	1.8	6.0	11.5	79.7	49.8
FW-1-0-8-S-1		0.1	0.5	1.9	6.0	11.3	80.3	49.8
8-M16-1		0.1	0.6	1.6	5.7	10.3	81.7	51.5
8-T16-1		0.3	0.7	1.7	5.5	10.7	81.1	51.3
8-M12-1		0.1	0.8	1.8	5.8	9.7	81.8	55.0
8-T12-1		0.2	0.4	1.9	6.1	10.1	81.3	56.0
FW-1-0-9-S-1		0.1	0.5	2.0	5.8	11.0	80.6	50.9
9-M16-1		0.2	0.6	1.7	5.7	10.5	81.3	54.7
9-T16-1		0.2	0.6	1.7	5.4	10.7	81.4	55.4
9-M12-1		0.3	0.7	1.5	5.8	10.5	81.2	52.7
9-T12-1		0.2	0.6	1.8	5.4	10.6	81.4	50.5
FW-1-0-10-S-1		0.1	0.7	1.6	6.3	10.7	80.6	50.8
10-M16-1		0.3	0.6	1.6	6.0	9.9	81.6	53.5
10-T16-1		0.3	0.6	1.7	5.4	10.5	81.5	53.6
10-M12-1		0.2	0.7	1.7	6.3	10.5	80.6	53.7
10-T12-1	↓	0.4	0.7	1.7	5.3	10.6	81.3	54.3

A-4 SLUDGE/FLY ASH RUNS

Tables A-12 to A-14 present the data gathered from pipe tests on digested sludge/fly ash mixtures.

TABLE A-12

RUN NO. FS-1-H
MATERIAL: Digested Sludge/Fly Ash Mixture
SOLIDS CONCENTRATION: 11% Wt.
GRAVITY (AVE): 1.05 = 65.5 lbs/ft^3
RHEOLOGY (AVE): η = 6.4 cP, τ_o = 4.8 dynes/cm^2
TEMPERATURE: 75°F
DATE: 11/2/68

Line No.	Time hr:min	Temp °F	Pressure psi	Specific Gravity	Solids Concentration Wt %	Flow gpm	Velocity		Pr
							12 Inch fps	16 Inch fps	12 I psi/
Start									
1	9:35	75	36	1.061	12.3	3120	8.85	5.48	1.9
2	9:45	73	36.5	1.048	10.5	2520	7.15	4.43	1.4
3	9:50	74	46	-	11.0	2040	5.79	3.58	0.9
4	10:00	75	50.5	-	11.9	1525	4.33	2.68	0.5
5	10:04	75	51.5	-	10.4	1020	2.89	1.79	0.3
6	10:14	75	54	-	9.9	500	1.42	0.88	0.1
7	10:25	76	55	-	9.6	225	0.64	0.40	0.1
8	10:28	76	54.5	-		620	1.76	1.09	0.1
9	10:34	76	54	-	9.5	830	2.35	1.46	0.2
10	10:39	75	53	-	13.3	1260	3.57	2.21	0.4
11	10:44	76	50	-	13.5	1830	5.19	3.21	0.7
12	10:49	76	39.5	1.041	10.2	2900	8.23	5.09	1.6
13	11:00	-	35	1.034	9.0	2280	6.47	4.01	1.1

A

locity	Pressure Drop		Rheology		Reynolds No.		Shear Stress		Friction Factor	
16 Inch fps	12 Inch psi/200'	16 Inch psi/200'	η / μ	τ_o dynes/cm^2	12 Inch x10^{-4}	16 Inch x10^{-4}	12 Inch lbs/ft^2	16 Inch lbs/ft^2	12 Inch x10^3	16 Inch x10^3
5.48	1.95	0.65	7.0	7.3	13.45	10.58	0.351	0.149	4.41	4.87
4.43	1.47	0.46	7.0	5.6	10.86	8.55	0.265	0.105	5.09	5.28
3.58	0.95	0.32	-	-	8.79	6.92	0.171	0.073	5.02	5.61
2.68	0.59	0.20	7.1	4.3	6.57	5.17	0.106	0.046	5.58	6.27
1.79	0.30	0.11	-	-	4.40	3.46	0.054	0.025	6.34	7.71
0.88	0.125	0.07	7.0	4.8	2.15	1.70	0.023	0.016	10.99	20.41
0.40	0.10	0.05	-	-	0.97	0.76	0.018	0.011	43.4	72.00
1.09	0.15	0.075	-	-	2.67	2.10	0.027	0.017	8.58	14.22
1.46	0.20	0.10	-	-	3.58	2.82	0.036	0.023	6.38	10.58
2.21	0.40	0.14	7.0	4.5	5.43	4.27	0.072	0.032	5.54	6.43
3.21	0.72	0.25	-	-	7.89	6.21	0.130	0.057	4.73	5.44
5.09	1.68	0.56	6.8	5.2	12.50	9.84	0.302	0.128	4.39	4.85
4.01	1.12	0.37	6.8	4.3	9.83	7.73	0.202	0.085	4.74	5.19

B

TABLE A-13

RUN NO.: FS-2-H
MATERIAL: Digested Sludge/Fly Ash Mixture
SOLIDS CONCENTRATION: 20% Wt.
GRAVITY (AVE): 1.10 = 68.5 lbs/ft^3
RHEOLOGY (AVE) η = 6.0 cP, τ_o = 7.4 dynes/cm^2
TEMPERATURE: 80° F
DATE: 11/2/68

Line No.	Time hr:min	Temp °F	Pressure psi	Specific Gravity		Solids Concentration Wt %	Flow gpm	Velocity		Pressu
				Lab	Densometer			12 Inch fps	16 Inch fps	12 Inch psi/200'
Start										
1	12:30	77	40	1.101	1.10	20.1	3000	8.5	5.3	1.98
2	12:36	77	45	1.101	1.11	19.6	2500	7.1	4.4	1.47
3	12:42	78	49.5	-	1.12	18.1	2000	5.7	3.5	0.97
4	12:47	79	52.5	-	1.126	20.6	1500	4.3	2.65	0.58
5	12:55	80	55	-	1.126	-	1000	2.84	1.76	0.275
6	13:00	80	56.5	-	1.12	22.2	500	1.42	0.88	0.125
7	13:06	82	57	-	1.12	20.3	280	0.79	0.49	0.125
8	13:12	80	57	-	1.12	18.5	600	1.70	1.05	0.150
9	13:17	81	57	-	1.12	19.5	820	2.33	1.44	0.175
10	13:23	81	56	-	1.12	24.4	1260	3.6	2.21	0.40
11	13:35	81	53	-	1.12	-	1760	5.0	3.1	0.72
12	13:40	81	49	1.095	1.12	19.8	2290	6.5	4.0	1.13
13	13:45	81	44.5	1.099	1.10	20.0	2760	7.8	4.9	1.62
14	13:50	82	42	-	1.09	-	2990	8.5	5.3	1.88

A

locity		Pressure Drop		Rheology		Reynolds No.		Shear Stress		Friction Factor	
ch.	16 Inch fps	12 Inch psi/200'	16 Inch psi/200'	η / μ	τ_o dynes/cm^2	12 Inch x10^{-4}	16 Inch x10^{-4}	12 Inch lbs/ft^2	16 Inch lbs/ft^2	12 Inch x10^3	16 Inch x10^3
	5.3	1.98	0.65	7.7	7.8	14.42	11.35	0.356	0.149	4.63	5.03
	4.4	1.47	0.49	7.6	7.1	12.02	9.46	0.265	0.112	4.95	5.47
	3.5	0.97	0.37	-	-	9.62	7.57	0.175	0.085	5.10	6.45
	2.65	0.58	0.20	8.5	7.8	7.21	5.68	0.104	0.046	5.42	6.20
4	1.76	0.275	0.125	-	-	4.81	3.78	0.050	0.029	5.78	8.71
2	0.88	0.125	0.10	8.0	7.1	2.40	1.89	0.023	0.023	10.51	27.88
9	0.49	0.125	0.10	-	-	1.35	1.06	0.023	0.023	33.53	88.91
0	1.05	0.150	0.11	7.9	6.9	2.89	2.27	0.027	0.025	8.76	21.30
3	1.44	0.175	0.12	-	-	3.94	3.10	0.032	0.028	5.47	12.44
	2.21	0.40	0.16	6.9	4.1	6.06	4.77	0.072	0.037	5.30	7.03
	3.1	0.72	0.26	-	-	8.46	6.66	0.130	0.060	4.89	8.55
	4.0	1.13	0.38	7.8	7.3	11.01	8.66	0.203	0.087	4.53	5.05
	4.9	1.62	0.55	7.3	7.4	13.27	10.44	0.292	0.126	4.47	5.03
	5.3	1.88	0.64	-	-	14.38	11.31	0.338	0.146	4.42	4.99

B

1

TABLE A-14

RUN NO.: FS-3-H
MATERIAL: Digested Sludge/Fly Ash Mixture
SOLIDS CONCENTRATION: 35% Wt.
GRAVITY (AVE) 1.25 = 78.2 lbs/ft^3
RHEOLOGY (AVE) η = 9.4 cP, τ_o = 11.8 dynes/cm^2
TEMPERATURE 67°F
DATE: 11/5/68

Line No.	Time hr:min	Temp °F	Pressure psi	Specific Gravity	Solids Concentration Wt %	Flow gpm	Velocity		Press
							12 Inch fps	16 Inch fps	12 Inch psi/200
Start									
1	8:40	63	50	1.257	37.2	2900	-	5.10	-
2	8:45	63	53.3	-	-	2450	-	4.30	-
3	8:50	64	57.3	1.256	34.6	2000	5.70	3.50	1.41
4	10:23	66	60 +	1.252	35.8	1490	4.20	2.62	0.67
5	10:30	67	60 +	-	43.2	980	2.78	1.72	0.33
6	10:35	67	60 +	1.243	34.2	520	1.50	0.91	0.25
7	10:40	67	60 +	-	33.9	780	2.20	1.37	0.28
8	10:45	67	60 +	1.243	34.3	1290	3.70	2.27	0.51
9	10:50	68	60 +	-	37.9	1700	4.80	3.0	0.82
10	10:55	67	57.5	1.248	35.5	2270	6.40	4.0	1.40
11	11:00	67	52	-	-	2760	7.8	4.9	2.0

A

ocity	Pressure Drop		Rheology		Reynolds No.		Shear Stress		Friction Factor	
16 Inch fps	12 Inch psi/200'	16 Inch psi/200'	η / μ	τ_o dynes/cm^2	12 Inch x10^{-4}	16 Inch x10^{-4}	12 Inch lbs/ft^2	16 Inch lbs/ft^2	12 Inch x10^3	16 Inch x10^3
5.10	-	0.75	9.1	12.6	-	7.99	-	0.172	-	5.45
4.30	-	0.55	-	-	-	6.75	-	0.126	-	5.60
3.50	1.41	0.39	8.9	9.9	7.01	5.51	0.212	0.089	5.43	5.95
2.62	0.67	0.23	9.1	11.5	5.22	4.11	0.121	0.053	5.56	6.33
1.72	0.33	0.18	9.4	11.2	3.43	2.70	0.059	0.041	6.33	11.44
0.91	0.25	0.15	9.3	10.4	1.82	1.43	0.045	0.034	17.03	33.87
1.37	0.28	0.16	9.5	11.6	2.73	2.15	0.050	0.037	8.48	16.06
2.27	0.51	0.23	8.8	11.4	4.52	3.56	0.092	0.053	5.65	8.44
3.0	0.82	0.32	10.0	12.5	5.96	4.69	0.148	0.073	5.23	6.76
4.0	1.40	0.51	9.0	11.5	7.95	6.26	0.252	0.117	5.01	6.04
4.9	2.0	0.70	9.6	12.7	9.67	7.61	0.360	0.160	4.84	5.61

B

1

Appendix B
NOMENCLATURE

B, b = coefficients in Blasius expression, dimensionless

c = ratio of yield stress to shear stress, τ_o / τ_w, dimensionless

D = diameter, ft.

f = Fanning friction factor, $(\Delta pD/4L)/(\rho V^2/2g_c)$, dimensionless

g = acceleration due to gravity, ft/sec^2

g_c = conversion factor (lb_m/lb_f) (ft/sec^2)

G = rate of shearing strain, sec^{-1}

K = consistency factor in Ostwald-de Waele model, lb_f/ft^2

L = length, ft.

n = flow index in Ostwald-de Waele model, dimensionless

N_{He} = Hedstrom number, $N_{Re} \cdot P_L$, dimensionless

N_{Re} = Reynolds Number, $DV\rho/\eta$ or $DV\rho/\mu_{eff}$, dimensionless

P_L = plasticity number, $(\tau_o/\eta)/(V/D)$, dimensionless

r = radius, ft.

U = local velocity, ft/sec

V = bulk velocity, ft/sec

Greek Letters

η = coefficient of rigidity, centipoise

μ = viscosity of suspending medium, centipoise

μ_{eff} = effective viscosity, centipoise

τ = shear stress, lb_f/ft^2 or $dynes/cm^2$

τ_o = yield stress, $dynes/cm^2$

τ_w = wall shear stress, lb_f/ft^2

ρ = density, lb_m/ft^3

ϵ = absolute pipe roughness, inches

κ = von Karman coefficient of turbulent exchange, dimensionless

Δp = pressure loss

ϕ = volume fraction (volume of solids/total slurry volume)(dimensionless)

Appendix C

REFERENCES

1. Cheung, D. C. H., Ray, D. J., and Valentin, F. H., "The Flow of Thixotropic Bentonite Suspension through Pipes and Pipe Fittings", Trans. Instn. Cheml. Engrs., Vol 43, pp. 176-186, 1965.

2. Weltmann, R. N. and Keller, T. A., "Pressure Losses of Titania and Magnesium Slurries in Pipes and Pipeline Transitions"., NASA Techl. note 3889, Jan. 1957.

3. Kearset, H. A., "The Rheology of Dispersed Suspensions of Thoria and its Relation to the Non-Newtonian Behavior of Flocculated Suspensions", Instn. Cheml. Engrs., Vol. 40, pp. 140-145, June 1962.

4. Gabrysh, A. F., Eyring H. and Cutler, I., "Rheological Factors for Attapulgite Suspended in Water", Journ. Am. Cera., Soc., Vol. 45, No. 7, pp. 334-343, July 1962.

5. Gabrysh, W. F., Eyring H., Pan, L. S., and Gabrysh, A. F. "Rheological Factors for Bentonite Suspensions", Jour. Am. Cera. Soc., Vol 46.

6. Michaels, A. S. and Bolger, J. C., "The Plastic Flow Behavior of Flocculated Kaolin Suspensions", Indl. and Engr. Chem. Fundamentals, Vol. 1, No. 3, pp. 153-162, Aug. 1962.

7. Starkey, T. V., Hewlett, V. A., Roberts, J. H. A., and James, R. E., "Principles Governing the Viscous Flow of Suspensoid Sols." British Jour. of Appl. Phys., Vol 12, pp. 545-553, October 1961.

8. McMath, R. E., "Silt Movement by the Mississippi", Van Nostrand's Engineering Magazine, p. 36, 1883.

9. Vanoni, V. A., "Transportation of Suspended Sediment by Water," Trans. A.S.C.E., Publ. 2267, 111, 67, 1964.

10. Zandi, I., "Decreased Head Losses in Raw Water Conduits," J. AWWA 59, 2, pp. 213-226, Feb. 1967.

11. Daily, J. W. and Bugliarello, G., "Basic Data for Dilute Fiber Suspensions in Uniform Flow with Shear," Tappi, 44, 7, 497, 1961.

12. Mooney, M., "The Viscosity of a Concentrated Suspension of Spherical Particles", Jour. Colloid Sci., Vol. 6, pp. 162-170., 1951.

13. Vand, V., "Viscosity of Solutions and Suspensions III Theoretical Interpretation of Viscosity of Sucrose Solutions", Jour. Phy. and Colloid Chem., Vol. 52, pp. 314-321, 1948.

14. Tomita, Y., "A Study of Non-Newtonian Flow in Pipe Lines, "Bulletin of A.S.M.E., 2, 5, pp. 10-16, 1959.

15. Metzner, A. B., "Non-Newtonian Technology: Fluid Mechanics, Mixing, and Heat Transfer", in Advances in Cheml. Engr., Academic P., New York, 1956.

16. Buckingham, E., Proc. Am. Soc. Testing Materials, 21, 1154-61, 1921.

17. Govier, G. W. and Winning, M. D., paper presented to the American Inst. of Chemical Engineers, Montreal, Canada, 1948.

18. Hedstrom, B. O. A., "Flow of Plastic Materials in Pipes", Jour. of Ind. Engrg. Chem. 44, 3, March 1952, pp. 651-656.

19. Hanks, R. W., J. A. I. Ch. E., 9, 3, May 1963, pp. 306-309.

20. Mooney, M., Journal of Rheology, 2, 210, 1931.

21. Behn, V. C. and Shane, R. M., "Capillary vs. Pipeline in Determining Sludge Flow Behavior", Wat. and Sw. Works, Vol. 110, pp. 272-274 July 1963.

22. Rankin, S., Thesis for Master of Chemistry Engineering presented to University of Delaware, Newark, Delaware, 1954.

23. Metzner, A. B. and Reed, J. C., "Flow of Non-Newtonian Fluids-Correlation of the Laminar, Transition, and Turbulent Flow Regions," Jour. of A. I. Ch. E., 1, Dec. 1955, pp. 434-440.

24. Caldwell, D.H. and Babbitt, H. E., "The Flow of Muds, Sludges, and Suspensions, in Circular Pipes," Trans. A.I.Ch.E. 37, Feb. 1941, pp. 237-66.

25. Alves, G. E., Boucher, D. F. and Pigford, R. L., "Pipe Line Design for Non-Newtonian Solutions and Suspensions", Chem. Engineering Progress, 48, 8, Aug. 1952, pp. 385-393.

26. Wilhelm, R. H., Wroughton, D. M., and Loeffel, W. F., "Flow of Suspensions Through Pipes, "Ind. & Engr. Chem. 31, 5, May 1939, pp. 622-629.

27. Winding, C. D., Baumann, G. P. and Krainch, W. L., "Flow Properties of Pseudo Plastic Fluids, Flow of GR-5 Latices in Commercial Tubing," Chem. Engr. Prog. 43, 10, Oct. 1947, pp. 527-536, & Nov. 1947, pp. 613-622.

28. Alves, G. E., "Flow of Non-Newtonian Suspensions," Jour. of Chem. Engr. 56, 5, May 1949, pp. 107-109.

29. Oldroyd, J. G. "A Suggested Method of Detecting Wall Effects in Turbulent Flow Through Tubes," Proc. First Int. Rheology Cong. Holland, 1948, II, pp. 1301-1304.

30. Bogue, D. C., "Velocity Profiles in Turbulent Non-Newtonian Pipe Flow," Ph. D. Thesis, University of Delaware, Newark, Delaware, 1960.

31. Weltman, R. N., "An Evaluation of Non-Newtonian Flow in Pipe Lines, "National Advisory Committee for Aeronautics, Wash., D. C. Tech. Note 3397, 1955.

32. Wang, C. T., "On the Velocity Distribution of Turbulent Flow in Pipes and Channels of Constant Cross Section, "Trans. ASME 68, Jour. of Applied Mech., June 1946, pp. A85-A90.

33. Thomas, D. G., "Transport Characteristics of Suspensions Part IX, "Jour. of A. I. Ch. E., 10, 3, May 1964, pp. 303-308.

34. Thomas, D. G., "Heat and Momentum Transport Characteristics of Non-Newtonian Aqueous Thorium Oxide Suspensions," A.I.Ch.E., 6, 4, Dec. 1960, pp. 631-639.

35. Binder, R. C. and Busher, J. E., "A Study of Flow of Plastics Through Pipes, "Trans. ASME, 68, Jour. of Appl. Mech. 13, June 1946, pp. A101-A105.

36. Dodge, D. W., "Turbulent Flow of Non-Newtonian Fluids in Smooth Round Tubes," PhD. Thesis, University of Delaware, Newark, Delaware, 1958.

37. Bird, R. B., "Correlation of Friction Factors in Non-Newtonian Flow, "Jour. of A. I. Ch. E., 2, 3, Sept. 1956, pp. 428-430.

38. Dodge, D. W., and Metzner, A. B., "Turbulent Flow of Non-Newtonian Systems "Jour. of A. I. Ch. E., 5, 2, June 1959, pp. 189-203.

39. Millikan, C.B. "A Critical Discussion of Turbulent Flows in Channels and Circular Tubes, "Proc. 5th Int'l Cong. for Applied Mechanics, John Wiley & Sons, New York, N.Y., 1939, pp. 386-390.

40. Shaver, R.G., "Turbulent Flow of Pseudoplastic Fluids in Straight Circular Tubes, "Thesis presented to Massachusetts Institute of Technology at Cambridge, Mass. in 1957, in partial fulfillment of the requirements for the degree of Doctor of Science.

41. Thomas, D.G., "Transport Characteristics of Suspensions Part (iv) Friction Loss of Concentrated Flocculated Suspensions in Turbulent Flow, "Jour. of A.I.Ch.E., 8, 2, May 1962, pp 266-27.

42. Thomas, D.G., "Non-Newtonian Suspensions, "I. & Engr. Chem., 55, 11 Nov. 1963, pp. 19-29.

43. Thomas, D.G., "Non-Newtonian Suspension Part II Turbulent Transport Characteristics, "I. & Engr. Chem., 55, 12, Dec. 1963, pp. 27-35.

44. Thomas, D.G., "Progress in International Research on Thermodynamic and Transport Properties, "Masi, J.F. and Tsai, editors, ASME, Academic Press, N.Y., 1962.

45. Eissenberg, D.M., "Measurement and Correlation of Turbulent Friction Factors of Thoria Suspensions at Elevated Temperatures," Jour. of A.I.Ch.E., 10, 3, May 1964, pp. 403-407.

46. Bogue, D.C. and Metzner, A.B., "Velocity Profiles in Turbulent Pipe Flow, "Jour of A.I.Ch.E. 2, 2 May 1963, pp. 143-149.

47. Murthy, V.R.K. and Zandi, I., "Turbulent Flow of Non-Newtonian Suspensions in Pipes", Jour. of Engr. Mech., A.S.C.E., 6427, pp. 1-17, Feb. 1969.

48. Govier, G.W. and Charles, M.E., Eng. J. 44, 8, pp. 50-57, 1961.

49. Durand, R., "Basic Relationships of the Transportation of Solids in Pipes - Experiementatal Research." Proc. Intln. Assoc. Hyd. Res., Minneapolis, Minn., Sept. 1-4, 1953.

50. Private Communication, Nov. 16, 1957.

51. Wirts, J.J., Water and Sewage Works., Oct. 1948, pp. 345-351.

52. Wever, J., "The Sewage System of the Hague...", Dept. of Public Works, The Hague, Holland.

53. Swan. I. D., Bomberger, D. R., and Barthauer, G. L., "Corrosion Control Achieved on Coal Slurry Pipeline", Materials Protection Vol. 2, No. 9, pp. 26-34. Sept. 1963.

54. Bain. A. G., "Getting Working Data on Coal Pipelines", Engr., Vol. 196, pp. 322-323, Sept. 13, 1963.

55. Smith, F. L. and Wasp, E. J., "Pipeline Movement of Bulk Materials", A. S. C. E., Phila. Pa., October 17, 1966, Colorado School of Mines Res. Foundation, Inc.

56. Symposium and Panel Discussion on the Handling and Placement of Hydraulic Backfill Underground, Canadian Mining and Metal, Bull. Vol. 53, pp. 687-692, Dis. 693-702, 1960.

57. Bomberger, D. R., "Hexavalent Chromium Reduces Corrosion in a Coal-Water Slurry Pipeline", Materials Protection, Jan. 1965, pp. 43-49.

58. McDermott, W. F., Cowper, N. T., Davis R. A. and Wasp., E. J., "The World's First Long Distance Iron Ore Slurry Pipeline" Soc. Min. Eng of AIME Minneapolis, Minnesota, Sept. 1968.

59. Babbitt, H. E., and Caldwell, D. H., Univ. of Illinois Bull. 319, 37, 12, Nov. 1939.

60. "The Transportation of Solids in Steel Pipelines", Colorade School of Mines, Res. Foundation, 1963, pp. 84-85.

61. Condolios, E., and Chapus, E. E., Chemical Engineering, July 22, 1963.

62. Koch, L., "Solids in Pipes", Internl. Sci. and Tech., 26, pp. 68-78, Feb. 1964.

63. Halvorsen, W. J., "Automating the Coal Pipeline", Coal Age, 69, pp. 107-108, July 1964.

64. Thompson, T. L., and Wasp, E. J., "Coal Pipelines - A Reappraisal" IEEE-ASME Joint Power Generation Conference, San Francisco September 1968.

1 *Accession Number*

W 70-04007

2 *Subject Field & Group*

05E, 06A, 05G

SELECTED WATER RESOURCES ABSTRACTS
INPUT TRANSACTION FORM

5 *Organization*

Bechtel Corporation, San Francisco, California.

6 *Title*

BULK TRANSPORT OF WASTE SLURRIES TO INLAND AND OCEAN DISPOSAL SITES: VOLUME III - TECHNICAL ASPECTS OF PIPELINING OF WASTE MATERIALS.

10 *Author(s)*

Kenny, J. P.

16 *Project Designation*

Contract No 14-12-156 FWPCA
Project No 14010 EMS

21 *Note*

Available from the Clearing-house as PB 189 759, $3 in paper copy, 65¢ in microfiche

22 *Citation*

Federal Water Pollution Control Administration Research Series Report DAST-16, Vol 3, September 1969. 167 p, 80 fig, 15 tab, 64 ref, 3 append.

23 *Descriptors (Starred First)*

*Sludge disposal, *Hydraulic transportation, *Pipelines, *Hydraulics, *Slurries, Waste disposal, Closed conduit flow, Pipe flow, Turbulent flow, Suspension, Mixing, Fly ash, Sewage sludge, Municipal wastes, Sanitary engineering.

25 *Identifiers (Starred First)*

Sludge transport, Solid waste disposal.

27 *Abstract*

The feasibility of using pipelines to transport waste materials, and to develop a reliable procedure for the design of such pipelines was studied. A series of laboratory and pipeline tests was performed. Digested sewage sludge and fly ash were chosen as representative materials for the tests. Both materials, sludge because of its fibrous nature and fly ash because the particles are very fine, were transported in homogenous flow in the turbulent regime. Samples taken from the top and the middle of the pipe test sections confirmed this. These materials, individually and in various combinations, were tested at various velocities in 1/2-inch, 12-inch, and 16-inch pipe test sections, for a number of solids concentrations. Digested sludge, fly ash, and fly ash/sludge mixtures can be successfully transported by pipelines. (Knapp - USGS)

(WRSIC ABSTRACT)

(See W70-04004)

Abstractor
George Knapp 3-2-70

Institution
U. S. Geological Survey, Water Resources Div.

WR:102 (REV. JULY 1969)
WRSIC

SEND TO: WATER RESOURCES SCIENTIFIC INFORMATION CENTER
U.S. DEPARTMENT OF THE INTERIOR
WASHINGTON, D. C. 20240

* GPO: 1969-359-339